

Old Dominion University

ODU Digital Commons

Mechanical & Aerospace Engineering Theses & Dissertations

Mechanical & Aerospace Engineering

Winter 2006

Development of a Nonlinear Estimator-Based Model of Pilot Performance During Brownout Conditions

Karl Ulrich Schultz
Old Dominion University

Follow this and additional works at: https://digitalcommons.odu.edu/mae_etds



Part of the [Aerospace Engineering Commons](#)

Recommended Citation

Schultz, Karl U.. "Development of a Nonlinear Estimator-Based Model of Pilot Performance During Brownout Conditions" (2006). Doctor of Philosophy (PhD), Dissertation, Mechanical & Aerospace Engineering, Old Dominion University, DOI: 10.25777/1jfr-jh64
https://digitalcommons.odu.edu/mae_etds/88

This Dissertation is brought to you for free and open access by the Mechanical & Aerospace Engineering at ODU Digital Commons. It has been accepted for inclusion in Mechanical & Aerospace Engineering Theses & Dissertations by an authorized administrator of ODU Digital Commons. For more information, please contact digitalcommons@odu.edu.

**DEVELOPMENT OF A NONLINEAR ESTIMATOR
BASED MODEL OF PILOT PERFORMANCE
DURING BROWNOUT CONDITIONS**

by

Karl Ulrich Schultz

B.S. May 1993, United States Naval Academy
M.S. June 1995, Massachusetts Institute of Technology

A Dissertation Submitted to the Faculty of
Old Dominion University in Partial Fulfillment of the
Requirement for the Degree of

DOCTOR OF PHILOSOPHY

AEROSPACE ENGINEERING

OLD DOMINION UNIVERSITY

December 2006

Approved by:

Thomas E. Alberts (Director)

Brett Newman (Member)

Colin P. Britcher (Member)

Braden J. McGrath (Member)

Angus Rupert (Member)

ABSTRACT

DEVELOPMENT OF A NONLINEAR ESTIMATOR BASED MODEL OF PILOT PERFORMANCE DURING BROWNOUT CONDITIONS

Karl Ulrich Schultz
Old Dominion University, 2006
Director: Dr. Thomas E. Alberts

During conditions of visual occlusion, pilots are forced to rapidly adapt their scan to accommodate the new observable states via instruments rather than the visual environment. During this transition, the provision of aircraft state information via other than visual modalities improves pilot performance presumably through the increase in situational awareness provided immediately following the visual occlusion event.

The Tactile Situational Awareness System (TSAS) was developed to provide continuous position information to the pilot via tactile rather than visual means. However, as a low-resolution display, significant preprocessing of information is required to maximize utility of this new technology.

Development of a nonlinear time varying estimator based multivariable model enables more accurate reproduction of pilot performance than previous models and provides explanations of many observed phenomena. The use of LQR feedback and an optimal estimator is heuristically consistent with reported strategies and was able to match pilot incorporation of multi-modal displays. Development of a nonlinear stochastic map of pilot “move-and-hold” control performance was able to accurately match increased pilot control noise at higher frequencies, a phenomenon formerly attributed to closed loop

neuromuscular effects. The continued improvement of this model could eventually result in the early stage mathematical prediction of the effectiveness of emerging cockpit technology and preprocessing algorithms, prior to costly hardware development and flight evaluation.

DEDICATION

To my beautiful wife Shannon, who has provided me unwavering support throughout this ordeal and to Ryland, in whose smile I see the face of God.

ACKNOWLEDGMENTS

There are many people who have contributed to the successful completion of this dissertation.

I would like to thank Captain Angus Rupert of Naval Aerospace Medical Research Laboratory. I called asking for career advice and you gave me a dissertation topic. Your mentorship throughout the years has been truly invaluable. I thank you for the numerous opportunities you've provided me and look forward to future collaboration.

To Commander Tim Bitzer, for selflessly allowing your XO to leave in the middle of the day to attend class. I truly couldn't have done it without your support.

To Commander Steve Halpern, for continuing the tradition set by your predecessor. See you in Houston.

To Professor Thomas Alberts, your patience and support these past four years has been incredible. I don't know if this would have been possible without your involvement.

I thank Professor Brett Newman, whose nonlinear actuators class will be the standard by which all other classes shall forever be judged. As GPD, your knowledge of the bureaucratic trappings of the University has been truly invaluable during the past months.

To Professor Colin Britcher: your enthusiasm has been a constant source of inspiration during this long and arduous task.

To Dr. Brad McGrath: Who would have thought that we'd end up here? Your insight and pragmatism have been invaluable during the experimental phase of this research. I look forward to our future collaborations.

To my Dad and my Mom, for coming down from New York to watch the boy while I finished this monstrosity. Thank you for your unwavering love and support.

TABLE OF CONTENTS

| | |
|--|-------------|
| LIST OF TABLES | ix |
| LIST OF FIGURES | x |
| ACRONYMS AND SYMBOLS | xiii |
| SECTION 1 INTRODUCTION..... | 1 |
| 1.1 Problem Solution..... | 3 |
| 1.2 Dissertation Goals | 4 |
| 1.3 Dissertation Structure | 5 |
| SECTION 2 LITERATURE REVIEW | 7 |
| 2.1 Skin and Tactile Sense | 7 |
| 2.1.1 Anatomy of the Skin | 8 |
| 2.1.2 Problems with Tactile Signals | 9 |
| 2.1.3 Quantifying Tactile Sense..... | 11 |
| 2.2 Tactile Displays | 13 |
| 2.2.1 Tactile Instruments..... | 13 |
| 2.2.2 Tactile Situation Awareness System..... | 16 |
| 2.3 Performance Measurements | 19 |
| 2.3.1 Performance Measures..... | 19 |
| 2.3.2 Workload..... | 20 |
| 2.3.2.1 Techniques for Assessing Pilot Workload..... | 20 |
| 2.3.2.2 Objective Measures..... | 21 |
| 2.3.2.3 Subjective Measures | 22 |
| 2.3.2.4 Physiological Measures | 23 |
| 2.3.2.5 Common Workload Measurement Techniques | 23 |
| 2.3.3 Situational Awareness..... | 25 |
| 2.3.3.1 China Lake Situational Awareness (CLSA) | 26 |
| 2.3.3.2 Situational Awareness Subjective Workload Dominance (SWORD) .. | 27 |
| 2.3.3.3 Perceptual Cue Rating..... | 27 |
| 2.4 Pilot Models | 28 |
| 2.4.1 Verbal Analytical Model..... | 29 |
| 2.4.1.1 Sources of Remnant | 31 |
| 2.4.2 Crossover Model..... | 32 |
| 2.4.3 Multi-Loop Model and Scanning..... | 35 |
| 2.4.4 Optimal Control Model (OCM)..... | 36 |
| 2.4.5 Modified Optimal Control Model (MOCM)..... | 38 |
| SECTION 3 METHODS | 41 |
| 3.1 Conventions | 41 |
| 3.2 Pilot Study..... | 42 |
| 3.2.1 High Hover Task..... | 43 |

| | | |
|------------------|--|-----------|
| 3.2.1.1 | Pilot Trial Results | 44 |
| 3.3 | Experimental Hardware and Software..... | 46 |
| 3.3.1 | Revised T-34 Simulator System | 47 |
| 3.3.2 | Plant Dynamics | 50 |
| 3.4 | Experimental Design..... | 53 |
| 3.4.1 | Subjects | 53 |
| 3.4.2 | Experimental Trials..... | 53 |
| 3.4.3 | Conditions Presented | 55 |
| 3.4.4 | Variables Recorded..... | 56 |
| 3.4.4.1 | Intra-Trial Questionnaire | 56 |
| 3.4.4.2 | Post Trial Questionnaire | 61 |
| 3.5 | Data Analysis..... | 61 |
| 3.5.1 | Subjective Data Analysis | 61 |
| 3.5.2 | Objective Data Analysis | 62 |
| 3.5.2.1 | Data Analysis Programming | 63 |
| 3.5.2.2 | Sliding Window Path Error Analysis..... | 63 |
| 3.6 | Model Development | 64 |
| SECTION 4 | RESULTS | 71 |
| 4.1 | Subjective Data..... | 71 |
| 4.1.1 | CLSA | 71 |
| 4.1.2 | Modified Cooper-Harper | 72 |
| 4.1.3 | Subjective Performance Self Evaluation | 73 |
| 4.1.4 | Perceptual Cue Rating..... | 74 |
| 4.1.5 | Visual Environment Information Percentage..... | 76 |
| 4.1.6 | Instrument Information Percentage..... | 77 |
| 4.1.7 | Subjective Workload Dominance (SWORD) | 78 |
| 4.2 | Objective Data..... | 79 |
| 4.2.1 | Summary Variables..... | 80 |
| 4.2.1.1 | Lateral Axis Position Error | 81 |
| 4.2.1.2 | Lateral Axis Error Rate, Roll Angle, and Roll Angle Rate | 82 |
| 4.2.1.3 | Aileron Response | 83 |
| 4.2.1.4 | Longitudinal Axis Error Signal..... | 83 |
| 4.2.1.5 | X-Axis Error Rate, Pitch Angle, and Pitch Rate..... | 84 |
| 4.2.1.6 | Elevator | 84 |
| 4.2.2 | Path Error | 85 |
| 4.2.2.1 | Lateral Axis Path Error | 86 |
| 4.2.2.2 | Longitudinal Axis Path Error..... | 89 |
| 4.3 | Model Structure | 91 |
| 4.3.1 | Optimal Feedback | 91 |
| 4.3.2 | Neuromuscular lag..... | 92 |
| 4.3.3 | Pilot Compensation..... | 93 |
| 4.3.4 | Nonlinear Effects | 94 |
| 4.3.5 | Final Model Structure | 95 |

| | | |
|------------------------|--|------------|
| 4.3.6 | Model Dynamic Equations | 97 |
| 4.4 | Validation of Model Subcomponents | 103 |
| 4.4.1 | Optimal Feedback Gain | 104 |
| 4.4.2 | Compensator Term..... | 105 |
| 4.4.3 | Neuromuscular Terms..... | 107 |
| 4.4.4 | Nonlinear Dynamics | 109 |
| 4.5 | Complete Model Solution | 116 |
| 4.5.1 | Parameter Identification Sequence | 117 |
| 4.5.2 | Estimator | 118 |
| 4.5.3 | Compensation Block..... | 121 |
| 4.5.4 | Nonlinear Stochastic Mapping..... | 122 |
| 4.5.5 | Closed Loop Model Performance | 123 |
| 4.5.5.1 | Linear Model Performance | 123 |
| 4.5.5.2 | Nonlinear Model Performance..... | 133 |
| 4.6 | Model Matching in the Longitudinal Axis..... | 138 |
| 4.6.1 | Longitudinal Axis Linear Model | 138 |
| 4.6.2 | Longitudinal Axis Nonlinear Model..... | 141 |
| SECTION 5 | DISCUSSION AND FUTURE RESEARCH..... | 144 |
| 5.1 | TSAS Effectiveness | 144 |
| 5.2 | Workload and Situational Awareness Measures | 145 |
| 5.2.1 | Subjective Measures | 145 |
| 5.2.2 | Model Measures..... | 145 |
| 5.3 | Model Development | 146 |
| 5.3.1 | Estimator Model..... | 147 |
| 5.3.2 | Optimal Feedback | 147 |
| 5.3.3 | Compensator Block..... | 148 |
| 5.3.4 | Nonlinear Block..... | 148 |
| 5.3.5 | Neuromuscular Model | 149 |
| 5.4 | Research Shortcomings | 150 |
| 5.4.1 | TSAS..... | 150 |
| 5.4.2 | Experimental Design..... | 150 |
| 5.4.3 | Model Development..... | 151 |
| 5.5 | Potential areas of future research | 152 |
| SECTION 6 | CONCLUSIONS | 155 |
| REFERENCES..... | | 157 |
| APPENDICES..... | | 169 |

LIST OF TABLES

| | |
|---|------------|
| Table 3-1 Plant Dynamics - Constants | 52 |
| Table 3-2 Pseudo-Random Sum-of-Sines Disturbance Signal | 55 |
| Table 4-1 Eigenvalues of Open Loop and Closed Loop GVE and DVE Systems ... | 120 |

LIST OF FIGURES

| | |
|---|-----------|
| Figure 1-1 Quality of Visual Field During Brownout Condition..... | 4 |
| Figure 2-1 Skin Structure..... | 8 |
| Figure 2-2 Homunculus | 12 |
| Figure 2-3 TSAS Vest | 17 |
| Figure 2-4 Modified Cooper-Harper Rating Scale | 24 |
| Figure 2-5 China Lake Situational Awareness Scale..... | 26 |
| Figure 2-6 Subjective WORKload Dominance Pilot Survey | 27 |
| Figure 2-7 Perceptual Cue Rating | 28 |
| Figure 2-8 Verbal Analytical Model..... | 29 |
| Figure 2-9 Crossover Model..... | 33 |
| Figure 2-10 Crossover and Extended Crossover Model..... | 33 |
| Figure 2-11 Optimal Control Model | 37 |
| Figure 2-12 Modified Optimal Control Model..... | 38 |
| Figure 3-1 Aircraft Axis Conventions | 41 |
| Figure 3-2 High Hover RMS Error in X, Y, and Z Axes | 44 |
| Figure 3-3 Pilot Mental Workload vs. Condition..... | 45 |
| Figure 3-4 NAMRL T-34 Simulator..... | 46 |
| Figure 3-5 Virtual Instrument Display | 47 |
| Figure 3-6 Visual Display and Modified VI Panel | 48 |
| Figure 3-7 Revised T-34 Simulator Data Stream..... | 49 |
| Figure 3-8 CLSA Questionnaire Format | 57 |
| Figure 3-9 Modified Cooper Harper Questionnaire Format..... | 58 |
| Figure 3-10 Subjective Performance Assessment | 58 |
| Figure 3-11 Perceptual Cue Rating..... | 59 |
| Figure 3-12 Visual Instrument Attention Division | 60 |
| Figure 3-13 TSAS Information Percentage Provided..... | 60 |
| Figure 3-14 Effect of Sampling Upon Power Spectrum | 68 |
| Figure 4-1 China Lake Situational Awareness Post Trial Reports | 72 |
| Figure 4-2 Pilot Mental Workload vs. Condition..... | 73 |
| Figure 4-3 Perceptual Cue Rating - Visual Attitude Cues | 74 |
| Figure 4-4 Perceptual Cue Rating - Visual Horizontal Drift Cues | 75 |
| Figure 4-5 Perceptual Cue Rating - Instrument Cues..... | 76 |
| Figure 4-6 Percentage of Information Acquired From Visual Environment..... | 77 |
| Figure 4-7 Source of Aircraft Information - Percentage..... | 78 |
| Figure 4-8 Reported SWORD Pairwise Comparisons | 79 |
| Figure 4-9 Lateral Axis Position RMS Error | 81 |
| Figure 4-10 Subjective Performance Evaluation | 82 |
| Figure 4-11 Aileron Response RMS | 83 |
| Figure 4-12 Longitudinal Axis Position RMS Error | 84 |
| Figure 4-13 Elevator Response RMS | 85 |
| Figure 4-14 Lateral Axis Path Error..... | 86 |
| Figure 4-15 Lateral Axis T-test Values Between Baseline and Test Conditions..... | 88 |
| Figure 4-16 Longitudinal Axis Path Error | 90 |

| | |
|--|-----|
| Figure 4-17 Modified Pilot Controller Model | 96 |
| Figure 4-18 Modified Pilot Controller Model - State Space Format..... | 102 |
| Figure 4-19 Optimal Feedback Gain - Frequency Domain Response..... | 104 |
| Figure 4-20 Optimal Feedback Reconstruction of Linear Aileron Signal..... | 105 |
| Figure 4-21 Various Structured Compensators' Performance - Time Domain..... | 106 |
| Figure 4-22 Comparison of Neuromuscular Models - Frequency Domain | 108 |
| Figure 4-23 Recorded Aileron Signal - "Move and Hold" | 109 |
| Figure 4-24 Stochastic Analysis of Pilot Decision | 110 |
| Figure 4-25 Length of Decision Phase vs. Command Signal Error..... | 111 |
| Figure 4-26 Cumulative Probability of Length of Hold vs. Command Signal Error | 112 |
| Figure 4-27 Cross Section of Cumulative Probability of Length of Hold vs. Command Signal Error..... | 113 |
| Figure 4-28 Cumulative Probability of Aileron Movement Left and Right vs. Command Signal Error..... | 113 |
| Figure 4-29 Magnitude of Aileron Change vs. Number of Timesteps | 114 |
| Figure 4-30 Cumulative Probability of Aileron Change vs. Length of Movement. | 115 |
| Figure 4-31 Cumulative Probability of Aileron Change to the Right..... | 115 |
| Figure 4-32 Frequency Domain Effects of Random "Move-and-Hold" | 116 |
| Figure 4-33 Poles and Zeros of GVE and DVE Closed Loop Plants..... | 118 |
| Figure 4-34 Slow Poles and Zeros of GVE and DVE Closed Loop Systems | 119 |
| Figure 4-35 Bode Plot of GVE and DVE Closed Loop Systems | 121 |
| Figure 4-36 Compensator Block Parameters | 122 |
| Figure 4-37 Stochastic Map - Simultaneous Display of Twelve Trials | 123 |
| Figure 4-38 Lateral Axis Position Error - Actual Trials and Model Prediction..... | 124 |
| Figure 4-39 Aileron Signal - Actual Trials and Model Prediction | 125 |
| Figure 4-40 Experimental and Simulated Aileron Signal - Frequency Domain | 126 |
| Figure 4-41 Linear Aileron Signal - "Move and Hold" Strategy | 127 |
| Figure 4-42 Aileron Signal - Effect of "Move and Hold" - Frequency Domain | 127 |
| Figure 4-43 Closed Loop Linear Plant - Frequency Spectrum..... | 128 |
| Figure 4-44 Pilot Loop - Experimental and Simulation | 130 |
| Figure 4-45 Pilot Loop with Plant Dynamics Superimposed | 130 |
| Figure 4-46 Pilot Loop - Neuromuscular Noise Removed..... | 131 |
| Figure 4-47 Lateral Axis Position Error - Linear Model and Discretized Aileron Signal..... | 132 |
| Figure 4-48 Aileron Signal - Linear Model and Discretized Aileron Signal | 133 |
| Figure 4-49 Lateral Axis Position Error - Actual Trials and Nonlinear Model Prediction..... | 134 |
| Figure 4-50 Aileron Signal - Actual Trials and Nonlinear Model Prediction | 134 |
| Figure 4-51 Nonlinear Model Aileron Signal - Frequency Domain | 135 |
| Figure 4-52 Nonlinear Model - Closed Loop Transfer Function..... | 136 |
| Figure 4-53 Nonlinear Model - Time Domain - Lateral Axis Position Error | 137 |
| Figure 4-54 Nonlinear Model - Time Domain - Aileron Signal | 137 |
| Figure 4-55 Power Spectral Density of Actual and Linear Model Elevator Signal | 139 |
| Figure 4-56 Longitudinal Axis - Magnitude of Actual and Linear Model Closed Loop System | 140 |

| | |
|--|------------|
| Figure 4-57 Longitudinal Position Error - Actual, Linear, and Linear Discretized Models | 140 |
| Figure 4-58 Elevator Signal - Actual, Linear, and Linear Discretized Models..... | 141 |
| Figure 4-59 Longitudinal Position Error - Actual and Nonlinear Model..... | 142 |
| Figure 4-60 Elevator Signal - Actual and Nonlinear Model | 142 |
| Figure 4-61 Closed Loop Transfer Function - Actual System and Nonlinear Model | 143 |
| Figure 5-1 Twelve Trial Repeatability | 153 |
| Figure 5-2 "Tweaked" Heuristic Model | 154 |

ACRONYMS AND SYMBOLS

ACRONYMS

| | |
|---------|---|
| ARE | Algebraic Riccati Equation |
| CLSA | China Lake Situational Awareness Measure |
| CSD | Cross Spectral Density |
| DEJ | Dermal Epidermal Junction |
| DF | Describing Function |
| DVEH | Degraded Visual Environment – High |
| DVEL | Degraded Visual Environment – Low |
| GVE | Good Visual Environment |
| HUD | Heads Up Display |
| LQR | Linear Quadratic Regulator |
| LQG | Linear Quadratic Gaussian |
| MCH | Modified Cooper-Harper Workload Measure |
| MILSPEC | Military Specification |
| MOCM | Modified Optimal Control Model |
| NAMRL | Naval Aerospace Medical Research Laboratory |
| OCM | Optimal Control Model |
| PCR | Perceptual Cue Rating |
| PSD | Power Spectral Density |
| PVO | Pre Visual Occlusion |
| RMS | Root Mean Square |
| SA | Situational Awareness |
| SWORD | Subjective Workload Dominance |
| TFE | Transfer Function Estimate |
| TSAS | Tactile Situational Awareness System |
| VOE | Visual Occlusion Event |
| VOSS | Visual Occlusion Steady State |
| VOX | Visual Occlusion Transition |

SYMBOLS

| | |
|-------------------|-----------------------------|
| dB | Decibel |
| F | Control rate cost matrix |
| K | Optimal feedback gain |
| L | Kalman estimator gain |
| Q | State cost matrix |
| R | Control cost matrix |
| Δ | Pilot effective time delay |
| x | Longitudinal position error |
| \dot{x} or dx | Longitudinal velocity |
| x_x | System state vector |
| y | Lateral position error |

| | |
|-----------------------------|--|
| \dot{y} or dy | Lateral velocity |
| y_x | System output vector |
| u_x | System command signal |
| v_u | Neuromuscular noise |
| v_y | Observation noise |
| w | Disturbance signal |
| w_c | Crossover frequency |
| w_n | Natural frequency |
| ζ | Damping coefficient |
| δ | Command signal (Aileron or Elevator) |
| θ | Pitch Angle |
| $\dot{\theta}$ or $d\theta$ | Pitch Rate |
| ϕ | Roll Angle |
| $\dot{\phi}$ or $d\phi$ | Roll Rate |
| x | Complete system state $[x_p \ x_{NM} \ x_c]^T$ |
| \hat{x} | Complete system state estimate |

SECTION 1 INTRODUCTION

When a rotary wing aircraft is operated in close proximity to loose sand, earth or snow, a visually occluding condition known as brownout (whiteout) occurs. As debris is blown into the air, a partial or full occlusion of the visual field takes place, eliminating the primary source of position, attitude, and velocity information prior to the occlusion. Although procedural attempts to prevent brownout have been marginally successful in reducing the problem, elimination of the problem seems unlikely while the necessity of operations in these environments exists. With the recent increase in the scope of operations conducted in the deserts of Southwest Asia and the mountainous terrain in both SW Asia and the Balkan Peninsula, the problem of brownout and whiteout has seen a corresponding increase, resulting in the loss of 20 U.S helicopters in Fiscal Year (FY) 2003 alone. Brownouts were by far the most prevalent accident events of 2003, accounting for 16% of all Army mishaps [Lyle, 2003]. Over 85% of these mishaps occurred in OPERATION ENDURING FREEDOM and OPERATION IRAQI FREEDOM related operations.

The problem of pilot performance during visually occluded situations is a complex one with many confounding factors including spatial disorientation, lack of aircraft state observability, and non-continuous controller strategy. These factors act in concert to degrade pilot-vehicle performance. Such degradation would be dangerous even during normal flight, but in such close proximity to the ground, with potentially high rates of descent and necessarily small margins of error, these dangers are exacerbated significantly.

During a normal helicopter landing to a spot, the pilot first decides upon an appropriate landing area. The landing zone may be designated by lights or visual markings, or may simply be the most appropriate spot given the terrain. The pilot then determines the proper approach path. The approach path is, in fact, a four dimensional trajectory through 3-D space with desired velocities corresponding to each point on the glide slope.

Factors such as terrain, obstacles, and wind direction will influence the construction of this invisible path to the landing spot.

Once the landing zone and approach path are determined, the pilot's actions can be modeled as a quasi-linear optimal regulator [McRuer and Krendel, 1974; Davidson and Schmidt 1992; Hess, 1989], attempting to minimize tracking error along the desired trajectory. A good pilot will use an "outside-in" scan, gathering information from both cockpit instruments and the visual environment to determine his actual position in relation to his desired position. During normal flight, the overwhelming majority of the information gathered by the pilot comes from the real-world visual environment.

A pilot's "scan" involves sharing time between two or more targets, "dwelling" on each target for a designated time, "transitioning" to another target, "acquiring" the new target, and dwelling again. An experienced pilot can scan several instruments each second and will change his scan depending on task, conditions, and scenario.

During transition periods, no foveal information is available to the pilot. Even once the pilot fixates on his new target, additional time is required for the pilot to gather any useful information. Essentially, when scanning, only the dwell period is productive in providing detailed foveal information to the pilot, though it should be noted that on a clear day some information can be gleaned peripherally from the visual environment (even during the transition period).

As challenging as it is to land a helicopter under the best conditions, brownout and whiteout complicate the evolution by obscuring the majority of the pilot's information at a critical time during the approach. The loss of this information forces the pilot to transition to an "inside" scan and rely solely upon cockpit instruments. This reduction in available information leads to a decrease in pilot performance and pilot bandwidth and an increase in pilot workload and tracking error. Most importantly, during the *transition time* from outside to inside scan, the pilot is provided *no* information regarding the aircraft states, further increasing the tracking error. If the loss of information occurs

during the last few moments prior to touchdown or during a period of high rate of descent, unplanned impact with the ground is likely.

1.1 Problem Solution

It is proposed that the use of continuous presentation of data to the pilot will improve performance during visually occluded conditions, particularly in the moments immediately following brownout. The use of visual, aural, or tactile instruments to present information has been the subject of much research. Each modality has been proven effective for specific tasks and environments.

Though aural presentation is effective in reducing pilot reaction time in responding to alerts or warning, the modality is limited in its utility in real time control of a dynamic system. Conversely, visual presentation of information, specifically enhanced vision and other heads up display (HUD) instruments, are perfectly suited toward control of a dynamic system. The fidelity and resolution possible with a visual display exceeds any other modality.

Despite this fact, a tactile presentation device is believed to possess more potential benefit in improving flight safety, particularly during times of visual or mental distraction. Though visual presentations can be quite rich in the amount of information available, they are subject to the same limitations of normal visual instruments and the visual environment. Most importantly, during periods of distraction, when gaze is fixed in locations other than the HUD or directly on the instruments, *zero* information is transmitted to the pilot. A tactile feedback device is capable of continuous presentation of information even during periods of visual or mental distraction.

It is theorized that a tactile feedback display device will improve pilot performance during visually occluded conditions. Sudden visual occlusion requires a scan transition from outside the aircraft (where visual cues were excellent) to inside the cockpit (where instrument cues are significantly worse). During this transition, the pilot is essentially

flying blind (no cues at all). By providing continuous inputs to the pilot via an intuitive tactile instrument, scan transition effects may be decreased. Furthermore, the presentation of additional information during the inside scan may improve performance after the transient stage and may even improve performance during flight with the good visual field. Figure 1.1 shows a graphical representation of the quality of the pilot's visual cues of aircraft attitude and position during a visually occluded event.

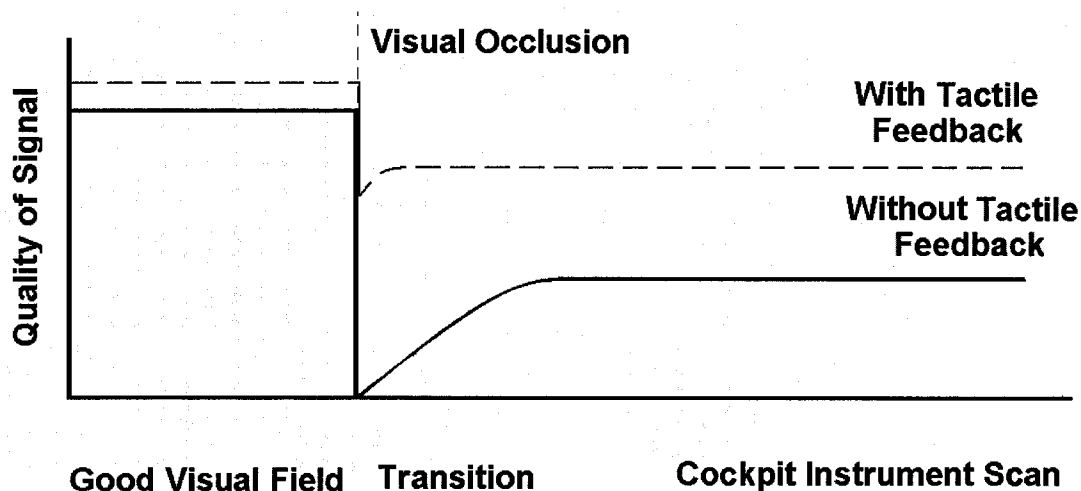


Figure 1-1 Quality of Visual Field During Brownout Condition

1.2 Dissertation Goals

The primary goal of this research is to improve the safety of flight in brownout and whiteout conditions through improved pilot performance during visually occluded environments. To accomplish the overall goal, two supporting objectives are addressed:

- To evaluate the Tactile Situational Awareness System and its efficacy in aiding pilot performance during normal and occluded visual environments.
- To develop a mathematical pilot model of pilot regulation task performance that includes visual and tactile feedback loops, with potential to include vestibular and proprioceptive, loops in later models.

This final goal is expected to require the most attention and be the source of the majority of intellectual contribution of this dissertation.

The goals of this dissertation will be addressed using test flight data, simulator trials, and mathematical models of the pilot controller. Initially, existing data collected during flight trials was used as a foundation for experimental design and model development. The trial protocols and performance measures were evaluated using a static visual simulator and a small number of test subjects. Appropriate modifications to both model and experimental trials took place following the initial evaluation. Once development of the model and the performance measures had matured to a satisfactory level, a more comprehensive and directed evaluation was conducted using the simulator with a larger number of subjects.

The development of the estimator based model uses heuristic knowledge of pilot strategies and existing structures of the pilot-vehicle system to determine the appropriate terms of the model. The heuristic terms of the model are evaluated using recorded simulator data and successful terms are incorporated into the final model structure. Accuracy of the model will be evaluated through closed-loop and open-loop simulation and comparison to recorded data in both the time and frequency domains.

Ultimately, the hardware and software developed will be evaluated through in-flight trials in an actual or simulated brownout environment. Ideally, these data would have been included in this research. However, funding and scheduling limitations have prevented the inclusion of such data.

1.3 Dissertation Structure

Following the introduction, the Section 2 will present a brief summary of skin, the nature of skin, and the problems associated with tactile inputs. A short review of tactile instruments will be followed by a review of pilot performance measures. The

background section will conclude with a literature review of pilot model development applicable to this research.

Section 3, methods, begins with a review of the pilot trials conducted prior to this experiment. Next, the methodologies employed during the construction and conduct of the experiment will be presented. Analytical methods will be presented, followed by methodologies used during the construction of the pilot model.

Section 4 presents all experimental results, beginning with subjective performance measurements, followed by objective measures. The section will conclude with a review of the final model structure and a presentation of its efficacy in modeling real pilot performance.

Section 5 discusses some of the potential benefits of this research, catalogs many of the mistakes and problems present in this research, and suggests areas of future research. Section 6 will list all conclusions drawn from this research.

SECTION 2 LITERATURE REVIEW

2.1 Skin and Tactile Sense

The skin is the body's largest organ, measuring approximately 1.8 m² in area with a mass of approximately 4 kg [Montagna 1956]. Skin is an extremely complex organ, the comprehensive discussion of which could fill several volumes. The purpose of this overview is not to exhaustively discuss the skin, but to present basic physiology and function of the skin and to convey the incredibly complex nature of the skin and the tactile sense. This overview will familiarize the reader with the problems and limitations particular to tactile display systems.

As with many organs of the body, the skin serves several purposes. It protects the body from physical injury, dehydration, microorganism invasion, and ultra violet radiation and also serves to regulate body heat. Finally, and most important to this dissertation, the skin houses the mechanisms for sensation of mechanical, vibratory, chemical, and thermal stimuli, collectively known as our ability to "feel" [Cholewiak and Collins, 1991].

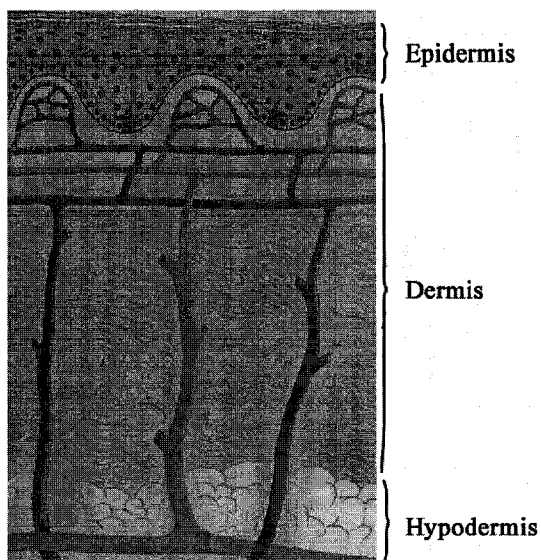


Figure 2-1 Skin Structure
from Rubin and Farber, 1994.

2.1.1 Anatomy of the Skin

The skin is a multi-layered sheet made up of three primary stratifications: the epidermis, the outermost layer of skin; the dermis, which houses most of the receptors believed to communicate “touch”; and superficial fascia, or hypodermis, which is made up of fat cells, vasculature, nerves, lymphatics and supportive structure. Additionally, hair follicles, apocrine and eccrine glands are confined to this depth. Skin covers the entire body and has a total thickness of approximately 1.5 to 4.0 millimeters, depending on the area of the body covered.

Of the cells that make up the epidermis, approximately 80 percent are *keratinocytes*, or skin cells. The remainder of the epidermis is made up of *melanocytes*, which protect the body’s DNA from UV radiation and cause tanning; *langerhans cells*, which aid the body in staving off infection by processing antigen information and passing it to T-cells through the lymph system; and *merkel cells*, which are attached directly to a free nerve ending and are mechanically activated by keratinocyte deformation. Their importance to the tactile sense bears further exploration later in this section.

Between the epidermis and the dermis is the Dermal/Epidermal Junction (DEJ), a thin layer bonding the two major layers of the skin. The DEJ provides resistance to shearing forces between the layers and is essentially composed of anchoring filaments, a membrane, and anchoring fibrils.

The dermis is composed of fibrous, filamentous, amorphous connective tissue, but also houses the majority of the vasculature and nerve network of the skin. Other cells are present (fibroblasts, macrophages, mast cells, and, to a smaller extent, lymphocytes and leukocytes) that aid in maintenance, repair, and defense of the body. Additionally, and most importantly to this research, the dermis houses *the meissner's corpuscles*, *pacinian corpuscles*, and *ruffini cylinders*, all of which are believed to be important receptors to touch.

The fibrous nature of the dermis provides the pliability, the elasticity, and the tensile strength of skin. The filament structure of collagen and elastic fibers makes up the interwoven fabric that provides all of the mechanical properties of the skin. The collagen provides 75% of the skin's tensile strength and elasticity. The elastic nature of both collagen and the connective tissue returns the skin to normal configuration after stretch or deformation and allows vibratory stimuli to travel *along* and *through* skin [Freeburg, 1991].

2.1.2 Problems with Tactile Signals

Earlier in this chapter, it was mentioned that, although several tactile receptors are named as such, the exact mechanism of the tactile sense is not clearly defined. Several reasons lead to this fact, including difficulty in producing “clean” stimuli, difficulty in measuring specific neural response, and the innate complexity of the neural architecture responsible for the tactile sense.

Producing a tactile stimulus for study seems a simple requirement. However, the complex physical nature of skin and its mechanoreceptors confound this seemingly simple task to an extremely complex level. The skin is an intricate web of neural pathways that measure chemical, thermal, electrical, or vibratory stimuli and overlap in unpredictable ways.

Additionally, a single stimulus may elicit a response in one or all of the tactile modes, confounding efforts to measure a single receptor response to a single event. As an example, consider the attempt to produce a simple vibrotactile signal in a subject. A tactor is placed on the forearm of the subject. The cold plastic or metal of the tactor creates an undesired thermal stimulus in the subject.

Furthermore, a vibratory stimulus may travel through the skin and elicit a response from receptors in several nearby fields, making a simple cause and effect measurement difficult, if not impossible. The very makeup of skin is one of the problems. As previously discussed, the collagen and keratin fibers that make up skin give it a property known as “viscoelasticity”, meaning that as a stimulus moves or deforms the skin, part of the energy is stored, allowing the skin to return to its original state (elastic), but part of that energy is transmitted through the skin (viscous). That energy may affect a receptor located nearby or at a completely different part of the body. It has been shown that mechanical vibration can generate traveling waves of energy across the surface of the skin. For example, a vibration delivered at a finger may travel up the arm [Keidel, 1968]. The propagation of these “surface waves” allows the possibility that a greater number of receptors might respond to a localized stimulus. The specific problem of surface waves may be reduced by adding a static ring around the moving vibratory contactor, called a “surround” [Verillo, 1962]. This technique succeeds in reducing surface vibrations, but deeper vibration signals may still spread laterally within the skin and subcutaneous structure. In fact, it is impossible to eliminate this phenomenon without amputation.

To further complicate issues, each unit may not respond in a time invariant fashion. Some units only respond to transient stimulus. Frequency sensitivity may, in fact

normally *does*, vary significantly. To demonstrate, the reader has probably been aware of, but not actively felt, their clothes for several hours. The tactile receptors have either ceased activity or, more likely, the brain has ignored the signal.

In addition to physical confounding factors, perceptual sensitivity reported by each subject may vary with awareness, training, and understanding of reporting instructions; multiple signals may mask or confound receptor signal or sensory interpretation; or speed of transmission of different signals may vary, contaminating cortical reconstruction of tactile signals.

Finally, the complexity of the tactile sense is not limited to anatomy of the physical receptors. The process of transmitting and processing tactile information contributes to further confound an already complex issue. Information from first-order neurons is distributed and combined with other first-order units and distributed among second-order units in the spinal cord. Convergence and divergence of these signals at both the cortical and sub-cortical level allows a cortex representation of the body surface stimuli [Cholewiak and Collins, 1991]. The location and intensity of the stimulus seems to be encoded on the number of receptors responding and the rate and duration of the response [Bolanowski and Zwislocki, 1984].

2.1.3 Quantifying Tactile Sense

Once somatosensory information reaches the brain, it is processed in several areas, Somatosensory I and II being the largest and most important [Kaas, Nelson, Sur, and Lin, 1979]. Areas with large innervation (fingertips, genitals, lips) have been found to have correspondingly higher areas of the brain associated with that innervation area. In the well-known homunculus in Figure 2.2 the size of the body part represents the size of the cortical area dedicated to that body part. Interestingly, a direct relationship has been established between cortical activity and sensory perceptions, even with tactile illusions; [Libet 1973] however, even these areas are not fixed. Significant changes in

somatosensory cortex organization can occur as a result of injury or experienced stimuli, essentially a rewiring of perceived tactile sense.

Concerted efforts to quantify tactile sensitivity have been recorded as far back as 1835 with the body of knowledge growing each year. To date, the most comprehensive and scientific of these efforts was conducted by Sidney Weinstein, who essentially reproduced the 1835 experiment, but employed the modern scientific method to balance the experiment and ensure uncorrupted results [Weinstein, 1968]. Weinstein and his colleagues measured two-point localization, pressure threshold, and two-point differentiation at various parts of the bodies of 24 right-handed males and 24 right-handed females. His research confirmed that sensitivity to touch is body part dependent and that the most sensitive areas of the body were the fingers, toes, and lips. The torso showed excellent pressure sensitivity, but subjects had some difficulty identifying the exact point of the tactile stimulus.

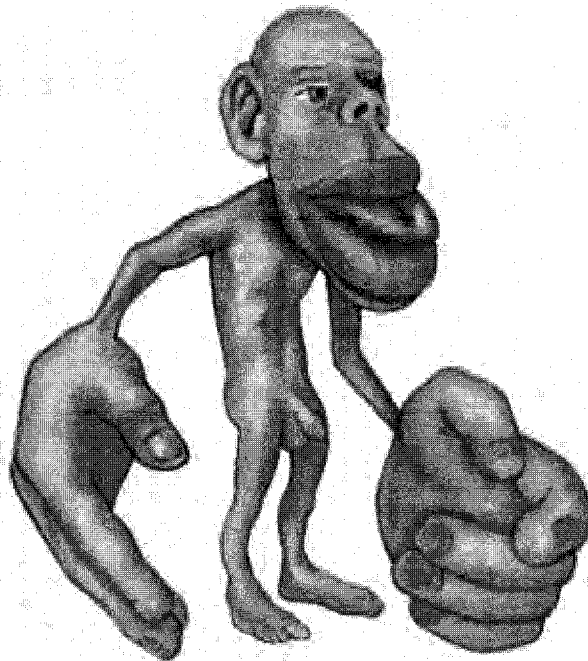


Figure 2-2 Homunculus
from Sherertz and Shenk, 2002

Taken collectively, this body of research might indicate that areas of high sensitivity to two-point localization, pressure threshold, and two-point differentiation would make the most suitable areas for transmission of tactile data.

While this assumption holds for isolated laboratory experiments and some practical tasks, i.e. Braille, research has shown that other factors must be considered when trying to relay information to subjects, particularly if that information is to be used in a control task or other closed loop system. Such factors include robustness of the signal, cortical effort required to process the signal, and the intuitive relationship between the tactile stimulus and the desired response [Wickens et al, 1983; Cholewiak and Craig, 1984; Ballard and Hessinger, 1954; Sanders and McCormick, 1982]. These experiments indicate that for complex or dynamic control tasks, an intuitive response to stimuli is preferable to increased sensitivity or point localization.

2.2 Tactile Displays

2.2.1 Tactile Instruments

The presentation of information via tactile modalities is not a new concept. Since the early twentieth century, researchers have been attempting to transmit information via tactile means. Most of the early attempts were centered around the development of sensory prosthetics for visually and auditorilly compromised persons. Attempts to transmit information through the skin involved head mounted; hand mounted, arm and leg mounted, and even back mounted tactile arrays. In fact, Braille writing is one of the more successful attempts to transmit information via tactile means.

The ability of the subject to receive and process information has been shown to be sensitive to body location, transmission mechanism, signal frequency, duration, and amplitude, and has been found to vary widely among subjects. However, researchers have been able to successfully transmit icons, graphs, maps, and even photos through tactile arrays [Dunlap, 1911; Geldard, 1957; Bliss, Katcher, Rogers, and Shepard 1970;

Loomis 1980; Cholewiak and Craig 1984; Wickens, Sandry, and Vidulich, 1983; Sherrick, 1985; Pring and Walker, 1993] to both blind and normal subjects.

While passing information in a sterile, controlled experiment is a necessary hurdle in the development of a useful tactile instrument; it is by no means sufficient. Robust, reliable, and intuitive information must be available if it is going to be used effectively in a modern cockpit.

The utility of non-visual instrumentation in high performance aircraft was most eloquently stated by James Ballard and Richard Hessinger, who wrote,

“In this age of instrumentation and servomechanisms, our machines are becoming so complicated that it taxes all the abilities of a human being to operate them... At the present time, the visual and aural senses of the pilot are employed to very near full capacity. Any change in the present complicated method of flying to relieve these two senses and to add to flying efficiency would be extremely valuable” [Ballard and Hessinger, 1954].

This realization sparked investigation of the use of tactile instruments to provide some of the information previously displayed to the pilot via visual means. Much early work focused on the use of tactile information as an alert, or alarm method. Researchers studied the effects of tactile cueing on indicating unexpected changes in the status of an automated cockpit system [Sklar and Sarter, 1999]. Tactile cueing resulted in higher detection rates *of* and faster response times *to*, uncommanded mode transitions. They also found that tactile information presentation did not interfere with, nor was it affected by, concurrent visual tasks. Raj found that vibrotactile cueing in addition to visual cueing reduced response times for reaction tasks in two axes [Raj et al, 2000].

Using tactile or aural signals as alert stimuli is useful, but more detailed information must be presented in order to be useful to the pilot during the active control of aircraft. In 1954 Ballard and Hessinger successfully used thumb mounted tactile instruments to

allow pilots to control the roll of a Link trainer. Sanneman reported success in 2-axis control using a cross-shaped tactile array worn on the pilot's chest [Sanneman, 1975].

Wickens, Sandry, and Vidulich [1983] found that when faced with visually demanding tasks, interference between tasks causes significant degradation in pilot performance. This phenomenon was found to be present even without scanning, and was even more pronounced when visual scanning was required. However, by providing information via a separate modality (auditory in this case) the task interference was reduced, and pilot performance improved. Furthermore, they found this result to be more dramatic as workload increased.

“Two tasks sharing common resource demands will be time-shared less efficiently than two tasks with non-overlapping demands. Furthermore, if the demand for a shared resource is increased by manipulating task difficulty, the disruptive effect on dual task performance will be greater than if the demand for a separate resource is increased.”

Wickens, Sandry, and Vidulich, 1983

In other words, the benefit of a separate modality display instrument will be more pronounced for tasks of greater difficulty.

Dobbins and Sanways [2002] found that navigation was possible using only tactile cues through either “virtual corridor” or “way point direction indicator” cueing protocols. By using a two-tactor set, and three distinct activation frequencies, they were able to communicate path deviation information to a submerged diver during undersea navigation trials. Results from these trials found that tactile cues provided similar cross track error as experiments using visual cues. Additionally, subjective feedback from the divers suggested that tactile feedback was easier to use, provided enhanced navigation, and was preferable to the visual display.

Despite the volumes of research available indicating ability of humans to successfully process tactile information and the effectiveness of tactile information in enhancing

performance of control tasks, prior to the early 1990s there was no focused effort on the development of a practical, in-cockpit tactile instrument, only esoteric experiments which, although successful, had limited general utility.

Naval Aerospace Medical Research Laboratory (NAMRL) in Pensacola, Florida undertook such a practical, focused effort. Over the past 10 years, NAMRL has sought to develop an effective, intuitive, and reliable tactile instrument. The result of this effort is the Tactile Situational Awareness System (TSAS), which represents the state of the art in tactile cueing instruments. TSAS is small, light, and unobtrusive, yet durable enough to survive modern cockpit environments and robust enough to provide a reliable signal even during complex flying tasks.

2.2.2 Tactile Situation Awareness System

The TSAS system, shown in Figure 2-3, was developed to provide flight or tactical information to a pilot by exploiting the previously untapped sense of touch, in the hopes of improving pilot situational awareness and reducing Spatial Disorientation. By transmitting relatively low bandwidth information, the intuitive nature of the tactile sense is preserved, thus providing additional information without affecting a pilot's cognitive abilities or interfering with his ability to utilize the visual or aural information available to him.

The system uses data from existing onboard aircraft systems, processes the data, and then relays designated information using miniature tactile stimulators called tactors. There are two types of tactors currently in use: pneumatic and electromagnetic. The pneumatic tactors are comprised of plastic bodies with latex bladders. Air is pulsed through the tactor and felt as a distinct tapping when placed against the body. The electromagnetic tactors have a magnet and electrical coil and, when energized, produce a unique buzzing sensation that "feels" different than the pneumatic tactors. The tactors are embedded in a MILSPEC, flight qualified, F-22 Raptor cooling vest, with two additional tactors embedded in a seat cushion.

The current TSAS configuration, shown in Figure 2.3, consists of eight vertical columns of pneumatic tactors inside the vest, each column consisting of three tactors. Four columns are located at each of the cardinal points on the body and four more columns midway between. In addition to the 24 pneumatic tactors, there are four (4) electromagnetic tactors, two mounted in the shoulders of the vest, and two in the seat cushion. Each of the tactors can be fired individually, or in concert with others. All of the tactors can be fired at three distinct intensities, low, medium, and high.

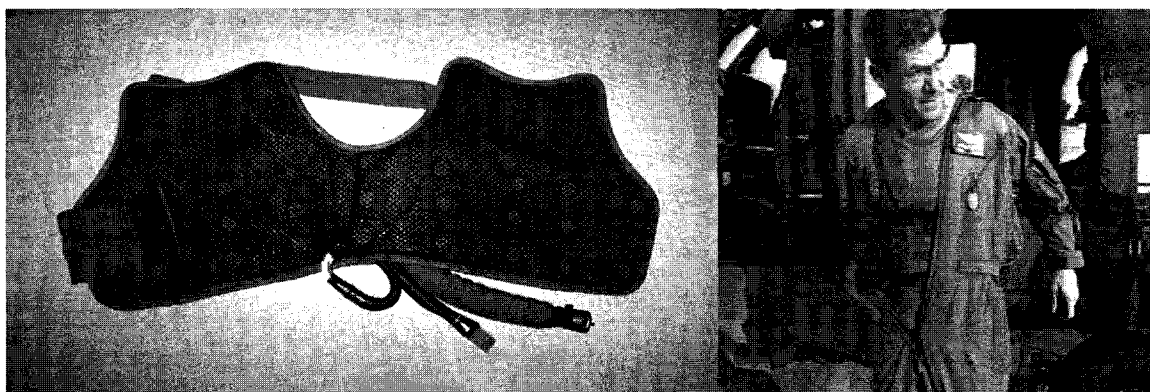


Figure 2-3 TSAS Vest

The TSAS has been proven effective in numerous simulator experiments and has been successfully tested and validated in three previous flight experiments: attitude orientation in the Navy T-34C Turbomenter, hover cues in the Army UH-60 Blackhawk, and hover cues in the Air Force MH-53M Super Stallion helicopter [Rupert et al 1994, McGrath 1999, Raj et al 1998].

The nature of information presented by the TSAS can vary significantly. Using onboard data bus information, the TSAS can present position, velocity, or even threat information to the pilot. For example, in hover mode, an aircraft position determined to be right of the desired position would elicit the activation of the tactors on the pilot's right side, indicating that left cyclic is required. In threat mode, activation of the left/back tactors

would indicate to the pilot that the threat is located at his 7:30 position. The specific modes of the TSAS will be discussed later in the methods section.

It should be noted that the current configuration of TSAS was not the original tactile instrument design. Earlier helicopter experiments conducted by NAMRL and other researchers transmitted altitude information to the pilot via two tactors mounted on the upper and lower sides of the left forearm. Activation of either tactor cued the pilot to increase or decrease collective pitch in order to climb or descend (collective is controlled by the left hand). Yaw information has been presented in a similar manner, with tactors mounted on each leg, signaling the pilot to add more left or right pedal as appropriate in order to correct yaw angle.

These earlier configurations are mentioned to draw attention to the deliberate nature of the evolution of TSAS. Each of these methods was successful in improving control of the aircraft. The intuitive location and appropriate response to stimuli was effective in transmitting necessary collective and yaw signals. The current configuration has drawn upon earlier successes and has attempted to further improve the performance of the man-machine system.

Despite their success in improving pilot performance during isolated experiments, neither configuration produced an improvement in pilot Situational Awareness. Perhaps because the tactors produced only a locally appropriate response, but did not provide any intuitive spatial information, pilots could react to the tactors, but were unable to glean any global information about the state of their aircraft. By mounting the tactors around the torso and, thus surrounding an intuitive spatial anchor, TSAS in its current configuration provides information that allows the pilot to quickly and easily expand his knowledge of his surroundings and then decide on the appropriate response [Rupert et al, 1993]. This added step allows not only performance improvement, but also increased situational awareness.

2.3 Performance Measurements

In order to effectively evaluate the utility of a cockpit instrument, appropriate measures must be defined. Controller performance (and, by extension, effectiveness of TSAS) can be defined not only as how well the pilot performed the primary assigned task, but also by how well the pilot's internal picture of his environment matches the true environment, or by how large a percentage of the pilot's energy must be focused to perform the assigned task. Occasionally when evaluating new cockpit technology, existing performance measurements will fail to accurately assess the utility of a new system. When that is the case, new and more sensitive measures must be developed in order to accurately and appropriately evaluate the new system.

2.3.1 Performance Measures

Performance is simply a measure of the pilot's success in accomplishing the assigned task. It is evaluated using observable and recordable variables. Depending on the experiment, such measures could include position, velocity, and acceleration of the aircraft, time on target, reaction times, number of errors made, control movements, and even physiological measures such as heart rate or eye movements.

For tracking tasks, like the one used in this experiment, the most important variable is the difference between the actual and desired states of the aircraft. This difference is defined as the error. Often, simple characteristics of error are utilized by the researcher: maximum and minimum error, range of error, or root mean square of error. Sometimes, more complex manipulations of error can provide insight into performance. Power spectral density, histogram evaluation, and temporal analyses have all been used to highlight performance changes. The specific objective performance measures used for this experiment will be elaborated upon in the Methods section.

2.3.2 Workload

Workload is a measure of the amount of pilot effort required to perform a given task. Although seemingly simple in concept, workload can be extremely difficult to measure accurately, precisely, and with repeatable results.

Efforts to define workload began over 60 years ago and have only recently gained a wide acceptance of a common definition. Early researchers defined workload as a “multi faceted concept, primary facets being formed by three variables: demands of the flight task, pilot effort, and results” [Roscoe, 1978]. Later researchers attempted to hone the definition, but the multi dimensional nature of the model persisted, with varying degrees of emphasis on the different facets. As recently as 1984, Miller and Hart defined nine dimensions of workload: “task difficulty, time pressure, own performance, mental effort, physical effort, frustration, stress, fatigue, and activity type” [Miller and Hart, 1984].

Arguably the most widely accepted definition was introduced in 1985 when a single element was deemed most important in identifying pilot workload. Ellis and Roscoe interviewed over 350 military and airline pilots and concluded that more than 80% of respondents identified “effort” as the defining characteristic of workload. This definition can be further refined to define “mental effort” as the percent of mental capacity required to perform a given task [Roscoe, 1987].

2.3.2.1 *Techniques for Assessing Pilot Workload*

Once defined, the problem still remains to accurately and reliably quantify the level of pilot effort required to perform a given task. Many researchers have developed methods to measure workload, with varied degrees of success. These methods for measuring pilot workload can be separated into three main categories:

- Objective Measures, primarily measures of primary or secondary task performance,
- Subjective measures, essentially survey driven, and

- Physiological measures, mostly involuntary bodily responses to stress.

Each of these groups has advantages and disadvantages, as do each of the individual methods within each group. Often, the appropriate measure depends upon the assigned task, subject population, and experimental design.

Rather than present a comprehensive list of all research conducted, and every measure introduced, only the measures relevant to this experiment will be presented. First, a brief overview of the three measurement groups will be presented.

2.3.2.2 Objective Measures

As mentioned previously, the primary objective workload measurement technique is that of measuring performance of a given task. These measures assume that as task workload increases, the additional effort required will result in degraded performance. The advantage of performance measures is that, assuming they are available for measurement, they are easily quantifiable and ready for analysis using any of the aforementioned methods (RMS, mean, max/min, etc.). The main disadvantage of these measures is that they are indirect measurements of workload. Performance may be influenced by other factors, such as motivation, learning, fatigue, and arousal and may not directly reflect the pilot workload required to perform a given task [O'Donnell and Eggemeier, 1986]. With all of the potential pitfalls, careful experiment design is required to reduce the possibility of performance data corruption by other factors. Additionally, ceiling or floor effects may be seen in performance if the task is too difficult or too easy.

Often, in addition to performance of the primary task, the subject is directed to perform a secondary task in an effort to measure spare attention or excess control capacity. A decrease in secondary task performance is an indication of reduced spare attention or increased primary task workload. Secondary tasks vary in complexity, intrusiveness, and expense and are subject to the same strengths and shortcomings as primary task

performance measurements. The major detractor of the secondary task is that it intrudes upon performance of the primary task [Williges and Wierwille, 1979].

In addition to task performance measurements, sometimes esoteric and task dependent variables have been used to try and objectively assess pilot or crew workloads. Most of these studies have involved some form of time and motion study. From observed behavior, models are constructed and workload indices calculated, allowing prediction of task load for a particular task or mission. These measures have proven sensitive for their specific studies, but lack a general applicability to other tasks and are not recommended for this experiment [Gawron, 2000].

Finally, a method that has shown high sensitivity to workload is the analysis of pilot control movements, the theory holding that as a pilot works harder to perform a task, this effort will be evident in the magnitude, frequency, and nature of his control inputs. This method is quantifiable, analyzable, and non-invasive. However, it does require that control positions are available for measurement. Furthermore, once the measure is recorded, there is some debate as to which analytical methods provide the best sensitivity to workload.

2.3.2.3 Subjective Measures

Subjective measurement techniques, in the form of pilot and observer surveys or rating scales, are probably the most commonly used and reliable form of workload assessment presently available. Pilot surveys are inexpensive, easy to administer in- or post-flight, and, given proper pilot training, can prove reliable, repeatable, and sensitive. The addition of numerical scales associated with the surveys adds the capability of quantifying workload and performing more powerful statistical analyses. However, these surveys are, like all surveys, limited to rating *conscious* processes and dependent upon short-term memory. Additionally, pilots often report “perception of performance” rather than workload (in essence making the performance-workload relationship assumption mentioned earlier), therefore requiring well-defined questions and highly trained subjects.

Some researchers have used outside observers to eliminate this problem. Observers are normally better trained and knowledgeable than their experimental subjects on experimental protocols. Therefore, their observations can be valuable in quantifying pilot workload but they are obviously limited to reporting only “observed” behavior and cannot possibly report internal cognitive states [Gawron, 2000].

2.3.2.4 *Physiological Measures*

Physiological measures have the advantage over subjective reports in that they measure involuntary responses to environmental stimuli. Before the pilot can verbalize that his workload has gone up (in fact, before he is even consciously aware of the fact) the human brain’s unconscious response mechanisms are already in full swing. Pulse, blood pressure, breathing rate, and neuro-chemical responses precede conscious awareness of increased arousal. Other measurements such as head or eye movements may indicate attention during complex scanning tasks. These measurements do not require any additional pilot tasking. However, they do require specialized equipment that can be very bulky, uncomfortable, and sensitive to electromagnetic interference (EMG) or aircraft motion in the case of eye movement trackers [Wierwille and Connor, 1983].

2.3.2.5 *Common Workload Measurement Techniques*

Due to the number of workload measures cited, and the breadth of their nature, Wierwille and Connor [1983] conducted a comprehensive evaluation of 20 different workload measures to determine which measures were most effective in capturing pilot workload. They evaluated subjective opinion scales, spare mental capacity (secondary tasks), physiological measurements, eye behavior, and primary task measures during a psychomotor task with three distinct difficulty levels: low, medium, and high. Of the 20 workload measures, they found five to be the most sensitive to difficulty of task (load).

Both opinion rating scales (Cooper-Harper and WCI/TE) demonstrated significant load effects. Of the seven spare mental capacity measures, only one (time estimation standard

deviation) proved sensitive to load. Only one of the six physiological measurements (means pulse rate) was responsive to task difficulty. Of the eye behavior measures, neither demonstrated a significant load effect. Finally, of the primary task measures, only control movement reversals was shown to be sensitive to load. Of these measures, Cooper-Harper and Control Movements showed the highest correlation to task difficulty.

Cooper-Harper Rating Scale

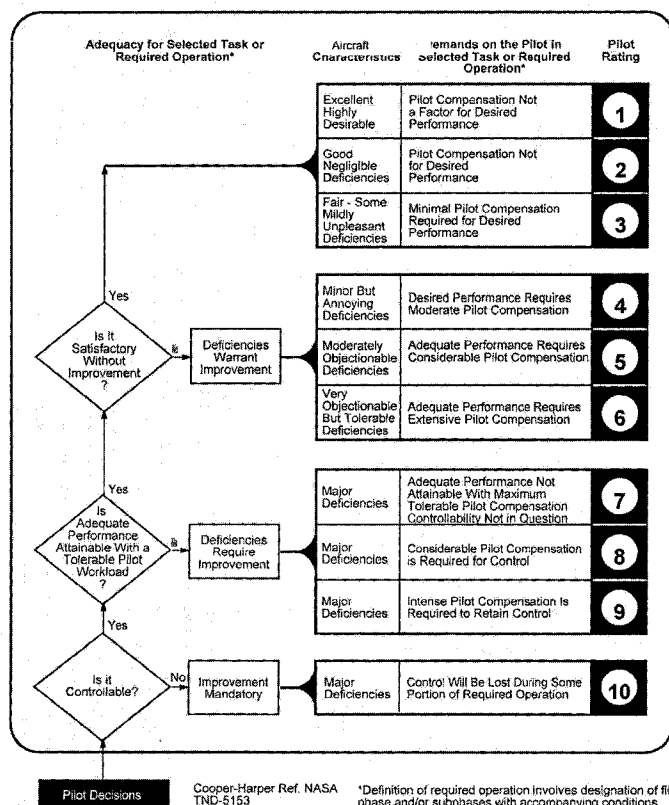


Figure 2-4 Modified Cooper-Harper Rating Scale
from Gawron, 2000.

The Cooper-Harper Rating Scale, shown in Figure 2-4, is a decision tree that uses controllability, attainable aircraft performance, and required pilot compensation to determine the overall handling qualities of an aircraft. This method of evaluation has become the gold standard in evaluation of aircraft handling qualities. Cooper-Harper requires minimum training and has been proven repeatable and sensitive to both

performance and workload. The decision tree and criteria have been adapted to reflect workload, rather than aircraft performance, but the methodology remains identical. Any shortcomings of Cooper-Harper are minor, but it does require a clear definition of desired and acceptable task performance [Gawron, 2000].

2.3.3 Situational Awareness

Situational Awareness (SA) is a measure of the agreement between an operator's knowledge of his surroundings and reality. SA may apply to the aircraft that the pilot is operating, or to external factors including other aircraft, terrain, or environmental information. Situational Awareness may also apply to air traffic controllers, machine operators, or plant monitors. Each of these professions requires that the operator maintain an accurate model of the environment. Although previously overlooked, the past 20 years have seen increased interest in the definition, measurement, and improvement of SA.

Endsley defines SA as “the perception of the elements in the environment within a volume of time and space, the comprehension of their meaning, and the projection of their status in the near future” [Endsley, 1989].

Like workload, situational awareness may be measured through performance, or through subjective or objective means. Advantages and disadvantages will be discussed for several possible measures of SA. However, a problem with using performance measures is even more striking than it is for workload measurements. The difference between a pilot's awareness of his surroundings and his ability to effectively control his environment is difficult to separate. While SA is required for successful task performance, it is not sufficient, and shortfalls in pilot abilities may be easily misinterpreted as poor SA. Therefore, this dissertation will center on only direct subjective and objective measures of SA.

2.3.3.1 China Lake Situational Awareness (CLSA)

| | |
|-----------------------|---|
| VERY GOOD 1 | Full knowledge of a/c energy state Full ability to anticipate/accommodate trends |
| GOOD 2 | Full knowledge of a/c energy state Partial ability to anticipate/accommodate trends No task shedding |
| ADEQUATE 3 | Full knowledge of a/c energy state Saturated ability to anticipate/accommodate trends Some shedding of minor tasks |
| POOR 4 | Fair knowledge of a/c energy state Saturated ability to anticipate/accommodate trends Shedding all minor tasks as well as many not essential to flight safety |
| VERY POOR 5 | Minimal knowledge of a/c energy state Oversaturated ability to anticipate/accommodate trends Shedding of all tasks not absolutely essential to flight safety |

Figure 2-5 China Lake Situational Awareness Scale
from Gawron, 2000.

The China Lake Situational Awareness scale, shown in Figure 2-5, is a subjective test designed to evaluate a pilot's self-perception of situational awareness. It is a five point rating scale based upon the Bedford Workload Scale, designed at the Naval Air Warfare Center at China Lake in 1998 to measure SA in flight.

Although the test is easy to administer and has been proven sensitive to SA, it is reliant on pilot reports that measure self-perception of SA and may not reflect the pilot's actual awareness of his surrounding. Also, the survey nature of this test requires that it not be administered during attention critical tasks (the most important time to measure SA), resulting in a compromise of safety [Gawron, 2000]. Postflight questionnaires, although safe and unobtrusive, rely upon pilots' recall of their own SA during the previous trial.

2.3.3.2 Situational Awareness Subjective Workload Dominance (SWORD)

The Situational Awareness Subjective Workload Dominance test uses judgment matrices to compare SA between task trials of different conditions. SWORD uses a numbered system to conduct comprehensive pairwise comparisons of all tasks completed. Geometric means can be determined between trials to determine important factors influencing SA. A typical SWORD survey is shown in Figure 2.6.

SWORD allows an objective and mathematical approach to defining differences in SA between trials. Again, however, SWORD is a subjective survey and is subject to pilot variability and recall problems. It has also been noted that SWORD is a relative measure rather than an *absolute* measure, limiting general application of results. Finally, since a pairwise comparison is required between *all* trials, the number of comparisons required for N trials is N factorial. Therefore experiments with more than five conditions can present a prohibitively high number of questions and normally preclude the use of SWORD.

| | Absolute | Very Strng | Strng | Weak | Equal | Weak | Strng | Very Strng | Absolute | |
|--------|----------|---------------|-------|------|-------|------|-------|---------------|----------|--------|
| Task A | | | | | | | | | | Task B |

Figure 2-6 Subjective WORKload Dominance Pilot Survey

2.3.3.3 Perceptual Cue Rating

Perceptual Cue Rating (PCR) is a generalized revision of the existing ADS-33-PRF *Visual Cue Rating*. Due to the addition of tactile information, this generalization was necessary. The PCR rating, shown in Figure 2-7 uses the same 5-point scale as the ADS-33E-PRF Visual Cue Rating scale but the pilots are asked to rate the quality of the overall visual *and* tactile cues. Pilots are directed to rate the quality of this information available

for attitude, and horizontal translation for both Outside Information (VFR Image) and Instruments (Flight Director, Artificial Horizon, and TSAS) from good to poor. This rating can be compared “inter-“ and “intra-trial” as well as “inter-“ and “intra-subject.”

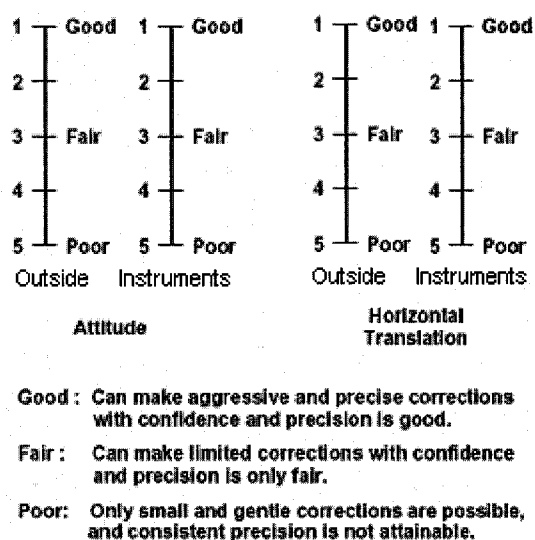


Figure 2-7 Perceptual Cue Rating

2.4 Pilot Models

Duane McRuer presciently noted that every advance in control systems theory has been accompanied immediately by an attempt to apply that advance to understanding the behavior of the human controller [McRuer, 1980]. This claim has certainly proved true, as the following overview will show. The review will begin with older models, which, although not used directly in this research, establish a solid foundation of pilot model architecture and provide valuable insight into pilot strategy. The review will conclude with more recent models that have a more direct impact on the structure and function of our model.

During the late 1950s and through the 1960s and 70s, McRuer and others developed a series of analytical models of the human operator, varying in their complexity and their

ability to capture the important aspects of manual control. Five of these models will be discussed.

2.4.1 Verbal Analytical Model

The earliest and simplest model is often referred to as the Analytical-Verbal model. The basic heuristic structure of the model is shown in Figure 2.8. This model is a single-loop feedback system (ignoring proprioceptive feedback loops internal to the pilot) that utilizes compensatory tracking, which means that the forcing function appears random and that no attempt is made to predict the future forcing function values.

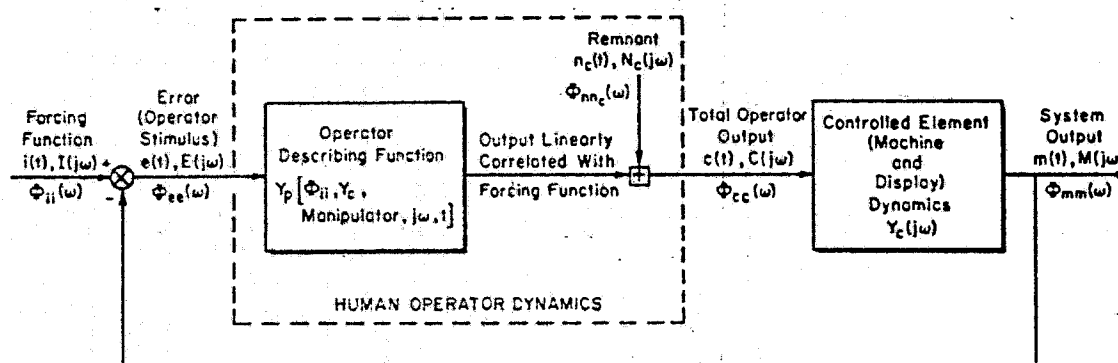


Figure 2-8 Verbal Analytical Model

from McRuer et al, 1967.

The pilot model shown can be described as quasi-linear, defining the human operator as a linear describing function (DF) plus a nonlinear remnant. The linear controlled element (aircraft) is described by its transfer function $Y_c(j\omega)$. The more complex human model requires two terms, the random input describing function Y_p (dependent upon the power spectral density of the forcing function Φ_{ii} , the transfer function Y_c , the frequency of the input ω , and the time t) and the remnant, $n_c(t)$.

By comparing results of previously conducted experiments, McRuer was able to create a general structure for the pilot describing function. The describing Function was found to

be sufficient for a majority of the research covered if a set of “adjustment rules” was applied in certain circumstances.

$$Y_p = K_p e^{-j\omega\tau} \frac{T_L j\omega + 1}{T_I j\omega + 1} \frac{\operatorname{erfc}\left[\frac{a_T}{\sqrt{2}\sigma_T}\right]}{\left[\left(\frac{j\omega}{\omega_N}\right)^2 + \frac{2\zeta_N j\omega}{\omega_N} + 1\right] (T_{N_1} j\omega + 1)} \quad \text{Eq. 2.1}$$

The formula above includes a gain, K_p , a reaction time constant τ , an equalization characteristic $\frac{T_L j\omega + 1}{T_I j\omega + 1}$, an indifference threshold describing function $\operatorname{erfc}\left[\frac{a_T}{\sqrt{2}\sigma_T}\right]$, and a

third order neuromuscular system characteristic $\left\{ \left[\left(\frac{j\omega}{\omega_N}\right)^2 + \frac{2\zeta_N j\omega}{\omega_N} + 1 \right] (T_{N_1} j\omega + 1) \right\}^{-1}$.

The exponential time delay term represents reaction, processing, and neuromuscular delays. For the majority of the experiments studied, the input signals were large enough that the threshold value was approximately equal to the RMS input of the threshold characteristic, allowing the indifference threshold term to be ignored. Additionally, at frequencies below ω_N , the neuromuscular effect could be simplified to a low frequency, first order lag term $(T_{N_1} j\omega + 1)$. The resulting simplified describing function is:

$$Y_p = \frac{K_p e^{-j\omega\tau} (T_L j\omega + 1)}{(T_{N_1} j\omega + 1)(T_I j\omega + 1)} \quad \text{Eq. 2.2}$$

The pilot controller then adjusts the parameters of the describing function to make the system stable with small error. McRuer and his collaborators theorized that once the basic response structure is established, the pilot adjusts the parameters using the following priorities:

- Stability. Make the overall man-machine system stable.
- Low frequency performance: A low frequency lag is generated when it could improve low frequency characteristics and it will not destabilize the system.
- Lead generation: Lead is generated to try and improve high frequency performance.
- Parameter adjustment: The operator adjusts all model parameters according to an optimization algorithm, normally to minimize RMS error.
- Invariance of the man-machine system: Once the initial adjustments are made, any change in the controlled element gains is offset by the operator gain, keeping the crossover frequency invariant.

2.4.1.1 Sources of Remnant

The component of pilot response not captured by the linear model is called the nonlinear remnant. The nature of the remnant signal can best be identified by looking at the Power Spectral Density (PSD) of the operator's output in comparison to the PSD of the forcing function. If the forcing function were comprised of a finite number of distinct frequency sinusoidal signals, N , the PSD of the forcing function would show non-zero values at those discrete frequencies, with zero power at all other frequencies. If the operator were a linear, constant gain compensator, his output would have non-zero peaks at the same frequencies as the forcing function, with only magnitudes differing, and zero power at all other frequencies. Nonlinearities or variable-rate sampling would add an infinite number of non-zero peaks, with frequency values related to the multiples of forcing function frequencies. A fluctuation in the controller characteristics would inject a continuous PSD signal into the controller's output. Finally, if the pilot was to initiate a dither into the controller (stirring the pot), this would add another PSD signal to the output, possibly completely unrelated to the PSD of the forcing function [McRuer and Krendel, 1978].

The presence of remnant has been explained in three possible ways:

- Random noise superimposed on the operator's linear output,
- Variant operator behavior, i.e. describing function changes during a run, or
- Nonlinear anticipation superimposed on linear output.

This general model proved to agree fairly well with documented data, and led to the development of the crossover model, a simple but flexible model that captures compensatory task pilot performance exceptionally well, particularly in the range of frequencies near the crossover frequency.

2.4.2 Crossover Model

The basic structure of the Crossover Model is shown in Figure 2.9. Notice that the pure time delay of the analytical model is present, as is a neuromuscular transfer function. However, the pilot-tracking group is expanded to include compensators ranging from pure integration to proportional, rate, and acceleration. It also includes processing, equalization, and filtering elements absent in the previous model. Future models would include additional compensators as well.

According to the model, the pilot operator selects the appropriate compensator(s) to achieve an overall closed-loop gain (including pilot and vehicle dynamics) equivalent to:

$$G = Y_{Pilot} Y_C = \frac{\omega_c e^{-s\tau}}{s} \quad \text{Eq. 2.3}$$

where ω_c is the crossover frequency

and τ is the equivalent delay

In other words, regardless of the plant dynamics, the pilot will add series dynamics resulting in a forward gain, pure integrator system with a pure time delay, with a -20 dB per decade rolloff at frequencies in the region of crossover (ω_c) [McRuer, 1980].

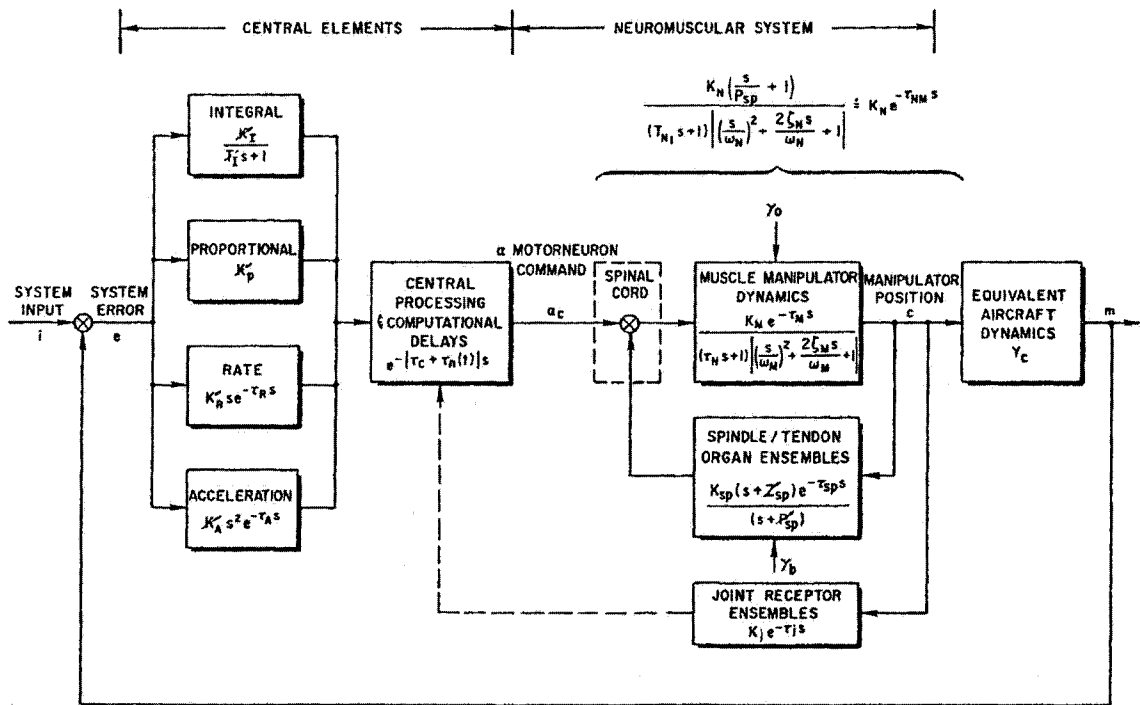


Figure 2-9 Crossover Model
from McRuer, 1973.

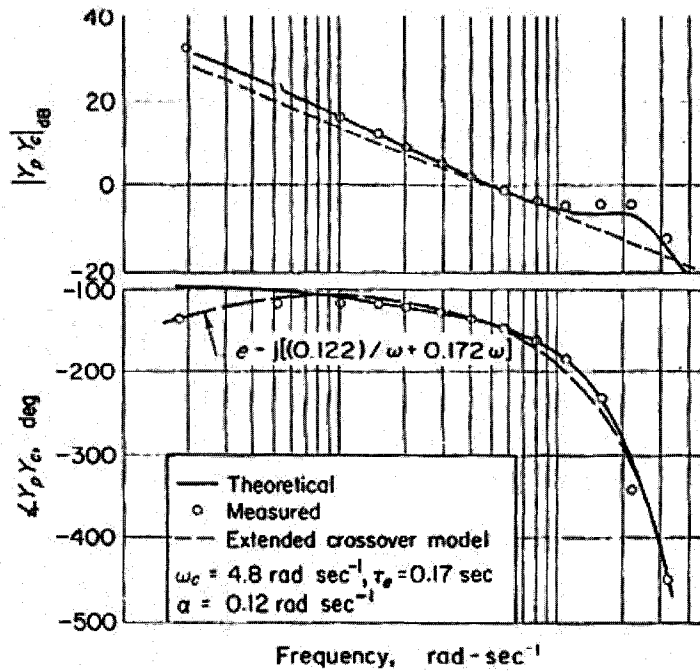


Figure 2-10 Crossover and Extended Crossover Model
from McRuer, 1973.

It should be noted that although the pilot will use whichever internal compensator is necessary to achieve crossover model performance, the pilot cannot arbitrarily choose any compensator that he desires. There are additional time delay penalties associated with the generation of rate and acceleration signals. The internal calculation of rates based upon observation takes time to compute, resulting in increased net delays. This delay can result in smaller phase margins and/or lower bandwidth, in this case, a lower ω_c .

As its name implies, the crossover model shows good agreement between theoretical and experimental values, particularly in the crossover region. However, at frequencies above or below ω_c , the model is slightly less accurate in magnitude, and shows particularly large inaccuracies in low frequency phase behavior. This phenomenon is referred to as “phase droop.” Additionally, there exists a small neuromuscular peak near 20 radians per second. This peak is believed to be due to physical limitations of the pilot controller. To correct these deficiencies, the Crossover Model was modified, creating the Extended Crossover Model and later the Precision Model, which accurately reproduced a broader frequency range than did the earlier Crossover Model, but also caused increased complexity and additional parameters [McRuer 1980]. The two additional models add value, but little additional insight into pilot strategies and model structure and therefore will not be discussed in detail.

2.4.3 Multi-Loop Model and Scanning

As the single loop model grew in complexity and in accuracy, researchers were also tackling the much more complex problem of modeling pilot performance during multiple task assignments or in multiple axes. Numerous structures of multi-loop feedback have been developed. Many of the multi-axis tracking experiments performed involved simple tracking tasks using two or more single-axis display instruments separated by a significant angle on the display panel. While those experiments proved valuable, their applicability to this research is limited [Levinson and Elkind, 1967; Weir and Klein, 1970; McRuer and Schmidt 1990].

Despite their collective limited applicability, one of the discoveries of multi-axis experiments that undoubtedly *is* applicable is the characterization of pilot “scanning.” When information is presented in more than one location, the operator is forced to divide his attention among the available instruments; with unavoidable losses occurring while his scan is between instruments [McRuer and Schmidt, 1990; Allen et al, 1970].

Several transcendent truths were discovered during these experiments:

- Pilots will chose the instruments or displays that allow control loops to be closed with minimum scanning and control effort,
- A stationary scanning strategy evolves for a given task/ instrument array,
- Pilot control is more continuous than simple scanning would suggest, implying a reconstruction methodology, and

Finally, and most importantly:

- The primary effects of scanning are to reduce the pilot gain and increase the remnant signal in the scanned channels.

This final effect, “increase in remnant,” exposes an area of potential benefit of continuous error display via tactile rather than visual means. By providing information via a separate

modality, and providing that signal on a continuous basis, the deficiencies from scanning are reduced or eliminated. This elimination could lead to higher pilot loop gain and higher bandwidth, resulting in improved performance and decreased workload.

2.4.4 Optimal Control Model (OCM)

Up to this point, all of the models discussed have relied upon “classical” control theory in developing transfer functions that accurately represent pilot performance. Even the multi-axis models involved separate, completely decoupled, feedback loops. Such a structure has obvious practical limits and falls short of capturing true pilot reconstruction and performance, particularly during complex or multiloop tasks.

In an effort to advance pilot models and to improve their ease of application, Kleinman et al [1970] applied modern optimal control theory to the estimation and description of human control behavior. The ultimate result of this effort was the development of the Optimal Control Model (OCM). The OCM operates on the assumption that a human controller behaves optimally, adjusting pilot compensation for given vehicle and task properties (one of McRuer’s original assertions).

The OCM models the human operator as a combination Kalman filter estimator and linear quadratic Gaussian stochastic controller. The system assumes the pilot operates to minimize a quadratic cost function in the presence of noises and disturbances. The use of the noisy Kalman Filter estimator implies imperfect and adaptable estimation of system states using available measured (either displayed or sensed directly by the pilot) output signals.

Construction of the OCM involves solution of the quadratic cost function:

$$J_{OCM} = E_{\infty} \{ \mathbf{y}^T \mathbf{Q}_y \mathbf{y} + \mathbf{u}^T \mathbf{R} \mathbf{u} + \dot{\mathbf{u}}^T \mathbf{F} \dot{\mathbf{u}} \} \quad \text{Eq. 2.4}$$

where Q , R , and F represent the costs associated with plant outputs, pilot controls, and control rates, respectively.

From an execution standpoint, the model allows easy, intuitive manipulation of controlled element dynamics, display signal noise, observations noise, and neuromotor noise. The overall linear OCM of a man machine system is shown in Figure 2.11.

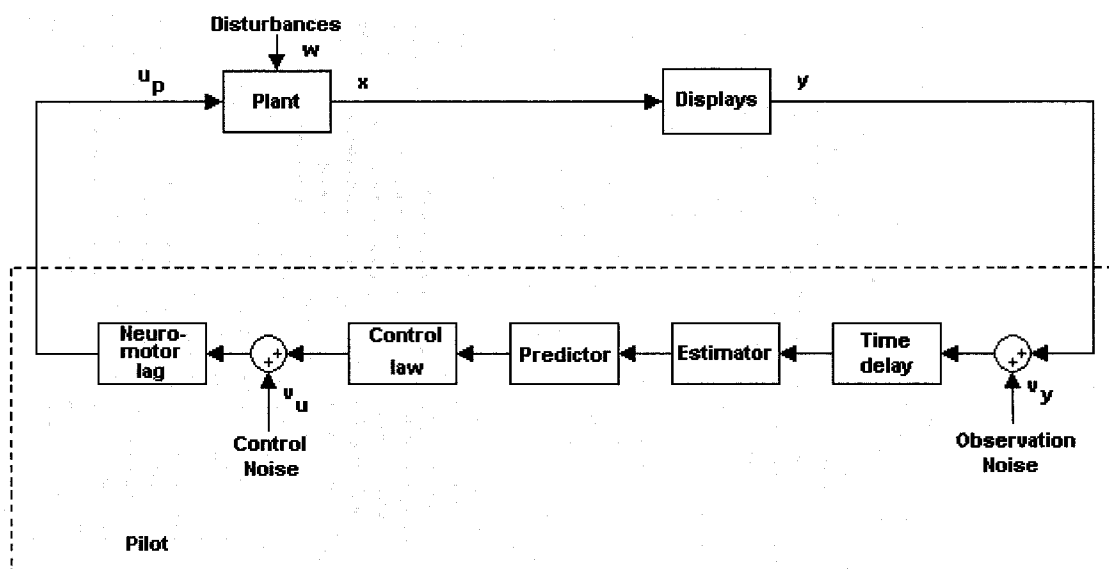


Figure 2-11 Optimal Control Model
adapted from Kleinman et al, 1970.

Note the presence of a neuromotor lag term and pilot delay, as before. However, the addition of the Kalman Filter estimator and predictor add potential pilot strategy and reconstruction capability. The control law is an optimal gain that uses a reconstruction of the entire pilot-plant system, including physical and intellectual limitations of the pilot.

The OCM was found to be a satisfactory model of pilot performance in a variety of control tasks. This model captures many of the important characteristics of pilot performance. The OCM allows for multi-axis operation, either coupled or uncoupled, and considers the adaptive nature of human operator performance while also including

time delays and nonlinear remnant. Properly designed, the model captures time response and frequency response characteristics of manual control. Physical corollaries are evident in motor noise, observation noise, neuromuscular lag and effective time delays.

2.4.5 Modified Optimal Control Model (MOCM)

In 1992, Davidson and Schmidt developed their Modified Optimal Control Model (MOCM). Shown in Figure 2-12, the MOCM retains all of the characteristics of the OCM, including the control rate in the cost function, an LQR solution for pilot gains, and a Kalman estimator. However, the MOCM structure allows direct calculation of system and pilot transfer functions and exploits many of the functions available in modern control systems software. The basic structure is similar to the OCM, with minor differences:

- Inclusion of a new time delay after the neuromotor lag, rather than after observation,
- Use of the KF-LQG structure including command signal feedback.

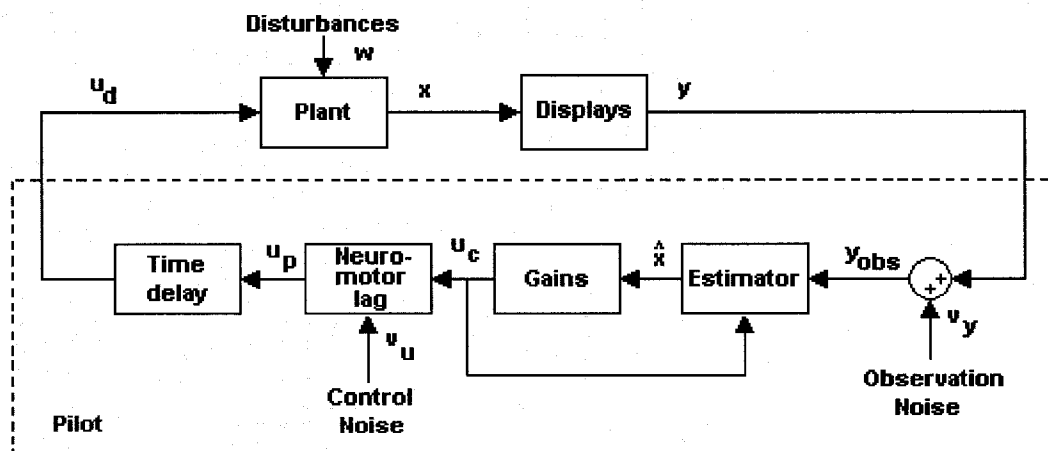


Figure 2-12 Modified Optimal Control Model
from Davidson and Schmidt, 1992.

The MOCM structure closely follows the OCM structure, utilizing optimal feedback, neuromotor lag, and a pure delay. The system is described by Equation 2.5

$$\frac{d}{dt} \begin{Bmatrix} x \\ x_d \\ u_p \end{Bmatrix} = \begin{bmatrix} A & BC_d & B \\ 0 & A_d & B_d \\ 0 & 0 & -\tau_\eta^{-1} \end{bmatrix} \begin{Bmatrix} x \\ x_d \\ u_p \end{Bmatrix} + \begin{bmatrix} 0 \\ 0 \\ \tau_\eta^{-1} \end{bmatrix} u_c + \begin{bmatrix} E & 0 \\ 0 & 0 \\ 0 & \tau_\eta^{-1} \end{bmatrix} \begin{Bmatrix} W \\ v_u \end{Bmatrix}$$

$$y_{obs} = \begin{bmatrix} C & DC_d & D \end{bmatrix} \begin{Bmatrix} x \\ x_d \\ u_p \end{Bmatrix} + v_y$$
Eq. 2.5

where A, B, C , and D define the plant dynamics

A_d, B_d, C_d and D_d define the delay states

u_c is the command signal

W is the magnitude of disturbance, w

τ_η is the neuromotor lag

v_u is the neuromuscular noise

and v_y is the observation noise.

Equation 2.5 can be simplified to

$$\dot{\chi} = A_1 \chi + B_1 u_c + E_1 w_1$$

$$y_{obs} = C_1 \chi + v_y$$
Eq. 2.6

The Algebraic Riccati Equation (ARE) is employed to find both the optimal feedback gain, ℓ_1 , and the estimator gain, F .

$$\frac{d}{dt} \begin{Bmatrix} \chi \\ \hat{\chi} \end{Bmatrix} = \begin{bmatrix} A_1 & -B_1 \ell_1 \\ FC_1 & A_1 - B_1 \ell_1 - FC_1 \end{bmatrix} \begin{Bmatrix} \chi \\ \hat{\chi} \end{Bmatrix} + \begin{bmatrix} E_1 & 0 \\ 0 & F \end{bmatrix} \begin{Bmatrix} w_1 \\ v_y \end{Bmatrix}$$

$$\begin{Bmatrix} y_{obs} \\ \delta \end{Bmatrix} = \begin{bmatrix} C_1 & 0 \\ C_\delta & 0 \end{bmatrix} \begin{Bmatrix} \chi \\ \hat{\chi} \end{Bmatrix}$$
Eq. 2.7

Equation 2.7 represents the complete, closed-loop model of the pilot and plant, using displayed variables to reconstruct the estimated states. The “input” to the system is found in the disturbance signal and the observation noise. The outputs of the system are the pilot observed states and the control signal from the pilot to the plant.

In addition to the basic structure of the model, Davidson and Schmidt laid out an iterative procedure of determining model parameters utilizing state magnitudes and their relationship to signal noise.

The intuitive nature of this model and the iterative solution procedure make it ideal for application to this dissertation, with some modification made to account for significance of the control rate, nested loop feedback, final state reconstruction, the presence of noise, and nonlinear attributes of control response. The specific changes to the model will be discussed in depth in the methods and results section.

SECTION 3 METHODS

This section will outline the basic research hardware, software, protocols and procedures utilized during this investigation. A brief listing of conventions utilized in this research will begin the section, followed by pilot trials and then experimental design hardware and software. Next the test subject population and trial protocols will be discussed. A discussion of all data analysis protocols will follow. Finally, this section will discuss the steps taken to develop the new visual-tactile pilot model.

3.1 Conventions

Throughout this dissertation, the aircraft (simulator) axes will be defined using conventional aircraft axis definitions. As shown in Figure 3.1, the x-axis or longitudinal axis runs through the tail and nose of the aircraft, with forward being positive. A right roll angle about the x-axis is considered positive. The y-axis or lateral axis runs from left to right, with right being positive. An upward pitch about the y-axis is considered to be positive.

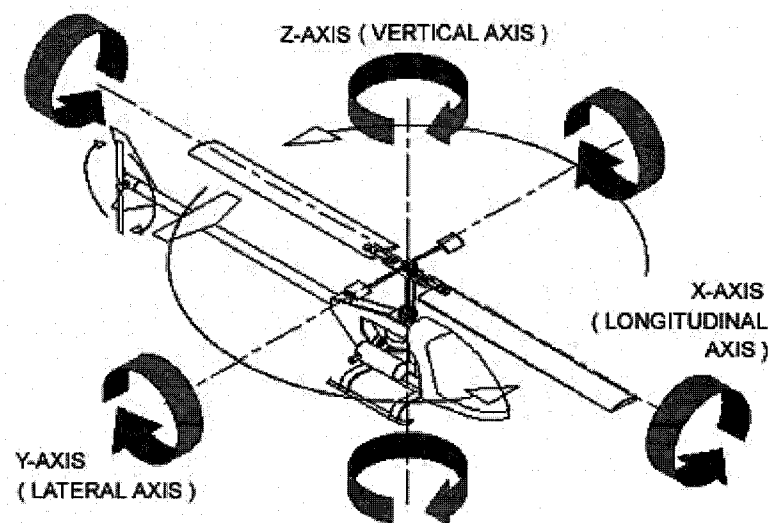


Figure 3-1 Aircraft Axis Conventions

The terms “aileron” and “elevator” refer to control movements in the lateral and longitudinal axes respectively. Although helicopters do not possess either of these control surfaces, the terms “lateral cyclic” and “longitudinal cyclic” become cumbersome. Aileron and elevator can be assumed to mean lateral and longitudinal cyclic.

Finally, all subjects are referred to as “he” or “him.” Though coincidentally, all subjects were male, such reference is used for convenience and consistency, and is not to be taken as deliberately exclusionary.

3.2 Pilot Study

The mature status of the TSAS vest and NAMRL’s extensive experience with the vest provide ample data from previous flight tests. Use of this data eliminated the necessity of long iterations of pilot testing and evaluation. The bulk of the data used in constructing a study plan was recorded in Ottawa, Canada during July and August of 2003, in a collaborative effort between ODU, NAMRL, Defense Research and Development Canada (DRDC) and the National Research Council – Flight Research Laboratory (NRC-FRL) [Craig et al 2004, Jennings et al 2004].

The cited experiment involved the flight evaluation of the TSAS vest in improving performance during two distinct tasks, a high-hover task that provided meager visual cues, and a visually saturated simulated shipboard landing task in which pilots were directed to track a moving visual target in two axes. Both tasks were performed with and without TSAS, in both good and degraded visual environments. Although both sets of data were usefully mined during the design of this experiment, the high hover task was more closely related to this research. Therefore, only the high hover task will be discussed at length.

3.2.1 High Hover Task

For the high hover task, a Bell 205 was flown by a safety pilot to a point over the field, 150 feet above ground level, with minimal visual cues available in the pilot's visual field. Once the test subject was comfortable, he was given control of the aircraft and directed to maintain a stable position over the ground in longitudinal (fore-aft), lateral (side-to-side), and vertical axes. The trial began when the subject pressed a designated button on the collective and ended after a three-minute trial duration.

Each subject performed the trial under good and degraded visual environments with and without TSAS. For the flight experiment, the degraded environment was simulated using ANVIS 9 Night Vision Devices (NVDs) that were fitted with broad spectrum reflective/absorptive filters, which had the effect of allowing less than 0.000 000 1% of incident light to reach the NVD sensors.

The TSAS signal displayed to the pilot was based upon three concentric cylinders, centered on the desired hover point. Cylinders, rather than spheres, were used to maintain the intuitive nature of the TSAS system, with the pneumatic tactor array providing horizontal drift information, while the electromagnetic tactors delivered the uncoupled vertical error signal to the pilots.

Utilizing three distinct error zones, if the pilot maintained his position inside the smallest cylinder, he would receive no correction information from the TSAS. As the predicted position drifted outside the first cylinder, into the second, a low amplitude sensation was delivered, notifying the pilot that he had drifted away from the desired position and needed to move in the direction opposite the tactile stimulus. As the position error drifted further, the signal amplitude was increased to medium, and then to high. The dimensions of the error cylinders were set at 10, 20, and 40 feet in the horizontal axes, and 5, 10, and 20 feet in the vertical axis.

3.2.1.1 Pilot Trial Results

The most profound validation of the efficacy of the TSAS can be found in analysis of the root mean square error of the aircraft position. Figure 3.2 shows the results of the pilot trials. With the benefit of TSAS, there is a clear performance improvement in the X, Y, and Z-axes. This performance was most dramatic during Degraded Visual Environments (DVE), when visual cues were worst and pilot performance suffered the most, but the improving trend was present for Good Visual Environment (GVE) trials as well.

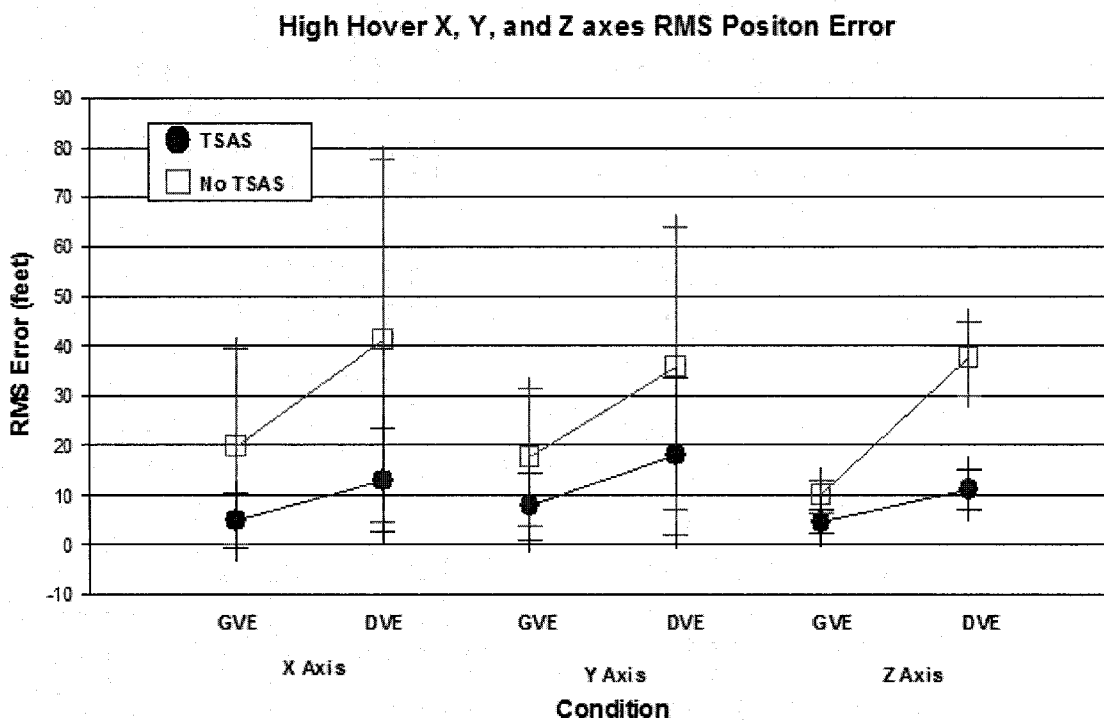


Figure 3-2 High Hover RMS Error in X, Y, and Z Axes

Most control experiments would anticipate a concurrent workload increase associated with the improved performance; “Performance has a price.” However, as Figure 3.3 shows, there was no significant change in pilot workload with the added benefit of TSAS. This fact can be attributed to one of two things. One possibility is that the workload measures employed are simply not sensitive enough to measure the small changes in pilot workload associated with TSAS. A second possibility is that TSAS, by employing the

previously untapped tactile modality, can provide intuitive information to the pilot without increasing cortical demand and, therefore, provide performance improvement without increasing pilot mental workload.

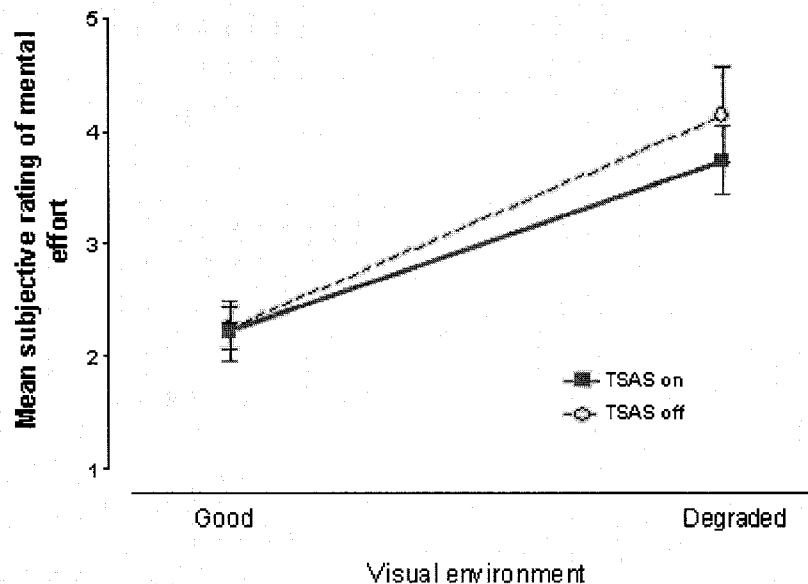


Figure 3-3 Pilot Mental Workload vs. Condition

Note that workload does increase significantly for the Degraded Visual Environment when compared to the GVE. This fact suggests that the measure itself is sensitive to workload changes, but that TSAS doesn't increase pilot mental workload.

The pilot trials revealed that the TSAS vest is an effective instrument in improving pilot performance during high hover tasks. Additionally, the results showed that the protocol followed in the pilot trials produced performance changes due to both visual and tactile presentation conditions. A similar experiment, run on the simulator, should provide adequate data to construct and validate a pilot model of hover performance. To address the workload question, new measures will be employed and evaluated during this experiment in an effort to prove the utility of TSAS and confirm the unchanged pilot workload.

3.3 Experimental Hardware and Software

The experimental data for this research was conducted using NAMRL's T-34 Helicopter Simulator, a PC based cockpit simulator with helicopter like controls (see Figure 3-2). Simulation was accomplished using off-the-shelf software including VegaSim for the visual simulation, C++ for the simulation dynamics, and LabView for the virtual cockpit instruments. The system used the flight ready TSAS driver box and a portable compressed air tank to drive the TSAS vest.



Figure 3-4 NAMRL T-34 Simulator

The original configuration of the T-34 simulator used two computers. The “simulator” computer received input information from the cockpit controls, and used VegaSim software and a C++ driving script to define, compute, and present aircraft dynamics via a single large monitor, shown in Figure 3-4. In addition to visual presentation, this computer provided position, velocity, and attitude information to the second, “controller” computer, which used a LabView script to simulate visual pilot instruments via two smaller screens, presented as shown in Figure 3-5. The controller computer provided information to the TSAS driver hardware, the small box to the left of the two small

instrument displays. The driver then presented information to the TSAS valve block that routed air to the appropriate pneumatic factor.

Despite the proven utility of this simulator, several on-site shortcomings, including the inability to manipulate plant dynamics, unsuitability of existing “instrument” displays, and the lack of recordable variables, necessitated revision of the existing system.

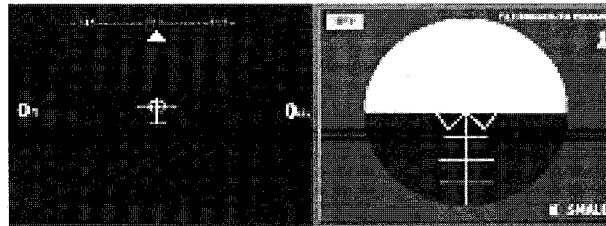


Figure 3-5 Virtual Instrument Display

3.3.1 Revised T-34 Simulator System

The plant dynamics of the existing system centered on a nonlinear computational fluid dynamics model which failed to meet the exact requirements of this experiment. Due to the lack of an appropriate C++ compiler on site, NAMRL programmers provided a new stripped down core program that drew the appropriate on-screen scene based upon externally supplied position and attitude. This “dummy” system allowed total flexibility in manipulating plant dynamics in all axes. A complete listing of the simulation code is available in Appendix A-1.

The “instrument” displays of the controller computer were modified using LabView software provided by NAMRL. The flight director, which had previously included velocity and acceleration information was stripped down to provide only position information. This modification was done to provide an input analogous to the TSAS and allow for an apples-to-apples comparison. Additionally, the artificial horizon gauge was moved to the extreme right of the visual field as shown in Figure 3-6, minimizing parafoveal reception of information between instruments.

Note the visual field present, the high quality drift cues available in the y-axis and the relatively poor quality cues in the x-axis. This difference in available information will lead to dramatically different performance between axes.

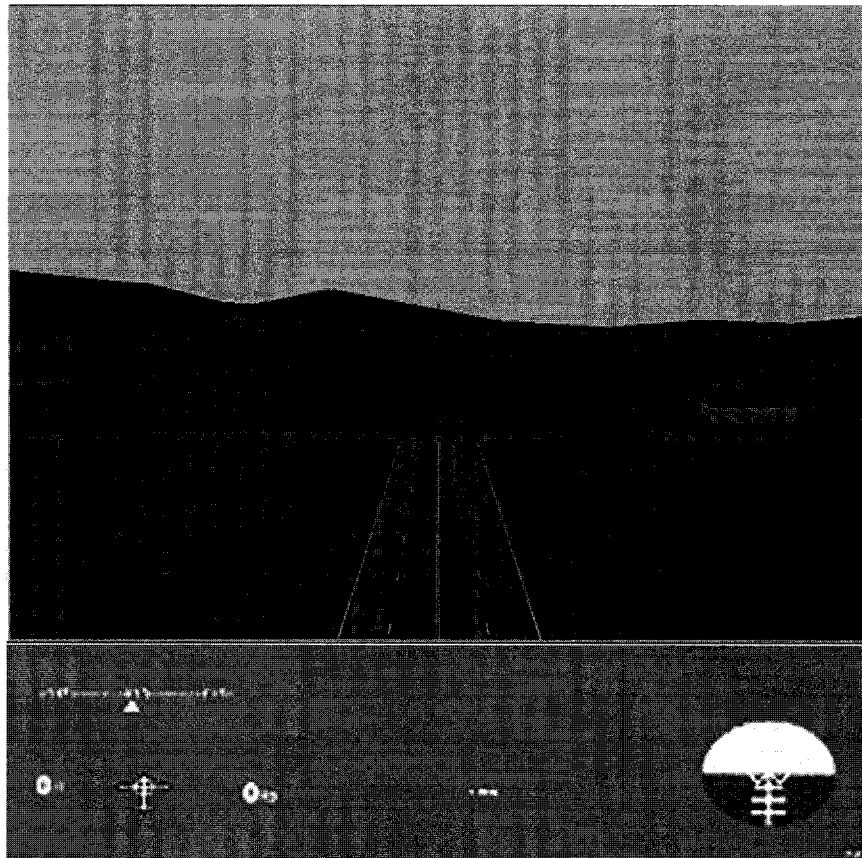


Figure 3-6 Visual Display and Modified VI Panel

Under the revised system, all plant dynamics were computed and recorded on a third “operator” computer. The use of a stand-alone operator, driven by available LabView software, provided the flexibility to achieve desired plant dynamics without costly and time consuming off-site rewrites. Additionally, system disturbances could be computed off-line and injected into the experiments in real time, allowing for repeatable results with the proper spatial and temporal characteristics. As a final benefit, the additional computer easily stored all generated and recorded data, facilitating nearly real time analysis of both pilot trials and final experiment data.

The “operator” received inputs from the flight controls, calculated the resulting dynamic changes, and provided the processed data to both the simulator and the controller computers and subsequently to the TSAS computer. The data stream schematic of the new system is shown in Figure 3-7.

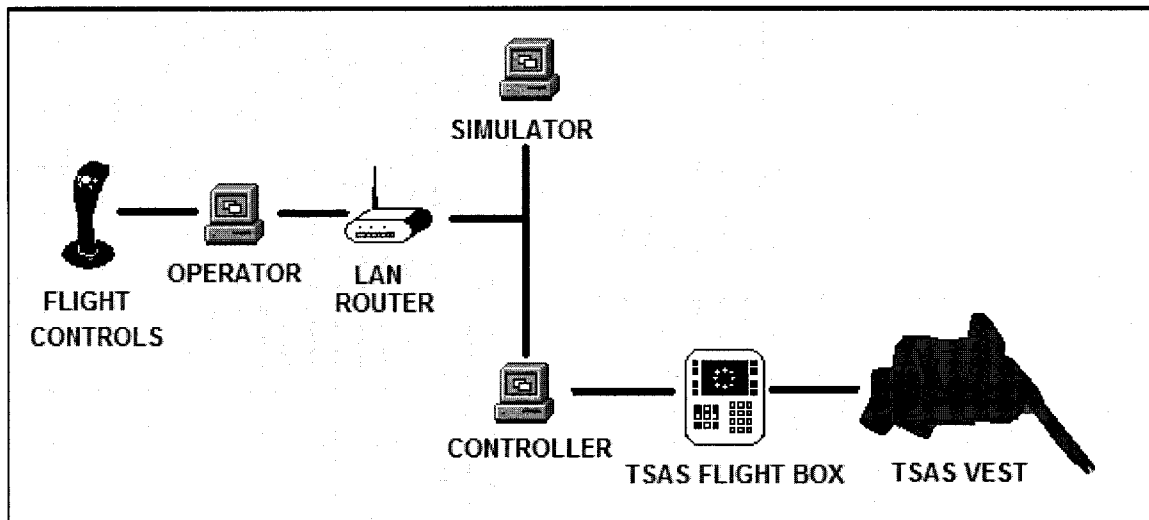


Figure 3-7 Revised T-34 Simulator Data Stream

Additional minor hardware changes were necessary to accommodate the new, three-computer configuration. A new joystick was required due to compatibility issues with the previously utilized controller. A Logitech Wingman, 11-button joystick was found to be compatible and commercially available. The off-the-shelf gaming device was disassembled and mounted into the existing simulator configuration. The interface was accomplished through existing USB connections directly into the “operator” computer.

For the TSAS, a compressed air source was required to drive the pneumatic factors. Compressed air was available on site. However, lack of an appropriate adapter led to the decision to use refillable SCUBA bottles as the sole air source. Although inert gas could have been used, air was more easily acquired. An electric compressor normally provides

the compressed air, but the additional noise created by the compressor was deemed too disruptive both to the test subjects and the other students in the lab.

3.3.2 Plant Dynamics

The plant dynamics were constructed to represent realistic helicopter dynamics, but maintain linear behavior throughout the full range of attitudes and positions. The plant was modeled using a rigid rotor-body system whose attitude was controlled via cyclic inputs. The pitch and roll inputs of the cyclic created a change in the attitude of the helicopter rotor disk. The attitude of the rotor disk in turn acted to create lateral or longitudinal forces acting on the mass of the helicopter, resulting in acceleration in the y and x-axes. The system was completely de-coupled between axes.

The pitch and roll of the system behaved like an underdamped stable pendulum, returning to zero (with mild overshoots) when the cyclic input was removed. The equations of motion in the x and y axes are completely analogous so only the x-axis equations will be presented. The basic equation governing the pitch of aircraft was:

$$\ddot{\theta} = \frac{1}{I_{xx}} (K_p C_\theta - K_d \dot{\theta} - \ell W \theta) \quad \text{Eq. 3.1}$$

where θ is the pitch angle (in radians),

K_x are constants,

C_θ is the cyclic input position (in unitless dimension),

ℓ is the equivalent length of the pendulum (in meters),

W is the equivalent weight of the pendulum (in Newtons),

and I is the moment of inertia (in kg meters²).

The pitch equation simplifies to:

$$\theta \left(s^2 + \frac{K_p}{I_{XX}} s + \frac{\ell W}{I_{XX}} \right) = \frac{K_p}{I_{XX}} C_\theta \quad \text{Eq. 3.2}$$

To keep the model development intuitive, the equation was further simplified to:

$$\theta = \frac{K_\theta}{s^2 + 2\zeta\omega_\theta s + \omega_\theta^2} C_\theta \quad \text{Eq. 3.3}$$

where ω is the natural frequency (in radians per second) and $\omega = \sqrt{\frac{\ell W}{I_{XX}}}$,

and ζ is the damping coefficient (unitless) and $\zeta = \frac{K_p}{2\sqrt{I_{XX}\ell W}}$.

The pitch to longitudinal velocity equation relates the thrust of the aircraft to the acceleration:

$$\ddot{x}m = T\theta - \dot{x}v_x \quad \text{Eq. 3.4}$$

where m is the mass of the aircraft (in kg),

v_x is the velocity damping constant (in kg/sec),

and T is the thrust (in Newtons).

This equation can be rewritten as:

$$x = \frac{\frac{T}{m}}{s^2 + s\frac{v_x}{m}} \theta \quad \text{Eq. 3.5}$$

where $\frac{T}{m}$ is equal to the gravitational constant g (in a hover),

and $\frac{v_x}{m}$ is simplified to V_x .

The roll/lateral dynamics follow an equivalent relationship, although the gains and natural frequencies were deliberately set at different values.

The new, complete dynamic equation can be written in matrix form as:

$$\frac{d}{dt} \begin{bmatrix} \dot{x} \\ x \\ \dot{\theta} \\ \theta \\ \dot{y} \\ y \\ \dot{\phi} \\ \phi \end{bmatrix} = \begin{bmatrix} -V_x & 0 & 0 & g & 0 & 0 & 0 & 0 \\ 1 & 0 & 0 & 0 & 0 & 0 & 0 & 0 \\ 0 & 0 & -2\zeta_\theta\omega_\theta & -\omega_\theta^2 & 0 & 0 & 0 & 0 \\ 0 & 0 & 1 & 0 & 0 & 0 & 0 & 0 \\ 0 & 0 & 0 & 0 & -V_y & 0 & 0 & g \\ 0 & 0 & 0 & 0 & 1 & 0 & 0 & 0 \\ 0 & 0 & 0 & 0 & 0 & 0 & -2\zeta_\phi\omega_\phi & -\omega_\phi^2 \\ 0 & 0 & 0 & 0 & 0 & 0 & 1 & 0 \end{bmatrix} \begin{bmatrix} \dot{x} \\ x \\ \dot{\theta} \\ \theta \\ \dot{y} \\ y \\ \dot{\phi} \\ \phi \end{bmatrix} + \begin{bmatrix} 0 & 0 \\ 0 & 0 \\ K_\theta & 0 \\ 0 & 0 \\ 0 & 0 \\ 0 & 0 \\ 0 & K_\phi \\ 0 & 0 \end{bmatrix} \begin{bmatrix} C_\theta \\ C_\phi \end{bmatrix} + \begin{bmatrix} 0 & 0 \\ 1 & 0 \\ 0 & 0 \\ 0 & 0 \\ 0 & 0 \\ 0 & 1 \\ 0 & 0 \\ 0 & 0 \end{bmatrix} \begin{bmatrix} w_x \\ w_y \end{bmatrix} \quad \text{Eq. 3.6}$$

The final dynamic constants are shown below in Table 3.1.

| Symbol | Value | Symbol | Value |
|---------------------------|-------|-------------------------|-------|
| V_x (kg/sec) | 4 | V_y (kg/sec) | 4 |
| ω_θ (rad/sec) | 3 | ω_ϕ (rad/sec) | 5 |
| ζ_θ (unitless) | 0.65 | ζ_ϕ (unitless) | 0.4 |
| C_θ (unitless) | 500 | C_ϕ (unitless) | 625 |

Table 3-1 Plant Dynamics - Constants

Note that the roll dynamics have a slightly higher natural frequency and a slightly lower attitude-damping coefficient. This behavior is indicative of most in-service helicopters, in that the aircraft is slightly more responsive in roll than pitch. The velocity damping coefficients are identical. The cyclic gain coefficients were chosen to provide adequate control authority during the most demanding disturbance inputs. It should be noted that

the system convention results in position and velocity in units of meters and meters per second. The cyclic position is a unitless dimension provided by the joystick.

3.4 Experimental Design

3.4.1 Subjects

In order to minimize required subject training and ensure subject population homogeneity, all subjects were qualified pilots and helicopter aircraft commanders. Their unique skill set, particularly their familiarity with simulator control configuration and test plant dynamic characteristics, allow this experiment to evaluate the efficacy of the TSAS, rather than measure the rapidity with which a subject can learn to fly.

A total of twelve subjects were chosen from local Navy helicopter squadrons. The use of twelve subjects allowed construction of a balanced experiment, eliminating order effects and evaluating the system as objectively as possible.

The Old Dominion University Institutional Review Board (IRB) approved the use of human subjects. The appropriate IRB application form and the proposed protocol are included in Appendix B. All subjects were advised of their rights and their status as experimental volunteers.

3.4.2 Experimental Trials

Based upon pilot trials, and the specific questions raised by previous research, the final task design was constructed to provide data for the visual/tactile pilot performance model. Additional experimental goals were to confirm the utility of the TSAS and to validate new workload measures.

The trial itself consists of a three minute, low hover task in the presence of a pseudo-random disturbance signal. The pilot was directed to maintain a constant position over

the ground. The visual environment provided relatively weak cues in the fore-aft or longitudinal axis and excellent cues in the port-starboard or lateral axis. Both yaw angle and altitude were held constant for this experiment.

The trial was divided into three phases, Pre Visual Occlusion (PVO) which lasted for 60 seconds, Visual Occlusion Transition (VOX) that lasted 30 seconds, and Visual Occlusion Steady State, which ran for 90 seconds. At the end of the first minute, Visual Occlusion occurred and the visual field transitioned to one of three conditions: Degraded Visual Environment-Heavy (DVE-H), Degraded Visual Environment-Light (DVE-L), or Good Visual Environment (GVE), which remains unchanged. The trial then continued for 120 more seconds (VOX and VOSS) under the new visual condition. The 30-second VOX attempted to capture transient dynamics of pilot performance. The final 90-second segment (VOSS) sought to identify steady state characteristics of pilot performance.

The pseudo-random disturbance signal is the sum of 12 sine waves. This signal was chosen because it allows analysis of pilot inputs at discrete frequencies, facilitating easier pilot plant identification, but still appears random in occurrence to the pilot, preventing any future disturbance signal generation (pursuit tracking). The frequency range was chosen to stimulate pilot response in the region of crossover. The specific frequencies were selected to result in whole periods during each phase of the run. However, no signal's total number of cycles could be a factor of any other signal. If such were the case, aliasing would occur, making it impossible to separate pilot response at the two frequencies. The amplitudes of each signal were scaled to provide a profound disturbance signal while remaining within the control range of the pilot-simulator plant. Three distinct signals were designed, one for each phase of the trial.

Table 3.2 shows the frequencies and amplitudes of the disturbance signal. The first column lists the desired frequencies. Practical limitations required choosing whole period signals whose frequency was close to the desired driving frequency. Note that the Visual Occlusion Transition signal has only eleven sine waves. This truncation was due

to the short period of the transition, prohibiting frequencies below 0.419 radians per second without violating the factor rule described above.

| Condition | Pre Visual Occlusion | | | Visual Occlusion Transition | | | Visual Occlusion Steady State | | |
|-----------------|----------------------|----------|-----------|-----------------------------|----------|-----|-------------------------------|----------|-----------|
| Time (sec) | 60 | | | 30 | | | 90 | | |
| Nominal Rad/Sec | Rad Sec | # Cycles | Amp (m/s) | Rad Sec | # Cycles | Amp | Rad Sec | # Cycles | Amp (m/s) |
| 0.2 | 0.2094 | 2 | 8 | | | | 0.2094 | 3 | 8 |
| 0.5 | 0.5235 | 5 | 8 | 0.4188 | 2 | 8 | 0.4886 | 7 | 8 |
| 1.0 | 1.1518 | 11 | 8 | 1.0471 | 5 | 8 | 1.0471 | 15 | 8 |
| 1.5 | 1.7801 | 17 | 8 | 1.4660 | 7 | 8 | 1.6056 | 23 | 8 |
| 2.0 | 1.9896 | 19 | 8 | 1.8840 | 9 | 8 | 2.0245 | 29 | 8 |
| 3.0 | 3.0367 | 29 | 6 | 2.7226 | 13 | 6 | 3.0018 | 43 | 6 |
| 6.0 | 6.1782 | 59 | 1 | 6.0735 | 29 | 1 | 5.9339 | 85 | 1 |
| 8.0 | 8.2726 | 79 | 0.8 | 7.7490 | 37 | 0.8 | 8.0282 | 115 | 0.8 |
| 10.0 | 10.1575 | 97 | 0.4 | 9.8433 | 47 | 0.4 | 9.9829 | 143 | 0.4 |
| 15.0 | 14.9744 | 143 | 0.1 | 15.2886 | 73 | 0.1 | 15.1490 | 217 | 0.1 |
| 19.0 | 19.1631 | 183 | 0.1 | 19.0584 | 91 | 0.1 | 18.9886 | 272 | 0.1 |
| 30.0 | 30.0536 | 287 | 0.1 | 29.9489 | 143 | 0.1 | 30.0885 | 431 | 0.1 |

Table 3-2 Pseudo-Random Sum-of-Sines Disturbance Signal

3.4.3 Conditions Presented

The previous TSAS experiments varied both TSAS and visual condition between trials. This trend was continued for this experiment, although with more resolution. Each three-minute run was presented in six conditions, GVE, DVE-L, and DVE-H, with TSAS and without. Each trial condition was performed twice, for a total of twelve trials.

The Degraded Visual Environment was divided into two distinct levels of visual field degradation in an effort to provide resolution for the pilot model with regard to incorporation of visual and tactile signals in the presence of noise.

Each trial began and ended with ten seconds of Good Visual Environment and no disturbance. The disturbance signals described above were present for PVO, VOX, and

VOSS and were seamless in their appearance. Visual field was unoccluded for the PVO phase and occluded at the appropriate level for the entire VOX and VOSS phases.

The TSAS vest was turned on or off as necessary prior to each trial run. If available, the TSAS signal was present throughout the entire three minute run, during PVO, VOX, and VOSS periods. Appendix C shows the Latin Square table used to balance the experiment and the algorithm used to generate the table of the trial condition order.

3.4.4 Variables Recorded

The LabView script on the “operator” laptop recorded all variables for the entirety of each trial. Variables recorded include positions, velocities, accelerations, attitude, and attitude rates. Additionally, the disturbances in each axis were recorded, as were the pilot control inputs. Finally, the time-step was recorded to verify that the software was performing at the proper sample rate throughout the trial.

In addition to the recorded objective variables, all pilots were required to fill in a pre-experiment questionnaire which is essentially a pilot data sheet, recording age, weight, height, and vision as well as recent and career flight experience. A copy of the pre-experiment questionnaire is included in Appendix D.

Following each trial, the pilot filled out an intra-trial questionnaire. The questionnaire included several subjective measures as well as a brief pilot wellness survey. A copy of the intra trial questionnaire can also be found in Appendix D. This questionnaire will be further explained in the following section.

3.4.4.1 Intra-Trial Questionnaire

In order to fully capture the utility of the TSAS system, subjective pilot interview sheets were used in addition to the objective measurements. These questionnaires were

designed to capture pilot perceptions of situational awareness, mental workload, quality of cues, and percentage of attention dedicated to various cockpit instruments.

China Lake Situational Awareness

The CLSA measure, described in Section 2, was employed to allow pilots to gauge the accuracy of their knowledge of their environment, in essence, how well did they know what was happening during the trial. In this case, pilots were asked to rate the accuracy of their perceived position over the ground during the time period following visual occlusion event?

- How would you rate your overall Situational Awareness during the previous run:

1 2 3 4 5

Very Good Good Adequate Poor Very Poor

Figure 3-8 CLSA Questionnaire Format

Pilots were provided a copy of the CLSA definition table (Figure 2-5) and asked to indicate their own perception of their SA during the trial. Integer responses were not mandatory. The specific form of the questionnaire is shown in Figure 3-8.

Modified Cooper-Harper

The Modified Cooper-Harper Workload scale was used to measure the pilot's perception of the mental workload required to satisfactorily complete the assigned task. The difference between SA, workload, and performance were stressed to the subjects throughout the experiment.

Again, pilots were provided a copy of the decision tree and asked to record their decisions on the numerical scale shown in Figure 3-9.

• How would you rate your mental effort during the previous run:

| | | | | | | | | | |
|-------------------------------|-------------------|-------------------------|----------------------------------|---|----------------------------------|------------------|------------------|------------------|------------------|
| 1 | 2 | 3 | 4 | 5 | 6 | 7 | 8 | 9 | 10 |
| Very Easy Highly Desirable | Easy Desirable | Fair Mild Difficulty | Minor but Annoying Difficulty | Moderately Objectionable Difficulty | Very Objectionable Difficulty | Major Difficulty | Major Difficulty | Major Difficulty | Major Difficulty |

Figure 3-9 Modified Cooper Harper Questionnaire Format

Subjective Performance Evaluation

The subjective performance evaluation was included to gauge the pilot's perception of how well they accomplished the assigned task. *Desired* and *adequate* performance were defined as maintaining an error of five and ten feet respectively. Pilots were given no feedback on their performance prior to submission of the intra-trial questionnaire. The questionnaire is presented in Figure 3-10.

• Rate your performance during the previous run:

| | | | | |
|---------|---|----------|---|--------------|
| 1 | 2 | 3 | 4 | 5 |
| Desired | | Adequate | | Sub Adequate |

Figure 3-10 Subjective Performance Assessment

Perceptual Cue Rating

Perceptual cue rating required the subject to evaluate the quality of the information from different sources for both attitude and horizontal position over the ground. The information was divided into the outside “VFR” information and that provided by all instruments, visual and tactile. The PCR rating scale is shown in Figure 3.9.

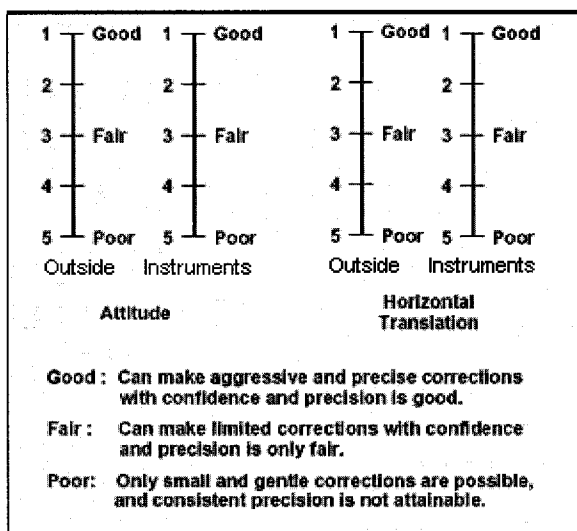


Figure 3-11 Perceptual Cue Rating

Attention Division for Visual Instruments

The final two measures were designed specifically for this experiment and were developed to measure the pilot’s perception of the source of his situational information.

The Visual Attention Division, shown in Figure 3.10, asked the pilot to graphically represent the percent of his attention that was focused on each instrument during both GVE and DVE conditions. Although pie graph representation was preferred, many subjects were more comfortable simply writing a percentage next to each instrument. For GVE trials, the second pie graph was marked “N/A” and was not filled in.

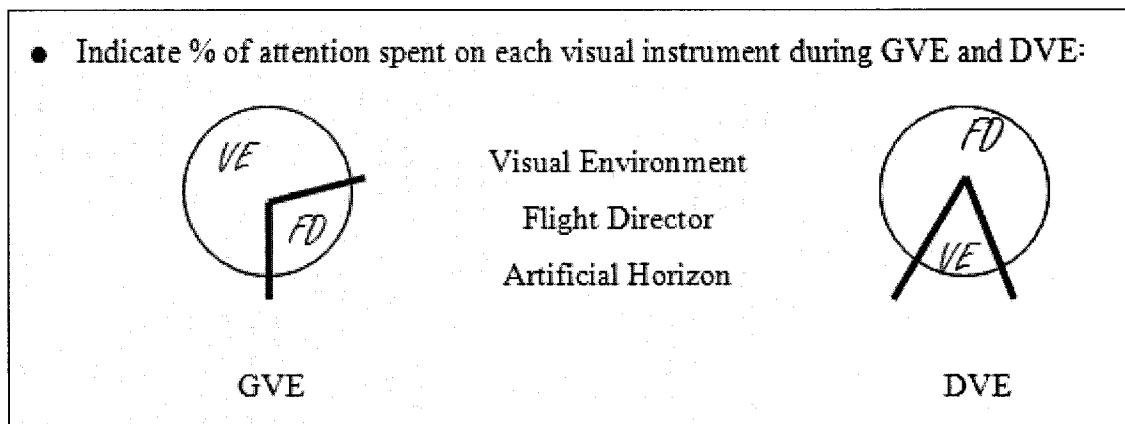


Figure 3-12 Visual Instrument Attention Division

TSAS information provided

The final subjective measure captured the pilot's perception of percent of information gathered from visual and tactile sources and is shown in Figure 3.11. This measure was taken for both GVE and DVE conditions, in order to measure whether pilots used tactile cues more, or less, during conditions of corrupted, noisy, or absent visual signals.

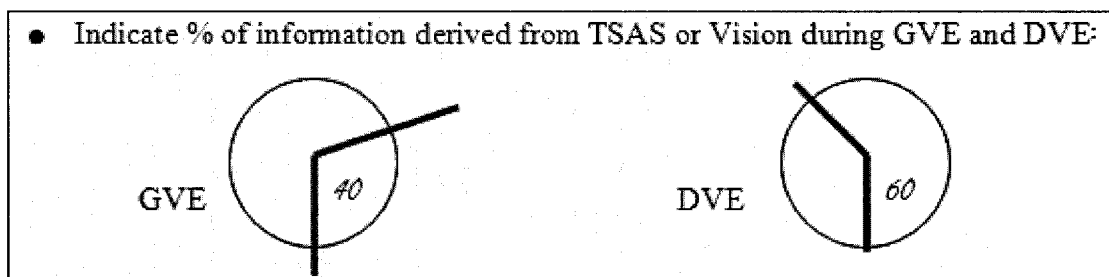


Figure 3-13 TSAS Information Percentage Provided

Physiological Response Questionnaire

At the end of each intra-trial questionnaire, the subjects were queried regarding any symptoms of illness, queasiness, or fatigue. These measures were taken in order to capture any additional factors that may have influenced pilot performance during each trial.

3.4.4.2 Post Trial Questionnaire

At the completion of the experiment, each subject completed a post trial survey. The post trial questionnaire was divided into two parts. Part one of the post trial questionnaire used SWORD to gain pairwise comparisons of the subjects' preferences regarding visual condition and TSAS. The second part involved questions regarding the desirability of the TSAS cueing and the fit and comfort of the TSAS vest itself. A copy of the post trial questionnaire is available in Appendix D.

3.5 Data Analysis

3.5.1 Subjective Data Analysis

The pilots' personal information was analyzed using cross-correlation statistical techniques to reveal any relationships between pilot performance and either anthropometric data or flight experience. Trends were sought within the raw performance as well as performance trends, to see if certain pilot characteristics might make him more or less predisposed to performance enhancement or degradations with the TSAS.

The intra-trial data was collected via numerical Lichert scales, allowing numerical analysis and trend determination as well as Wilcoxon Ranked Sum statistical analysis to determine statistically significant changes in reported subjective measures with respect to trial conditions. A cross correlation analysis was also conducted between variables, in an effort to uncover relationships among the variables themselves. For example, "Did pilot reported situational awareness correlate to pilot reported subjective performance?"

Further correlation analysis was conducted between subjective data and the objective data. The purpose of this analysis was to reveal relationships between subject perception and actual pilot performance.

3.5.2 Objective Data Analysis

Of the recorded variables, all of the positions, attitudes and rates were analyzed for mean, root mean square, standard deviation, maxima and minima, and range. Variables were compared across conditions and plotted by visual and tactile condition. Data was viewed in its raw form.

The original experiment was designed to allow comparison of PVO, VOX, and VOSS conditions both within and among subjects. However, because the disturbances presented in each phase were designed to match in the frequency spectrum, they produced different path error magnitudes in all subjects, essentially prohibiting comparison of PVO to VOX or VOSS data. Instead, each condition was compared to all other conditions within each phase of the trials. For example, RMS error of each Pre-Visual Occlusion condition (GVE / DVE-L / DVE-H, and TSAS / No TSAS) was compared to every other PVO condition. Similar analysis was conducted with Visual Occlusion Transition and Visual Occlusion Steady State respectively.

The a priori intent was to normalize data by subject to remove any inter-subject variability in performance, essentially allowing each subject to serve as their own baseline. However, the similarity between subjects made such a step unnecessary. Normalization saw no improvement in statistical significance of results or in appearance of trends with respect to visual or tactile condition. The consistent performance among all subjects can be attributed to the homogenous nature of the pilot population used as test subjects.

Outliers were defined as any data that fell more than $2 \frac{1}{2}$ standard deviations from the mean. Any outliers were discarded for summary analysis. Statistical analysis was performed before and after outlier removal. Removal of outliers will be disclosed for any significant results.

3.5.2.1 *Data Analysis Programming*

The data were analyzed using several Matlab scripts. The summary data were recorded using Excel spreadsheets. Summary data was then plotted and analyzed statistically.

The script *FINALDATAPARSEANDSAVE.m* loaded the data and stripped the appropriate channels for analysis. The script then sorted each trial according to visual and tactile condition, and computed all of the objective summary data (mean, RMS, range, etc.). Finally, it compiled all subject trials together and saved the data.

The script *FINALDATAANALYZE.m* loaded the saved data, searched for outliers at each time-step, removed outliers, and saved the data. This script also contained a routine to smooth the data using a sliding 3-second average. However, preliminary analysis revealed that such manipulation unnecessarily corrupted the data, particularly during the transition phase. As a result, this subroutine was deactivated.

The data was plotted for preliminary analysis with the script *PATHERRORPLOT.m*. This script allowed side-by-side comparison of trials by condition, subject, and trial number. The full text of the important Matlab scripts is included in Appendix E.

Statistical analysis was performed using a two-tailed heteroscedastic t-test. Each condition was compared to every other condition. Additionally, all GVE trials were compared to DVE results and TSAS trials were compared to No TSAS. The resulting p -values were recorded and tabulated.

3.5.2.2 *Sliding Window Path Error Analysis*

Due to the rapid adaptability of the pilot controller, gross average analysis often failed to reveal performance differences between conditions. In an effort to provide additional resolution, a moment-by-moment analysis of the x- and y-axes' path error was performed.

The aircraft position was recorded every 12 milliseconds for the duration of the run. The values were sorted by visual and tactile condition, averaged for each condition, and outliers removed. The homogenous nature of the subject population eliminated the need to remove outliers. The errors were then plotted by condition in an effort to display transient effects of visual and tactile presentation conditions.

Though not a normal analysis method, a t-test was performed on the path error data at each time point. This procedure was performed to record the transient nature of any statistical significance achieved following Visual Occlusion Event.

3.6 Model Development

The basic methodology of the model development for this research is predicated upon the belief that to the maximum extent possible, a model should reflect not only the gross behavior of the system being modeled, but a structure born of a comprehensive understanding of the entire system and the complex interaction between and among subsystems. With that in mind, each part of the developed model was based upon heuristic evidence, implicit or anecdotal, that a certain strategy or behavior is present. Though many of these assumptions were found to be either inconclusive or incorrect, the remaining components of the model reflect not only a mathematical representation of the system's performance, but a structural one as well.

The MOCM has proven to be a successful and satisfactory model of pilot performance. The MOCM captures the gross performance characteristics of the pilot-plant system. It has well defined methods for iterative solutions to potentially complex systems and is mathematically elegant in that optimization techniques are exploited to represent physical pilot limitations.

Despite these traits, several problems exist with the MOCM, primarily heuristic in nature. First, the basic structure of the model doesn't construct an appropriate physical analogy to the real world. For example, placing the delay after the neuromotor lag implies that

the pilot's brain sends a signal to the muscles, that signal is subject to the physical limitation of the neuromuscular system and an output emerges. Then, that output is delayed. Perhaps a more analogous setup would place the delay immediately following the estimator/gain loop, implying a cortical processing delay prior to muscular command determination. The delayed output signal is then subject to the neuromuscular limitations as before.

Admittedly, for a linear plant, the order of the operations is insignificant. Acceptable mathematical accommodations can be made to achieve computational equality. Some incidental differences include the input of control noise and its subsequent delay under the MOCM, while the new model injects the noise following the delay. For the case of this model, the delay was incorporated into the pilot compensation model.

When defining the estimator dynamics, the MOCM makes two assumptions that will be challenged. The first is that the magnitude of the observation noise is 0.003 times the variance of the state being observed. For this experiment, empirical measurements of pilot observation accuracy were taken to quantify observation and estimation error in lieu of assumptions of blanket ratios between noise and variance.

Second, the MOCM uses a single estimator gain for the duration of the trial, essentially assuming time-invariant behavior by the pilot-estimator. Heuristically, it stands that as the pilot's error signal changes, so will his ability to estimate the state of the system, particularly if the magnitude of the observation noise is dependent upon the magnitude of the error, as it is in this case. Additional noise may affect estimator reconstruction dynamics and, ultimately, performance. Therefore, a time-varying estimator was constructed for this research.

One of the more brilliant aspects of the MOCM is also, in the opinion of the author, one of the most heuristically inappropriate. As described in Section 2, the use of a control rate term in the optimal control cost function, Eq. 2.3, eventually decouples into a pilot control first order lag term that is injected into the plant dynamics. This solution is

elegant and serves to provide a lag term not unlike the neuromuscular lag exhibited by human controllers.

An objection to this approach is that it implies that the reason for the neuromuscular lag is a pilot assigned cost (conscious or sub-conscious) associated with control rates. According the MOCM model structure and methodology, it is this pilot desire to limit input control rates that causes the neuromuscular lag. Heuristically, the neuromuscular dynamics are defined not by cognition or control strategies, but by the physical limitations of nerves, tendons, and muscle fibers.

Admittedly, the control rate term in the optimal cost function is required when dealing with pilot controllers during most control tasks. The desire to elicit smooth response and avoid overshoots and oscillations causes the pilot to dampen his responses somewhat. In fact, control rate is decidedly more important than the control variable itself. For example, a driver attempting to maintain his course over the road will move the wheel to whatever position is required to allow him to track properly over his desired course. The pilot will not, however, recklessly turn the wheel from left to right as quickly as possible. Self-preservation and the cost associated with large control rates prevent him from overcontrolling by limiting control rates.

An alternative methodology to control rate defining the neuromuscular lag is proposed in which the optimal cost function retains the state and control costs, but the neuromuscular term is defined by the physical limitations of the human machine rather than a control strategy. The new structure places the neuromuscular term after both the estimator and cognitive delay. The control noise is still added at the neuromuscular block, which captures the imperfect nature of human control.

In addition to the new neuromuscular block, the new model contains a pilot compensation module, the structure of which is dependent upon the system being controlled. Based upon McRuer's pilot strategy rules, the compensation module contains a second order Pade approximation of a pure time delay, lag (low frequency performance) and lead (high

frequency performance) terms, as well as a scalar gain (set crossover frequency). This block was identified using an off-the-shelf Matlab script *PEM*. *PEM* uses numerical, partial differential equation techniques to iteratively solve the prediction error estimate of a linear model. Although extremely powerful, there are risks involved. First of all, the initial guess must be close in order to ensure that the solution converges. Second, the order must be chosen wisely, as numerical errors tend to compound and higher order models routinely drive unstable. The solution and effectiveness of each of these terms is explored using the Matlab script *XAXIS_MODEL_REVIEW.m* which is included in Appendix E. The specific solution will be discussed in the results section.

Regardless of the appropriateness and accuracy of the component of a model, a linear model will always fail to accurately capture all the important elements of a system as complex and nonlinear as that of a human pilot. Particularly, no satisfactory method exists to explain the high frequency noise that the pilot injects into the system. Previously, this disparity was attributed to nonlinear “remnant.” The PSD of the remnant was calculated, but little else was done to heuristically model the phenomenon.

It is theorized that nonlinear behavior, unpredictable, but stochastically definable, may contribute to the high frequency noise. With this hypothesis clearly in mind, a nonlinear stochastic analysis was performed relating linear command signals to the actual, nonlinear signal. The relationship was investigated between the linear output signal and the actual output signal (command output error) and movement likelihood, movement direction, length of movement, and magnitude of movement. The results of nonlinear character identification are believed to have tremendous potential and will be fully explained in the results section. The Matlab script *XAXIS_NONLINEAR_ANALYZE.m* defines the probability of action and the stochastic maps. The scripts *XAXIS_SIM_LINEAR.m* and *XAXIS_SIM_NONLINEAR.m* use the model structure and stochastic information to conduct time domain simulations of each pilot trial, varying visual and tactile information as appropriate. Again, the full text of these scripts is available in Appendix E.

For the actual trial data, the histogram of movement was superimposed on the linear control signal generated by the linear model in order to explore the possible cause of a high frequency *remnant* and *neuromuscular peak*. To demonstrate why the “move and hold” may cause additional high frequency noise, a review of sampling effects is necessary. Whenever a signal is sampled at frequency F_s , information is lost. Specifically, the sampled signal is unable to accurately reconstruct any of the original signal information above the Nyquist frequency, which is equal to half the sampling rate. (More correctly, the Nyquist sampling rate must be twice the maximum frequency of the original signal to avoid data corruption.) Failure to sample at or above the Nyquist rate results in *aliasing*.

Aliasing is the appearance of sampled signal content at frequencies not present in the original signal. Aliasing results when signal content above the sample interval is reflected about the half-sampling frequency. Figure 3-14 shows the general effect of sampling and aliasing.

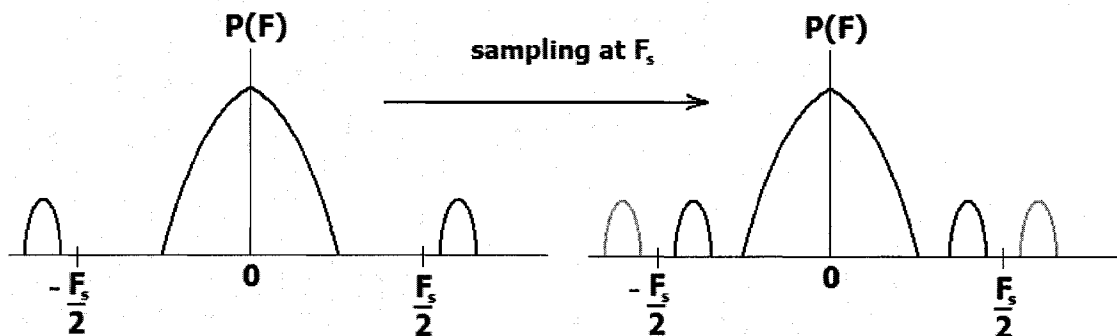


Figure 3-14 Effect of Sampling Upon Power Spectrum

Mathematically, the phenomenon of aliasing can be explained through Fourier series analysis. Assume an original function $f(t)$ for a given range $T_1 < t < T_2$ and a sampling interval of $\Delta T = 1/F_s$. Sampling the function at time ΔT is accomplished by multiplying

the original function by a *comb* function, which is unity at each ΔT and zero at all other points. The new function can be defined by the following equation:

$$f^*(t) = s(t; \Delta T)f(t) = \sum_{n=-\infty}^{n=\infty} f(t)\delta(t - n\Delta T) \quad \text{Eq. 3.7}$$

where δ is the impulse function

s is the comb function

and n is the infinite integer series

The Fourier series of the comb function is:

$$s(t; \Delta T) = \frac{1}{\Delta T} \sum_{n=-\infty}^{n=\infty} e^{jn\omega_0 t} \quad \text{Eq. 3.8}$$

$$\text{where } \omega_0 = \frac{2\pi}{\Delta T}$$

The Fourier coefficients of the comb function are always equal to $1/\Delta T$.

Solving the Fourier series of the sampled function yields:

$$F^*(j\omega) = \int_{-\infty}^{\infty} f^*(t)e^{-j\omega t} dt \quad \text{Eq. 3.9}$$

Substituting for $f^*(t)$:

$$F^*(j\omega) = \frac{1}{\Delta T} \sum_{n=-\infty}^{n=\infty} \int_{-\infty}^{\infty} f(t)e^{jn\omega_0 t} e^{-j\omega t} dt \quad \text{Eq. 3.10}$$

and

$$F^*(j\omega) = \frac{1}{\Delta T} \sum_{n=-\infty}^{n=\infty} F(j(\omega - n\omega_0)) \quad \text{Eq. 3.11}$$

Substituting back for ω_0 yields:

$$F^*(j\omega) = \frac{1}{\Delta T} \sum_{n=-\infty}^{n=\infty} F\left(j\left(\omega - \frac{2\pi n}{\Delta T}\right)\right) \quad \text{Eq. 3.12}$$

Equation 3.12 reveals that the Fourier transform of the sampled function $f^*(t)$ is identical to the original transform, but repeated in the frequency domain every $1/\Delta T$, resulting in an apparent reflection of the power spectrum around a point equal to half of the sampling frequency.

The importance of this phenomenon as it applies to pilot performance is that the move-and-hold strategy employed by all pilot subjects is tantamount to a sampling of the smooth, linear control strategy. Although random sampling has a slightly more complex effect than constant period sampling, any discrete sampling of a continuous signal serves to inject additional frequency content into the final signal as previously discussed.

SECTION 4 RESULTS

This section will outline the analytical results of both subjective and objective variables. Additionally, the final pilot model will be presented and discussed. Subjective results will be presented first, followed by basic objective variable analysis. More complex analysis of objective variables will be presented next. Following analytical presentation, the pilot model will be discussed, including developmental discoveries, pilot strategies, and mathematical modeling of these strategies.

4.1 Subjective Data

The subjective data for this experiment was collected wholly from the pilot questionnaires filled out before, between, and after the experimental trials. The results will be presented in the order in which the pilot was queried, beginning with the intra-trial questionnaire.

4.1.1 CLSA

Although the China Lake Situational Awareness measure failed to produce consistently statistically significant results, Figure 4-1 shows that some interesting trends were revealed.

First, pilots reported worse Situational Awareness with degraded visual environments: slightly for DVE-Light, and more noticeably for the DVE-Heavy condition (lower numbers represent better reported SA). In fact, for the No-TSAS trials, the DVE-H condition Situational Awareness was significantly higher than the reported SA for Good Visual Environment ($p=0.04$). No other significant differences were noted between visual conditions.

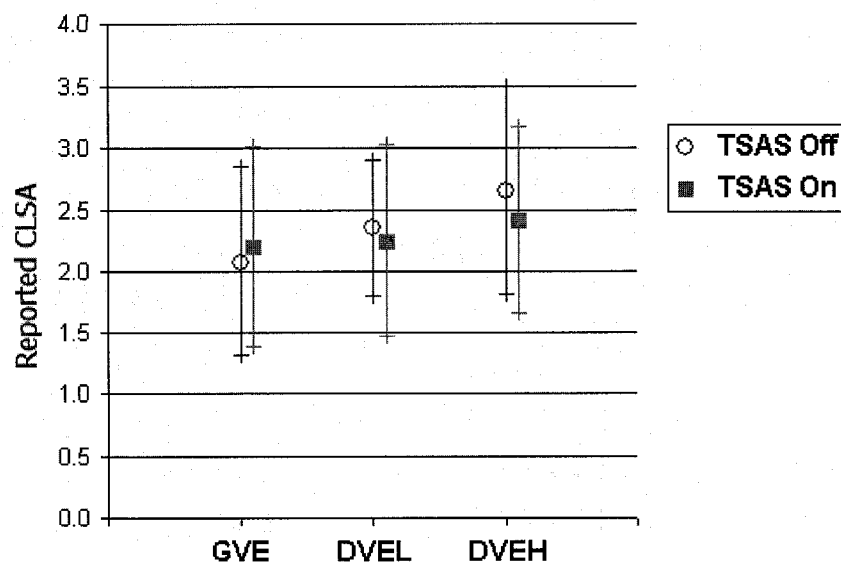


Figure 4-1 China Lake Situational Awareness Post Trial Reports

The second trend is that TSAS appears to slightly improve pilot reported situational awareness. Additionally, reported Situational Awareness with the TSAS appears to be less affected by visual condition, as evidenced by the shallower slope of the TSAS trials. The trials without TSAS showed a more marked decrease in SA as the visual environment became more degraded. However, all of these trends are very small and none of them achieved statistical significance.

Normalization of these data produced nearly identical results, confirming the earlier assertion that the homogenous subject pool led to consistent results across subjects.

4.1.2 Modified Cooper-Harper

As shown in Figure 4-2, the Modified Cooper-Harper subjective workload scale presented results very similar to the CLSA. Again there exists a statistically significant difference between reported workload during GVE and DVEH without TSAS ($p=0.0162$).

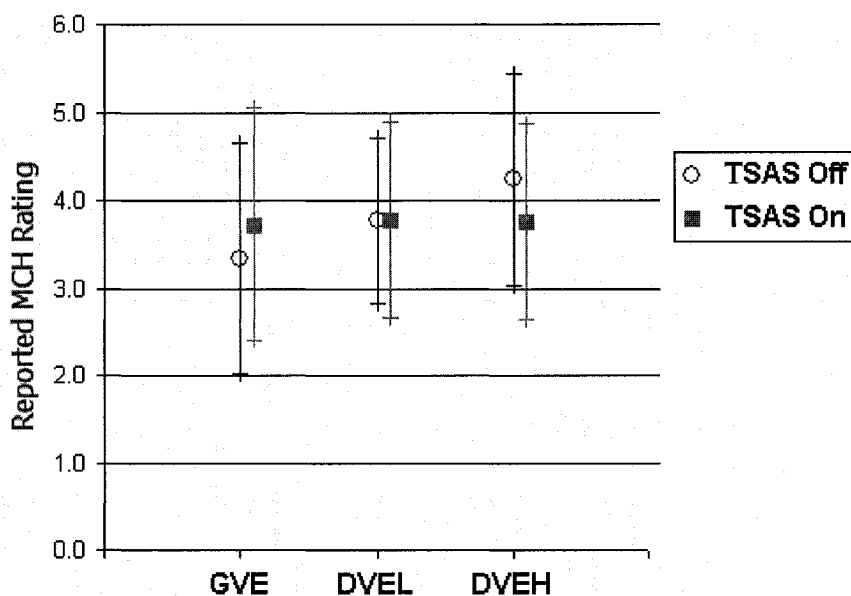


Figure 4-2 Pilot Mental Workload vs. Condition

Again the TSAS appears to lessen the effects of visual environment with regard to reported workload. The difference between TSAS and No TSAS was nearly negligible and clearly condition dependent. Each of these trends failed to achieve statistical significance. As before, normalization produced nearly identical results.

4.1.3 Subjective Performance Self Evaluation

This subject will be discussed in depth following presentation of the objective position error data. This change in presentation order has been done to allow a side-by-side comparison of the subjects' perception of their performance and the actual measured performance.

4.1.4 Perceptual Cue Rating

The Perceptual Cue Rating was broken up into four separate measurements, each evaluating the quality of the signals presented to the pilot via different modalities and in different axes.

The pilot's rating of the attitude cues (Figure 4-3) showed a strong and expected inverse relationship between the amount of visual degradation and the subsequent rating by the pilot. For the No TSAS condition, the GVE condition was statistically better than both the DVE-L and DVE-H conditions ($p=0.0004$ and $p=0.0000$). Furthermore, DVE-L was rated statistically better than the DVE-H condition ($p=0.008$). With the benefit of TSAS, the trend was the same, with statistical significance achieved between GVE and both DVE-L and DVE-H ($p=0.0037$ and $p=0.0004$). For the TSAS condition, DVE-L did not show a significant difference with DVE-H ($p=0.2302$). Since this measure is essentially an indirect measure of the quality of the visual signal, failure to achieve these results would have been surprising.

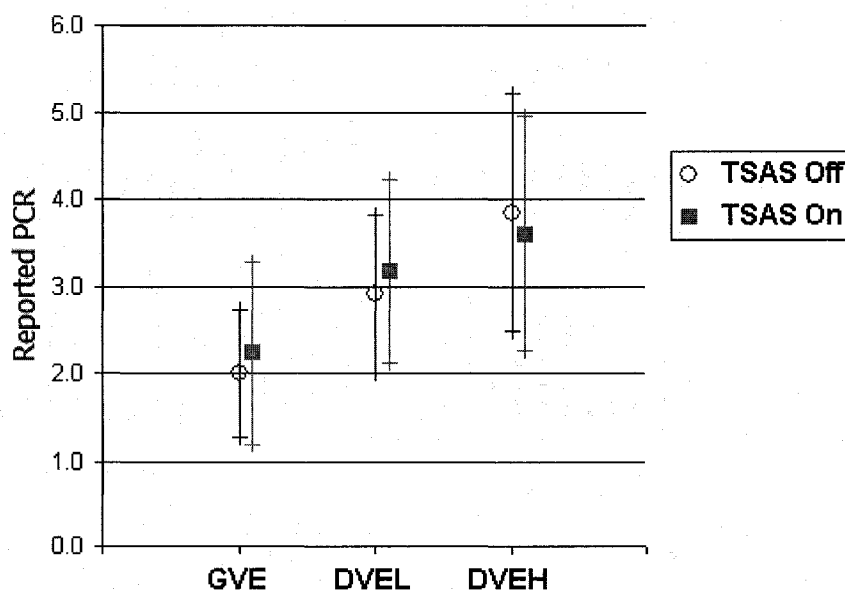


Figure 4-3 Perceptual Cue Rating - Visual Attitude Cues

The trend was identical for the pilot ratings of the horizontal cues (Figure 4-4). Again each No TSAS visual condition was different than the others ($p=0.0002$, $p=0.0000$, $p=0.0116$). As before, the TSAS condition showed a difference only between GVE and both DVE-L and DVE-H ($p=0.0023$, $p=0.0005$), but failed to achieve statistical significance between DVE-L and DVE-H ($p=0.35$).

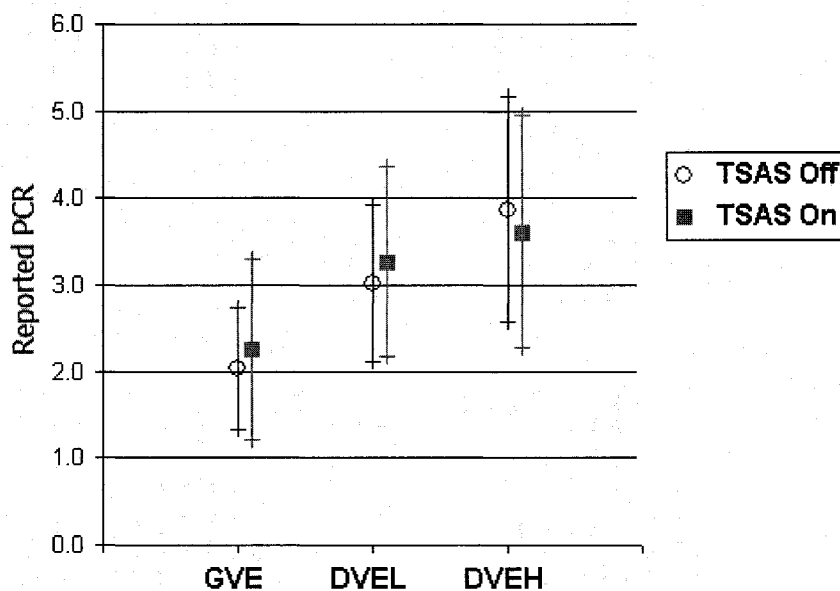


Figure 4-4 Perceptual Cue Rating - Visual Horizontal Drift Cues

In addition to rating the quality of the visual signals, pilots were asked to evaluate the quality of cues presented by the instruments (all instruments, visual and tactile). These results revealed an insensitivity to visual condition in pilot reported quality of cues. Figures 4-5 a. and b. clearly show that neither visual nor tactile condition had any significant effect upon reported instrument cue PCR. Predictably, none of the conditions achieved statistical significance.

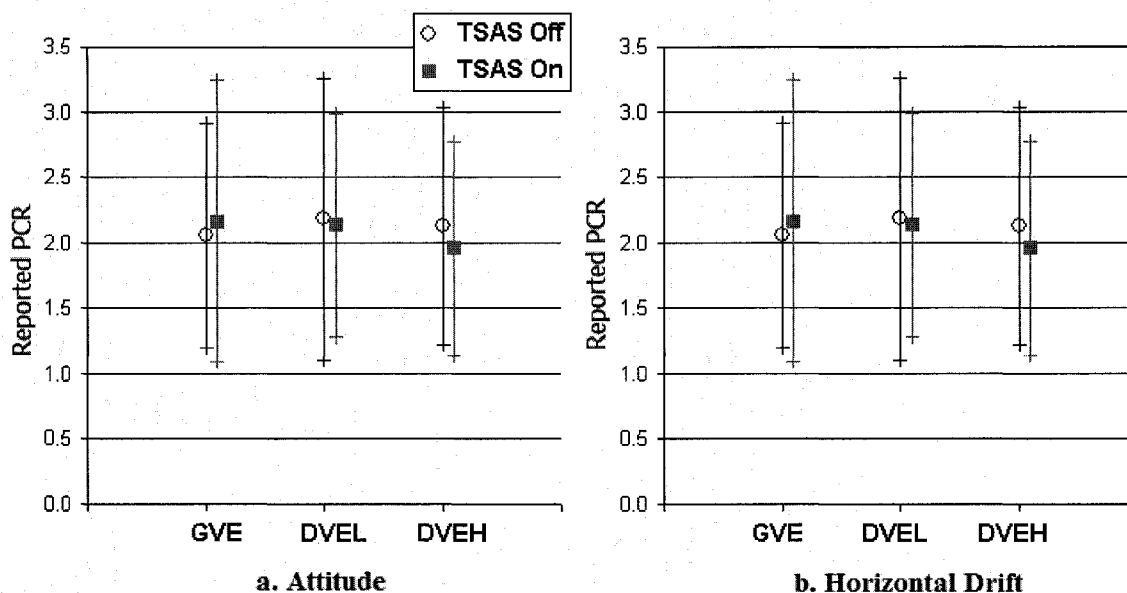


Figure 4-5 Perceptual Cue Rating - Instrument Cues

4.1.5 Visual Environment Information Percentage

As one of the more esoteric measures of this research, the Visual Environment Information Percentage measured the pilot reports of the fraction of their information that came from the “visual environment” as opposed to instruments (Figure 4-6). Predictably, pilots reported that as the visual environment became more degraded, a smaller percentage of their total information was derived from a VFR scan. A few subjects admitted “experimenting” with different scans which may explain the high variability within the GVE and DVE-L conditions. However, despite the high standard deviations, the three conditions were found to be significantly different ($p=0.0007$, $p=0.0000$, $p=0.0001$). The relatively linear decrease was consistent both with and without TSAS. Surprisingly, the presentation of tactile cues did not appear to have affected the pilots’ chosen ratio of information collection from visual or instrument sources. In fact, TSAS appears to have had almost no affect on subjective pilot reports of visual scan dwell fraction.

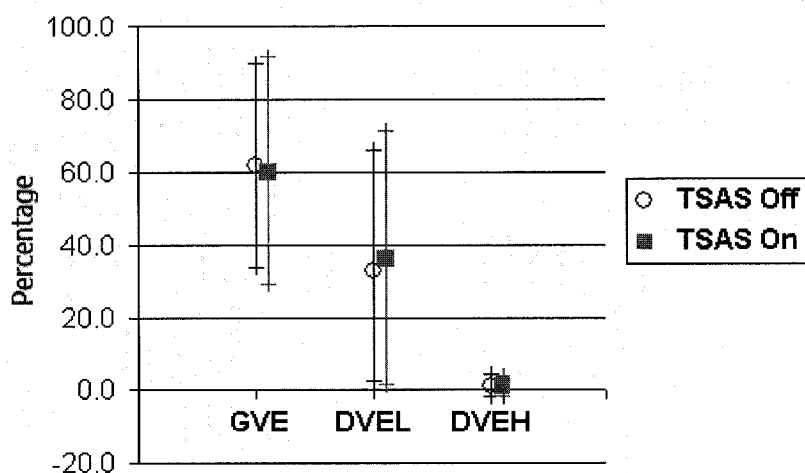


Figure 4-6 Percentage of Information Acquired From Visual Environment

4.1.6 Instrument Information Percentage

In an effort to present a comprehensive picture of pilot scan strategies, the percentage of information derived from tactile instruments was combined with the visual instrument percentages. The result is a full reconstruction of pilot attention during GVE, DVE-L and DVE-H conditions. As Figure 4-7 shows, the percentage of information derived from TSAS increases slightly, though not statistically significantly, from the GVE condition to both DVE conditions. However, the largest and most significant increase in pilot reported attention is found for the Flight Director. In fact, the pilot attention seems to have been diverted directly from the VFR outside scan to the flight director.

As an aside, from data analysis and anecdotal reports from the subjects, it is theorized that the Artificial horizon was ignored by most of the pilot subjects because the attitude of the aircraft was not defined as a task parameter. Additionally, the non-motion simulation provided no additional indication or penalty for large attitude swings. These experimental conditions, combined with the physical separation between the FD and AH may explain the fact that artificial horizon received little attention.

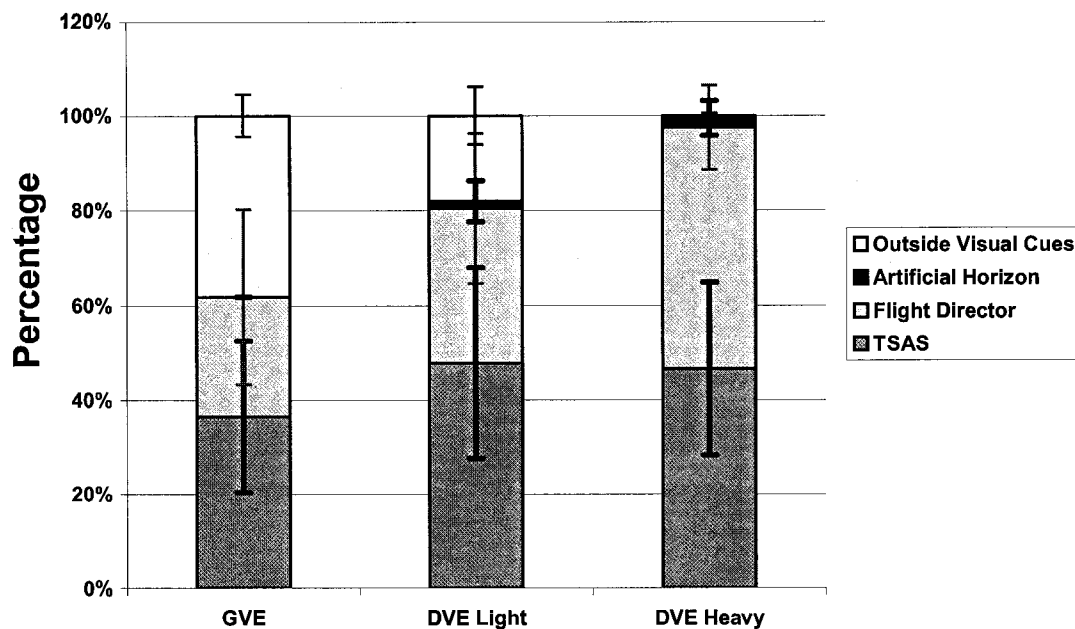


Figure 4-7 Source of Aircraft Information - Percentage

4.1.7 Subjective Workload Dominance (SWORD)

The SWORD surveys were conducted post flight, providing a pairwise comparison of each of the visual conditions presented. The pilots were instructed to rate the degree to which one condition was preferable to another. Plotting the six pairwise comparisons on a single plot reveals the reported trends. Figure 4-8 is an unconventional presentation structure, but effectively summarizes the subjective measures. Each condition is compared to every other condition, with GVE on the left and DVE on the right, TSAS on the bottom and No TSAS on the top. To reduce the number of pairwise comparisons, DVEL and DVEH were combined into a single “Trial Condition.” The vertical and horizontal lines represent comparisons in which only one condition (visual or tactile) was varied. Diagonal lines represent trials where both visual and tactile presentation is different. A point that is closer to one node than the other indicates a pilot preference for the closer condition. Figure 4-8 clearly shows that, of the six conditions, GVE TSAS was most effective in reducing pilot reported mental workload. During DVE trials, TSAS

again proved effective in reducing mental workload. As expected, without the benefit of TSAS, pilots rated GVE less mentally taxing than DVE. The p values shown in Figure 4-8 are the t-test for means different from zero. Of the single condition comparisons, the strongest response was between DVE No TSAS and DVE TSAS, followed closely by DVE No TSAS and GVE No TSAS. This response seems to indicate that TSAS is as valuable as visual environment in reducing pilot controller mental workload.

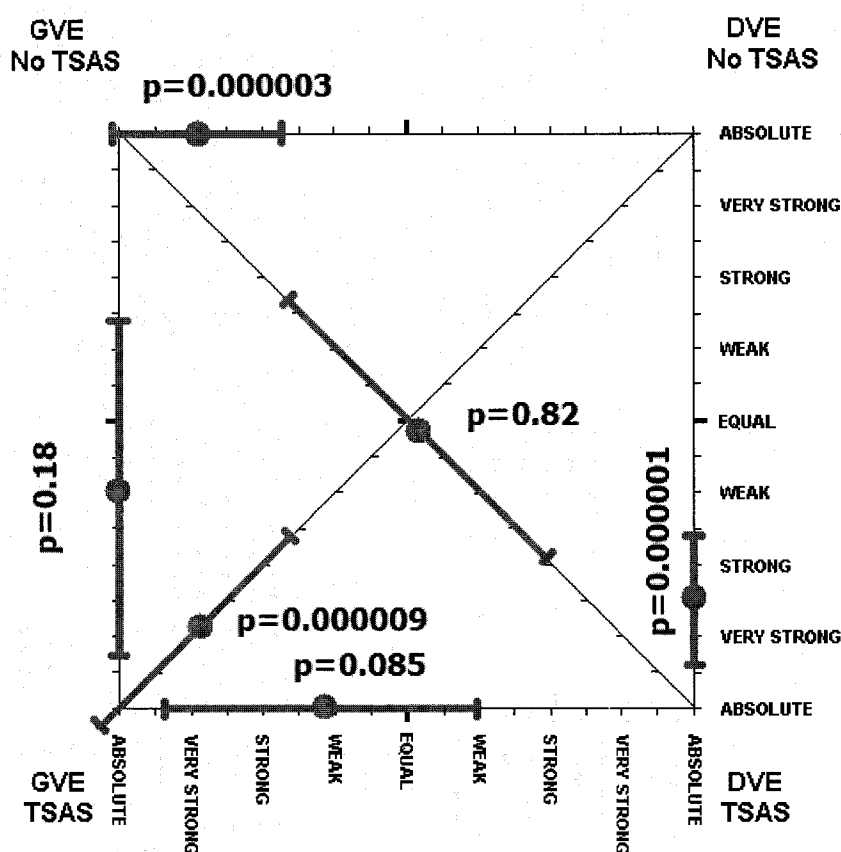


Figure 4-8 Reported SWORD Pairwise Comparisons

4.2 Objective Data

The analyzed objective data can be easily separated into three categories: simple descriptive variables, advanced workload, and model matching parameters. Additional path error analysis was conducted as well, to provide increased resolution. Each category

reveals different information about the influence of vision and TSAS in pilot performance and strategy.

4.2.1 Summary Variables

The descriptive or summary variables revealed a basic difference between pilot performance in the lateral (Y) or left-right axis and the longitudinal (X) or fore-aft axis. The disparity in performance is theorized to be due to the difference in quality of the visual signal presented to the pilot in the two axes. Due to the chosen hover location, the Y-axis provided excellent cues to the pilot for even miniscule drift away from the target position. Contrarily, the X-axis provided only vague cues but, due to the lack of peripheral display, failed to provide the detailed drift information present in the Y-axis.

Originally, it was desired to make direct comparisons between all variables within the PVO, VOX, and VOSS phases. However, despite construction of similar disturbance signal content, the open-loop and closed-loop errors and command signals were dramatically different, preventing an intra-phase comparison. Therefore, all variables are compared only within phase, to other conditions within each phase.

Generally, many of the results expected were not witnessed through gross analysis of the recorded variables in each phase. Closer inspection revealed a higher than expected recovery rate during the transition period, hinting that for the chosen experimental setup, a 30 second transition period may have been too large a time period to be sensitive to pilot performance changes. Alternative analyses will be discussed later.

Additionally, the mean and range variables failed to produce interesting results in any of the recorded variables. Their analysis was performed for completeness' sake, but none of these results will be presented.

4.2.1.1 Lateral Axis Position Error

The Y-axis, with its high quality visual signal, showed a significant decrease in performance during both the transition and the steady state phases. As Figure 4-9 (a) below shows, the PVO conditions were statistically identical. [Note: The labels GVE, DVEL, and DVEH refer to the overall trial condition. The Pre Visual Occlusion events were all displayed without visual occlusion. However, comparative analysis was performed to reveal trial order effects.] Without TSAS, the transition displayed a statistical difference between the GVE conditions and both DVEL and DVEH ($p=0.04$ and $p=0.01$). With TSAS, the DVEH condition proved to be statistically higher ($p=0.05$) than GVE. The DVEL condition showed the same increasing trend, but failed to achieve statistical significance ($p=0.3$). During the VOSS condition, the same increasing trend was present, but none of the conditions proved to be statistically different. The failure to achieve statistical significance during the VOSS phase could be attributed to the highly adaptive nature of the pilot controller and the high quality of the flight director signal. Additionally, when compared to the No TSAS condition, TSAS was not found to influence the Y-axis RMS to a significant degree in any of the phases or conditions.

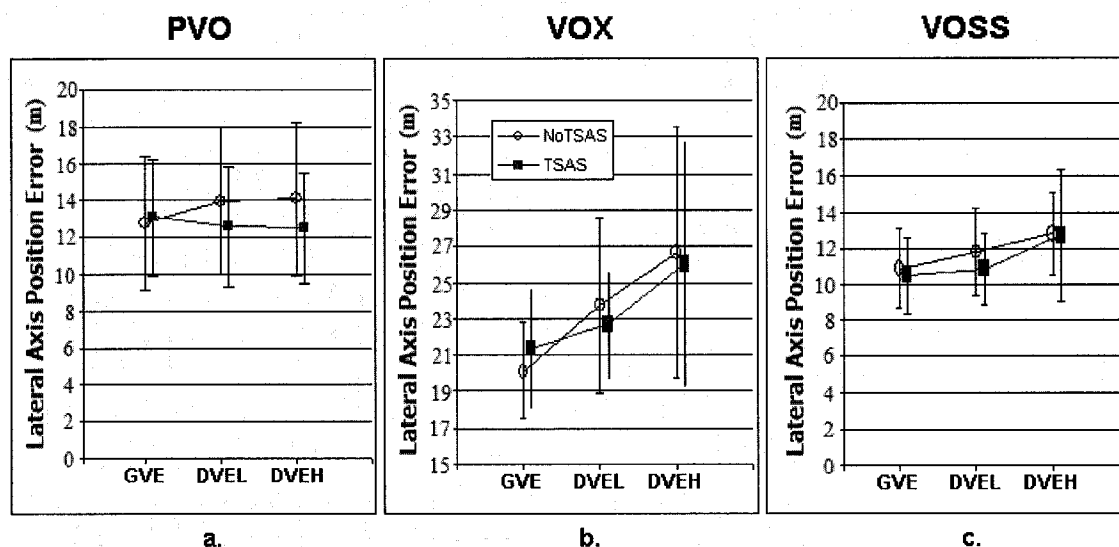


Figure 4-9 Lateral Axis Position RMS Error

The previously introduced Subjective Performance Evaluation, shown in Figure 4-10, shows a good correlation with actual performance with the exception that, during Good Visual Conditions pilots reported feeling that they performed worse with TSAS than without.

This dichotomy was likely due to one of two factors. First, 4 of 12 pilots reported the unfamiliarity with the TSAS made it distracting, particularly during the GVE when they felt the additional information was unnecessary. A second possibility is that the presentation of additional information via the TSAS made pilots more aware of their errors. This error awareness led to a perceived decrease in performance despite a slight improvement in actual performance.

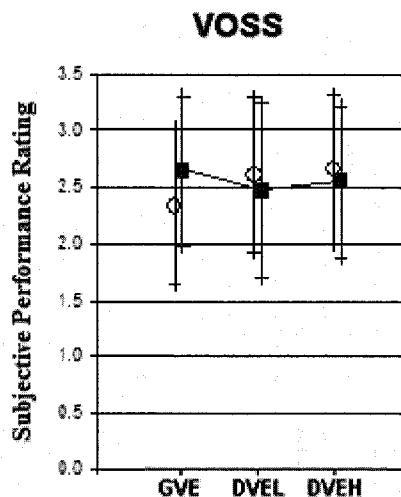


Figure 4-10 Subjective Performance Evaluation

4.2.1.2 Lateral Axis Error Rate, Roll Angle, and Roll Angle Rate

The lateral-axis error rate and roll angle each failed to present any statistically significant trends, in any phase, between any conditions. This result is not surprising since control of aircraft rate or attitude was not a stated goal. Any changes present would have been incidental to the pilot's attempts to control position.

In contrast to roll angle and error rate, roll rate showed consistent and significant trends in both VOX and VOSS phases, for both TSAS and No TSAS. However, it is theorized that this change was incidental to changes in aileron response.

4.2.1.3 Aileron Response

The pilot's lateral control input can be measured through the RMS value of the lateral cyclic (aileron) input. As Figure 4-11 shows, there is a slight decreasing trend during the VOX phase, but this trend disappears during the steady state. In either case, statistical significance is not achieved.

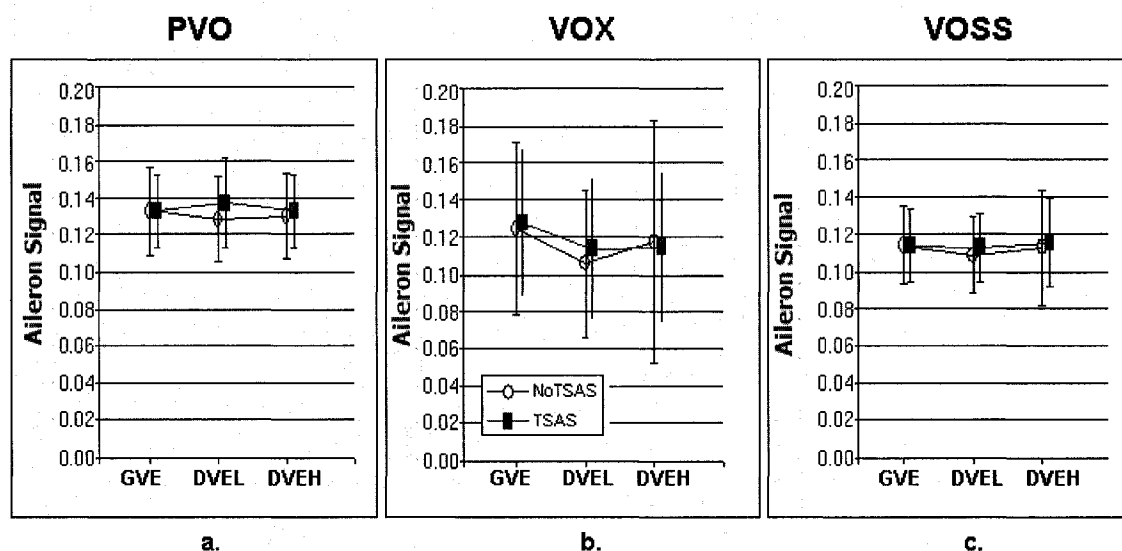


Figure 4-11 Aileron Response RMS

4.2.1.4 Longitudinal Axis Error Signal

The X-axis, with its poor quality visual cues, showed no significant trends in either the PVO or VOX phases. During the VOSS phase, the X-axis error was significantly **lower** for DVEH condition when compared to the GVE condition. This difference was present both with and without TSAS.

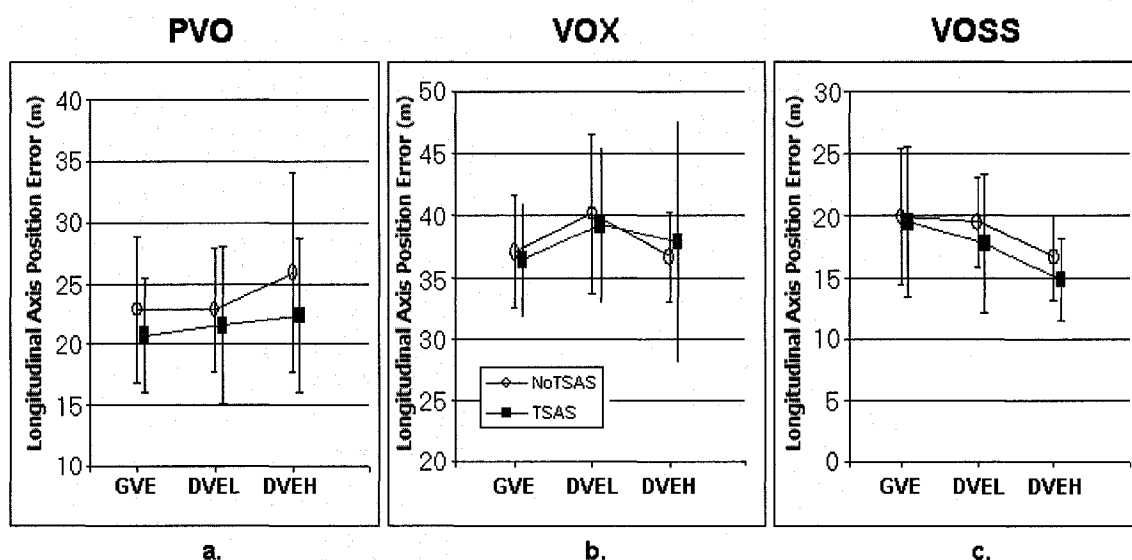


Figure 4-12 Longitudinal Axis Position RMS Error

This decrease in error may have been due to the poor quality of the visual signal in the X-axis and the comparatively high-resolution information available to the pilot when using the virtual “flight director” instrument. The absence of this trend during DVEL conditions may be attributable to the fact that the slightly degraded environment still provided visual cues and did not force a visual transition to a solely instrument scan, as was the case with the DVEH condition.

4.2.1.5 X-Axis Error Rate, Pitch Angle, and Pitch Rate

Error rate, pitch angle, and pitch rate failed to achieve any consistent significant results.

4.2.1.6 Elevator

Given the dynamic relationship between elevator position and pitch angle, rate and X-axis position, one would expect the trends to be similar for these variables; such was the case. Also, as was the case with the previous variables, an increasing trend is noted

during the DVEL condition. This trend is continued to a higher degree during the DVEH condition.

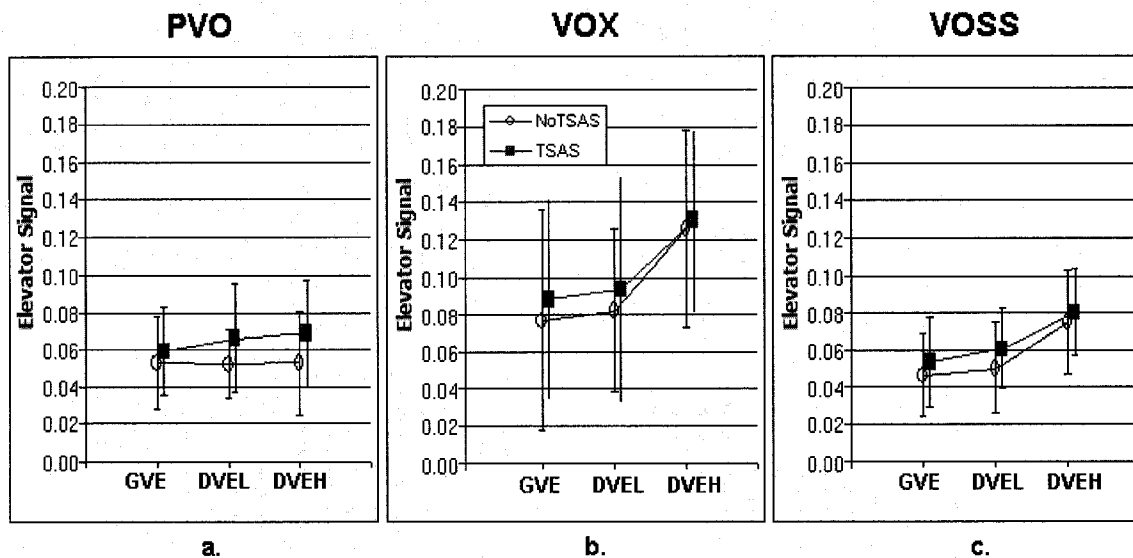


Figure 4-13 Elevator Response RMS

Without the benefit of TSAS, both the VOX and VOSS phases yielded statistically significant results ($p=0.04$ and $p=0.01$). With TSAS, the VOX condition did not achieve statistical significance between GVE and DVEH, but the VOSS condition did ($p=0.01$). This result might be caused by the increased position errors within this axis and the pilots' response to those errors.

4.2.2 Path Error

Due to the rapid adaptability of the pilot subjects, the gross summary variables failed to illuminate the true performance of the subjects and the effects of visual and tactile condition on the transient performance following the Visual Obscuration Event. By viewing the second-by-second path error of each condition immediately following the VOE, two things become apparent: that both visual and tactile conditions affect pilot performance and that the highly adaptable nature of the pilot quickly overcomes these

effects: following a brief transition period of degraded performance, the pilot is able to reevaluate the new scenario and can continue to function effectively.

4.2.2.1 Lateral Axis Path Error

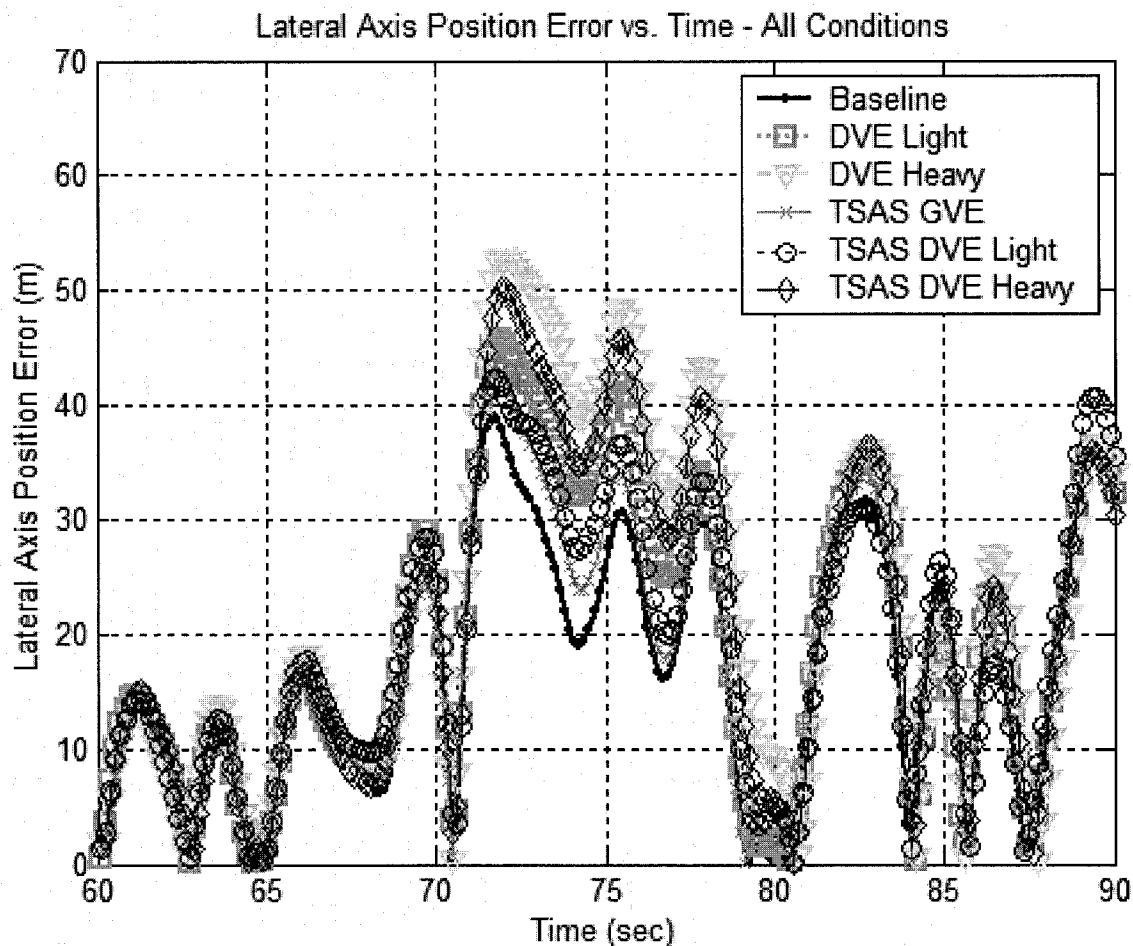


Figure 4-14 Lateral Axis Path Error

Figure 4-14 shows the average position error of the 12 pilots for each of the six conditions, plotted simultaneously. The absolute value of the error is presented since it was decided that the sign of the error was unimportant. Inspection of the full trial run revealed a statistically equivalent error among all conditions for the entire run with the exception of the seconds immediately following VOE. This result was expected during the PVO phase, when the visual condition is untrammelled for all trial conditions.

Perhaps unexpectedly, the error signal was also virtually the same during the VOSS phase, despite significant difference in the quality of the visual field. Viewing Figure 4-14, note that in all cases there is an increase in error. This increase is due to the disturbance signal. However, the pilots' ability to correct that disturbance is significantly lessened during conditions of degraded visual environment, more so for DVEH than DVEL. Additionally, in both cases TSAS assisted the pilots in regulating the disturbance signal and reducing the error.

Although a non-standard form of analysis, plotting the value of the t-test throughout the course of the trial is revealing in determining statistically different pilot performance. Figure 4-15 shows the t-test value at each data point for the time surrounding VOE. The value is found using the equation:

$$t = \frac{\bar{x}_1 - \bar{x}_2}{\sqrt{\frac{\sum x_1^2 - \frac{(\sum x_1)^2}{n_1} + \sum x_2^2 - \frac{(\sum x_2)^2}{n_2}}{n_1 + n_2 - 2} \left(\frac{1}{n_1} + \frac{1}{n_2} \right)}} \quad \text{Eq. 4.1}$$

The p-value can be found using the appropriate t-test table and the correct degrees of freedom, in this case 24, with two trials for each of the twelve subjects. For 24 degrees of freedom, the t value corresponding to a p-value of 0.05 is 2.064. The line of statistical significance is plotted in Figure 4-15. Note that there is no consistent statistical significance between any of the conditions prior to the visual obscuration event at 70 seconds. During the VOSS phase, there are occasional statistical differences between trials, particularly between the baseline and DVEH conditions, but the error vacillates between significantly higher error and lower error.

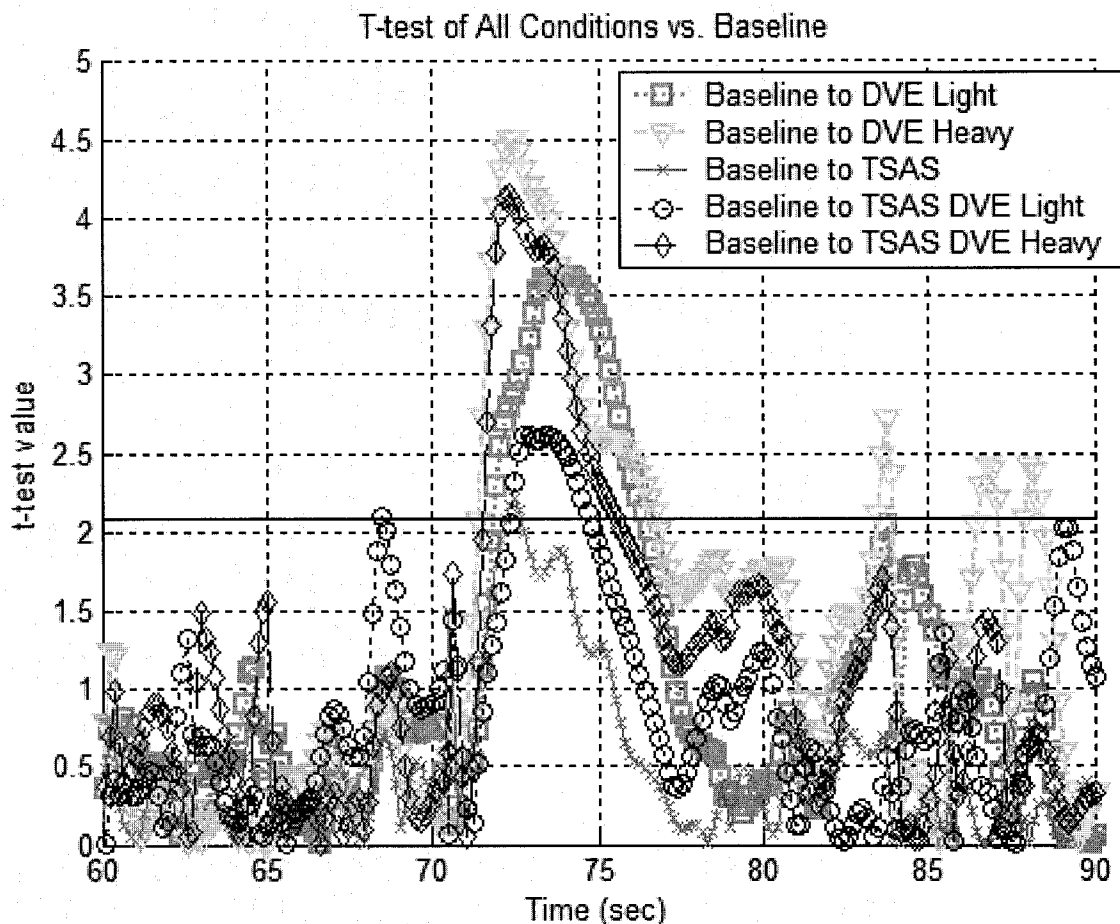


Figure 4-15 Lateral Axis T-test Values Between Baseline and Test Conditions

Only the transition period immediately following the VO shows a consistent trend in error and statistical significance between conditions. Although the inertia of the system requires a few moments for the disturbance to drive the various trials to levels of statistically significant difference, all five conditions showed significant differences from the baseline condition.

Figure 4-15 shows that the GVE TSAS trial barely achieves a level of statistical significance before pilot adaptation drives performance back to normal baseline behavior. Both DVEL conditions reach significance, although TSAS aids the pilot in maintaining a smaller difference and a faster recovery following the VOE. A similar trend is noted for

the DVEH condition where again both TSAS and No TSAS are significantly different and again TSAS is slightly closer to baseline and recovery is slightly faster.

Of all the findings, most impressive is the fact that in every case, the pilot adapted to bring the DVE condition back within the limits of statistical sameness within 7 seconds. Within 15 seconds, there is no discernable difference in pilot performance between conditions. Clearly the original assumption of a 30 second transition period grossly underestimated the speed and efficiency within which the human brain is able to construct a new strategy for effective control of the system, even with a severely degraded primary scan.

4.2.2.2 Longitudinal Axis Path Error

Perhaps due to the poor quality of the visual cues in the X-axis, path error analysis failed to yield results comparable to those found in the Y-axis analysis. The paths of the various conditions alternately cross above and below each other, with no correlation to visual condition or TSAS.

Figure 4-16 shows the position errors of the six conditions plotted simultaneously. As with the Y-axis, the path errors are consistent between pilots and conditions. However, unlike the Y-axis, the sameness is present during PVO, VOX, and VOSS conditions. Although there are occasional differences between conditions, there are no consistent trends present and the differences seem to indicate random occurrence rather than a measurable change in performance. Even immediately following VOE, the increase in error is nearly identical for all six cases. Neither visual nor tactile display status had any discernable affect on pilot performance. The poor quality of the X-axis visual cues may explain this result.

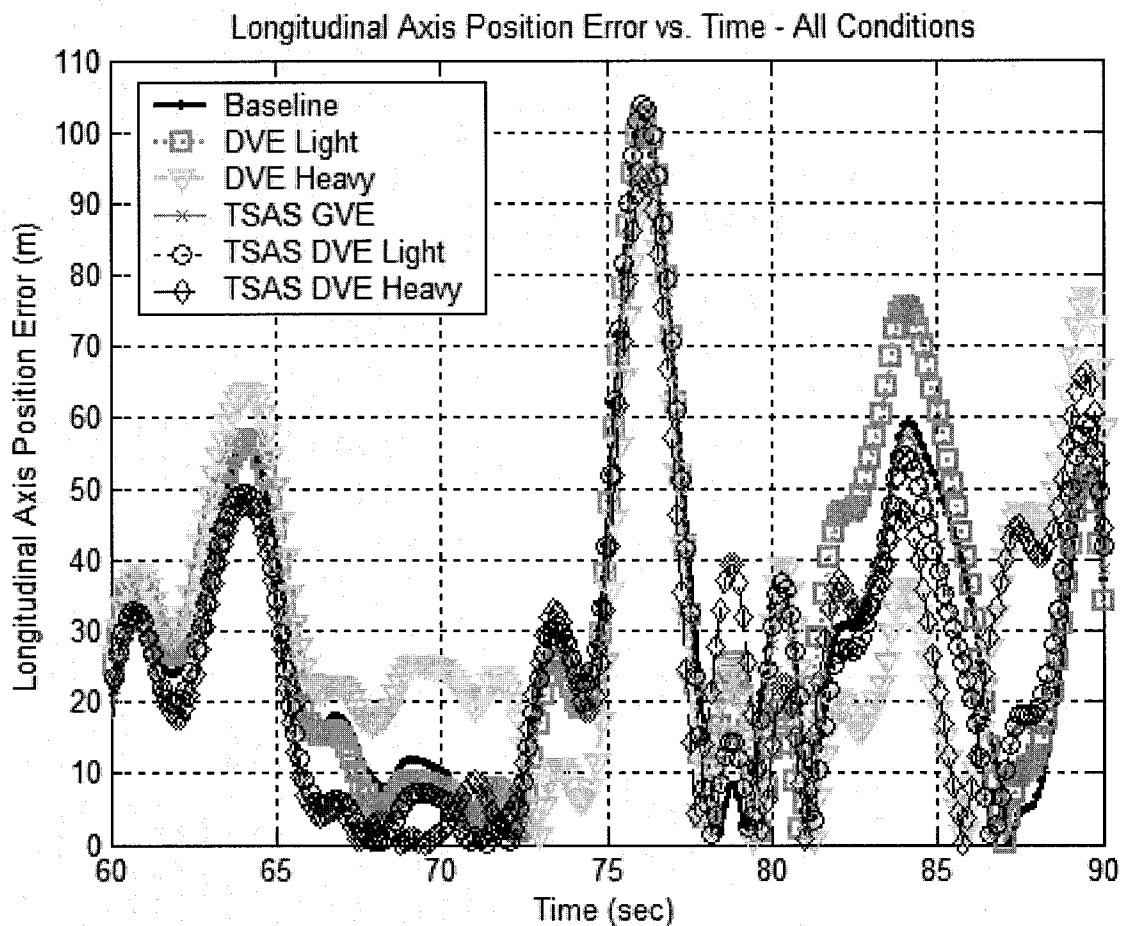


Figure 4-16 Longitudinal Axis Path Error

As for the longitudinal-axis, a t-test was performed between the X-axis baseline and all other conditions. There was no consistent significant difference between any conditions, even immediately following VOE.

Due to the lack of consistent change in performance, it is impossible to draw any conclusions regarding the speed with which a pilot can adapt. Future research must be designed to provide better visual cues in the X-axis in order to capture the nature of transient behavior in both, and perhaps in three, axes.

4.3 Model Structure

The final structure of the model will be revealed following introduction of each of the blocks in its final form. Following the heuristic strategy mentioned earlier, the blocks will be introduced in the following order: optimal feedback, neuromuscular effects, compensation block, nonlinear effect and estimator block. The final block is computed last since it assumes the pilot possesses full knowledge of his own strategic and physical dynamics.

4.3.1 Optimal Feedback

The optimal feedback gain follows the standard Algebraic Riccati Equation (ARE) to minimize the cost function stated in Equation 2.4 with two exceptions. First, the control rate term is not included. Instead, only the original Q and R matrices are used as cost matrices for the state and control magnitude. The devolution of control rate cost into a lag term was previously discussed and is unnecessary with the chosen model structure. Second, the matrices Q and R serve only to define the direction of the K vector, not the magnitude of it. The pilot compensation block will reset the feedback gain appropriately so the sole purpose of Q and R is to determine the relative gains applied to each state.

Pilot interviews stated unanimously that the only state that had an associated cost was the position error. Velocity, attitude and attitude rate were virtually ignored. This selection is consistent with the instructions given to the subjects; that only position is to be controlled. Though not the case for this investigation, in an actual aircraft, and perhaps even in a full-motion simulator, a non-zero cost would undoubtedly be assigned to all aircraft states. Unchecked oscillations in attitude or velocity could lead to disorientation, illness, or even (in the case of semi-rigid, underslung rotorheads) catastrophic “mast bumping.” Regardless, in the non-motion simulator, there was no perceived or actual penalty for large excursions in non-position states and no value was assigned.

Pilot interviews also stated that zero cost was associated with control inputs. This assignment is again consistent with pre-trial instructions. However, mathematical singularities prevent assignment of zero to the R matrix, which must be inverted in the ARE. Therefore, a small value of 10^{-12} was assigned.

As a point of interest, it should be noted that for small R , the vector K assigns very small values to the first, third, and fourth states (\dot{x} , $\dot{\theta}$, and θ) with the largest value assigned to the x state, just as one would expect. Interestingly, as R increases, the vector K becomes less weighted toward x and more weighted toward θ . Given the dynamics of the plant, this makes sense. The system is essentially an attitude command system, with a given aileron input driving the system to a given roll angle. Therefore, to prevent large control inputs, the system tends to minimize the associate state, in this case: θ .

4.3.2 Neuromuscular lag

The pilot neuromuscular term was not solved explicitly. Instead, estimated structures were assigned based upon previous research, predominantly the work of McRuer [1970] and Hess [1990]. For this research, comparative analysis of three potential models was performed, a zero order model (no neuromuscular effect), a 2nd order model, and a 3rd order model.

The basic structure of the second order model is:

$$\delta = \frac{\omega_n^2}{s^2 + 2\zeta\omega_n s + \omega_n^2} u_{NL} \quad \text{Eq. 4.2}$$

where δ is the command control signal (in unitless dimensions),

ω_n is the natural frequency (in radians per second),

ζ is the damping coefficient (in unitless dimensions),

and u_{NL} is the nonlinear control output (in unitless dimensions).

Hess found that values of $\omega_n = 20$ radians per second and $\zeta = 0.7$ were satisfactory parameters for a wide range of performance tasks.

The third order model includes the underdamped pair as before, but adds an additional lag term. The final structure is:

$$\delta = \frac{\omega_n^2}{(L_i s + 1)(s^2 + 2\zeta\omega_n s + \omega_n^2)} u_{NL} \quad \text{Eq. 4.3}$$

where δ is the command control signal (in unitless dimensions),

L_i is the lag time constant,

ω_n is the natural frequency (in radians per second),

ζ is the damping coefficient (in unitless dimensions).

and u_{NL} is the nonlinear control output (in unitless dimensions).

All three models were compared in order to ascertain the necessity of additional degrees of freedom.

4.3.3 Pilot Compensation

The pilot compensation block was identified in parallel with the neuromotor lag using the *PEM* function described in the Methods section. In this case the combination of pilot compensation structure with neuromuscular model order was evaluated in its ability to accurately model pilot performance. Numerous compensation structures were evaluated, including unstructured models that allowed the computer to find the best model of the assigned order.

Ultimately, the most consistent model structure contained a gain, a lead term, a lag term, and 2nd order Pade approximation of a pure time delay. The structure is shown below

$$u_c = \frac{G(s + n_{lead}) \left(s^2 - \frac{6}{\Delta} s + \frac{12}{\Delta^2} \right)}{(s + n_{lag}) \left(s^2 + \frac{6}{\Delta} s + \frac{12}{\Delta^2} \right)} u_o \quad \text{Eq. 4.4}$$

where u_c is the neuromuscular command signal output (in unitless dimensions),
 G is the forward loop gain of the compensator (in unitless dimensions),
 n_{lead} is the lead term frequency (in radians per second),
 n_{lag} is the lag term frequency (in radians per second),
 Δ is the effective time delay of the pilot model (in seconds),
and u_o is the optimal command signal (in unitless dimensions).

This result is completely consistent with McRuer's stated pilot strategies. In this case, once the system is stable (which it is, even open loop) the pilot adjusts the lag term to improve low frequency performance. Next the pilot develops a lead signal to try and improve high frequency performance. The delay is an inevitable part of any human task performance. Cognitive and neuromuscular delays are all represented by this term.

4.3.4 Nonlinear Effects

Up to this point, all of the effects discussed can be easily modeled using off-the-shelf linear tools. Though a large percentage of pilot performance can be captured using these tools, certain characteristics of pilot in the loop dynamics cannot be duplicated without delving into the nonlinear realm.

From the data recorded, the most obvious nonlinear effect is the non-continuous control strategy employed by every pilot throughout every trial. While the linear combinations of states all produce a smooth, continuous signal, the actual pilot output is notably discontinuous, with brief periods of movement followed by extended periods of inactivity. This "position-and-hold" strategy bespeaks the limitations of the pilot to think

and act simultaneously. Time is required to absorb incoming data, process it, decide upon the correct action, and then take action.

Stochastic analysis of the pilot control movement revealed several consistent interesting trends:

1. The pilot behavior can be broken down into periods of action (Movement) and inaction (Hold).
2. The decision to choose one action over another appears to be governed by a “fuzzy” equation.
3. Once the decision is made to act, the length of time of the action appears to be defined by a linear relationship with respect to command signal error, with Gaussian white noise injected over it.
4. The relationship between the length of the period and the magnitude of the control change also appears to be linear in nature, with normally distributed white noise present in the decision.
5. The variable periodicity of pilot movement has the effect of variable sampling rates of the continuous signal. This sampling introduces aliasing above the sampling Nyquist frequency. The end result is the introduction of broad-spectrum noise into the feedback signal. This phenomenon is particularly noticeable at the higher frequencies.

Graphical representations of the existing relationships will be discussed following a presentation of the complete model structure.

4.3.5 Final Model Structure

The complete model structure is shown in Figure 4-17. Note that the plant and display blocks are identical to the MOCM, as are the observation noise blocks, the optimal feedback gains, and the Kalman filter estimator. The desired signal is then processed by additional pilot strategy in a block called “Compensator & Time delay.” This block contains the gain and the lead/lag term discussed earlier, as well as the 2nd order Pade

approximation of a pure time delay. This delay represents the sum total of all of the computational and transmission delays, from display to control output.

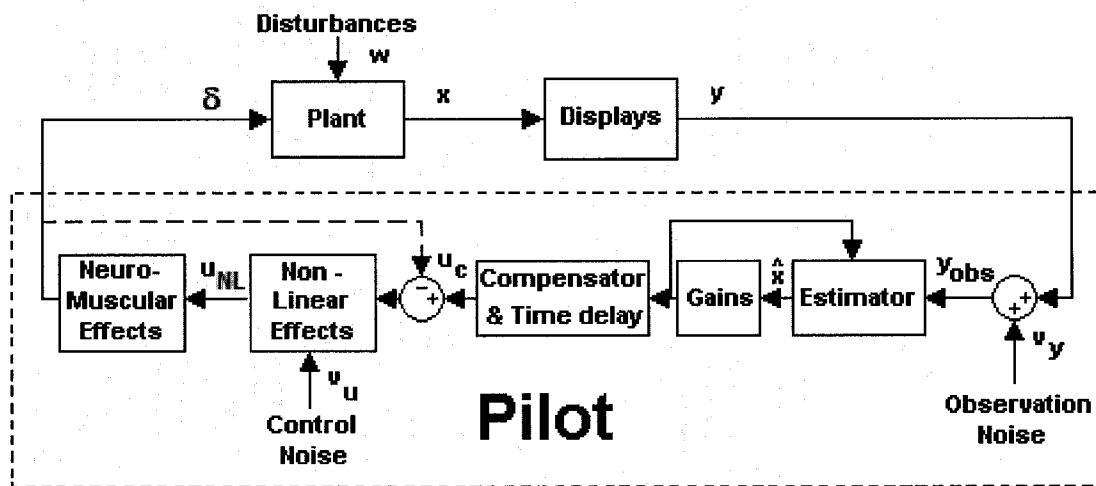


Figure 4-17 Modified Pilot Controller Model

Following the compensation block is the control signal negative feedback loop. This loop represents predominantly proprioceptive and, to some extent, visual feedback. It is logical that the pilot would use both muscular and visual means to identify that the position of the control matches the commanded control output, though during particularly demanding tasks, the majority of visual bandwidth would most likely be employed for primary task performance. This loop encompasses both the nonlinear block and the neuromuscular dynamics term. The proprioceptive feedback loop was applied only to the nonlinear model. It was deliberately removed from the linear model in an effort to eliminate neuromuscular feedback as the cause of the neuromuscular peak phenomenon. The nonlinear block uses a stochastic, or “fuzzy,” decision engine that drives the decision to move or remain static. The model then incorporates Gaussian white noise onto the command signal, which is driven through the neuromuscular dynamics. Given that most Bode plots of human performance exhibit a neuromuscular peak at around 20 radians per second, a third-order neuromuscular model is used here. The neuromotor dynamics and

nonlinear effects are applied to all output channels; in this case, both the aileron and elevator control output signals.

4.3.6 Model Dynamic Equations

The basic structure of the pilot plant system remains as defined in Equation 3.6, with the plant dynamics governed by the following equation:

$$\begin{aligned}\dot{x}_p &= Ax_p + B\delta + Ew \\ y_{obs} &= Cx_p + D\delta + v_y\end{aligned}\tag{Eq. 4.5}$$

where x_p is the plant state, $[x \ dx \ \theta \ d\theta]$,

δ is the control input to the plant from the pilot system (unitless),

w is the disturbance signal (meters per second),

v_y is the observation noise (same units as respective state),

and y_{obs} is the observed output, which includes all system states.

Due to the dynamics of the model used in this investigation, the D matrix is zero. This is typical of mechanical or massive systems, in which system inertia forces inputs to be shaped by the system dynamics prior to output.

Since it is assumed that the pilot estimator can reconstruct all states, including internal pilot states, the model will be built backward, starting with the controlled element, then the neuromuscular term, and finally the compensator term. Finally, the estimator dynamics will be applied to the entire pilot-vehicle model.

Given the new structure, the next relationship that must be identified is the neuromuscular term, which is governed by the following equations:

$$\begin{aligned}\dot{x}_{NM} &= A_{NM}x_{NM} + B_{NM}u_{NL} \\ \delta &= C_{NM}x_{NM} + v_u\end{aligned}\tag{Eq. 4.6}$$

where x_{NM} represents the internal states of the neuromuscular term,
 u_{NL} is the output from the nonlinear term,
 v_u represents the nonlinear neuromuscular control noise,
and δ is the control output of the pilot system.

To facilitate the closed form linear model, the nonlinear dynamics are simplified as a simple gain plus noise.

$$u_{NL} \approx C_{NL}(u_c - \delta)\tag{Eq. 4.7}$$

where u_c is the command signal input to the nonlinear term,
 δ is the control output of the pilot system,
and u_{NL} is the nonlinear term output.

Again it should be noted that for the linear model, control output feedback was eliminated.

The compensation dynamics are represented by the equations:

$$\begin{aligned}\dot{x}_c &= A_c x_c + B_c u_o \\ u_c &= C_c x_c + D_c u_o\end{aligned}\tag{Eq. 4.8}$$

where x_c represents the internal states of the compensation term,
 u_o is the optimal control signal,
and u_c is the command signal from the compensation term.

The complete model relating u_o to y_{obs} is:

$$\frac{d}{dt} \begin{bmatrix} x_p \\ x_{NM} \\ x_c \end{bmatrix} = \begin{bmatrix} A & BC_{NM} & 0 \\ 0 & A_{NM} & B_{NM}C_{NL}C_c \\ 0 & 0 & A_c \end{bmatrix} \begin{bmatrix} x_p \\ x_{NM} \\ x_c \end{bmatrix} + \begin{bmatrix} 0 \\ B_{NM}C_{NL}D_c \\ B_c \end{bmatrix} u_o + \begin{bmatrix} E & B \\ 0 & 0 \\ 0 & 0 \end{bmatrix} \begin{bmatrix} w \\ v_u \end{bmatrix} \quad \text{Eq. 4.9}$$

$$y_{obs} = \begin{bmatrix} C & 0 & 0 \end{bmatrix} \begin{bmatrix} x_p \\ x_{NM} \\ x_c \end{bmatrix} + v_y$$

or

$$\begin{aligned} \dot{\chi} &= A_1\chi + B_1u_o + E_1w_1 \\ y_{obs} &= C_1\chi + v_y \end{aligned} \quad \text{Eq. 4.10}$$

Here the model development reverts to the standard optimal Linear Quadratic Gaussian formulation, first using the optimal cost function to determine the feedback gain and then using the noise intensity to calculate the estimator gains.

The overall cost function can be rewritten

$$J_{OCM} = E_{\infty} \{ \chi^T Q_1 \chi + u_o^T R u_o \} \quad \text{Eq. 4.11}$$

where

$$Q_1 = \begin{bmatrix} Q & 0 & 0 \\ 0 & 0 & 0 \\ 0 & 0 & 0 \end{bmatrix} \quad \text{Eq. 4.12}$$

with no associated cost placed upon any of the internal pilot states.

Now, using the full plant described in Equation 4.10, the standard Algebraic Riccati Equation applies:

$$0 = (A_1)^T \Sigma + \Sigma A_1 + Q_1 - \Sigma B_1 R^{-1} (B_1)^T \Sigma \quad \text{Eq. 4.13}$$

and the solution relates u_o to the state χ :

$$u_o = -R^{-1} (B_1)^T \Sigma \chi \quad \text{Eq. 4.14}$$

or

$$u_o = -K \chi \quad \text{Eq. 4.15}$$

Once the optimal feedback gains are determined, the estimator gains can be computed. The estimator structure can be determined by solving the Algebraic Riccati Equation:

$$0 = A_1 \Sigma_1 + \Sigma_1 A_1^T + E_1^T W_1 E_1 - \Sigma_1 C_1^T (V_y)^{-1} C_1 \Sigma_1 \quad \text{Eq. 4.16}$$

where W_1 is $\text{diag}(W, V_w)$ $W_1 \geq 0$, and $(V_y) > 0$.

The solution to the equation yields the Kalman filter estimator gain L .

$$L = \Sigma_1 (C_1)^T (V_y)^{-1} \quad \text{Eq. 4.17}$$

The estimated states are then defined by:

$$\dot{\hat{\chi}} = A_1 \hat{\chi} + B_1 u_o + L (y_{obs} - \hat{y}) \quad \text{Eq. 4.18}$$

which can be simplified to:

$$\dot{\hat{\chi}} = (A_1 - LC_1) \hat{\chi} + LC_1 \chi + B_1 u_o + L v_y \quad \text{Eq. 4.19}$$

Now, by combining the actual and estimated states, the complete closed loop state space equation becomes:

$$\frac{d}{dt} \begin{bmatrix} \chi \\ \hat{\chi} \end{bmatrix} = \begin{bmatrix} A_1 & -B_1K \\ LC_1 & A_1 - LC_1 - B_1K \end{bmatrix} \begin{bmatrix} \chi \\ \hat{\chi} \end{bmatrix} + \begin{bmatrix} [E_1] & 0 \\ 0 & 0 & L \end{bmatrix} \begin{bmatrix} w \\ v_u \\ v_y \end{bmatrix} \quad \text{Eq. 4.20}$$

By evaluating the model and using matrix algebra, the matrices representing the pilot response can be found. Defining the input as the observed system outputs y_{obs} (although it could be argued that the observation noise is internal to the pilot model and therefore the input is the uncorrupted system output y) and the output as the control signal δ , the matrices are found to be analogous to the entire system. The ultimate structure desired for the pilot plant is:

$$\begin{aligned} \dot{\chi}_p &= A_p \chi_p + B_p y_{obs} \\ \delta &= C_p \chi_p + D_p y_{obs} \end{aligned} \quad \text{Eq. 4.21}$$

Equations 4.6 through 4.8 can be manipulated to yield:

$$\begin{aligned} \frac{d}{dt} \begin{bmatrix} x_{NM} \\ x_c \end{bmatrix} &= \begin{bmatrix} A_{NM} & B_{NM} C_{NL} C_c \\ 0 & A_c \end{bmatrix} \begin{bmatrix} x_{NM} \\ x_c \end{bmatrix} + \begin{bmatrix} B_{NM} C_{NL} D_c \\ B_c \end{bmatrix} u_o + \begin{bmatrix} 0 \\ 0 \end{bmatrix} v_u \\ \delta &= [C_{NM} \quad 0 \quad 0] \begin{bmatrix} x_{NM} \\ x_c \end{bmatrix} + 0u_o + v_u \end{aligned} \quad \text{Eq. 4.22}$$

The governing equations for the estimator and optimal gains remain the same, although the system states cannot be properly included in the final pilot matrices. By using the estimated states, the uncontrolled and unestimated system can be written as:

$$\frac{d}{dt} \begin{bmatrix} \hat{\chi} \\ x_{NM} \\ x_c \end{bmatrix} = \begin{bmatrix} A_1 - LC_1 - B_1K & 0 & 0 \\ -B_{NM}C_{NL}D_cK & A_{NM} & B_{NM}C_{NL}C_c \\ -B_cK & 0 & A_c \end{bmatrix} \begin{bmatrix} \hat{\chi} \\ x_{NM} \\ x_c \end{bmatrix} + \begin{bmatrix} L \\ 0 \\ 0 \end{bmatrix} y + \begin{bmatrix} L \\ 0 \\ 0 \end{bmatrix} v_y$$

Eq. 4.23

$$\delta = \begin{bmatrix} 0 & C_{NM} & 0 \end{bmatrix} \begin{bmatrix} \hat{\chi} \\ x_{NM} \\ x_c \end{bmatrix} + v_u$$

which can be simplified as:

$$\begin{aligned} \dot{\chi}_p &= A_p \chi_p + B_p y + E_p v_y \\ \delta &= C_p \chi_p + v_u \end{aligned}$$

Eq. 4.24

The resulting complete state space model is represented in Figure 4-18.

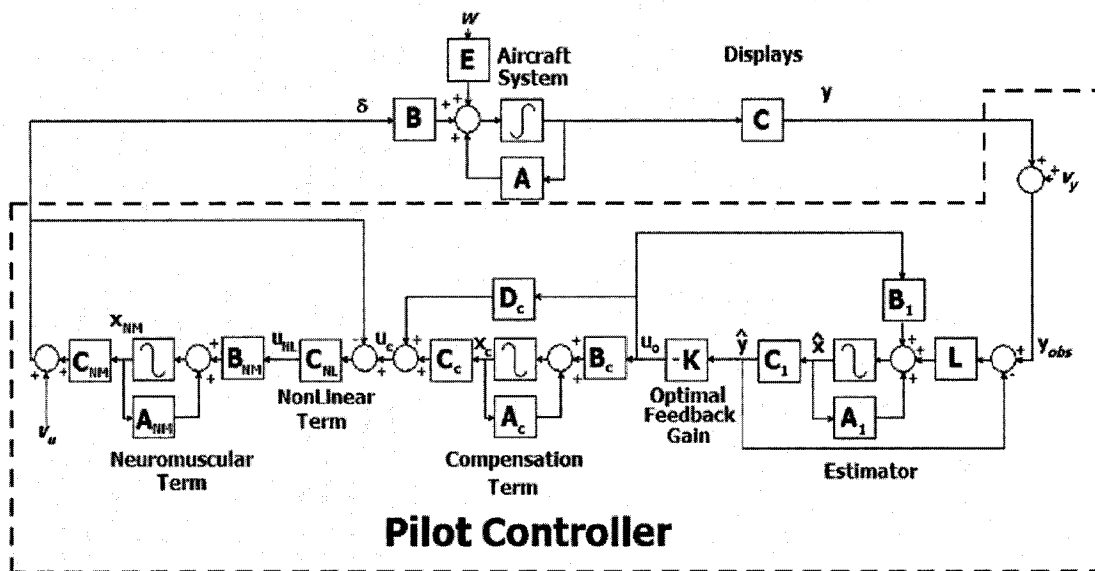


Figure 4-18 Modified Pilot Controller Model - State Space Format

Isolating the nonlinear term is possible by breaking the system at u_o , and eliminating the neuromuscular term, defining u_{NL} as the system input and $\delta - u_c$ as the system output.

Following removal of the neuromuscular term, the remaining x and x_c variables have the relationship:

$$\begin{aligned} \frac{d}{dt} \begin{bmatrix} x_p \\ x_c \end{bmatrix} &= \begin{bmatrix} A & 0 \\ 0 & A_c \end{bmatrix} \begin{bmatrix} x_p \\ x_c \end{bmatrix} + \begin{bmatrix} 0 \\ B_c \end{bmatrix} u_o + \begin{bmatrix} B \\ 0 \end{bmatrix} u_{NL} + \begin{bmatrix} E & B \\ 0 & 0 \end{bmatrix} \begin{bmatrix} w \\ v_u \end{bmatrix} \\ u_c - \delta &= \begin{bmatrix} 0 & C_c \end{bmatrix} \begin{bmatrix} x_p \\ x_c \end{bmatrix} + D_c u_o - u_{NL} - v_u \end{aligned} \quad \text{Eq. 4.25}$$

Since we have already shown that $u_o = -K\hat{\chi}$ and the dynamics for the estimator are known, the final set of equations can be written:

$$\begin{aligned} \frac{d}{dt} \begin{bmatrix} \hat{\chi} \\ x_p \\ x_c \end{bmatrix} &= \begin{bmatrix} A_1 - LC_1 - B_1K & L_1C & 0 \\ 0 & A & 0 \\ -B_cK & 0 & A_c \end{bmatrix} \begin{bmatrix} \hat{\chi} \\ x_p \\ x_c \end{bmatrix} + \begin{bmatrix} 0 \\ B \\ 0 \end{bmatrix} u_{NL} + \begin{bmatrix} 0 & 0 \\ E & B \\ 0 & 0 \end{bmatrix} \begin{bmatrix} w \\ v_u \end{bmatrix} + \begin{bmatrix} L \\ 0 \\ 0 \end{bmatrix} \begin{bmatrix} y \\ \end{bmatrix} \\ u_c - \delta &= \begin{bmatrix} -D_cK & 0 & C_c \end{bmatrix} \begin{bmatrix} \hat{\chi} \\ x_p \\ x_c \end{bmatrix} - u_{NL} - v_u \end{aligned} \quad \text{Eq. 4.26}$$

which can be simplified as:

$$\begin{aligned} \dot{\chi}_{NL} &= A_{NL}\chi_{NL} + B_{NL}u_{NL} + E_{NL}w_{NL} + v_y \\ u_c - \delta &= C_{NL}\chi_{NL} + D_{NL}u_{NL} - v_u \end{aligned} \quad \text{Eq. 4.27}$$

The structure shown in Equation 4.27 allows the logic of the nonlinear term to be evaluated with the model system dynamics in place.

4.4 Validation of Model Subcomponents

The model showed excellent ability to match both time and frequency domain characteristics of pilot performance. The effect of the terms will be introduced using a “building block” methodology, with each new term adding to the effectiveness of the

previous. The MATLAB script *XAXIS_MODEL_REVIEW.m* performed all calculations and plots.

4.4.1 Optimal Feedback Gain

The use of the optimal feedback gain in pilot modeling was well documented as an effective means of replicating man-in-the-loop performance and this investigation was no exception. Figure 4-19 compares the experimental transfer function to the calculated closed loop system. The transfer function is calculated by dividing the cross spectral density of system disturbance w in relation to position error x (CSD_{wx}) by the power spectral density of x (PSD_{xx}). Note the nearly perfect match of the closed loop system to the experimental transfer function at the discrete frequencies present in the disturbance function.

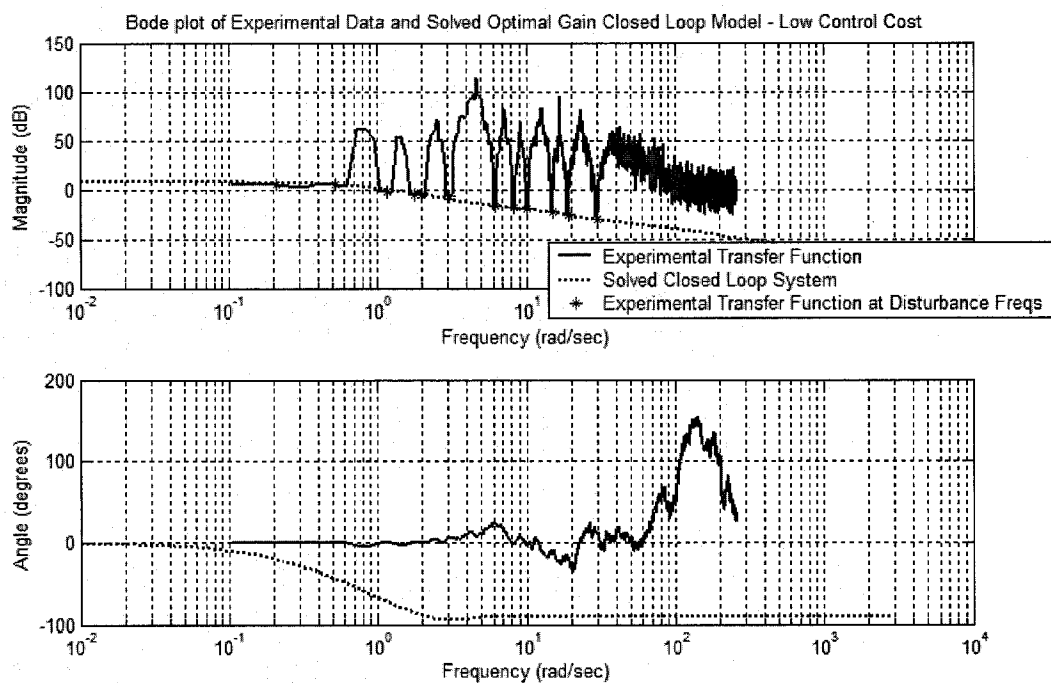


Figure 4-19 Optimal Feedback Gain - Frequency Domain Response

However, note the excessive noise present at other frequencies and the lack of fidelity in phase throughout all frequencies. The noise is presumably due to the pilot injected neuromuscular noise which has not been modeled for this single-term evaluation. The lack of phase fidelity may be partially due to the inability of the script to properly *unwrap* the phase signal, resulting in an inaccurate experimental phase result.

The time domain plot of the linear modeled command signal and the actual aileron signal shows that, despite transfer function agreement at driving frequencies, the model fails to accurately model the character of the real aileron signal. Although many of the gross dynamics are present, the peaks are not as large, the faster dynamics are completely missed and the nonlinear “move-and-hold” response is not evident.

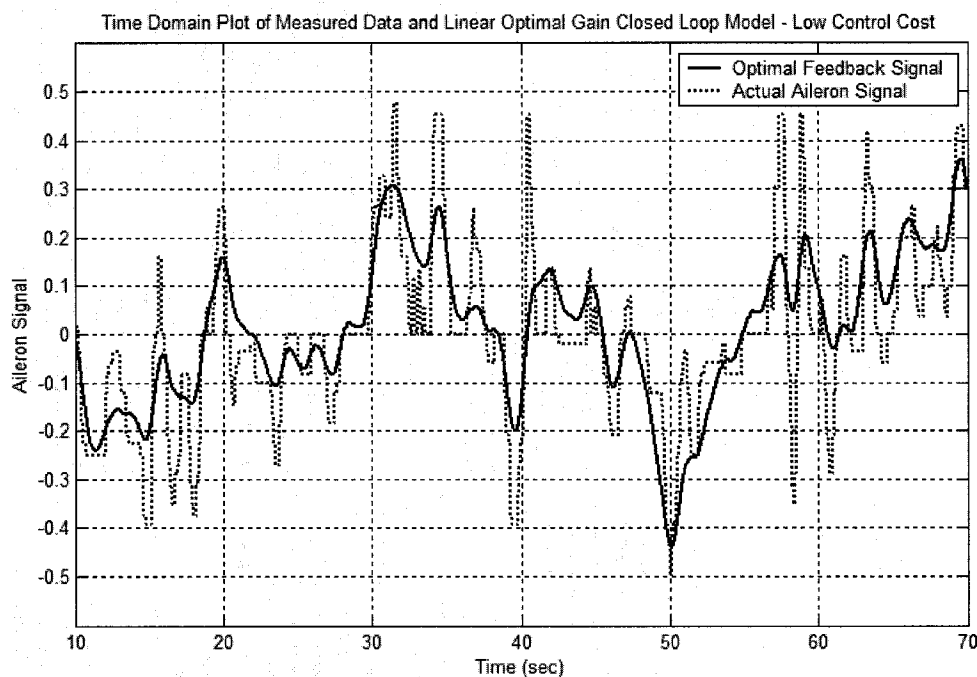


Figure 4-20 Optimal Feedback Reconstruction of Linear Aileron Signal

4.4.2 Compensator Term

The structured form of the compensator is of the form given in Equation 4.4. Analysis of an indicative run is shown in Figure 4-21, in this case Subject A, Trial # 1. The figure

compares the structured model solution to three unstructured solutions in which the computer finds the best fit of that order. Note that even the third order unstructured model did not achieve a solution comparable to that of the structured model. The fit is printed to the right of the plot for clarification. The failure of the unstructured models to accurately capture the pilot strategy is primarily due to the computer's inability to solve for a pure time delay using partial differential numerical methods. The algorithm must be directed to include a Pade approximation of a pure time delay. The solution using only unpaired poles and zeros yields a solution significantly less accurate than the structured model.

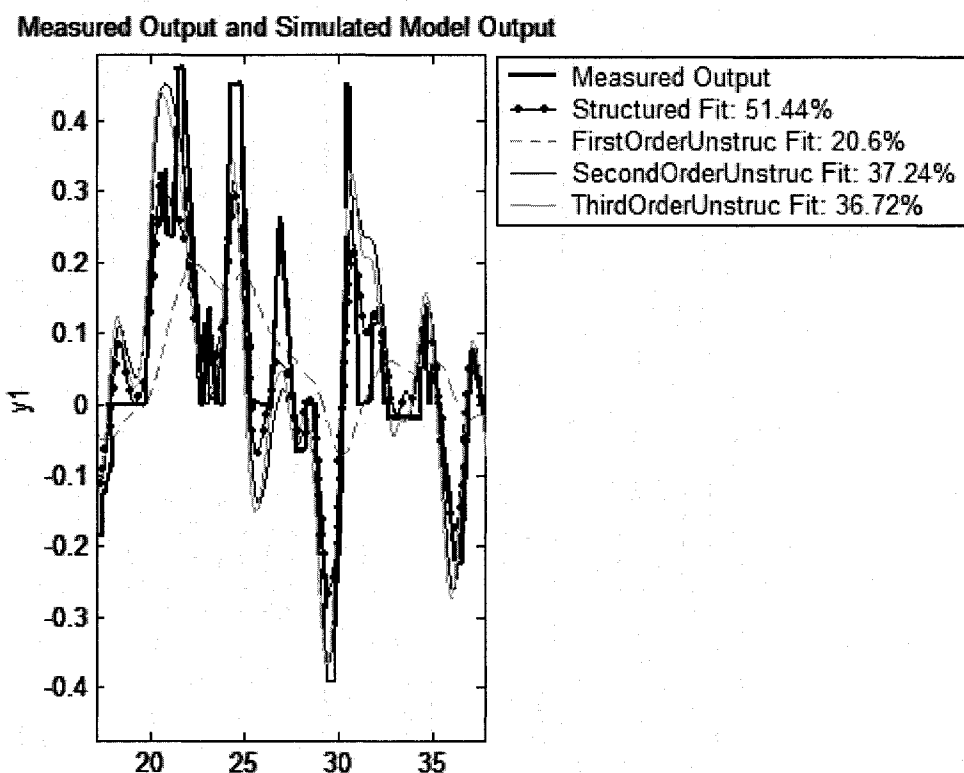


Figure 4-21 Various Structured Compensators' Performance - Time Domain

The structured model is, however, able to attain a satisfactory model of actual performance (linear). In this case, the final model solution is:

$$u_c = \frac{3.75 \times 10^{-7} (s + 1.07) \left(s^2 - \frac{6}{0.14} s + \frac{12}{0.14^2} \right)}{(s + 6.18) \left(s^2 + \frac{6}{0.14} s + \frac{12}{0.14^2} \right)} u_o \quad \text{Eq. 4.28}$$

Note the relative magnitudes of the lead and lag terms. In this case, the pilot lead term takes effect at a lower frequency than the lag term. This is indicative of additional effort by the pilot on maintaining good performance at higher frequencies. The delay of 0.14 seconds is a realistic estimate of cognitive delays during system reconstruction and strategic planning. The specific parameters associated with all subjects and conditions will be discussed later.

4.4.3 Neuromuscular Terms

The effectiveness of each of the three neuromuscular models in matching the frequency domain performance is plotted below in Figure 4-22. Note that of the three models, the zero-order model most closely matches the value of the actual transfer function, particularly at the discrete frequencies of the disturbance signal. At the higher frequencies, the underdamped pair pushes the magnitude far lower than that of the actual transfer function magnitude.

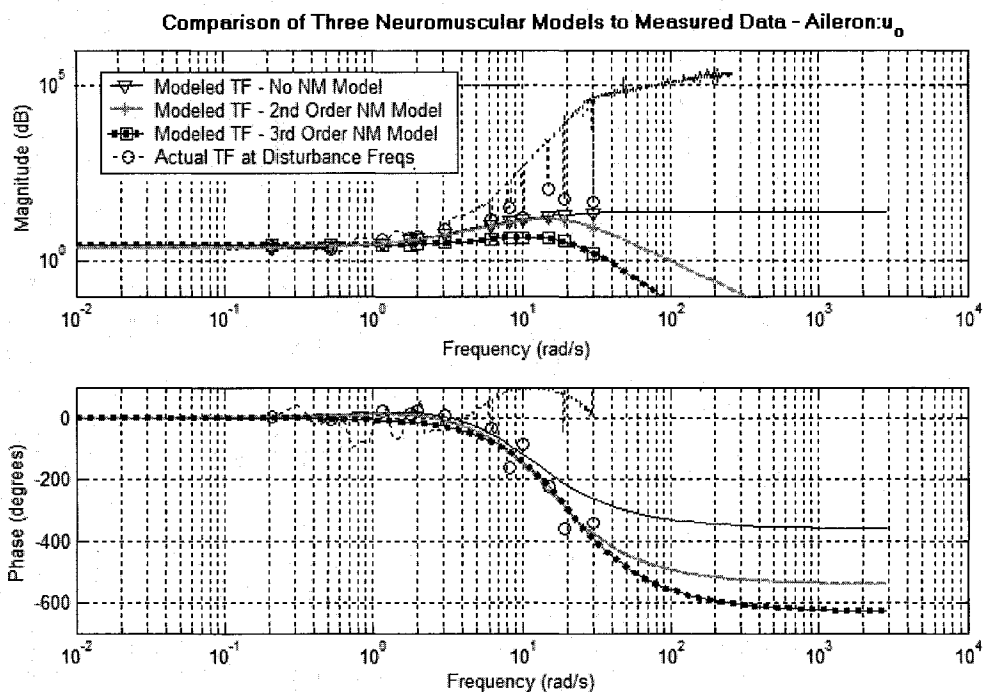


Figure 4-22 Comparison of Neuromuscular Models - Frequency Domain

However, none of the models satisfactorily models the frequency spectrum of the transfer functions at frequencies other than those present in the disturbance function. The high frequency noise is again present and again defies accurate modeling by the present structure.

A time domain analysis of the actual aileron signal vs. the neuromuscular term signal showed that again, the zero-order model appears to be the best fit, but none of the models is close to 100% effective in matching the actual control signal. The lack of fidelity and a potential cause for the lack of agreement between actual and recorded data will be discussed following presentation of the final model.

4.4.4 Nonlinear Dynamics

This term was a late development based upon observed behavior and the failure of linear terms to accurately model all characteristics of pilot performance. The final structure of the nonlinear model consists of three components:

1. Determination of Action (Hold, Move Aileron Left, Move Aileron Right)
2. Determination of Length of Action (How many time steps)
3. Determination of Magnitude of Action (How far to move Aileron)

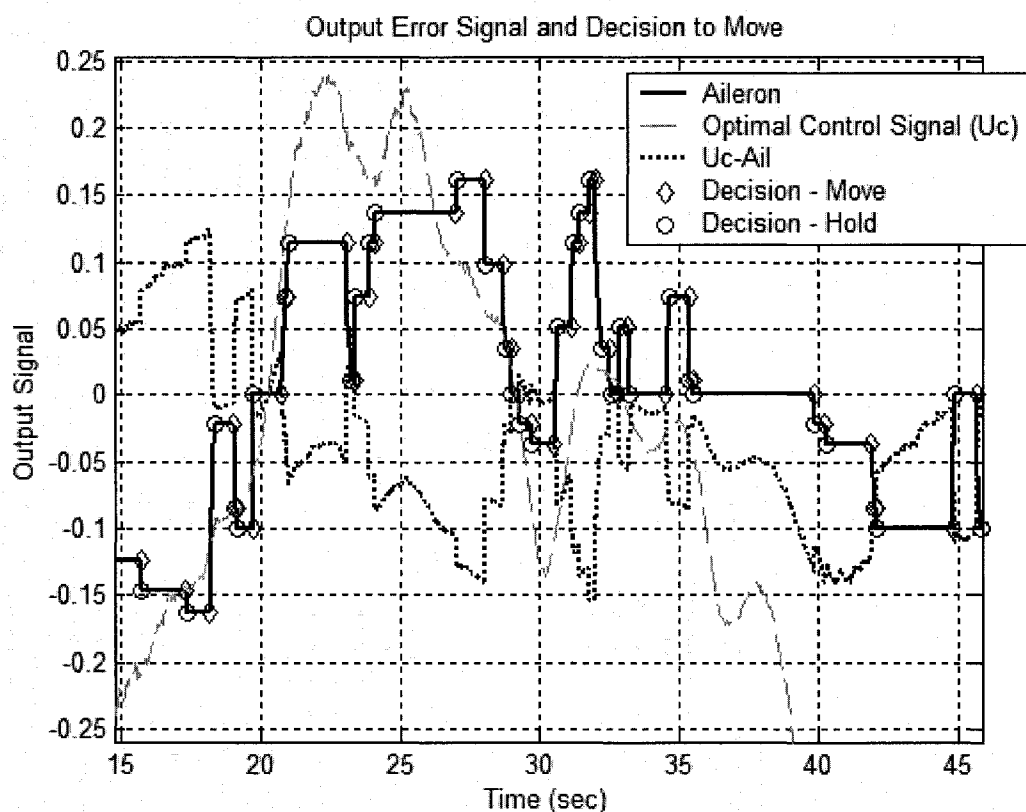


Figure 4-23 Recorded Aileron Signal - "Move and Hold"

The behavior of the pilot is not continuous, but rather a string of movements, each of which is of a predetermined length and character. Analysis of the aileron signal allows each phase to be captured and defined. Figure 4-23 shows a typical control run, in this

case Subject C, trial #3. Note the characteristic “move-and-hold” nature of the response, with brief periods of motion interspersed with long periods of inactivity.

The decision to move the controls or hold them immobile is not a clearly definable function, but rather a stochastic relationship by which each value of “command signal error” is associated with a likelihood of each of the three choices. Figure 4-24 shows a typical stochastic function versus command signal error. There is clearly a relationship between signal error and the decision to move up (right) or down (left), though likelihood of remaining immobile seems invariant with respect to signal error. This relationship was found to be present and consistent for all subjects and all conditions.

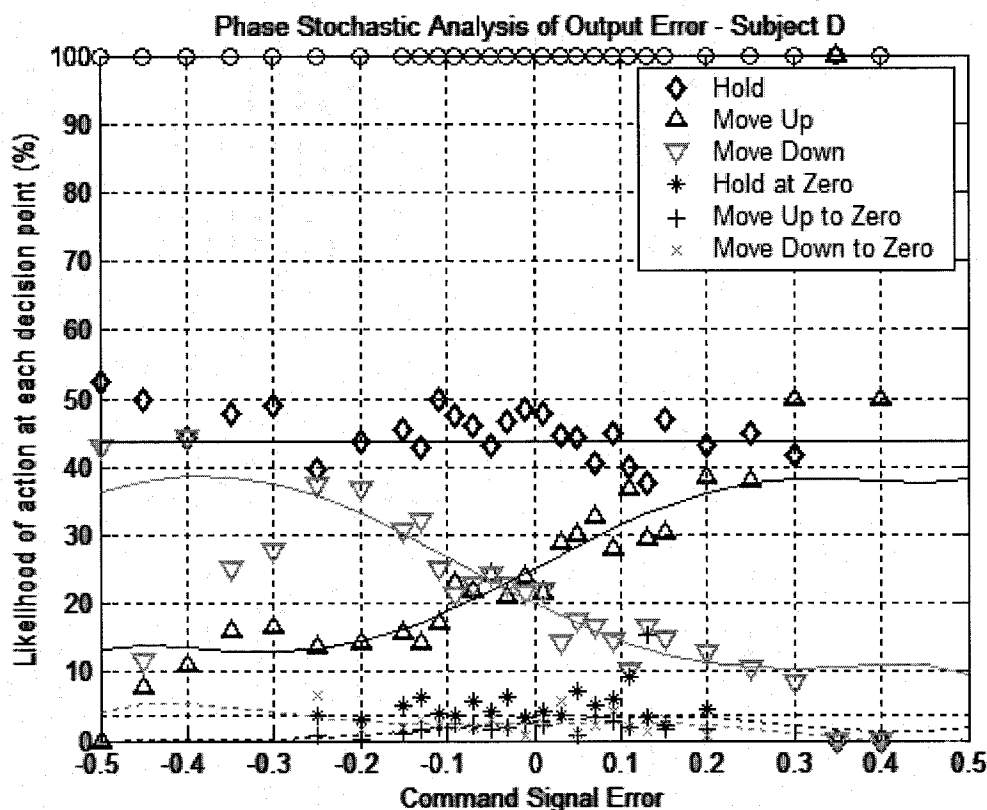


Figure 4-24 Stochastic Analysis of Pilot Decision

Once the pilot decides whether to move the aileron or hold, the duration of the period must be determined. Inspection of the relationship in Figure 4-25 shows a spread of data

across the range of command signal error whose exact relationship is difficult to quantify through a simple linear regression. A different means of analysis is required.

As an alternative, each decision was analyzed separately, with a stochastic analysis conducted relating the likelihood of each period length (number of timesteps) to the command signal error at the beginning of the phase. The individual likelihood of action at each point was then summed to yield a cumulative probability. The result is the three dimensional plot shown in Figure 4-26.

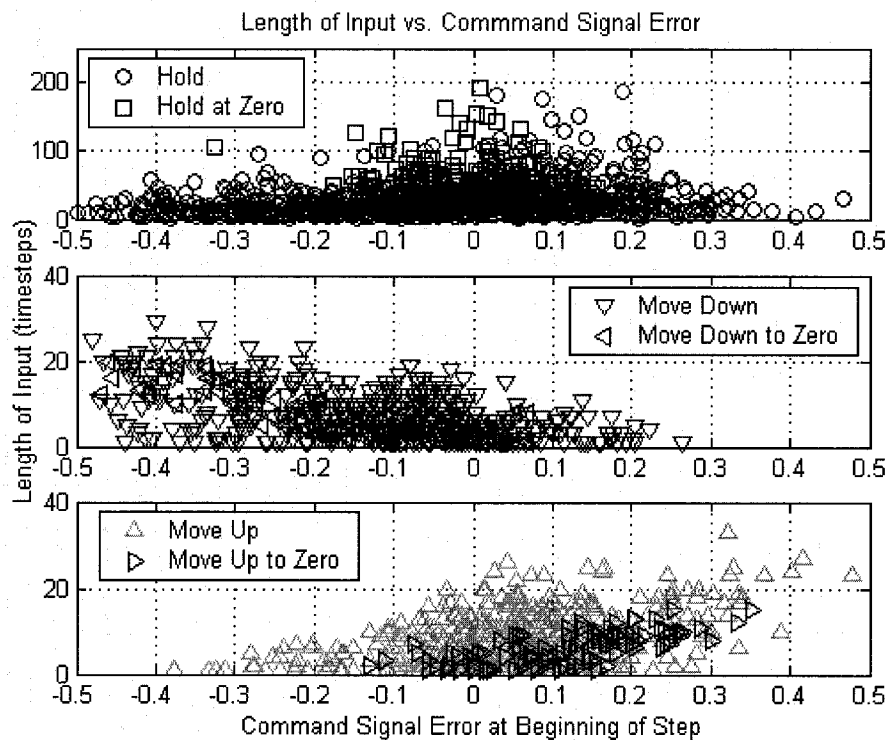


Figure 4-25 Length of Decision Phase vs. Command Signal Error

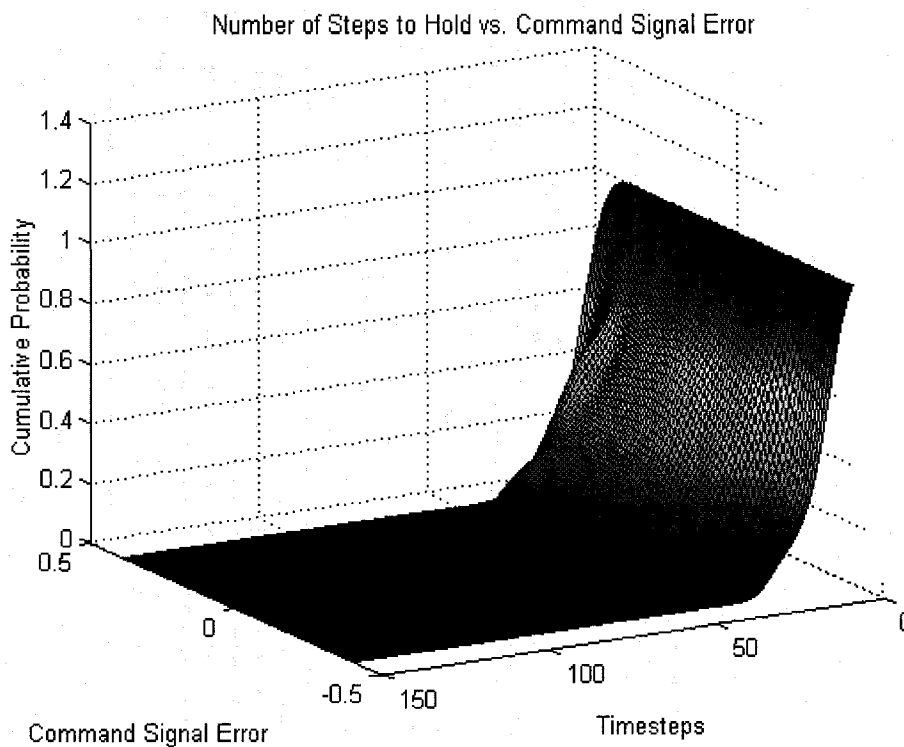


Figure 4-26 Cumulative Probability of Length of Hold vs. Command Signal Error

There is a small, but undeniable effect of signal error upon length of the hold, with a higher likelihood of longer holds at or near zero error. Interestingly, a cross section of the plot, shown in Figure 4-27 looks almost exactly like the cumulative probability distribution of a half of a normally distributed function. This may indicate that the relationship between length of hold and command signal error is, in fact, a linear relationship with Gaussian white noise added.

A similar relationship exists between command signal error and the length of aileron movement left or right (down or up), although the length of the periods are shorter. Figure 4-28 a. and b. shows the analogous relationship and the relative homogeneity of the relationships. Again, a cross section of the plot reveals a relationship that most likely can be represented by a linear relationship between command signal error and length of movement with Gaussian white noise added.

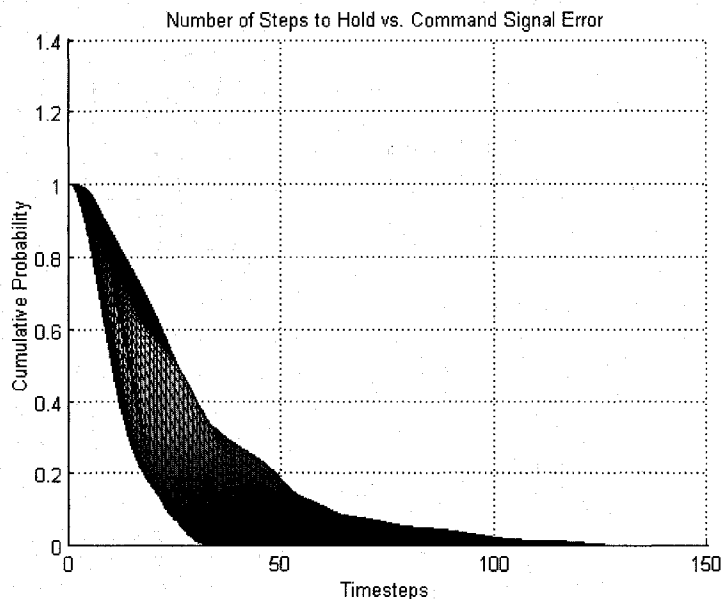


Figure 4-27 Cross Section of Cumulative Probability of Length of Hold vs. Command Signal Error

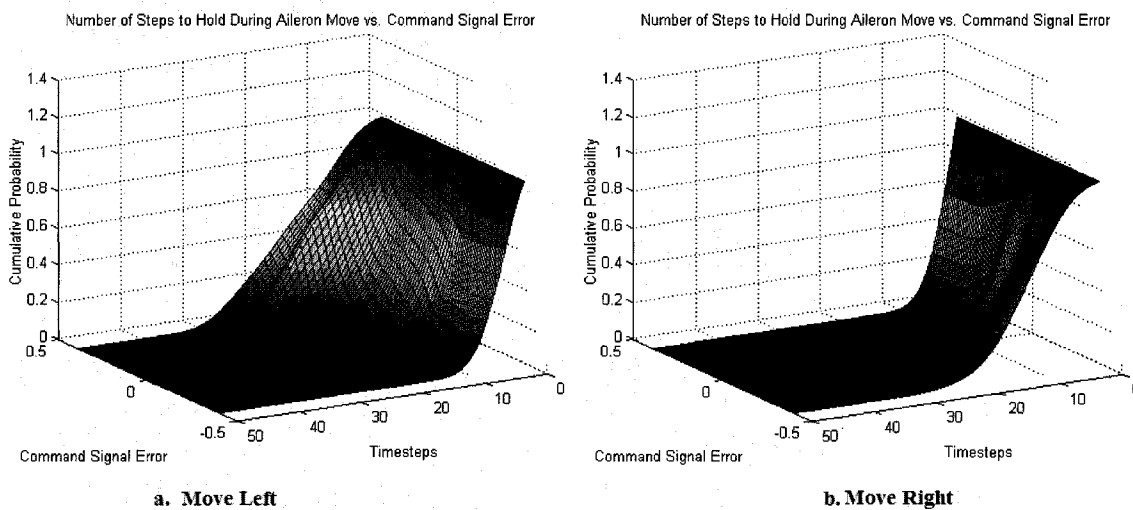


Figure 4-28 Cumulative Probability of Aileron Movement Left and Right vs. Command Signal Error

Once the length of period is determined, the magnitude of the change in control output must be determined (for movement only). Figure 4-29 shows that there is clearly a

relationship between the length of the movement and the magnitude of the control change in that longer movement correlates nearly linearly to longer aileron movement.

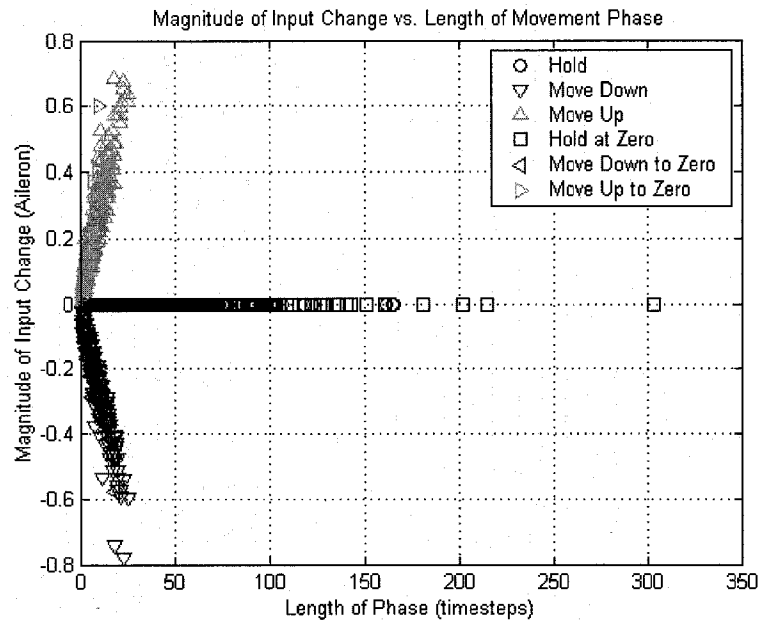


Figure 4-29 Magnitude of Aileron Change vs. Number of Timesteps

Stochastic mapping, shown in Figure 4-30 shows the three dimensional cumulative probability of both left and right movement vs. number of timesteps. Note the extremely smooth shape of the probability surface due to the very linear relationship between number of timesteps and distance moved. The cross section of the right movement, shown in Figure 4-31, is a perfect match of the cumulative probability distribution of half of a Gaussian signal (half of the distribution is due to the impossibility of negative movement).

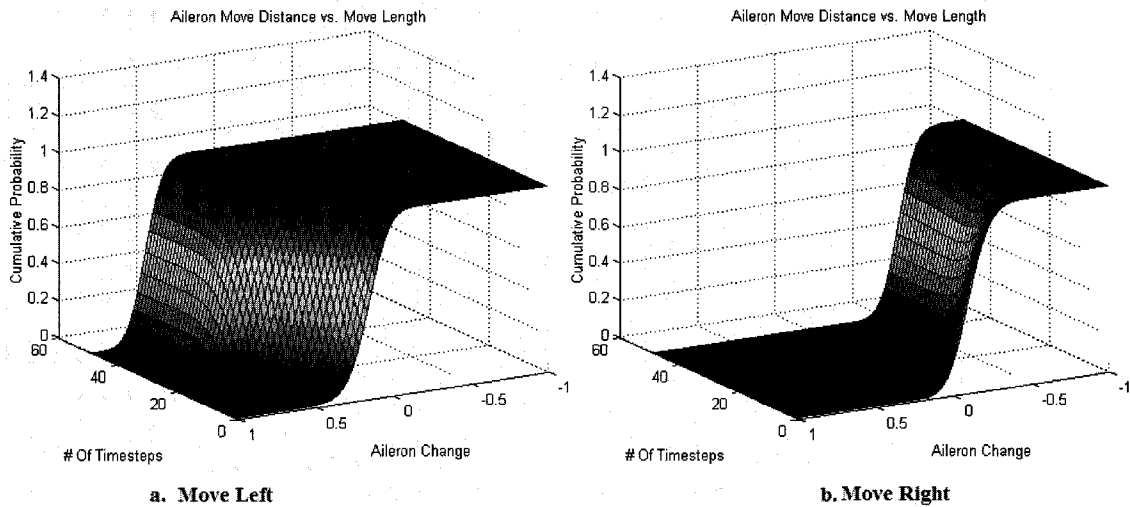


Figure 4-30 Cumulative Probability of Aileron Change vs. Length of Movement

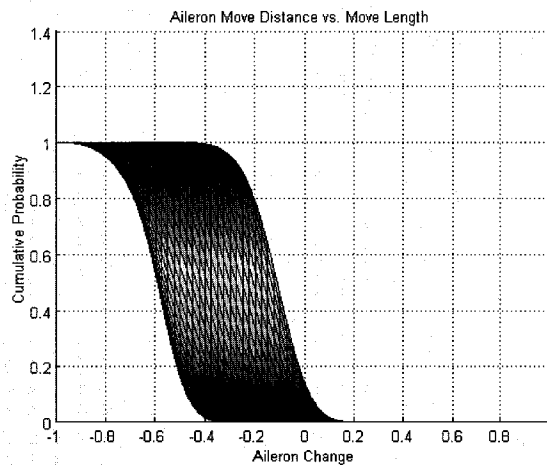


Figure 4-31 Cumulative Probability of Aileron Change to the Right

Although the stochastic nature of the nonlinear term precludes identical match of the time domain signal, the frequency domain signal shows significant improvement in correlation. Figure 4-32 shows the first order effect of discretization of the linear signal through nonlinear move and hold behavior. The additional noise causes the Bode plot magnitudes to increase dramatically, coming within a few decibels of matching the nonlinear signal exactly.

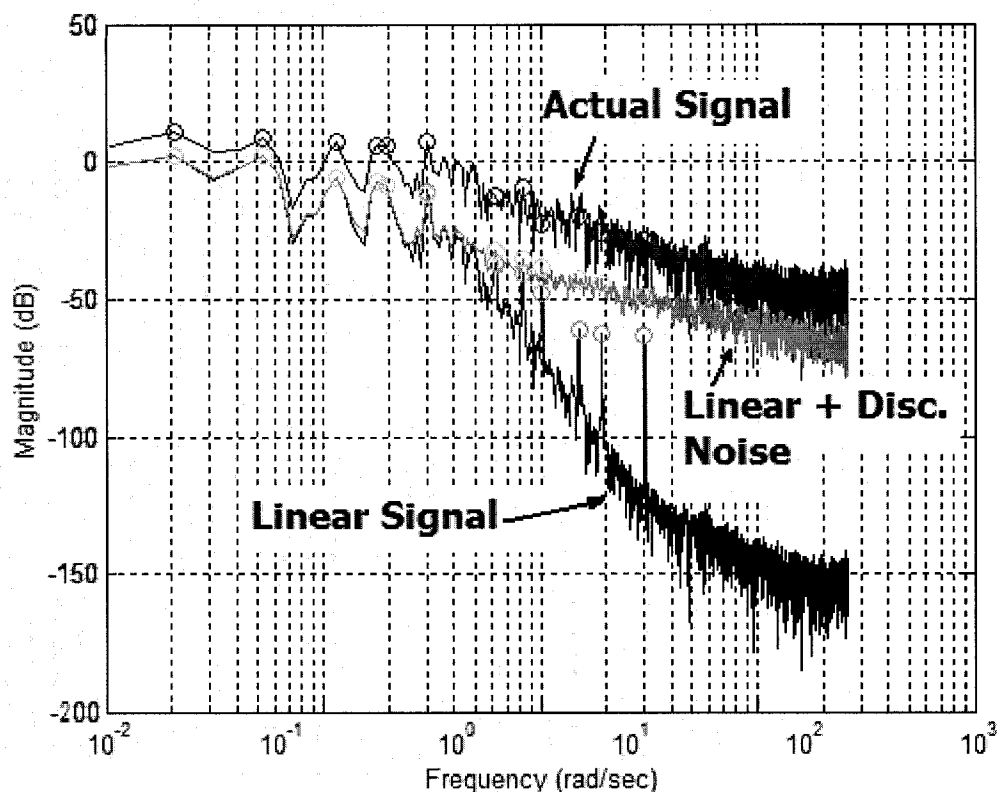


Figure 4-32 Frequency Domain Effects of Random "Move-and-Hold"

This "move-and-hold" phenomenon and its effect upon frequency domain characteristics will be revisited during the in depth explanation of model performance.

4.5 Complete Model Solution

Inspection of the model parameters revealed several features of the pilot performance during visually occluded conditions. They will be discussed by individual blocks, then as an entire model. First, a summary of the solution protocols will be reviewed.

4.5.1 Parameter Identification Sequence

The model solution involves identification of model parameters that best match empirical data. The parameter identification was calculated using the following steps:

The script `XAXIS_NM_MODELCALC` performs steps 1 through 7.

1. Construct matrices appropriate to controlled element dynamics.
2. Augment the system using the 3rd order neuromuscular term.
3. Assign a Q and R appropriate to the pilot reports of cost for state and control.
4. Solve for optimal control feedback gain K .
5. Load experimental data and extract appropriate variables.
6. Using the state variables and K , calculate the control term u_o .
7. Solve the structured compensator *Gain, Denominator, Numerator, and Delay*.

This script utilizes the built-in MATLAB function `PEM` and the scripted function `PILOTPARAM.m` to solve the parameters for each trial.

The script `XAXIS_MODEL_SIM_LINEAR` performs steps 8 through 11.

8. Augment the system matrices with the new compensator dynamics.
9. Calculate the linear time invariant transfer functions for closed loop and pilot loop.
10. Utilize the empirical observation error values to solve the estimator gain at each time step. This results in a linear, time-varying estimator.
11. Simulate full run through step-by-step simulation and calculation.

The script `XAXIS_SIM_PLOT_LINEAR` performs step 12.

12. Calculate summary variables, PSD values, and transfer functions.

In summary, most of the structure is unchanging from trial to trial. The pilot structure is defined through selection of the neuromuscular block, the optimal feedback matrices, and the empirical observation errors, which were determined empirically during independent trials. The NM block, feedback matrices, and observation noise remain constant for each subject. For each trial, the recorded variables are used to solve the pilot compensation

dynamics, and then to generate the closed loop performance of the model. The estimator gain is calculated at each timestep based upon the magnitude of each of the states and their corresponding observation error.

4.5.2 Estimator

The estimator dynamics were defined by the magnitudes of the observation noise with respect to the magnitude of the disturbance signal, in this case, both the disturbance and the neuromuscular noise. As can be seen in Figure 4-33, the Good Visual Environment succeeded in changing the closed loop poles more significantly than the Degraded Visual Environment.

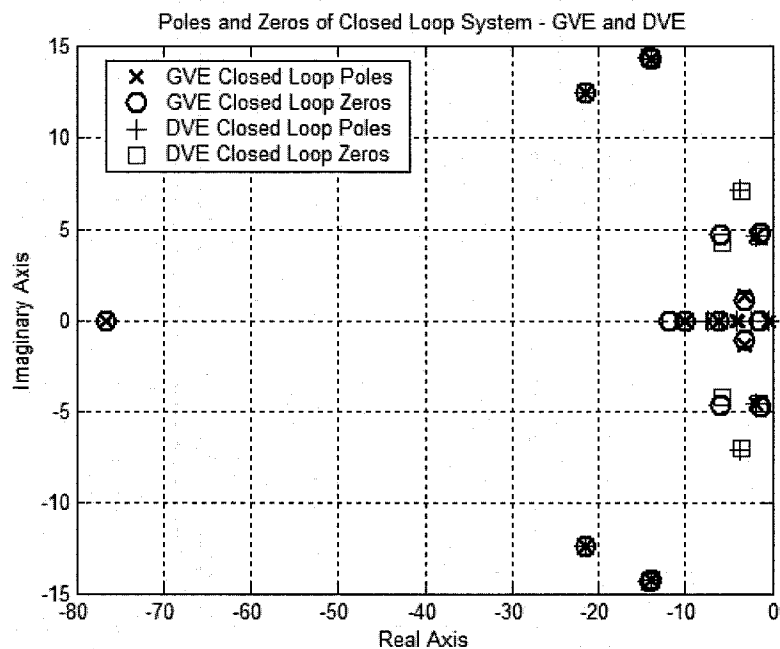


Figure 4-33 Poles and Zeros of GVE and DVE Closed Loop Plants

However, note that the largest effects took place on the faster poles, the poles associated with the compensator and the neuromuscular terms. The slowest poles (and therefore most important in controlling) are less significantly effected by the estimator dynamics, although it can be seen that the DVE condition has slightly slower dynamics with less

damping. Figure 4-34 zooms in on the slower dynamics to highlight the difference between GVE and DVE closed loop systems.

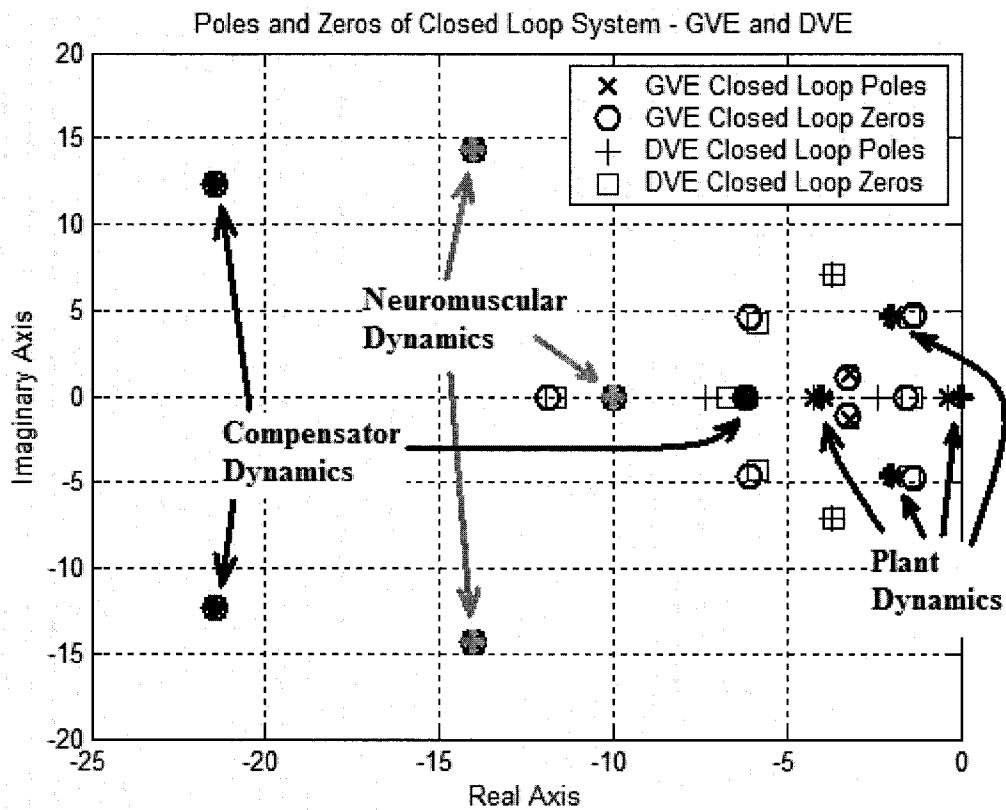


Figure 4-34 Slow Poles and Zeros of GVE and DVE Closed Loop Systems

Inspection of Figures 4-33 and 4-34 and Table 4-1 reveals that both the estimator and the optimal feedback gain primarily affect the poles of the controlled system, which are the slowest poles and which most profoundly affect the closed loop performance. The optimal feedback poles are identical for both GVE and DVE systems, with the greatest effect on the pure integration pole at $s=0$.

The estimator poles differ between visual conditions in that the GVE system is able to move the poles further to the left, affecting a faster, more accurate reconstruction of the actual closed loop system states and ultimately allowing a more effective control implementation.

| Closed Loop Eigenvalues | | Feedback and Associated Term | Open Loop Eigenvalues | Closed Loop vs. Open Loop |
|-------------------------|---------------------|---------------------------------------|--------------------------|------------------------------------|
| GVE | DVE-H | | | |
| $-21.43 \pm 12.37i$ | $-21.43 \pm 12.37i$ | K / A_c | $-21.43 \pm 12.37i$ | = |
| -6.08 | -6.08 | K / A_c | -6.18 | \approx |
| $-14.00 \pm 14.28i$ | $-14.00 \pm 14.28i$ | K / A_{nm} | $-14.00 \pm 14.28i$ | = |
| -10.0034 | -10.0034 | K / A_{nm} | -10.00 | \approx |
| $-2.00 \pm 4.63i$ | $-2.00 \pm 4.63i$ | K / A | $-2.00 \pm 4.58i$ | \approx |
| -0.37 | -0.37 | K / A | -0.00 | \neq |
| -4.23 | -4.23 | K / A | -4.00 | \approx |
| $-21.43 \pm 12.37i$ | $-21.43 \pm 12.37i$ | L / A_c | $-21.43 \pm 12.37i$ | = |
| -6.18 | -6.18 | L / A_c | -6.18 | = |
| $-14.00 \pm 4.28i$ | $-14.00 \pm 14.28i$ | L / A_{nm} | $-14.00 \pm 14.28i$ | = |
| -10.00 | -10.00 | L / A_{nm} | -10.00 | = |
| $-3.17 \pm 1.36i$ | $-3.69 \pm 7.11i$ | L / A | $-2.00 \pm 4.58i$ | \neq |
| -3.92 | -2.41 | L / A | -0.00 | \neq |
| -75.90 | -7.35 | L / A | -4.00 | \neq |

Table 4-1 Eigenvalues of Open Loop and Closed Loop GVE and DVE Systems

Despite the seemingly important difference between the closed loop poles, the bode plot in Figure 4-35 shows the relatively small effect the noise had upon closed loop dynamics. The total effect on closed loop performance will be further explored in the following section though initial indications point to a lack of sensitivity to system noise.

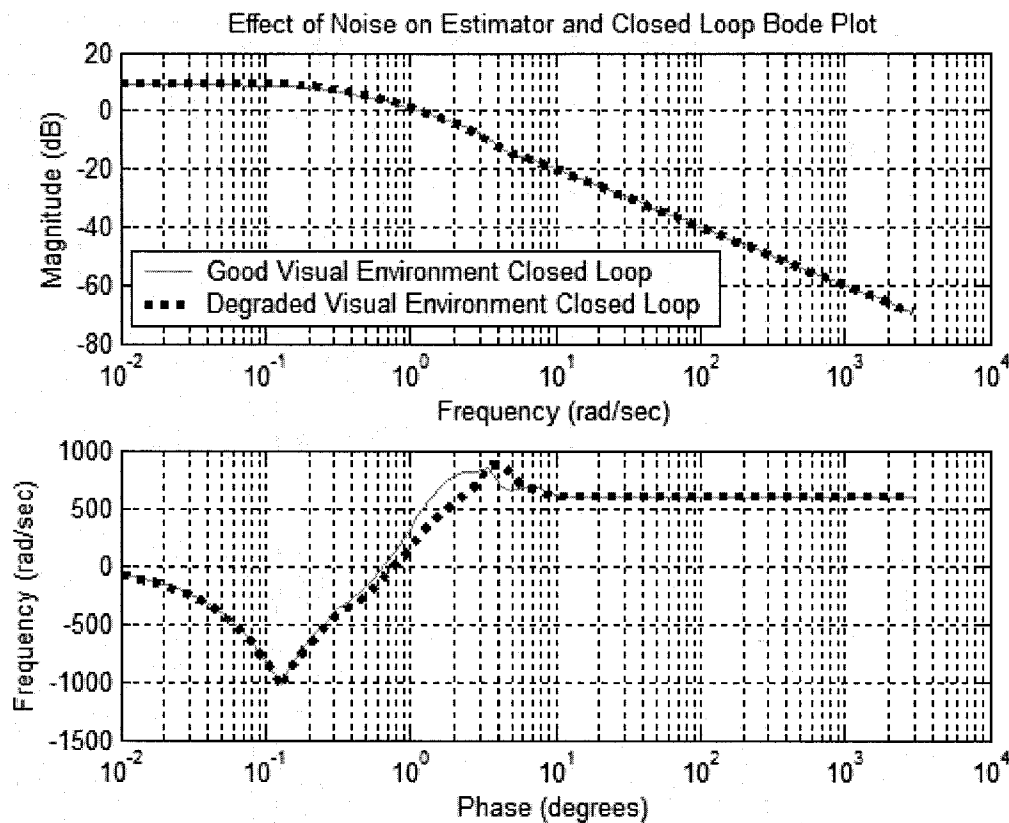


Figure 4-35 Bode Plot of GVE and DVE Closed Loop Systems

4.5.3 Compensation Block

The linear compensator blocks showed some consistent significant changes with respect to condition and some interesting trends were revealed. PVO condition showed no difference between TSAS/No TSAS. Figure 4-36 shows the summary results for all subjects during the VOSS condition. Note that pilot compensator delay increases during the DVEL condition, but remains relatively constant for DVEH with respect to GVE. The forward loop gain is at its lowest during the DVEL condition, with a slight decrease shown DVEH over GVE. The denominator and numerator showed large variability, particularly for the DVEL conditions. This may be due to the reported various strategies employed during DVEL. During GVE, pilots remained “outside,” using the visual field presented. During DVE-Heavy, pilots immediately moved their scan “inside” to utilize

the instruments. In contrast, during DVEL, pilots were unsure which strategy provided the best information and shuttled back and forth between the visual field and instruments.

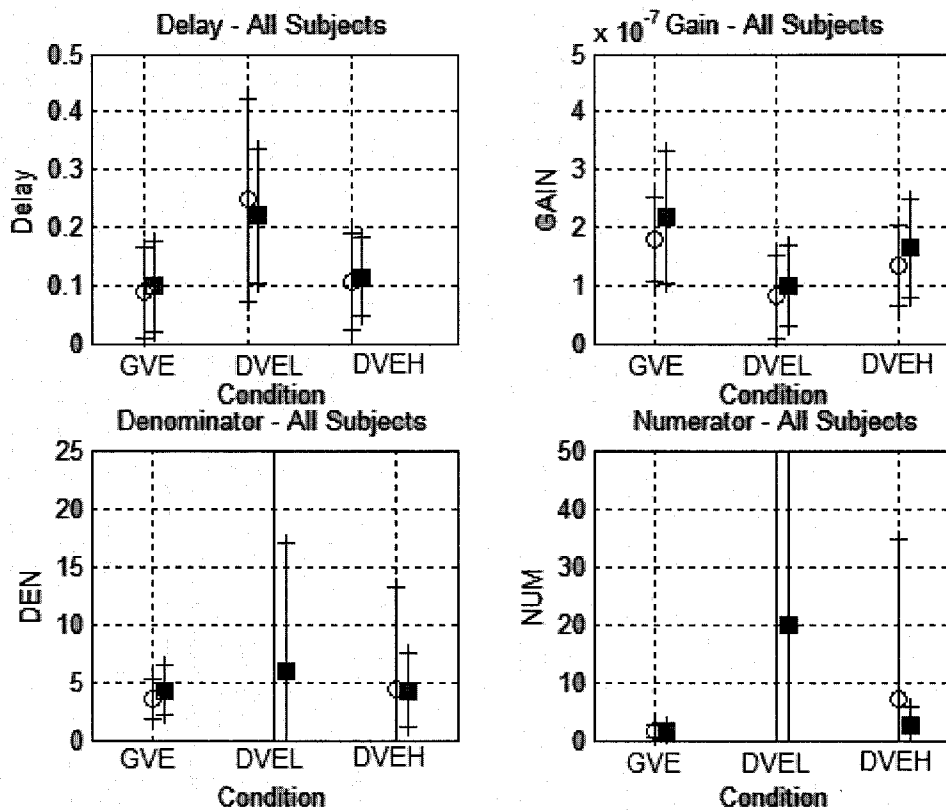


Figure 4-36 Compensator Block Parameters

4.5.4 Nonlinear Stochastic Mapping

The nonlinear dynamics were found to be relatively stable within subjects, but exhibited large differences in specific nonlinear parameters between pilots. Nonlinear pilot performance was relatively static with respect to visual and tactile conditions. A typical series of stochastic maps is shown in Figure 4-37, in this case the map depicting the cumulative probability for the length of a hold based upon the difference between the linear and actual command signal (Subject E, All trials, all conditions.) The maps are semi-transparent to allow visibility within. Note that the variability is quite limited. Although some difference was apparent between conditions, the small number of trials

per subject led to high variability and the lack of consistent significant results. Therefore, a single set of stochastic maps was used for each subject, for all conditions.

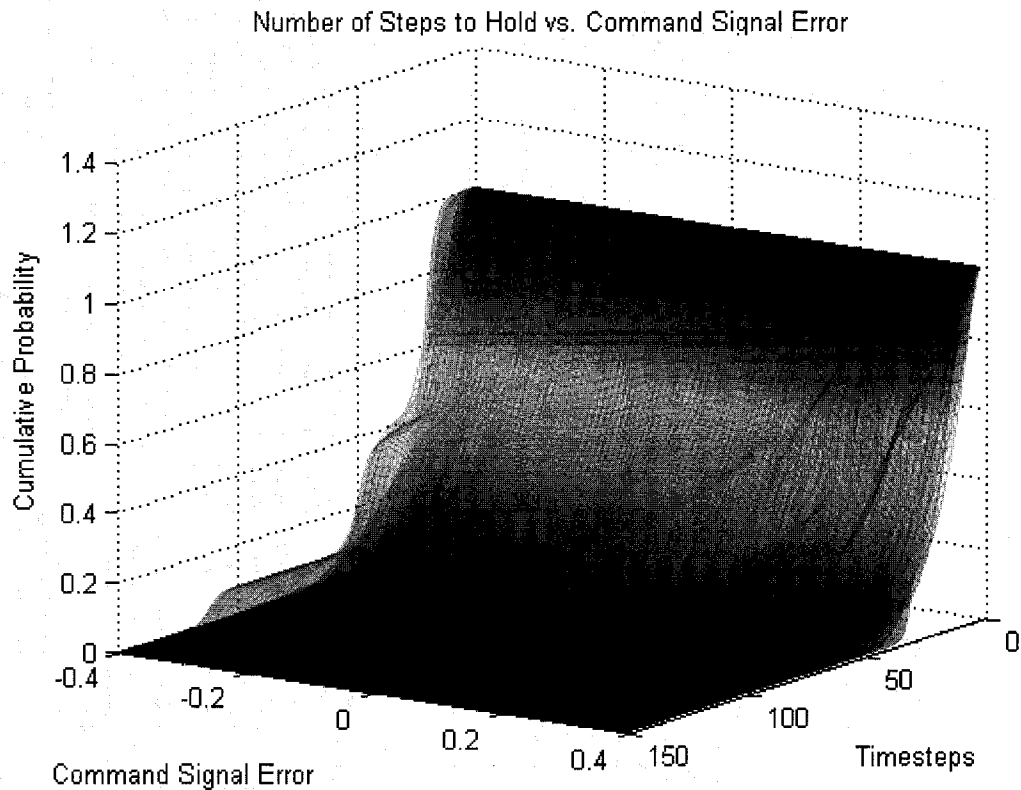


Figure 4-37 Stochastic Map - Simultaneous Display of Twelve Trials

4.5.5 Closed Loop Model Performance

Three models were evaluated, the linear closed loop term defined in Equation 4.20, the linear pilot model defined in Equation 4.25, and the nonlinear model defined in Equation 4.27, with the nonlinear input defined by the stochastic process previously described.

4.5.5.1 Linear Model Performance

The linear model, although it obviously lacks some of the advanced dynamics of the nonlinear model is very useful for first order approximations of closed loop pilot-plant

system performance. It should be noted that no model “tweaking” was performed to improve matching performance. The model presented was constructed based upon the previously discussed assumptions. Modification to improve parameter matching will be presented later. Comparison of actual and model data is presented in Figure 4-38.

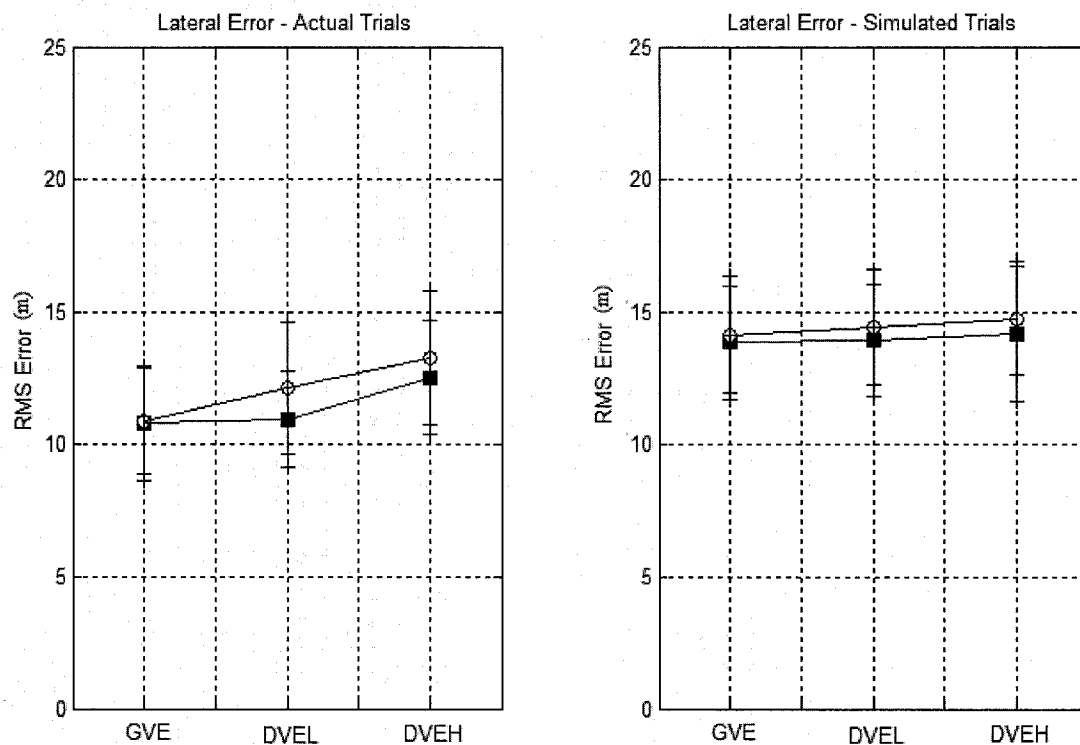


Figure 4-38 Lateral Axis Position Error - Actual Trials and Model Prediction

The lateral-axis position error shows the excellent correlation between actual and calculated data, although the model fails to exhibit the increasing rate of system degradation with increasing obscuration. Furthermore, the model has significantly less variability than real pilot performance. The relative lack of repeatability of the pilot data speaks to the importance of the nonlinear dynamics.

Additional analysis was performed on the control signal. Figure 4-39 shows again the relative agreement between actual and calculated aileron signal. The slightly lower aileron signal is most likely the result of a truly optimal response, leading to matched

performance with less “effort.” As with the position error, there is significantly less variability for the model.

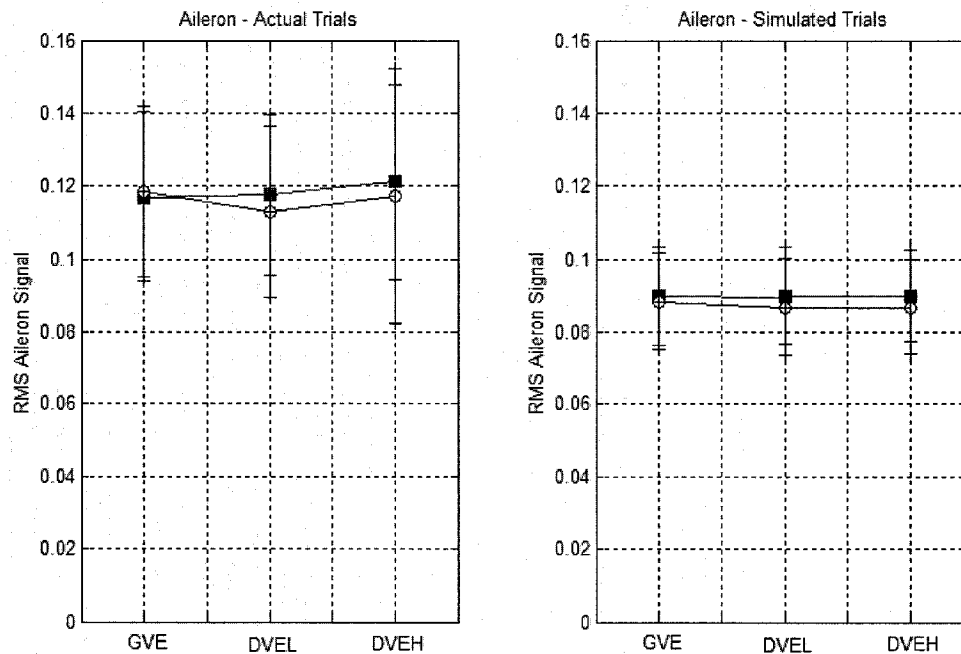


Figure 4-39 Aileron Signal - Actual Trials and Model Prediction

The frequency spectrum performance of the linear model was expectedly poor. The linear model failed to accurately reconstruct the real aileron signal. Figure 4-40 shows the Power Spectral Density ($PSD_{\delta\delta}$) of the experimental aileron signal and the modeled aileron signal. The model achieves a match at the low frequency input frequencies but not at the higher input frequencies and never between. Figure 4-40 b shows the magnitude difference between the real aileron signal and the closed loop calculation. The result is the “neuromuscular peak” that is present in most pilot control research. The source of the peak is normally attributed to proprioceptive feedback of the neuromuscular loop. Through active feedback and gain manipulation, such a response can be teased out of a linear system.

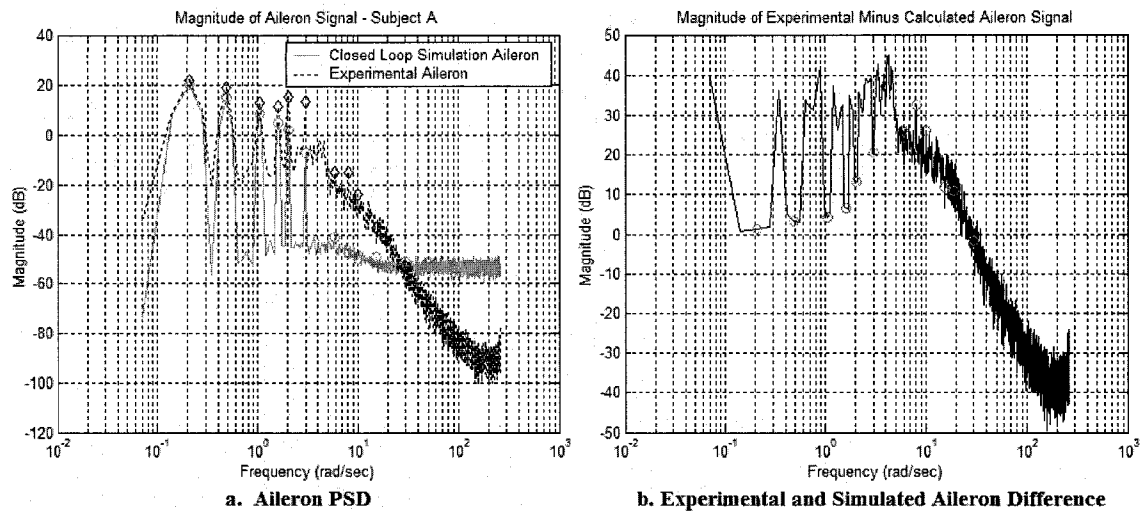


Figure 4-40 Experimental and Simulated Aileron Signal - Frequency Domain

However, as previously discussed, the source of the extra information may be the sampling frequency of the pilot response. As was previously demonstrated, sampling of the response creates aliasing and adds additional power at higher frequencies. The same effort is used for the linear model. This time, instead of using a measured histogram of actual pilot data, as an example of potential sources of neuromuscular peak, the system uses a normally-distributed hold times to extend the present state of aileron response. The resultant signal was scaled to maintain a reasonable signal. The time domain aileron signal is plotted with the experimental signal and the original linear signal in Figure 4-41.

The resultant signal succeeded in matching the power spectral density of the signal almost exactly, as shown in Figure 4-42. Although not a perfect match, the result demonstrates the potential effect of “move and hold” strategies in introducing high frequency gain into the frequency domain of the aileron signal. Again, this increase in power magnitude was not due to “neuromuscular peak” but the effect of random time-period sampling.

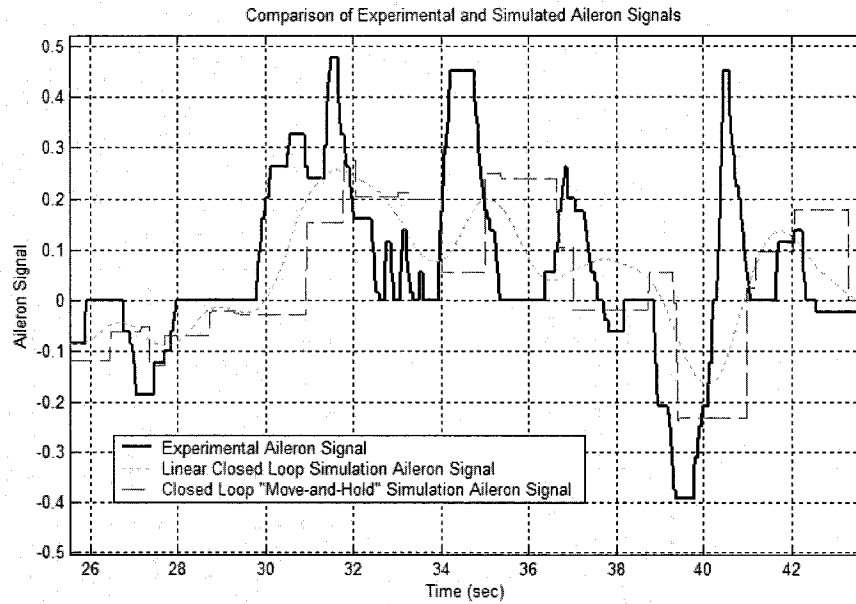


Figure 4-41 Linear Aileron Signal - "Move and Hold" Strategy

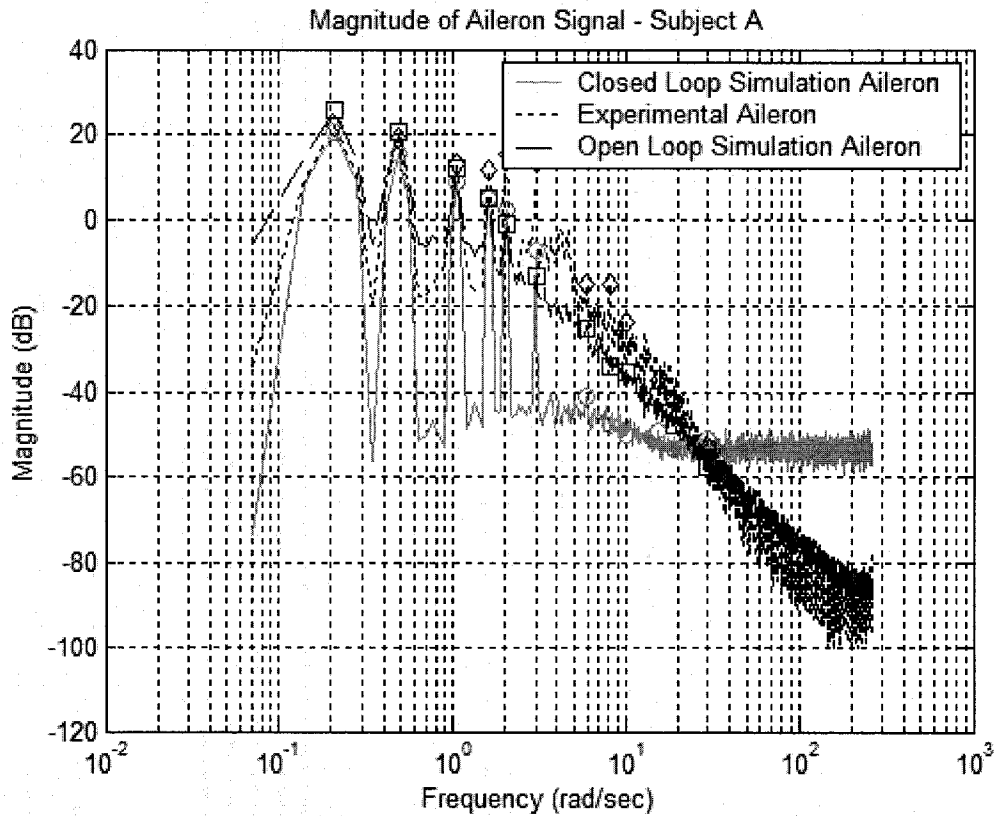


Figure 4-42 Aileron Signal - Effect of "Move and Hold" - Frequency Domain

The linear model succeeded in replicating frequency domain characteristics of the actual pilot controlled closed loop plant both with and without the “move and hold” strategy employed. Figure 4-43 shows the closed loop transfer function of the real and simulated systems. The actual closed loop system was calculated by dividing the cross spectral density of disturbance signal w with respect to position error x by the power spectral density of w . The simulated closed loop system was calculated using Equation 4.20. The figure shows excellent agreement among all systems, particularly at the driving frequencies of the disturbance signal. The off-frequency noise, which is injected by the pilot’s nonlinear performance, is replicated adequately through the inclusion of neuromuscular noise v_u .

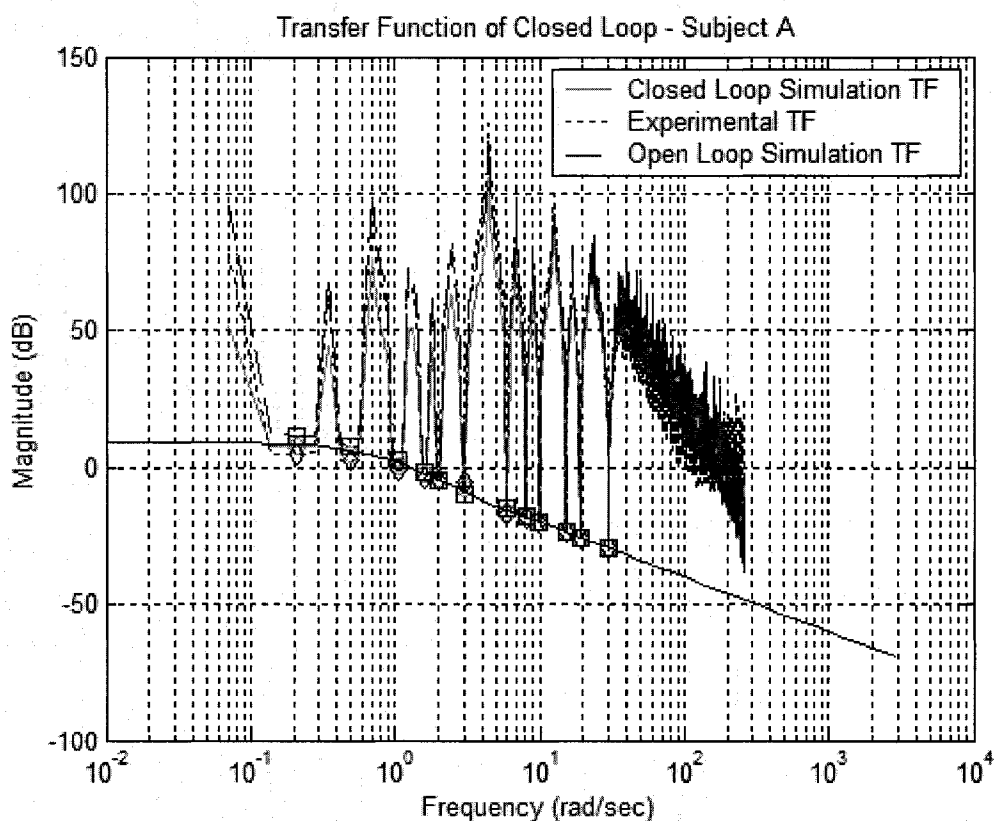


Figure 4-43 Closed Loop Linear Plant - Frequency Spectrum

The linear plant model yielded the following solution:

$$x = 2.86 \frac{(-10.07)(-1.46)(-1.85 \pm 4.53i)(-3.85 \pm 1.80i)(-3.76 \pm 1.38i)}{(-0.59)(-10.00)(-1.12)(-2.00 \pm 4.61i)(-3.64 \pm 0.22i)(-3.73 \pm 3.85i)} w \quad \text{Eq. 4.29}$$

where $(-x.xx)$ indicates a single pole or zero

and $(-x.xx \pm x.xx i)$ indicates an underdamped pair

Incredibly, with minimal loss of information, the equation can be simplified to

$$x \approx \frac{2.86}{(s + 0.59)} w \quad \text{Eq. 4.30}$$

Equation 4.30 yields a structure very similar to McRuer's Crossover Model.

The actual pilot loop was solved by dividing the cross spectral density of the position error x with respect to the aileron signal δ by the power spectral density of the position error x . The linear models were solved using Equation 4.25.

Figure 4-44 shows that the linear model simulation was able to accurately capture closed loop pilot performance at all frequencies. However, two things are interesting about the transfer function plot. First of all, what is the source of the increase in magnitude of the transfer function at higher frequencies? Second, why does the linear model (no noise) fail to account for the increase in magnitude, even at the disturbance signal driving frequencies.

In an effort to isolate the source of the increase in magnitude, a contemplative reflection on the plot reveals the answer. Figure 4-44 plots the relationship between δ and x . However, the entire closed loop system also relates x to δ through the original plant dynamics. Therefore, if the original plant bode plot is inverted and superimposed on the original plot, Figure 4-45 shows that the source of the increased magnitude has been

found. White noise injected by the pilot in the form of neuromuscular noise, v_u is then shaped by the system dynamics and inverted due to the structure of the transfer function.

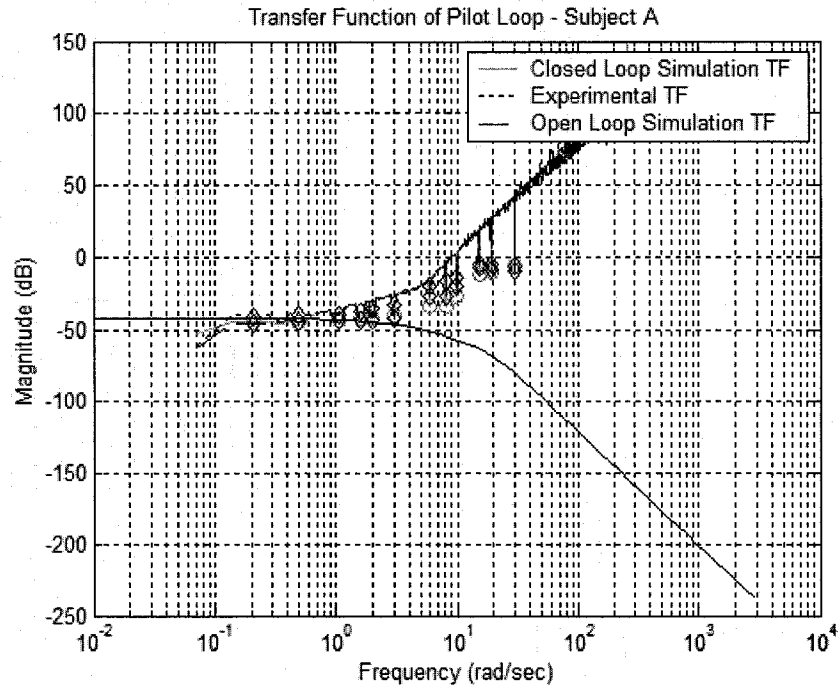


Figure 4-44 Pilot Loop - Experimental and Simulation

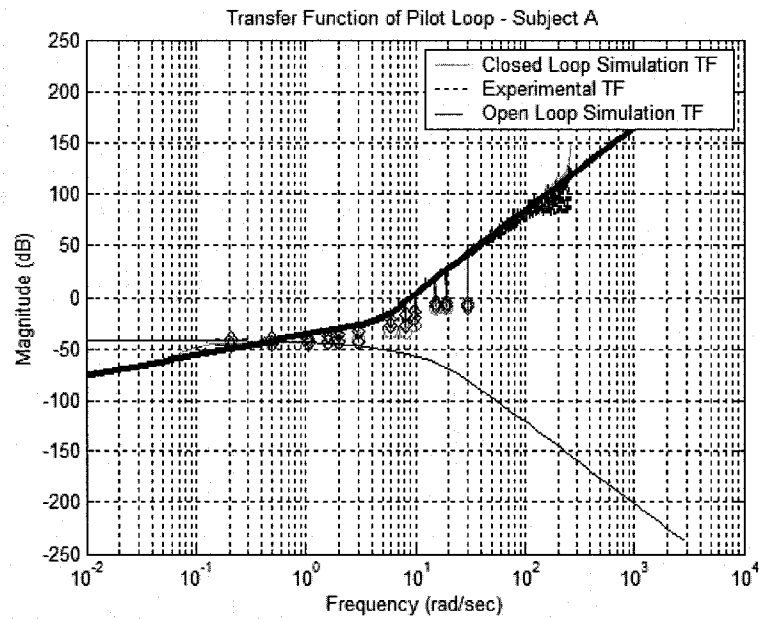


Figure 4-45 Pilot Loop with Plant Dynamics Superimposed

The second question, regarding the failure of the linear model (no noise) to accurately match the empirical data, has a self revealing solution. Removal of the noise signal, v_u , shows that the resultant transfer function, shown in Figure 4-46, is basically flat, with amplitudes of the driving frequencies matching the linear system magnitudes perfectly. This again validates the model structure, in particular the inclusion of neuromuscular noise and its magnitude.

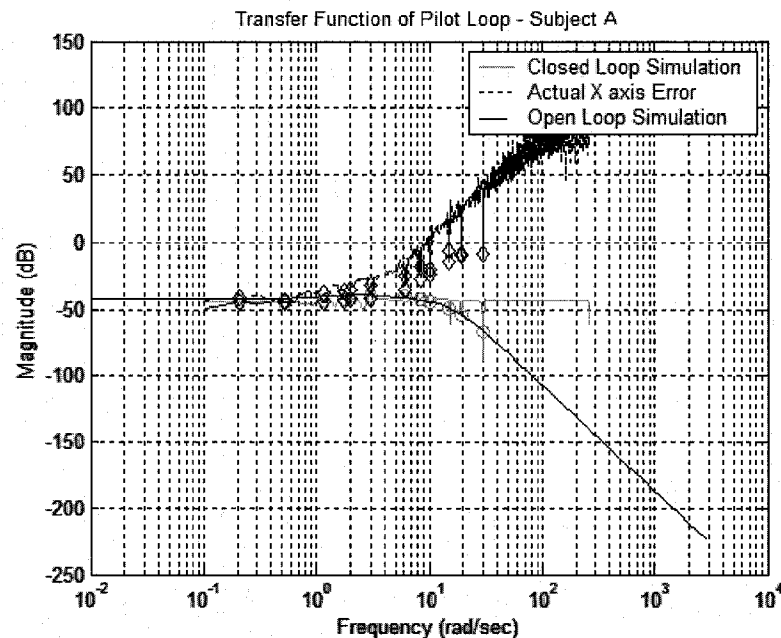


Figure 4-46 Pilot Loop - Neuromuscular Noise Removed

The ultimate governing equation of the pilot loop is defined by the equation:

$$\delta = -.0077 \frac{(39965)(-10.49)(-1.63)(-20464 \pm 34890)(-3.74 \pm 1.43i)(280.63 \pm 162.02i)}{(-1.31)(-2.89)(-3.52 \pm 1.81i)(-10.93 \pm 4.20i)(-13.93 \pm 13.97i)(-280.63 \pm 162.02)} \times \text{Eq. 4.31}$$

Note the extremely fast dynamics in the numerator, and the presence of a non-minimum phase zero. By ignoring the faster dynamics and allowing rough cancellations of poles and zeros, Equation 4.31 can be simplified to approximately:

$$\delta \approx -0.0077 \frac{1}{(-10.93 \pm 4.20i)(-13.93 \pm 13.97i)} x \quad \text{Eq. 4.32}$$

The gain and structure of Equation 4.32 match the corner frequency and high frequency 80 dB per decade rolloff of the actual pilot model.

Of course, arbitrary modification of the optimal signal cannot be accomplished without consequence. An undesirable result of the first order discretization approximation is the lack of fidelity in the time domain. Figures 4-47 and 4-48 show the resultant effect of discretization upon mean error and aileron response for the new system. Note the higher error and higher aileron signal.

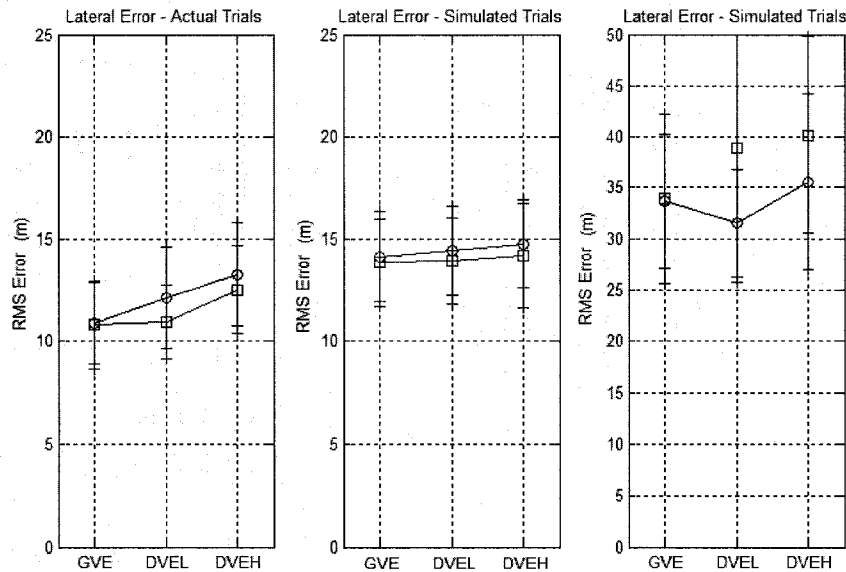


Figure 4-47 Lateral Axis Position Error - Linear Model and Discretized Aileron Signal

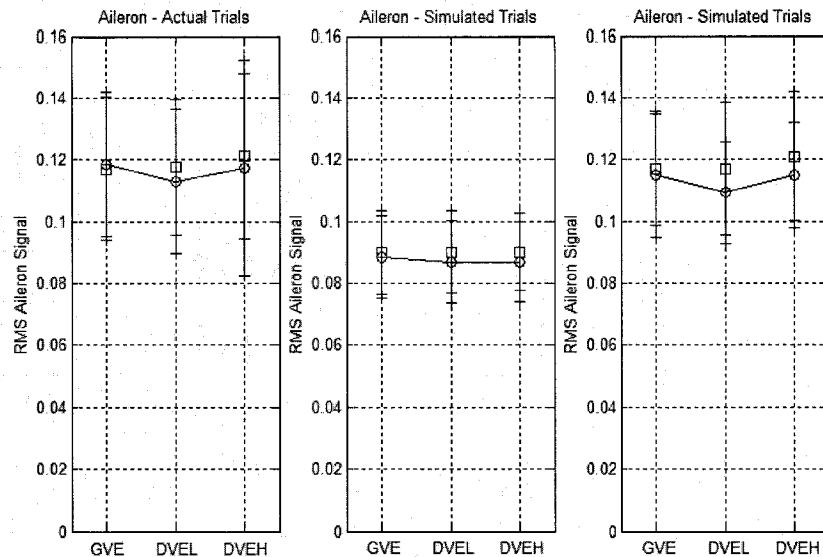


Figure 4-48 Aileron Signal - Linear Model and Discretized Aileron Signal

Recall that Figure 4-42 shows that the PSD of the discretized aileron signal matches the real signal. Despite this match, the lack of time domain accuracy seems to indicate that the arbitrary discretization of the linear signal is not the best way to mimic pilot performance.

4.5.5.2 *Nonlinear Model Performance*

By opening the loop after the nonlinear term, the system can be stepped through an entire run of nonlinear move-and-hold dynamics. Due to the stochastic nature of the nonlinear term, each condition was run 10 times. Within subjects, the model showed significantly less variability in summary variables than the actual pilot subjects, eliminating the need for increased number of iterations.

Figure 4-49 represents the RMS error found in each condition. The model exhibits significantly more variability than the linear model, nearly comparable to the actual system. The RMS error signal is significantly higher for all conditions and, again, the model was unable to replicate the higher performance degradation associated with the degraded visual environments. Figure 4-50 shows the higher aileron signal present during all nonlinear trials, this despite the significantly degraded performance.

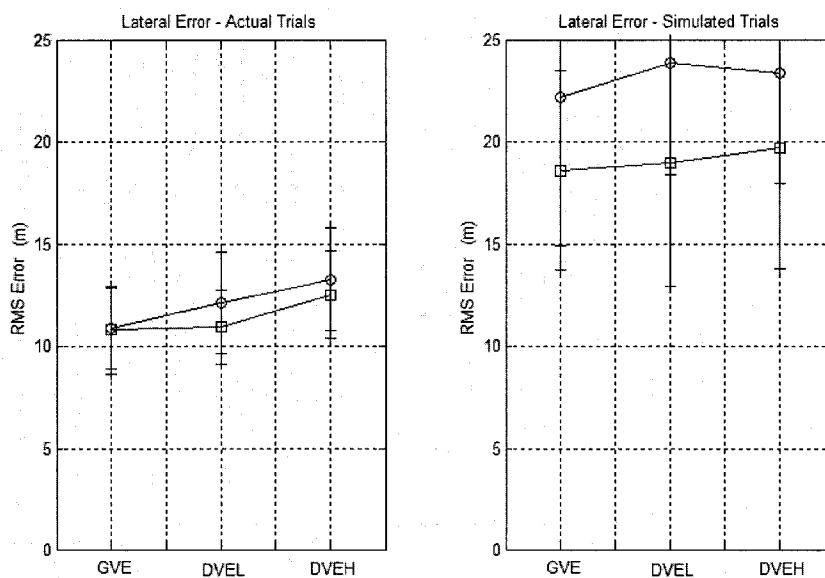


Figure 4-49 Lateral Axis Position Error - Actual Trials and Nonlinear Model Prediction

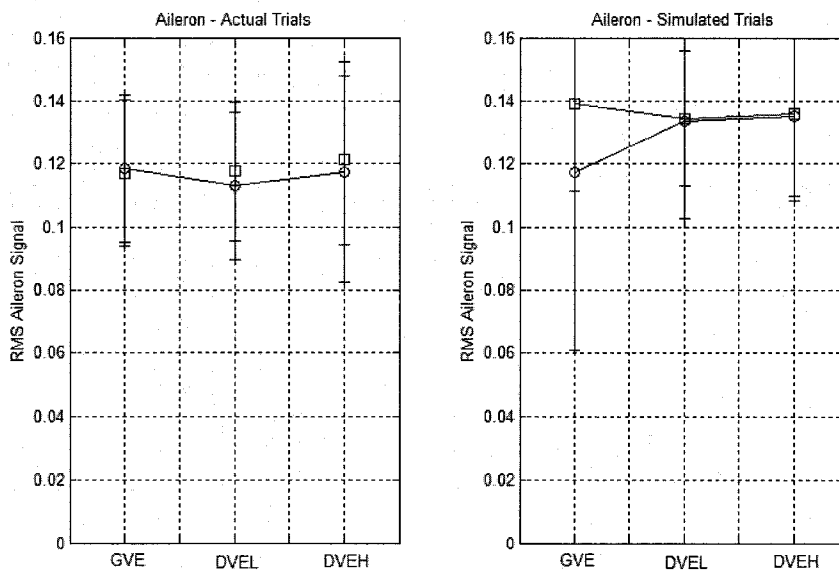


Figure 4-50 Aileron Signal - Actual Trials and Nonlinear Model Prediction

Figure 4-51 shows the Power Spectral Density ($PSD_{\delta\delta}$) of the recorded and computed aileron signals. The frequency response of the nonlinear model showed excellent matching of the true aileron signal with no additional “neuromuscular peak” or noise-adding tricks. The power spectrum is the result of the nonlinear move-and-hold method and neuromuscular noise that accurately mimics the true pilot behavior.

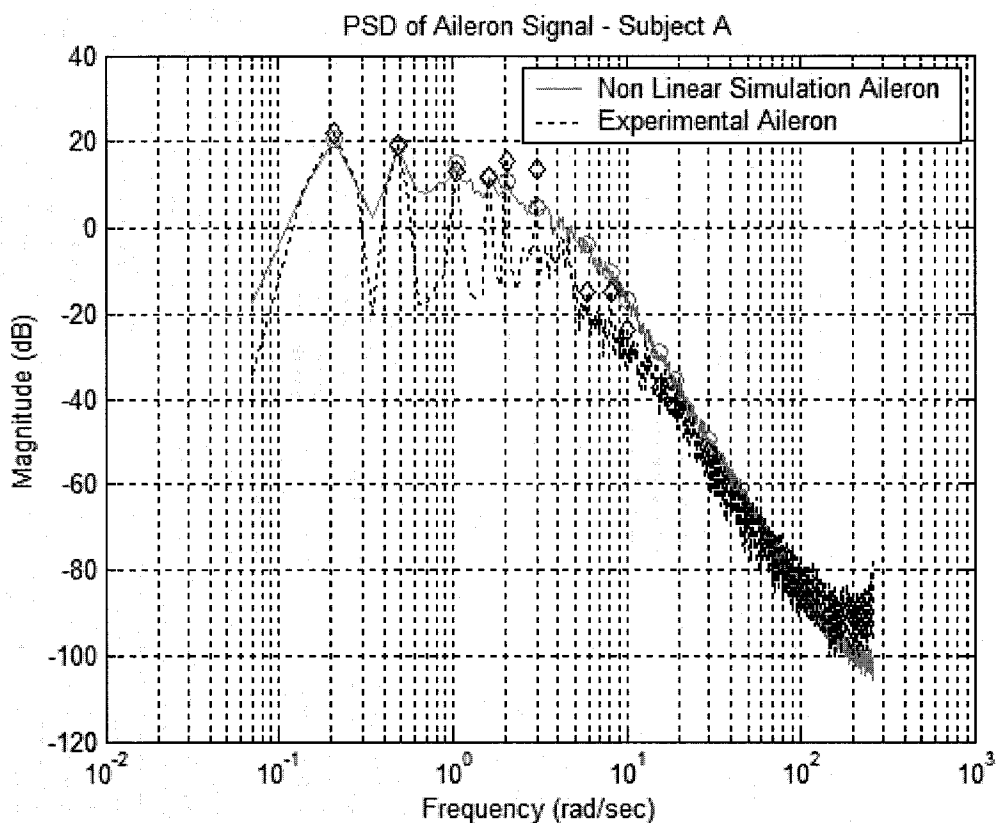


Figure 4-51 Nonlinear Model Aileron Signal - Frequency Domain

The relationship between disturbance signal w and output error x is shown in Figure 4-52 (CSD_{wx}/PSD_{xx}). The closed loop model showed similarly acceptable matching data for the closed loop transfer function. In contrast to the linear model comparison, both the experimental and the nonlinear model data were solved using cross spectral density and power spectral density functions. The nonlinear nature of the model precluded a closed form mathematical solution. The previously solved linear model is shown for

comparison. In this case, the nonlinear model is able to match frequency information across the entire spectrum, at driving frequencies and between.

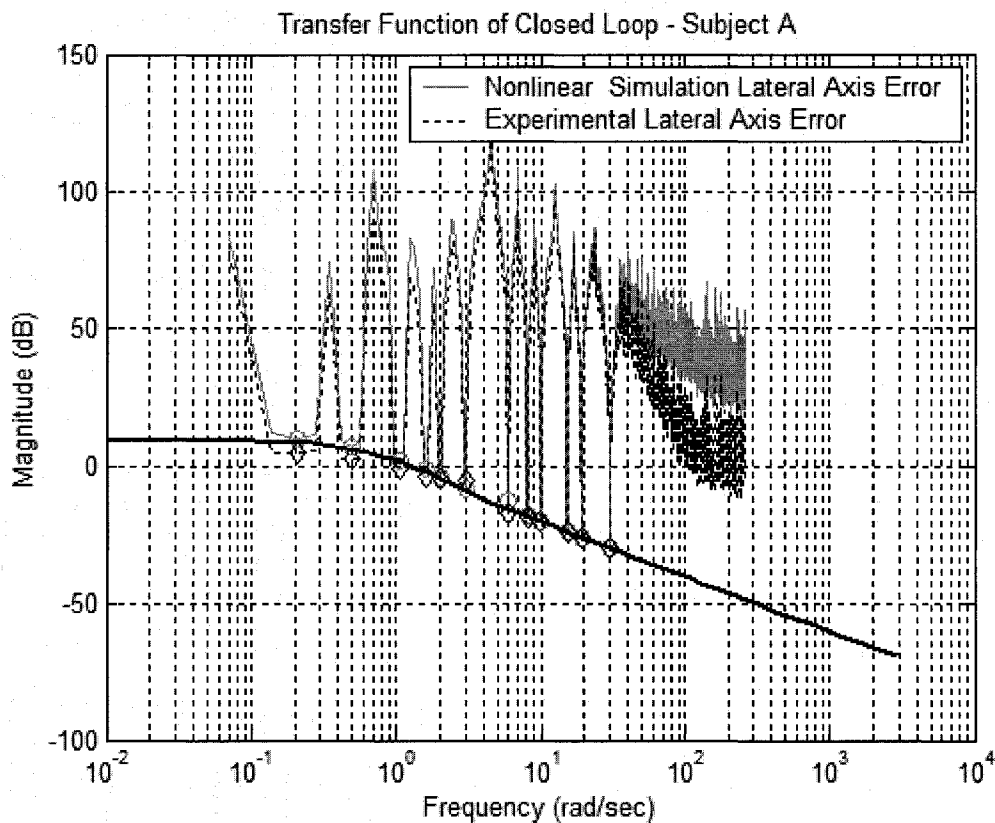


Figure 4-52 Nonlinear Model - Closed Loop Transfer Function

Despite excellent matching in the frequency domain, as Figure 4-53 shows, the nonlinear model is unable to accurately copy the exact timeline of lateral axis error. Even the estimated error has visibly larger excursions than the real data. The true error of the model is slightly worse than the estimated state. This indicates that despite stochastic similarities between the actual and simulated signals, the nonlinear model has failed to capture the essence of the true pilot behavior.

The aileron signals are shown in Figure 4-54. The linear command signal shows reasonable correlation to the real aileron, although the gain is lower and much of the high frequency content of the recorded signal is absent in the modeled signal. The nonlinear

modeled aileron departs significantly from the command signal, yet another indication that the stochastic maps fail to completely identify all inputs into the pilot nonlinear decision matrix.

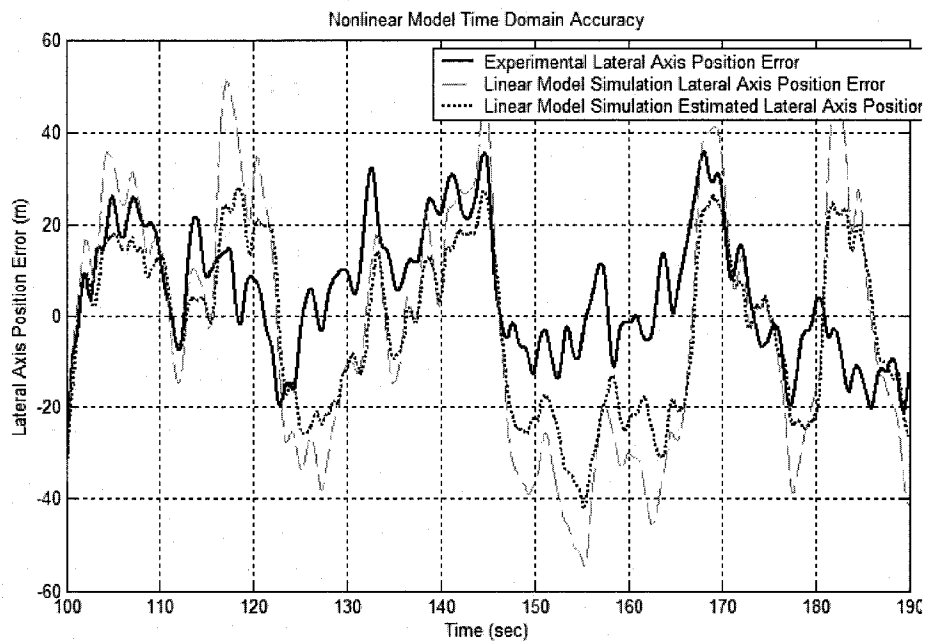


Figure 4-53 Nonlinear Model - Time Domain - Lateral Axis Position Error

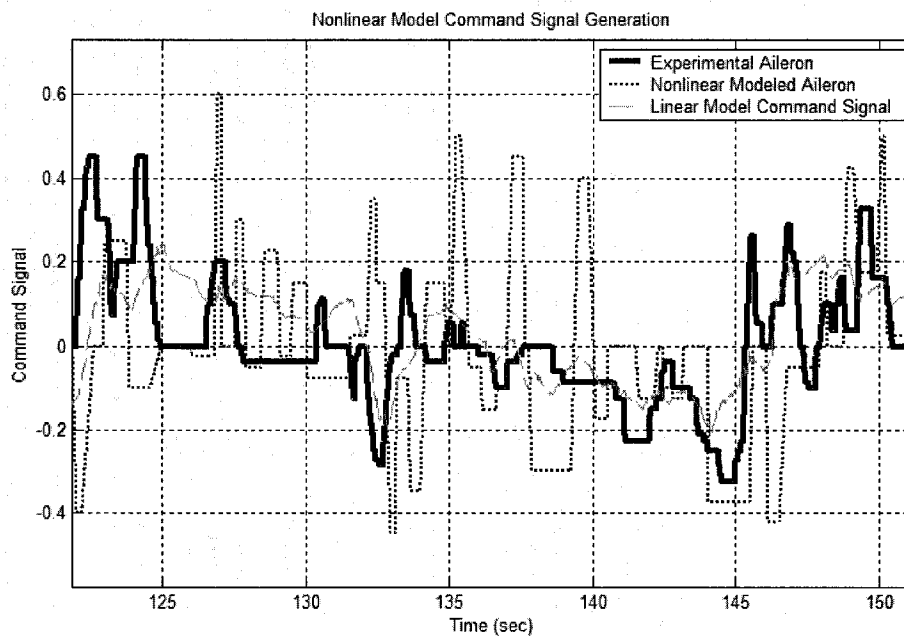


Figure 4-54 Nonlinear Model - Time Domain - Aileron Signal

Despite the inability of both models to accurately capture the time domain performance of the pilot subjects, they are both able to generate matching results within the frequency spectrum and produce summary results that are within the deviation of the experimental recorded pilot controller data.

4.6 Model Matching in the Longitudinal Axis

The ultimate litmus test of a model's utility is its ability to not only match, but also to predict behavior based upon known quantities. Despite the profound difference in quality of visual presentation signals, and small differences in the plant dynamics, an attempt will be made to model the longitudinal axis VOSS behavior based upon PVO model data.

4.6.1 Longitudinal Axis Linear Model

The structure of the linear model is identical to that of the lateral axis. Using techniques established during model development, and PVO data (including neuromuscular model, compensation term, and stochastic mapping) the model was developed in its entirety without additional validation trials. This was done in an effort to evaluate the predictive value of the model. Additionally, the linear elevator signal was injected with randomly distributed sampling in an effort to match the true elevator PSD function. Both closed loop and random sampled signals will be presented.

Figure 4-55 shows the PSD_{88} of the actual, linear, and linear move-and-hold elevator signals. Note that the addition of discretized hold periods again succeeds in bringing the frequency spectrum of the simulated signal closer to that of the real signal.

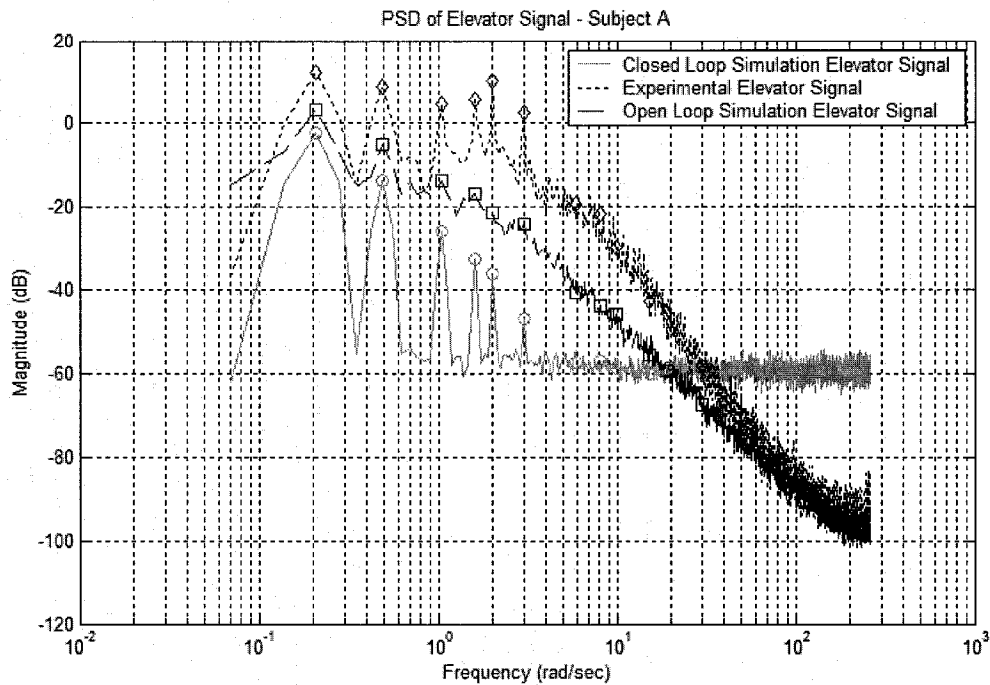


Figure 4-55 Power Spectral Density of Actual and Linear Model Elevator Signal

Figure 4-56 shows the closed loop dynamics (CSD_{wy}/PSD_{yy}) of the real, linear, and discretized simulation. Note that both the linear and discretized models succeed in matching the closed loop frequency spectrum of the real plant. As with the lateral axis, the linear model matches the transfer function of the real pilot-plant system at the driving frequencies of the disturbance signal. Again, the injection of neuromuscular noise succeeds in matching the frequency spectrum of recorded pilot performance at off-frequencies.

The “move and hold” strategy showed improved matching in the frequency domain. For the time domain summary variables however, Figure 4-57 shows that the original linear signal did a much better job in replicating the closed loop performance than the linear “move and hold.” Neither the trends nor values of the discretized system were in agreement with actual pilot data. Note that the linear model with discrete control has an RMS error nearly double that of the real and linear models.

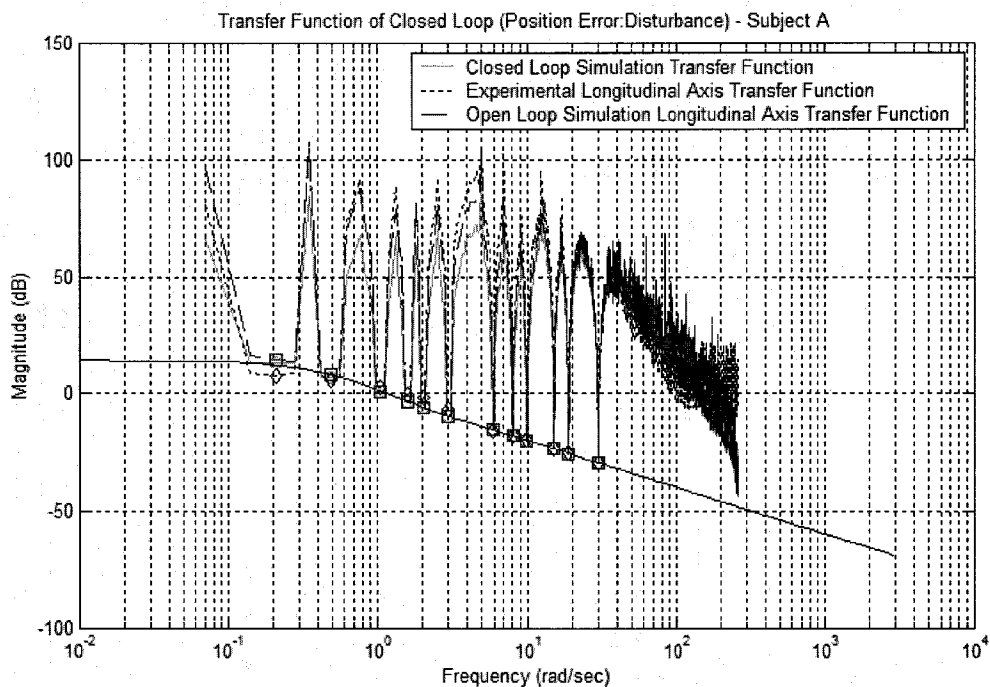


Figure 4-56 Longitudinal Axis - Magnitude of Actual and Linear Model Closed Loop System

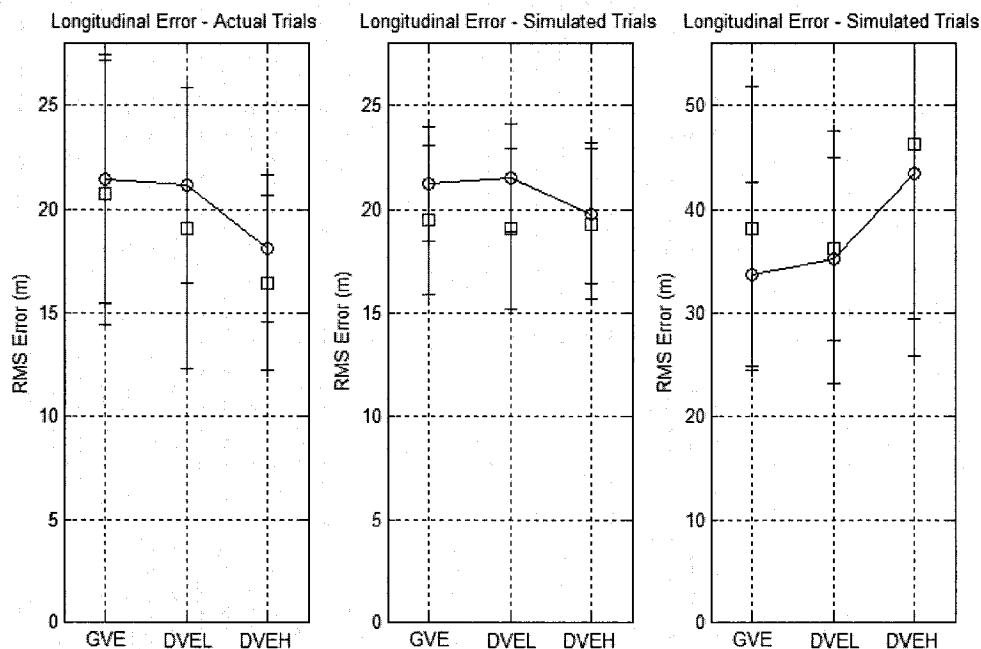


Figure 4-57 Longitudinal Position Error - Actual, Linear, and Linear Discretized Models

As shown in Figure 4-58, the linear model and the linear discretized model both have significantly less elevator activity than the real pilot, though the trends are the same. Note that the smaller elevator signal associated with the linear model yields a roughly equal longitudinal axis error, but the discretized model yields a significantly poorer performance.

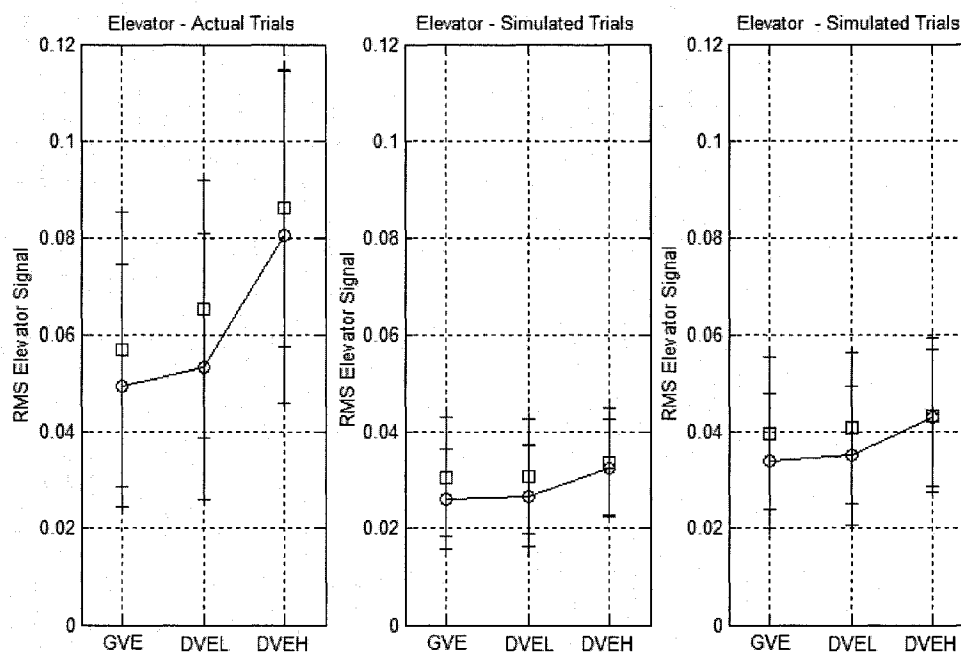


Figure 4-58 Elevator Signal - Actual, Linear, and Linear Discretized Models

4.6.2 Longitudinal Axis Nonlinear Model

Like its linear counterpart, the nonlinear model was simulated using only PVO data from the Y axis, in order to fairly assess its predictive value.

Figures 4-59 and 4-60 show that the nonlinear model clearly failed to match the time domain performance of the real pilot performance. The trends are not the same and the

magnitude of the error is nearly triple the real performance. The elevator signal is nearly double that of the recorded pilot data. It seems that, despite excellent linear model performance, the addition of the stochastic map clearly reduces the fidelity of the system.

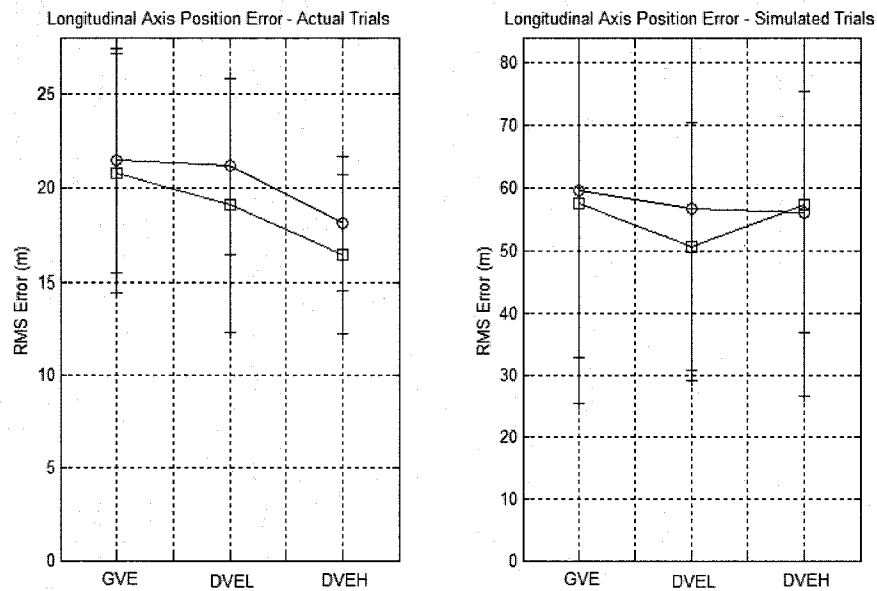


Figure 4-59 Longitudinal Position Error - Actual and Nonlinear Model

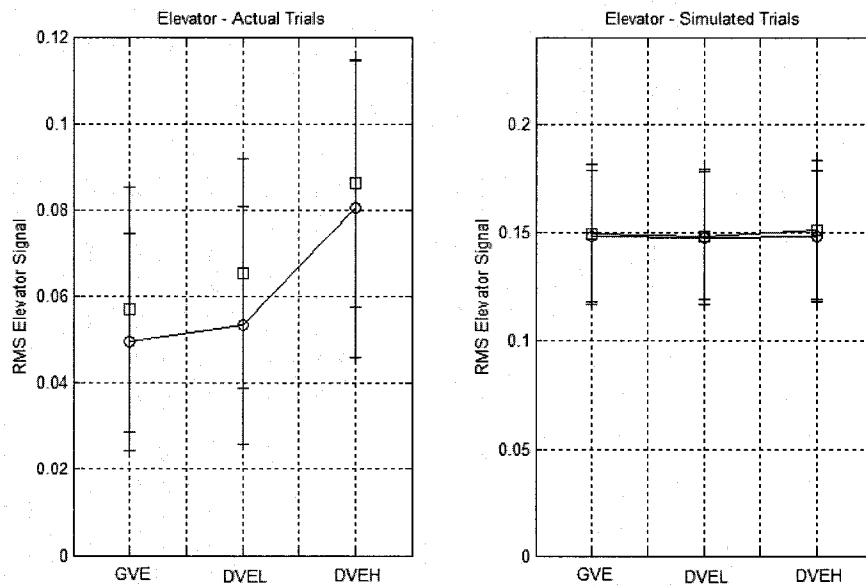


Figure 4-60 Elevator Signal - Actual and Nonlinear Model

Although the time domain response of the nonlinear model was not a match for the real data, as the transfer function analysis (CSD_{wy}/PSD_{yy}) in Figure 4-61 shows, the model does an excellent job of matching the real performance of the pilot subjects in the frequency domain, both at disturbance signal input frequencies and at the noise frequencies in between. Again the linear model has been shown for comparison. Note that the input frequencies fall on the linear model, while all other frequencies are much higher, though the model is able to replicate the PSD at all frequencies, presumably through proper modeling of the noise content of the elevator signal. The consequences of these results will be discussed in Sections 5 and 6.

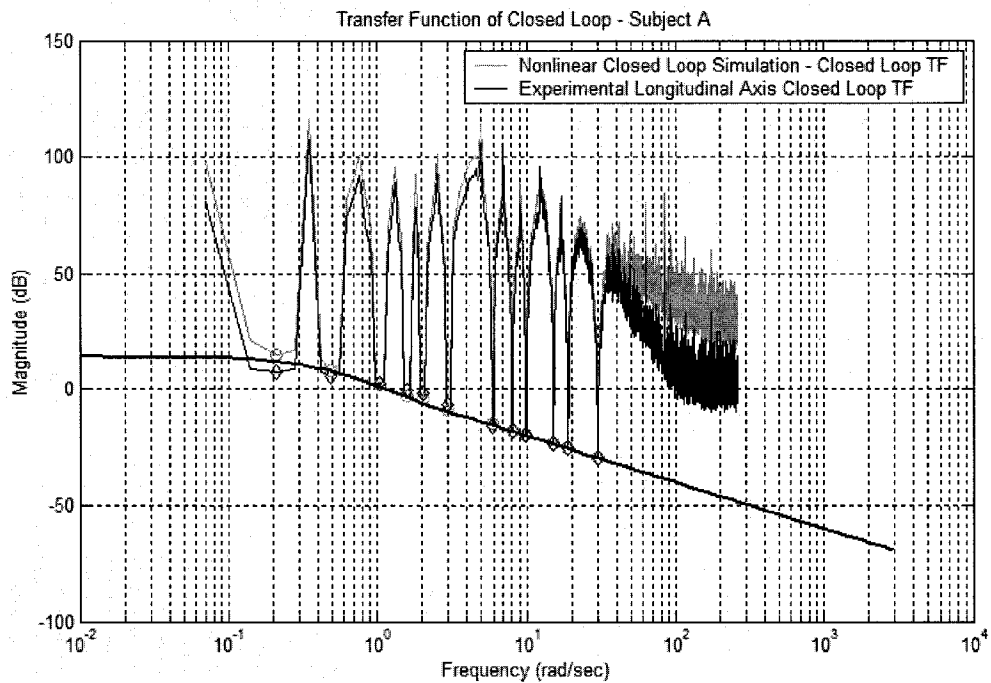


Figure 4-61 Closed Loop Transfer Function - Actual System and Nonlinear Model

SECTION 5 DISCUSSION AND FUTURE RESEARCH

The success of this research can be judged according to its ability to achieve the goals stated at the beginning of this document:

- To evaluate the Tactile Situational Awareness System and its efficacy in aiding pilot performance during normal and occluded visual environments, and
- To develop a pilot model of pilot regulation task performance that includes visual and tactile feedback loops, with potential to include vestibular and proprioceptive, loops in later models.

This section will begin by outlining the successes associated with this research. Next an overview of some of the shortcomings of these efforts will be presented. This section will conclude with some recommendations for future research.

5.1 TSAS Effectiveness

The answer to the question regarding the TSAS and its efficacy is “yes, if...” Though no statistically significant differences were present, the trends showed TSAS to be effective in improving pilot performance during visually occluded conditions. The quality of the additional information provided by TSAS was sufficiently superior to the information provided by the visual instrument to affect an improvement in performance. During normal visual conditions, the TSAS succeeded in producing a small performance improvement in the lateral axis, where there were excellent visual indications of lateral drift, and a slightly larger improvement in the longitudinal axis, where visual drift indications were poor.

The effectiveness in some conditions and not others suggests that performance improvement is present only when the quality of the new signal is significantly better than the previously existing displayed information. This observation is completely

consistent with the model structure and can be attributed to the estimator block and the eigenvalues of the estimator-closed-loop system, $(A-LC)$.

If the additional signal is of poor quality and fails to affect an improvement (i.e. increase frequency) in the eigenvalues of the closed loop estimator, the speed and quality of state reconstruction is unaffected. Conversely, a cleaner signal leads to faster eigenvalues and allows a faster and more accurate reconstruction of the system states, ultimately leading to performance improvement. The mathematical relationship between observation noise, v_y , disturbance magnitude, W , and Kalman Estimator gain, L , is consistent with this phenomenon.

5.2 Workload and Situational Awareness Measures

5.2.1 Subjective Measures

The subjective measures were reported via intra-trial or post-trial questionnaires. Due to their subjective nature and consequent lack of repeatability and precision, it was believed that these measures would be marginally successful in measuring the difference in workload and situational awareness due to changes in visual and tactile conditions. This a priori belief was certainly not the case, with all subjective measures reporting significant degradations in workload and situational awareness during visually occluded conditions. Of the subjective measures, only SWORD revealed consistent preferences for TSAS over No TSAS conditions, although this opinion was unanimous and very pronounced.

5.2.2 Model Measures

The trend of model compensator loop parameter, *Delay*, with respect to both visual and tactile condition is consistent with expected and reported changes in state reconstruction by the pilot subjects during the various runs. The increased delays witnessed during

periods of uncertainty, or in the presence of poor quality signals, seem to be a reasonable penalty for the more difficult control conditions.

Additionally, the decreased gain associated with the DVEL condition may indicate that pilot forward loop gain is reduced during a period of visual occlusion. The presence of changes for the DVEL condition, but lack of significant changes for the DVEH condition may be attributed to the comparable quality of signal provided by the instrument panel “Flight Director” or by the rapid adaptability of the pilot controller.

5.3 Model Development

This research was moderately successful in development of a multivariable estimator based model that adequately captured both the frequency domain and time domain characteristics of pilot performance. The development of linear and nonlinear blocks also has the potential to reveal consistent pilot responses during varying visual and tactile (and potentially other modalities) conditions.

The originally stated goal of a linear model development was abandoned when inspection of closed loop data revealed a significant portion of performance was attributable to nonlinear behavior and that the relationship, though nonlinear, appeared to be quantifiable.

The goal of expandability to include vestibular and proprioceptive loops seems to have been met, although not in the originally anticipated manner. In fact, the model seems insensitive to the modality of any observed states. The estimator structure of the new model uses all inputs to compile a holistic view of the system states. Therefore, only the noise of the observed signal (not the method of observation) is important in defining the effectiveness of the new observed state. Of course, in keeping with the heuristic nature of the model, it must be assured that placement of the observed state is consistent with pilot physiological structure and strategy. Additional sensory dynamics may be inserted

into the observation loop to accurately model vestibular or proprioceptive data acquisition.

5.3.1 Estimator Model

The estimator block of the model was successful in reconstructing the full system state through optimal filtering of noisy observable outputs and knowledge of internal system structure. Furthermore, the relationship between observation noise v_y and the eigenvalues of the closed loop system $A-LC$ was shown to reveal a close relationship between the quality of signal and the state reconstruction speed and accuracy. This fact is particularly of value when addressing the presentation of existing data through new means or modalities. The utility of such presentation can be evaluated a priori by inspecting the anticipated noise signal on the new observed state and its effect on the closed loop estimator eigenvalues.

5.3.2 Optimal Feedback

The optimal feedback gain appears to be an effective and heuristically sound means of calculating pilot feedback strategy. Although innumerable methods for such calculation exist and the presence of a more suitable means cannot be ruled out, the idea that a pilot assigns costs to states and control inputs and attempts to minimize a cost function accordingly is appealing on a heuristic level. The mathematical fit of this method led to its adoption.

Given the structure of this model, the magnitude of the gain, K , was unimportant. The compensator block, with a variable gain, will automatically rescale the optimal control signal. A larger gain K will result in a smaller compensator gain, G . Only the direction of the K vector (relative gains associated with each state) is important. The acceptability of this methodology will be discussed in Section 6.

5.3.3 Compensator Block

The compensation block for this model was effective in modeling the linear pilot output. In fact, the structured model yielded a better match of pilot output than an unstructured model, validating the chosen structure.

The calculation of realistic delay terms and consistent lead/lag terms further indicates that the selected structure accurately represents pilot strategy and performance. Though parameter variability was present among subjects and conditions, and notable trends were observed, the number of observations was too small to draw any general conclusions about pilot performance. The previously mentioned changes in pilot delay and forward loop gain seem to validate this model structure as a choice.

5.3.4 Nonlinear Block

The nonlinear block was the last term to be added to the model. This enhancement was done after inspection of the data revealed that to ignore these effects would severely limit the ability of the model to capture all important characteristics of pilot performance, particularly the presence of additional noise at higher frequencies with the power spectrum. The presence of the “fuzzy” term in the decision process is heuristically sound and consistent with previous theories on pilot performance and strategy. The resultant accuracy of the decision reinforces the theory of imperfect pilot observation and performance.

Most interesting was the revelation that, once the decision is made to move the controls or hold them, the time to hold seems to exhibit a linear relationship to the command signal error (with a normally distributed white noise signal superimposed) and that the distance to move the controls seems to be linearly related to the time to hold (again with normally distributed noise added).

The fuzzy term, variable hold, and variable movement terms combine to match pilot performance extremely well in the frequency domain, but perform less well in the time domain.

The fact that the relationship between command signal error, time to hold, and distance to move are invariant with visual or tactile conditions indicates that pilot strategy is also invariant and that differences in control output and performance are attributable to either reconstruction dynamics or differences in the compensation block.

5.3.5 Neuromuscular Model

The Neuromuscular model was taken from previous research. The only determinations necessary were the appropriate order of neuromuscular dynamics for this model, and the use of proprioceptive loop closure within the neuromuscular model. Although all three models (0th, 2nd, and 3rd Order) were nominally successful in replicating pilot performance, the 3rd order model is clearly superior in matching the frequency domain results, particularly at higher frequencies. The presence of the additional lag term causes the magnitude to fall off faster than would have otherwise been the case, matching empirical results extremely well.

Regarding loop closure, it was found that the linear closed loop system was virtually unaffected by the presence of proprioceptive feedback within the neuromuscular block. Interestingly, when the nonlinear block was constructed, presence of the neuromuscular block prevented construction of realistic output signals (quick movements, and crisp “hold” periods.) This fact seems to indicate that either the neuromuscular block precedes the nonlinear block in actual pilot reconstruction, or that neuromuscular dynamics are accounted for by the nonlinear term, resulting in the final, observed control output signal.

5.4 Research Shortcomings

5.4.1 TSAS

Despite promising trends across a variety of conditions, the TSAS failed to produce statistically significant results comparable to the results found in previous research. However, it must be noted that the bar was deliberately set much higher for this experiment, evaluating TSAS in the presence of excellent visual environment and visual instrument cues. Regardless, the TSAS still proved to be an effective means of displaying data to the pilot, particularly in the moments immediately following VOE.

5.4.2 Experimental Design

A few of the details of the experimental design may have reduced the effectiveness of the research effort. Though no profound errors were discovered, different protocols might have been more effective in generating the desired results.

The use of a relatively complex fourth order model undoubtedly complicated the experiment more than necessary. The presence of both attitude and position dynamics made the system much more difficult to control and model. For original model development, a simpler linear model would have been preferable, followed by validation with a more complex linear dynamic model. All of the literature cited used first or second order models for the controlled element dynamics.

Regarding the dynamic effects of the disturbance, in this experiment disturbance signal directly affect the velocity rather than the acceleration. This implementation was done in an effort to avoid corrupting the disturbance signal through system dynamics. However, it resulted in open loop plant dynamics diverting from the dynamics set by the A matrix. The time rate of change of the x state was not simply equal to the \dot{x} state. Instead, the disturbance signal was added (or subtracted, axis dependent). Although it most likely had no effect from a mathematical standpoint, from a bookkeeping standpoint this

decision necessitated much more care and caution during the mathematical modeling and made pilot state reconstruction more difficult.

The failure to break out x and y-axes in many of the subjective measures resulted in the loss of potential insight into pilot workload and situational awareness. The failure to realize the profound difference in the quality of signal provided in each axis led to this oversight. A priori, it was not anticipated that the visual field would result in different control models. This oversight could be easily remedied in future research.

5.4.3 Model Development

In designing the Pilot compensator term, the parameters *Den*, *Num*, and *Delay* all changed the gain of the forward loop. The use of parameters that affected the forward loop gain of the term made physical meaning of parameters less intuitive. A better probably would have been to have unity value on all final terms and embed the delay, denominator, and numerator parameters on the higher orders of *s*. For example, to define the lead term as $\frac{1}{\frac{s}{Den} + 1}$ instead of $\frac{1}{s + Den}$ would not have changed the physical

significance of the *Den* parameter, and would have allowed the forward loop gain of the compensator to be solely defined by the *Gain* parameter.

The decision to use the Linear Quadratic Regulator only to set the vector of *K*, but not match the magnitude of the *u_c* signal to the aileron signal could be questioned. Though heuristically sound, one could argue that *R* and *Q* should have been chosen to result in an optimal feedback gain *K* that produced a linear command signal equal in magnitude to the actual output. This decision can be defended by pointing out that using low control cost was consistent with pilot reported strategies and yielded acceptable results.

The inability of the model to predict the exact magnitude of performance penalty due to the Degraded Visual Environment indicates that causes other than estimation dynamics

may affect closed loop dynamics during condition changes. It is possible that either the pilot loop gain may be affected by a lack of confidence in the quality of signals or that the empirical measurements of observation noise under each condition was inaccurate.

Regarding the nonlinear dynamics, surprisingly, the nonlinear block resulted in universally poorer time domain matching performance than the actual pilot strategy employed, indicating that either the stochastic measures were incomplete in defining pilot strategy, or that an additional control loop is present in defining final pilot control output.

5.5 Potential areas of future research

Certainly, the improved definition and measurement of pilot strategic indicators bears further research. Despite the shortcomings of this research, the use of stochastic maps and fuzzy decision-making has potential to accurately model pilot performance, which, by most accounts, defies logic at times. As mentioned previously, other factors than those used to define stochastic maps are clearly important in influencing pilot decision-making. Identification of those factors and quantification of them is a realistic and attainable goal.

The construction of a simpler simulator task, with fewer conditions may ease the completion and validation of the heuristic model. Additionally, the presentation of a Gaussian disturbance signal, rather than a sum-of-sines signal may provide insight into broad band pilot dynamics and may present an opportunity to explore the utility of control movement analysis as it applies to workload measurement.

Regarding the model development, there are several courses of action that have potential to add to the fidelity of the existing heuristic model. First of all, many of the model terms may be unnecessarily complex. A comparative analysis of optimal gain upon closed loop matching is necessary. Furthermore, it is possible that a simpler compensator plant (without lead/lag terms) will suffice in modeling closed loop pilot performance.

The use of imperfect plant knowledge may add an additional dynamic to the model. The heuristic model has, until this point, assumed perfect knowledge of the plant. To perturb the estimator model with imperfect plant structure will effect the reconstruction of plant states and may more closely match pilot performance degradation during degraded visual environments. This is a potentially complex task and should only be explored after validation of a simpler model.

Without a doubt, the arena of nonlinear pilot development has the potential to aid in the development of new cockpit technology. An accurate model of pilot performance may one day reduce development time by identifying effective hardware for further evaluation and eliminating non value-added systems early in the development phase.

As a point of interest, Figure 5-1 shows the simultaneous plot of all twelve trials of subject A. The relative repeatability suggests that the pilot strategy is less random and more structured than assumed. This result indicates that the pilot decision making process *can* be defined, but the wrong or incomplete variables were evaluated in this case.

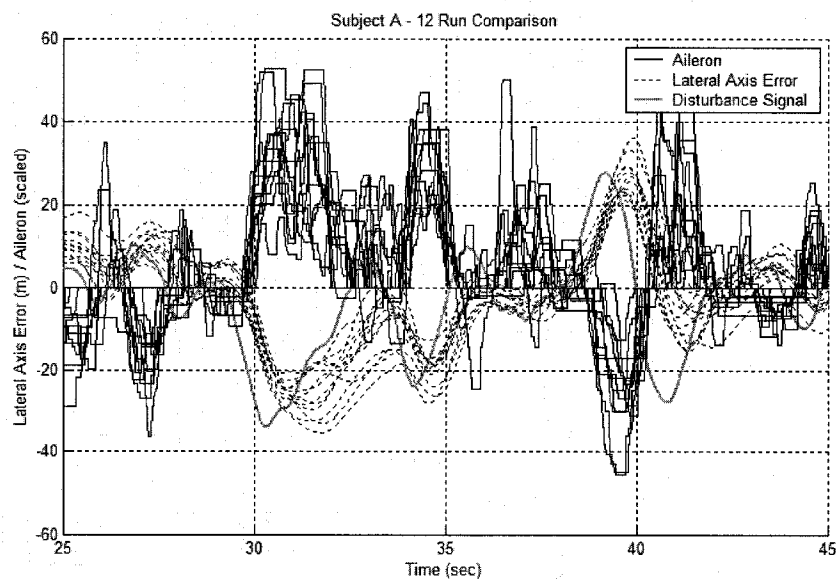


Figure 5-1 Twelve Trial Repeatability

Model Adjustment is also necessary for further research. The models presented here were generated with basic assumptions about pilot performance and strategy. The assumptions translated into well defined optimal gains and observation noise signals. By allowing empirical, rather than heuristic, definition of those values, model matching can be improved. Figure 5-2 shows the result of “tweaking” the existing model structure by massaging the optimal feedback gain K and the observation noise signal v_y .

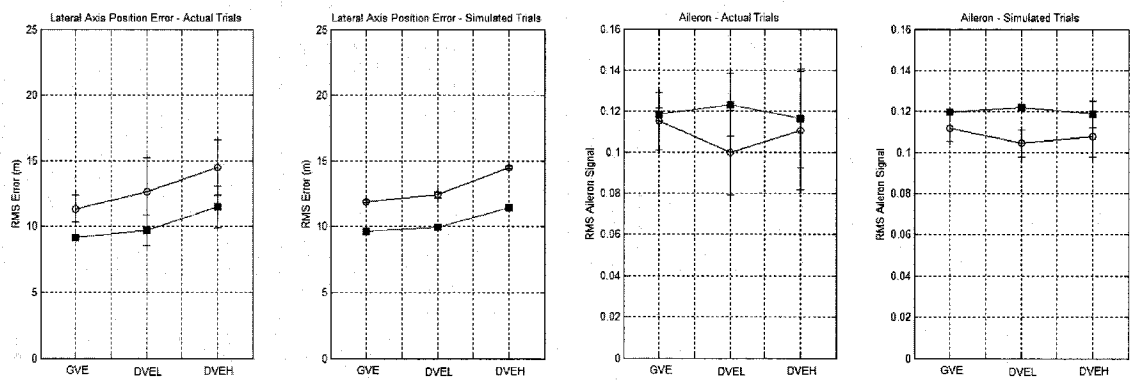


Figure 5-2 "Tweaked" Heuristic Model

It is relatively easy to achieve excellent matching, though the physical meaning of all changes must be accounted for logically.

SECTION 6 CONCLUSIONS

The Tactile Situational Awareness System is an effective means of improving pilot performance, increasing situational awareness, and reducing workload. These improvements are more pronounced during conditions of degraded or absent visual cues. The system is most effective in the moments immediately following loss of visual cues, resulting in improved performance and faster transition recovery times.

The use of subjective measures of pilot workload and situational awareness was validated as an effective means of evaluation. All subjective measures proved sensitive to visual condition, indicating an increase in workload and decrease in situational awareness during degraded visual conditions.

The development of a heuristic linear model was successful in matching both time and frequency domain characteristics of closed loop pilot performance. The inclusion of heuristically derived terms and feedback elements that are consistent with stated and observed pilot control strategies is effective in replicating the gross qualities of pilot behavior.

The inability of the nonlinear term to accurately replicate the pilot decision process is most likely due to an incorrect choice of the decision drivers, rather than the appropriateness of the stochastic analysis method, which is likely employed by pilots during control tasks. Certainly, the improved definition and measurement of pilot strategic indicators bears further research. Despite the shortcomings of this research, the use of stochastic maps and fuzzy decision-making has potential to accurately model pilot performance, which, by most accounts, defies logic at times. As mentioned previously, other factors than those used to define stochastic maps are clearly important in influencing pilot decision-making. Identification of those factors and quantification of them is a realistic and attainable goal.

This research has shown the potential benefit of an accurate multi-modal mathematical model of pilot behavior. Perfecting such a model has the potential to dramatically reduce time and cost of development of new technology. An accurate model of pilot performance, either linear or nonlinear, may one day reduce development time by identifying effective hardware for further evaluation and eliminating non value-added systems early in the development phase.

References

Adams, C., Dryden, R., John, G., and P. Hall. Nurse Minerva. 1997. 24 Oct. 2004. <<http://www.nurseminerva.co.uk/diagrams.htm>>.

Allen, R. W., Clement, W.F., and H.R. Jex. "Research on Display Scanning, Sampling, and Reconstruction Using Separate Main and Secondary Tracking Tasks." Technical Report No. 170-2, NASA CR-1569, July 1970.

Anderson, M. R., and D. K. Schmidt. "Closed Loop Pilot Vehicle Analysis of the Approach and Landing Task." Journal of Guidance 10.2. (1987): 187-194.

Ball, D. LTC. "Brownout: Reducing the Risk." FlightFax, Army Aviation Risk Management Information Nov. 2003: 13-15.

Ballard, J. W. and R. W. Hessinger. "Human-engineered Electromechanical Tactual Sensory Control System." Electrical Manufacturing Oct. 1954: 118-121.

Barnhill, R.L. Ed. Textbook of Dermatopathology. New York: McGraw Hill, 1998.

Baron, S., Kleinman, D.L., and W.H. Levinson. "An Optimal Control Model of Human Response Part II: Prediction of Human Performance in a Complex Task." Automatica. 6 (1970). 371-383.

Biezad, D. J. and R. Cheng. "Controls Design with Crossfeeds for Hovering Rotorcraft Using Quantitative Feedback Theory." Annual Progress Report, NASA CR-195765. Mar. 1994.

Blanken, C. L., Pausder, H. J., and C. J. Ockier. An Investigation of the Effects of Pitch-Roll (De)Coupling on Helicopter Handling Qualities. U.S.Army Aeroflightdynamics

Directorate (USAATCOM), Ames Research Center. Springfield, VA: National Technical Information Service, 1995.

Bliss, J.C., Katcher, M.H., Rogers, C.H., and R.P. Shepard. "Optical-to-tactile image conversion for the blind." IEEE Transactions on Man-Machine Systems 11.1 (1970): 58-65.

Bolanowski, S.J. Jr., and J.J. Zwislocki. "Intensity and Frequency Characteristics of Pacinian Corpuscles: 1. Action potentials." Journal of Neurophysiology. 51.4 (1984): 793-811.

Bologna, J.L., Jorizzo, J.L., and R.P. Rapini, eds. Dermatology. Mosby Publishing: Spain, 2003.

Braithwaite M.G., DeRoche S.L., Alvarez E.A., and M.A. Reese. The impact of SD on rotary-wing operations. Proceedings of the First Tri-service Conference on Rotary Wing Spatial Disorientation: Spatial Disorientation in the Operational Rotary-Wing Environment, 23-26 Sep. 1996, Fort Rucker, AL: Aircrew Health and Performance Division, 1997.

Burgess, P.R. and E.R. Perl. "Cutaneous Mechanoreceptors and Nociceptors." Ed. A. Iggo. Handbook of Sensory Physiology: Somatosensory System, Vol. 2. New York: Springer-Verlag, 1973: 29-78.

Cholewiak, R. W., and J.C. Craig. "Vibrotactile pattern recognition and discrimination at several body sites," Perception & Psychophysics. 35.6 (1984): 503-514.

Cholewiak R.W., and A.A. Collins. "Sensory and Physiological Bases of Touch." The Psychology of Touch. Eds. M.A. Heller and W.E. Schiff. Hillsdale, NJ: Lawrence Erlbaum Associates, 1991. 23-60.

Craig, G., Jennings, S., Cheung, B., Rupert, A., and K. U. Schultz. "Flight-Test of a Tactile Situational Awareness System in a High-Hover Task." American Helicopter Society 60th Annual Forum, Baltimore, MD, June 7-10, 2004.

Davidson, J.B. and D.K. Schmidt. "Modified Optimal Control Pilot Model for Computer Aided Design and Analysis." NASA Technical Memorandum 4384, 1992.

Davidson, J.B., and D.K. Schmidt. "Extended Cooperative Control Synthesis." NASA Technical Memorandum 4561, August 1994.

Dell'Acqua, R., Turatto, M., and P. Joliceur. "Cross-modal attentional deficits in processing tactile stimulation." Perception and Psychophysics 63.5 (2001): 777-789.

Dobbins, T. and S. Samways. The Use of Tactile Navigation Displays for the Reduction of Disorientation in Maritime Environments. RTO HFM Symposium on "Spatial Disorientation in Military Vehicles: Causes, Consequences, and Cures." 15-17 Apr. 2002, La Coruna, Spain:RTO-MP 2002.

Doman, D. B., and M.R. Anderson. "A fixed-order optimal control model of human operator response." Automatica 26 (2000): 209-418.

Dunlap, K. "Paesthetic difference sensibility for rate." American Journal of Physiology 29 (1911): 180-114.

Endsley, M.R. "A Methodology for the Objective Measurement of Pilot Situation Awareness." Presented at the AGARD Symposium on Situation Awareness in Aerospace Operations, Copenhagen, Denmark, Oct., 1989.

Endsley, M.R. and D. J. Garland. Situation Awareness Analysis and Measurement. Mahwah, NJ: Lawrence Erlbaum Associates, 2000.

Eschow, M. M. "Flight Investigation of Variations in Rotorcraft Control and Display Dynamics for Hover." Journal of Guidance, Control, and Dynamics 15.2, (1992): 482-490.

Forssberg, H. and S. Grillner. "The Locomotion of the Acute Spinal Cat Injected with Clonidine I.V." Brain Research. 50 (1973): 184-186.

Freeberg, I. M.. Fitzpatrick's Dermatology in General Medicine, 5th ed. New York, NY: MCGraw Hill, 1999.

Freed, M. A and M.G. Shafto. Human-System Modeling: Some Principles and a Pragmatic Approach. Proceedings of the 4th International Workshop on the Design, Specification, and Verification on Interactive Systems, Granada, Spain, 1997

Gartner, W.B. and M.R. Murphy. "Concepts of Workload." AGARDograph No. 246, Survey of Methods to Assess Workload. Eds. Hartman, B.O. and R.E. McKenzie. London: Technical Editing and Reproduction, Ltd. 1979. 1-5.

Gawron, V.J. Human Performance Measures Handbook. Mahwah, NJ: Lawrence Erlbaum Associates, 2000.

Geldard, F. A. "Adventures in tactile literacy." American Psychologist 12 (1957): 115-124.

Goff, G.D. "Differential Discrimination of Frequency of Cutaneous Mechanical Vibration." Journal of Experimental Psychology. 74 (1967): 294-299.

Gottlieb, G. "Conceptions of Prenatal Development: Behavioral Embryology" Psychological Review 83.3 (1976): pp215-234.

Hartman, B. O. and R. E. McKenzie. Survey of Methods to Assess Workload. AGARDograph No 246. London: Technical Editing and Reproduction, Ltd. 1979..

Hess, R. "Theory for Aircraft Handling Qualities Based Upon a Structural Pilot Model." Journal of Guidance 12.6 (1989): 792-797.

Hess, R. "Analyzing Manipulator and Feli System Effects in Aircraft Flight Control." IEEE Transactions on Systems, Man, and Cybernetics 20-4 (1990). 923-931.

Hess, R. A. "Human-in-the-Loop Control." The Control Handbook. Ed. S. Levine. IEE Press, 1996. 1497-1505.

Hess, R. A. and S. A. Snell, "Flight Control System Design with Rate Saturating Actuators." Journal of Guidance, Control, and Dynamics. 20.1 (1997): 90-96.

Jennings, S., Craig, G., Cheung, B., Rupert, A., and K.U. Schultz. "Flight-Test of a Tactile Situational Awareness System in a Land-based Deck Landing Task." American Helicopter Society 60th Annual Forum, Baltimore, MD, June 7-10, 2004.

Johnston, D. E. and D. T. McRuer. "Investigation of Limb-Side Stick Dynamic Interaction with Roll Control." Journal of Guidance 10.2 (1986): 178-186.

Kaas, J.H., Nelson, R.J., Sur, M., and C.S. Lin. "Multiple Representations of the Body Within the Primary Somatosensory Cortex of Primates." Science. 205 (1979): 521-523.

Keidel, W.D. "Electrophysiology of Vibratory Perception." Ed. W.D. Neff, Contributions to Sensory Physiology, Vol. 3. New York: Academic Press, 1968. 1-79.

Keller, J. D. An Investigation of Helicopter Dynamic Coupling Using an Analytical Model. NASA, Springfield, VA: National Technical Information Service, 1995.

Kennet, S, Spence, C, and J. Driver. "Visuo-tactile links in covert exogenous spatial attention remap across changes in unseen hand posture." Perception & Psychophysics 64.7 (2002): 1083-1094.

Kleinman, D.L., Baron, S., and W.H. Levinson. "An Optimal Control Model of Human Response –Part I: Theory and Validation." Automatica. 6.3 (1970): 357-369.

Lakatos, S. and R. N. Shepard. "Constraints Common to Apparent Motion in Visual, Tactile, and Auditory Space." Journal of Experimental Psychology: Human Perception and Performance 25.4 (1997): 1050-1080.

Lee, D., Horn, J. F., Sezer-Uzol, N., and L. N. Long. "Simulation of Pilot Control Activity During Helicopter Shipboard Operation." American Institute of Aeronautics and Astronautics. 2003.

Levinson, W. H. and J. I. Elkind. "Studies of Multivariable Manual Control Systems: Two Axis Compensatory Systems with Separated Displays and Controls." NASA CR-875, Oct. 1967.

Libet, B. "Electrical Stimulation of Cortex in Human Subjects and Conscious Sensory Aspects." Ed. A. Iggo, Handbook of Sensory Physiology: Somatosensory System. Vol. 2. New York: Springer Verlag 1973. 743-790.

Loomis, J.M. "Interaction of Display Mode and Character Size in Vibrotactile Letter Recognition." Bulleting of the Psychonomic Society. 16, (1980): 385-387.

Lwekowicz, D. L. "Heterogeneity and heterochrony in the development of intersensory perception." Cognitive Brain Research 14 (2002): 41-63.

Lyle, C. "FY03Aviation Safety Performance Review." FlightFax, Army Aviation Risk Management Information. Dec 2003: 7.

Maravita, A., Spence, C., Kennett, S., and J. Driver. "Tool-use changes multimodal spatial interaction between vision and touch in normal humans." Cognition 83 (2002): B25-B34.

McDonnell, J.D., and H.R. Jex. A Critical Tracking Task for Man-Machine Research Related to the Operators Effective Delay Time. Part II: Experimental Effects of System Input Spectra, Control Stick Stiffness, and Controlled Element Order. NASA CR-674, Jan. 1967.

McFarland, M.W., ed. The Papers of Wilbur and Orville Wright, Vol. I, New York: McGraw-Hill, 1953. 90-100.

McGrath, B.J. "Tactile Instrument for Aviation." Dissertation, University of Sydney, 1999.

McRuer, D., Graham, D., and E. Krendel. "Manual Control of Single Loop Systems: Part I." Journal of the Franklin Institute 283.1 (1967): 1-29.

McRuer, D., Graham, D., and E. Krendel. "Manual Control of Single Loop Systems: Part II." Journal of the Franklin Institute 283.2 (1967): 144-168.

McRuer, D. "Development of Pilot-in-the Loop Analysis." Journal of Aircraft 10.9 (1973): 515-524.

McRuer, D. T., Ashkenas I, and D. Graham. Aircraft Dynamics and Automatic Control. Princeton NJ: Princeton University Press, 1973.

McRuer D.T. and E. S. Krendel, "Mathematical Models of Human Pilot Behavior", AGARDograph No. 188, London: Technical Editing and Reproduction, Ltd. 1974. 29-39.

McRuer, D T. "Human Dynamics in Man Machine Systems." Automatica 16 (1980): 237-283.

McRuer, D. T. and D. K. Schmidt. "Pilot Vehicle Analysis of Multiaxis Tasks." Journal of Guidance 13.2 (1990): 348-355.

Miller, R.C., and S.G. Hart. "Assessing the subjective workload of directional orientation tasks." 20th Annual Conference on Manual Control, Vol. 2 (1984): 85-96.

Montagna, W. The Structure and Function of Skin. New York: Academic Press. 1956.

O'Donnell, R. D and F. T. Eggemeier. "Workload Assessment Methodology." in K. R. Boff, L. Kaufman, and J.P. Thomas (Eds.) Handbook of Perception and Human Performance New York, NY: John Wiley and Sons, 1986.

Prather, S. C., and K Sathian. "Mental rotation of tactile stimuli." Cognitive Brain Research 14 (2002): 91-98.

Pring, L, and J. Walker. "Degree of accuracy in perceiving graphic and representational information through touch." International Journal of Rehabilitation Research 16 (1993): 277-287.

Raj, A.K., Suri, N, Braithwaite, M.G., and A Rupert. The Tactile Situation Awareness System in Rotary Wing Aircraft: Flight Test Results. RTO HFM Symposium on "Current Medical Issues in Rotary Wing Operations." 19-21 Oct. 1998. San Diego, CA: 1998.

Raj, A.K., Kass, S. J, and Perry, J.F. Vibrotactile Displays for Improving Spatial Awareness. Proceedings of the Human Factors and Ergonomics Society, Annual Meeting, 2000.

Roscoe, A.H. "Assessing Pilot Workload." AGARDograph No. 233, Neuilly Sur Seine, France: Advisory Group for Aerospace Research and Development, 1978.

Roscoe, A.H. "The Practical Assessment of Pilot Workload." AGARDograph No 282. Loughton, Essex: Specialised Printing Services, 1987.

Roscoe, M. F. and C. J. Wilkinson. "DIMSS – JSHIP'S Modeling and Simulation Process for Ship/Helicopter Testing and Training." AIAA Modeling and Simulation Technologies Conference and Exhibit, 5-8 August 2002, Monterey, California..

Rubin, E., and J.L. Farber, Eds. Pathology. 2nd Ed. Philadelphia, J.B. Lippincott, 1994.

Rupert, A.H., Guedry, F.E., and M.F. Reshke. "The Use of a Tactile Interface to Convey Position and Motion Perceptions." *Virtual Interfaces: Research and applications*, Lisbon, Portugal. October 18-22, 1993.

Rupert, A.H., Guedry, F.E., and M.F. Reshke. "The Use of a Tactile Interface to Convey Position and Motion Perceptions." Neuilly Sur Seine, France: Advisory Group for Aerospace Research and Development. AGARD CP-541:20 (1994) 11-75.

Sanders, M. S., and E.J. McCormick, Eds. Human Factors in Engineering and Design, 5th Ed. New York, NY: McGraw Hill, 1982.

Sanneman, R.A. Tactical Display for Aircraft Control, DARPA A010258, Office of Naval Research, Arlington, VA, 1975.

Sherertz, T. and B. Schenk. The Homunculus: Vanderbilt Undergraduate Neuromajors Club Newsletter. 2002, 8 Oct. 2002 <http://www.vanderbilt.edu/neuro_majors/homunculus.htm>.

Sheridan, T. B. Man-Machine Systems: Information, Control, and Decision Models of Human Performance Cambridge, MA: MIT Press, 1974.

Sherrick, C. E. "A scale for rate of tactual vibration." Journal of the Acoustical Society of America 78.1, (1985): 78-83.

Sklar, A.E., and N.B. Sarter "Good Vibrations: Tactile Feedback in Support of Attention Allocation and Human-Automation Coordination in Event Driven Domains." Human Factors 41.4 (1999) 543-552.

Spence, C., Pavani, F., and J. Driver. "Crossmodal Links Between Vision and Touch in Covert Endogenous Spatial Attention." Journal of Experimental Psychology: Human Perception and Performance 26.4 (2000): 1298-1319.

Stapleford, R. L., McRuer, D. T., and R. Magdaleno. "Pilot Describing Function Measurements in a Multiloop Task." CR-542, Aug. 1966, NASA.

Stapleford, R. L., Craig, S. J. and J. A. Tennant, "Measurement of Pilot Describing Functions in Single Controller Multiloop Tasks," NASA CR-1238, Jan. 1969.

Spraycar, M. Ed. Stedman's Medical Dictionary, 26th Ed. Baltimore, MD: Williams and Wilkins Publishing, 1995.

Stengel, R. F. "Toward Intelligent Flight Control." IEEE Transactions on Systems, Man, and Cybernetics 23.6 (1993): 1699-1717.

Suri, N. and A. Rupert. "Tactile Situational Awareness System." Naval Aerospace Medical Research Laboratory Annual Update, 1997.

Verillo, R.T. "Investigation of Some Parameters of the Cutaneous Threshold for Vibration." Journal of the Acoustical Society of America. 37 (1962): 843-846.

Weinstein, S. "Intensive and Extensive Aspects of Tactile Sensitivity as a Function of Body Part, Sex, and Laterality." The Skin Senses. Ed. D.R. Kenshalo. Springfield, IL: Thomas, 1968. 195-222.

Weir D.H. and R.H. Klein. "The Measurement and Analysis of Pilot Scanning and Control Behavior During Simulated Instrument Approaches." NASA CR-1535, 1970.

Weir, D.H. and D.T. McRuer. "Dynamics of a driver/vehicle steering control." Automatica. 6 (1987).

Whillans, M.G. Human Factors in Aircraft Design, Chapter in Anthropometry and Human Engineering, 1963 Bournemouth England

Wickens, C. D., "The effects of Control Dynamics on Performance." Human Performance. Ed. Paul M. Fitts and Michael I Posner. Belmont, CA: Brooks/Cole Publishing Company. 1967. Chapter 39.

Wickens, C. D., Sandry, D. L., and M Vidulich. "Compatibility and Resource Competition between Modalities of Input, Central Processing, and Output." Human Factors 25.2 (1983): 227-248.

Wierwille, W.W., and S.A. Connor. "Evaluation of 20 Workload Measures Using a Psychomotor Task in a Moving Base Aircraft Simulator." Human Factors 25.1 (1983): 1-16.

Wilkinson, C. H., Roscoe, M. F., and G. M. VanderVliet. "Determining Fidelity Standards for the Shipboard Launch and Recovery Task." AIAA Modeling and Simulation Technologies Conference and Exhibit. 6-9 August 2001 Montreal, Canada.

Williges, R.C., and W.W. Wierwille. "Behavioral Measures of Aircrew Mental Workload." Human Factors 21 (1979), 549-574.

Wood, D. "Tactile Displays: present and Future." Displays 18 (1998): 125-128.

Zeyada, Y and R.A. Hess. "Modeling Human Pilot Cue Utilization with Applications to Simulator Fidelity Assessment." Journal of Aircraft 37.4 (2000): 588-597.

Appendices

| | |
|-------------------------|---|
| Appendix A | Computer Programming Code |
| Appendix B | Institutional Review Board Certification |
| Appendix C | Latin Square Trial Order |
| Appendix D | Pilot Questionnaires |
| Appendix E | Data Analysis MATLAB Code |

Appendix A Computer Program Source Code

| | |
|---|-----|
| NAMRL C++ Code for Aircraft Dyanmics..... | 171 |
|---|-----|

NAMRL C++ Code for Aircraft Dynamics

```

#####
//
// SFB_Sim.c
// Vega Helicopter Simulation
// Carl S. Cole 12.7.2004
//
// summary of keyboard commands
// t or T :: Time of day; 1=day, 0=night
//=====
#include <vg.h>           // include file for Vega
#include <vgFx.h>         // special effects
#include <vgAudio.h>     // vega audio
#include <aw.h>           // audio works
#include <vgsym.h>       // for symbology
#include <math.h>
#include "SFB_Sim.h"     // header file

#####
// main
//=====
int main() {
//=====
// assign remote parameters to address structure
    WSAStartup(0x202,&wsaData);

// assign winsock parameters
    local_addr.sin_family = AF_INET;           // address to receive on
    local_addr.sin_port = htons(receive_port);
    local_addr.sin_addr.s_addr = INADDR_ANY;   // listen on any adaptor

// initiate local socket
    receive_socket = socket(AF_INET, SOCK_DGRAM, 0);

// place socket in to non-blocking mode
    retval = ioctlsocket(receive_socket, FIONBIO, (unsigned long *) &mode);

// bind socket to address structure
    bind(receive_socket, (struct sockaddr*)&local_addr, sizeof(local_addr));

    fromlen = sizeof(from_addr);           // must initialize

//=====
// init, define and config vega
    vgInitSys();           // initialize system
    vgInitAudio();
    vgInitSym();
    vgDefineSys(adf_file);
    vgConfigSys();
//=====
    helo_pos = vgNewPos(); // initialize position objects
//=====
// find instances
// players

```

```

helo_player =    vgFindPlyr("Helo"); // get player reference

// windows and scenes
window = vgFindWin("Default");    // get window reference

// iSectors
helo_isec = vgFindIsect("HeloHAT"); // helicopter height above terrain for motoin model

myEnv = vgFindEnv("Default");
//=====
// loop forever
while (1) {
//=====
// get height above terrain
vgUpdate (helo_isec);
hat_status = vgGetIsectResult (helo_isec, VGIS_GETHAT, &helo_hat);
// let's do everything in meters
// helo_hat = M2FT * helo_hat;
if (fabs(helo_hat) > 500) helo_hat = 500;
//=====
// toggle time of day if no UDP input
key_press = vgGetWinKey (window);
if ((key_press == 'n' || (key_press == 'N'))) {
timeOfDay -= 0.1f;
if (timeOfDay < 0.0f) timeOfDay = 1.0f;
}
//=====
// UDP receive info from LabView control process
timeOut = 0;
while (timeOut < 100) {
retval = recvfrom(receive_socket, receive_str, sizeof(receive_str), 0,
(struct sockaddr *)&from_addr, &fromlen);
// printf("%i\n", retval);
// data received
if (retval > 0) {
receive_str[retval] = 0;    // terminate string
// printf("%s\n", receive_str);
sscanf(receive_str, "%10f%10f%10f%10f%10f%10f%10f%10f",
&delta_t, &timeOfDay,
&h_helo, &p_helo, &r_helo, &x_helo, &y_helo, &hat_cmd);
// convert to meters
// x_helo = x_helo / M2FT;
// y_helo = y_helo / M2FT;
// hat_cmd = hat_cmd / M2FT;
printf("%i %7.3f %4.1f %8.1f %8.1f %8.1f %8.1f %8.1f %8.1f\n",
retval, delta_t, timeOfDay,
h_helo, p_helo, r_helo, x_helo, y_helo, hat_cmd);
timeOut = 100;
}
else {
Sleep(10);
timeOut += 10;
printf("no data %i\n", timeOut);
}
}
//=====

```

```

// set degraded visual environment
    vgProp(myEnv, VGENV_TOD, timeOfDay); // time of day, 1=day
    //      vgEnvColor(myEnv, VGENV_VISCOLOR, 0.7f, 0.7f, 0.7f); // fog color
    //      vgProp(myEnv, VGENV_VISRNG, 300.0f); } // fog far range
//=====
// control "bouncing" over terrain features
    z_terrain = z_helo - helo_hat; // meters
    if ((delta_t > 0) && (helo_hat < 200) && hat_status) {
// compute required velocity and acceleration
        last_hat_d = hat_d;
        hat_d = (hat_cmd - helo_hat) / delta_t;
        hat_dd = (hat_d - last_hat_d) / delta_t;
// limit acceleration -- different limits if velocity oppisite acceleration
        if ((hat_dd >= 0) != (last_hat_d >= 0)) // opposite directions
            hat_dd_limit = 3.0f * hat_dd_max;
        else
            hat_dd_limit = hat_dd_max;
        hat_dd = max(-hat_dd_limit, hat_dd);
        hat_dd = min(hat_dd_limit, hat_dd);
// compute limited velocity
        hat_d = last_hat_d + delta_t * hat_dd;
// damp velocity if close to desired z
        delta_z = fabs(hat_cmd - helo_hat);
        if (delta_z < 10)
            hat_d = 0.9 * hat_d;
// calculate final z
        z_helo = z_terrain + helo_hat + delta_t * hat_d;
//      printf("%f %f %f\n", z_helo - z_terrain, hat_d, hat_dd);
    }
    else
        z_helo = z_terrain + hat_cmd;
//=====
// position Helo
    vgPosVec(helo_pos, x_helo, y_helo, z_helo,
            h_helo, p_helo, r_helo); // convolve
    vgPos(helo_player, helo_pos); // set position of Helo
//=====
    vgSyncFrame (); // update vega
    vgFrame ();
//=====
} // end loop forever
closesocket(receive_socket);
    WSACleanup();
} // end main

```

Appendix B Institutional Review Board Documentation

The use of human subjects during this research necessitated the filing and approval of all research procedures. Included in Appendix B is the final approved proposal. This proposal was approved by the board on January 18th, 2004. Approval expiration occurs in October, 2005. Any questions regarding this process may be directed to Old Dominion University Institutional Review Board office at

Appendix B
OLD DOMINION UNIVERSITY
HUMAN SUBJECT RESEARCH REVIEW APPLICATION FORM

| Responsible Project Investigator (RPI) | | |
|--|--|--------------------------------------|
| Responsible Project Investigator: The RPI must be a member of ODU faculty or staff who will serve as the project supervisor and be held accountable for all aspects of the project. Students cannot be listed as RPIs. | | |
| First Name: Thomas | Middle Initial: E. | Last Name: Alberts |
| Telephone: 683-3736 | Fax Number: 683-3200 | E-mail: talberts@odu.edu |
| Office Address: 241 Kaufman Hall | | |
| City: Norfolk | State: VA | Zip: 23529-0247 |
| Department: Aerospace Engineering | College: Engineering and Technology | |
| Complete Title of Research Project: Use Of A Tactile Instrument To Enhance Pilot Performance During Brownout Conditions | | Code Name (one word): TSAS |
| Investigators | | |
| If more investigators exist than lines provide, please attach a separate list. | | |
| Investigator(s): Individuals who are directly responsible for any of the following: the project's design, implementation, consent process, data collection, and/or data analysis. | | |
| First Name: Karl | Middle Initial: U. | Last Name: Schultz |
| Telephone: 624-3705 | Fax Number: 445-8516 | Email: karl.schultz@navy.mil |
| Office Address: 733 Graydon Ave | | |
| City: Norfolk | State: VA | Zip: 23507 |
| Department: Aerospace Engineering | College: Engineering and Technology | |
| Affiliation: <input type="checkbox"/> Faculty <input checked="" type="checkbox"/> Graduate Student <input type="checkbox"/> Undergraduate Student <input type="checkbox"/> Staff <input type="checkbox"/> Other | | |
| | | |
| First Name: Braden | Middle Initial: J. | Last Name: McGrath |
| Telephone: 850-452-4441 | Fax Number: 613-452-9290 | Email: brad@namrl.navy.mil |
| Office Address: 51 Hovey Road | | |
| City: Pensacola | State: FL | Zip: 32508 |
| Department: Aerospace Engineering | College: Engineering and Technology | |
| Affiliation: <input type="checkbox"/> Faculty <input type="checkbox"/> Graduate Student <input type="checkbox"/> Undergraduate Student <input type="checkbox"/> Staff <input checked="" type="checkbox"/> Other <input type="checkbox"/> Adjunct Faculty | | |
| List all information for additional investigators on attachment and check here: <input type="checkbox"/> | | |

8. Are research subjects being used whose ability to give informed voluntary consent may be in question? (e.g., children, persons with AIDS, mentally disabled, psychiatric patients, prisoners.)

Yes (If yes, explain the procedures to be employed to enroll them and to ensure their protection).

No

8b. What type of vulnerable subjects are being enrolled? (check all that apply)

Critically Ill Patients

Mentally Disabled or Cognitively

Impaired Individuals

Prisoners

Physically Handicapped

Pregnant Women

Children

Other _____

Recruitment

9. How will participants be recruited? (Please submit a copy of the sign-up sheet, newspaper advertisement, or any other protocol or procedure which will be used to recruit subjects.)

Internet

Newspaper/radio/television advertising

Posters/brochures/letters

Other LOCAL MILITARY SQUADRONS

Comments: Volunteers will be sought from local naval helicopter squadrons.

Inclusion and Exclusion Criteria

10. Are subjects equitably chosen for participation in the study? (no one group is excluded without justification)

Yes

No (If no, specify criteria and justify in detail below.)

10a. Does the study require special evaluation and screening of potential subjects to determine their appropriateness for inclusion in the study?

Yes (If yes, briefly elaborate on the screening process and attach the screening questionnaire.)

No

Experimental Procedures

11. Describe the experimental procedures that will be followed. (Include a succinct, but comprehensive statement of the methodology relating to the human subjects. You are encouraged to include a discussion of statistical procedures used to determine the sample size.)

Twelve subjects will be used. The rationale for this number is economic and practical. The unfunded status of this research effort precludes large sample size, as does the availability of well-trained helicopter pilots in the local area. Additionally, the existence of twelve trial conditions lends itself to the use of twelve subjects to achieve a balanced trial order.

Subjects will be instructed to control a static helicopter visual flight simulator to maintain a position in the fore-aft axis. A secondary task, roll angle, will vary in difficulty dependent upon primary task performance. During the three-minute trial, the pilot will naturally reach an equilibrium between primary task performance and secondary task difficulty.

Twelve trials will be conducted, varying fidelity of the visual field and provision of tactile information as well as visual.

Intra-trial questionnaires will be conducted to measure pilot situational awareness and workload during each visual/tactile condition.

Post trial surveys will be conducted to gather information pertaining to tactile vest fit, comfort, and utility.

11a. Will any aversive or painful procedures be employed (e.g., shock, the threat of shock or punishment, experimentally induced stress?)

Yes (If yes, specify and justify in detail below.)
 No

11b. Will the deliberate deception of research participants be involved as part of the experimental procedure?

Yes (If yes, explain the nature of the deception, why it is necessary, any possible risks that may result from the deception, and the nature of the debriefing with specific reference to the deception.)
 No

Attach copies of the following items:

Research Protocol(s)

Questionnaire

Copies of any instructions or debriefings given

If the research is part of a research proposal submitted for federal, state or external funding, submit a copy of the FULL proposal

| Compensation | |
|------------------|--|
| 12. | How much time will be required of each subject? 2 hours |
| 12a. | Will research subjects receive course credit for participating in the study? <input type="checkbox"/> Yes (If yes, please explain in comments section.) <input checked="" type="checkbox"/> No Comments: |
| 12b. | Are there any other forms of compensation that may be used? (e.g. Money) <input type="checkbox"/> Yes (If yes, please explain in comments section.) <input checked="" type="checkbox"/> No Comments: |
| 12c. | Are there any penalties for subjects who do not show up for a research session? <input type="checkbox"/> Yes (If yes, please explain in comments section.) <input checked="" type="checkbox"/> No Comments: |
| Informed Consent | |
| | 13. Do you intend to obtain informed consent from subjects? <input checked="" type="checkbox"/> Yes (please answer question 13a) <input type="checkbox"/> No (please complete Appendix F: Request for Waiver of Consent Form) |
| 13a. | Describe the procedures that will be used to obtain Informed Consent and attach the Informed Consent Document (follow the guidelines for preparation of the University Informed Consent Form). |
| | See attached document. Informed Consent Form is in full compliance with ODU Informed Consent Checklist. |
| Risks | |

14. What are potential risks of the research? (Check all that apply)

- physical harm
 psychological harm
 Release of confidential information
 Other Mild spatial disorientation

14a. Describe any potential risks to subjects for the activities proposed and describe the steps that will be taken to minimize the risks. Include any risks to the subject's physical well being, privacy, dignity, emotions, employability, and criminal and legal status. A detailed, comparative statement of the risk (harm or likelihood) must also be described in the consent form.

Mild Spatial Disorientation and nausea possible during some of the trials, due to visual vestibular conflict. In the event that the subject begins to feel nausea, they can halt the experiment at any time.

Please attach the following (if you have developed them)

- The script by the experimenter to disclose potential harm and likelihood (risk) prior to the subject's choice to participate.

Benefits

15. Assess the potential benefits that may accrue to the individual subject as well as to others as a result of the proposed study. Do the potential benefits justify the possible risks involved? Although you may mention general benefits to society, such speculative benefits should not be presented to a subject as a direct benefit for informed consent.

There are no direct benefits for the test subjects. Evaluation of the TSAS system may lead to improved algorithms for the TSAS system itself, ultimately leading to improved pilot situational awareness and performance, decreased pilot workload, and safer flying conditions, saving lives, airframes, and money.

Protection of Anonymity

16. Describe in detail the procedures for protecting the anonymity (meaning that no one will ever be able to know the names) of the research subjects. If anonymity is impossible, then describe in detail the procedures for safeguarding data and confidential records. These procedures relate to how well you reduce the risk that a subject may be exposed or associated with the data.

Research subjects will be assigned a letter for analysis and presentation. Their names or any other information that would allow a reader to identify them will not be used in any presentation or publication.

| |
|--|
| Drugs or Devices |
| <p>17. Will any drugs, devices, or chemical biological agents be used with the subjects? <input type="checkbox"/> Yes (If yes, please attach Appendix G: Drugs, Agents, and Devices Form) <input checked="" type="checkbox"/> No</p> |
| Biological Materials |
| <p>18. Will this research involve the collection, analysis, or banking of human biological materials (cells, tissues, fluids, DNA?) <input type="checkbox"/> Yes (If yes, please attach Appendix H: Biological Materials Form) <input checked="" type="checkbox"/> No</p> |
| Training |
| <p>19. Briefly explain the nature of the training and supervision of anyone who is involved in the actual data collection, research design, or in conducting the research. The RPI must document completion of NIH Training. Attach a copy of the RPI's NIH Certificate for Human Participants Protections Education for Research Teams.</p> <p>All training and experimental protocols will be supervised by Professor Alberts, Lieutenant Commander Schultz, or both. No trials will be conducted without the presence of at least one of the two. Both have completed NIH Training, certificates attached</p> |
| PLEASE NOTE: |
| <p>You may begin research when the University Human Subjects Review Board gives you final WRITTEN notice of its approval. You MUST inform the committee of ANY adverse event, changes in the method, personnel, funding, or procedure. At any time the committee reserves the right to re-review a research project, to request additional information, to monitor the research for compliance, to inspect the data and consent forms, to interview subjects that have participated in the research, and if necessary to terminate a research investigation.</p> |
| |
| <p>Responsible Project Investigator (Must be original signature)</p> |

INFORMED CONSENT DOCUMENT

OLD DOMINION UNIVERSITY

PROJECT TITLE: Use Of A Tactile Instrument To Enhance Pilot Performance During Brownout Conditions

INTRODUCTION

The purposes of this form are to give you information that may affect your decision whether to say YES or NO to participation in this research, and to record the consent of those who say YES. The research in question is designed to evaluate the utility of a Tactile instrument in improving pilot performance and decreasing pilot workload during hover tasks.

RESEARCHERS

This research is being conducted in partial fulfillment of requirements for Ph.D. in Aerospace Engineering for Lieutenant Commander Karl U. Schultz. The research team is headed by Professor Thomas Alberts, ODU Department of Aerospace Engineering. Other research advisors include Professors Brett Newman and Colin Britcher, ODU Department of Aerospace Engineering, Braden McGrath, Ph.D., Naval Aerospace Medical Research Laboratory, and Captain Angus Rupert, MD, Ph.D., NASA Flight Surgeon.

DESCRIPTION OF RESEARCH STUDY

Several studies have been conducted looking into the subject of the use of a Tactile cockpit instrument in improving pilot performance. Naval Aerospace Medical Research Laboratory (NAMRL) in Pensacola Florida has developed the Tactile Situational Awareness System (TSAS) to provide information to a pilot via tactile, rather than visual means. Although several successful flight tests have been conducted on TSAS, NAMRL presently lacks sufficient ground based data to build a comprehensive cognitive model of pilot visual/tactile interaction. Such a model could lend insight into pilot strategies in combining parallel information paths, ultimately leading to the development of more effective TSAS algorithms, the presentation of more valuable information to the pilot, and improved flight safety.

If you decide to participate, then you will join a study involving research of pilot workload and performance in good and degraded visual environments, both with and without TSAS. You will be required to control a static helicopter flight simulator in both pitch and roll for twelve trials lasting approximately 3 minutes each. If you say YES, then your participation will last for approximately 2 hours at the ODU Vibrations Laboratory, Building 241, Room 126. Approximately 12 subjects will be participating in this study.

EXCLUSIONARY CRITERIA

You should have completed the TSAS experiment screening questionnaire. Your status as an aviator guarantees that you do not have any exclusionary conditions

RISKS AND BENEFITS

RISKS: If you decide to participate in this study, then you may face a risk of slight nausea due to visual-vestibular conflict (not unlike other Navy visual, static trainers.) The limited field of view of the TSAS simulator makes this event unlikely. However, if you do feel nauseous, or suffer any other discomfort, you may terminate your involvement in this experiment at any time. And, as with any research, there is some possibility that you may be subject to risks that have not yet been identified.

BENEFITS: There are no direct benefits derived from your participation in this experiment. The main benefit to you for participating in this study is your involvement in developing emerging cockpit technology. Your opinion will be invaluable to improving the utility of this instrument, as well as improving aviation safety for you, your squadron mates, and those who will follow you.

COSTS AND PAYMENTS

The researchers want your decision about participating in this study to be absolutely voluntary. While they recognize that your participation may pose some inconvenience, the researchers are unable to give you any payment for participating in this study.

NEW INFORMATION

If the researchers find new information during this study that would reasonably change your decision about participating, then you will be personally contacted by either Dr. Alberts or Lieutenant Commander Schultz.

CONFIDENTIALITY

The researchers will take all reasonable steps to keep private information, including all questionnaires and surveys confidential. With the exception of your experiment screening questionnaire, all records will refer to each subject by a subject letter. Copies of trial data will be sent to research offices at Naval Aerospace Medical Research Laboratory in Pensacola, Florida. None of the records sent to NAMRL will contain your name or any personal data. The screening questionnaires will remain on-site within the Aerospace Department at ODU. The results of this study may be used in reports, presentations, and publications; but the researcher will not identify you. Of course, your records may be subpoenaed by court order or inspected by government bodies with oversight authority.

WITHDRAWAL PRIVILEGE

It is OK for you to say NO. Even if you say YES now, you are free to say NO later, and walk away or withdraw from the study -- at any time. Your decision will not affect your relationship with Old Dominion University, or otherwise cause a loss of benefits to which you might otherwise be entitled.

COMPENSATION FOR ILLNESS AND INJURY

If you say YES, then your consent in this document does not waive any of your legal rights. However, in the event of illness or injury arising from this study, neither Old Dominion University nor the researchers are able to give you any money, insurance coverage, free medical care, or any other compensation for such injury. In the event that you suffer injury as a result of participation in any research project, you may contact Dr. Alberts at 757-683-3736 or Dr. David Swain the current IRB chair at 757-683-6028 at Old Dominion University, who will be glad to review the matter with you.

VOLUNTARY CONSENT

By signing this form, you are saying several things. You are saying that you have read this form or have had it read to you, that you are satisfied that you understand this form, the research study, and its risks and benefits. The researchers should have answered any questions you may have had about the research. If you have any questions later on, then the researchers should be able to answer them:

| | | |
|-----------------------|---------|--------------|
| Professor Tom Alberts | ODU | 757-683-3736 |
| LCDR Karl U Schultz | US Navy | 757-445-5191 |
| Dr. Braden McGrath | NAMRL | 850-452-4441 |

If at any time you feel pressured to participate, or if you have any questions about your rights or this form, then you should call Dr. David Swain, the current IRB chair, at 757-683-6028, or the Old Dominion University Office of Research, at 757-683-3460.

And importantly, by signing below, you are telling the researcher YES, that you agree to participate in this study. The researcher should give you a copy of this form for your records.

| | |
|---|-------------|
| Subject's Printed Name & Signature | Date |
|---|-------------|

INVESTIGATOR'S STATEMENT

I certify that I have explained to this subject the nature and purpose of this research, including benefits, risks, costs, and any experimental procedures. I have described the rights and protections afforded to human subjects and have done nothing to pressure, coerce, or falsely entice this subject into participating. I am aware of my obligations under state and federal laws, and promise compliance. I have answered the subject's questions and have encouraged him/her to ask additional questions at any time during the course of this study. I have witnessed the above signature(s) on this consent form.

| | |
|--|-------------|
| Investigator's Printed Name & Signature | Date |
|--|-------------|

Appendix C Latin Square Development

The Latin Square Development Algorithm is a method that balances the experiment against order effects. By varying the order of presentation of each trial condition, the Latin Square eliminates the possibility of learning or fatigue effects confounding the data and being confused with actual condition related changes in performance.

The Latin Square method guarantees that each trial condition will appear in each temporal position once and only once. It further guarantees that each condition will follow and precede each other condition only once.

Assuming N number of trial conditions, the equation for the order of trials for subject number one is:

Condition # 1, 2, N, 3, N-1, 4, N-2, ...

To find the condition order for subject number two, each trial is stepped up by one:

Condition # 2, 3, 1, 4, N, 5, N-1, ...

This trend continues until subject N+1, at which time the previous N orders can be reversed, creating N more orders and maintaining a balanced experiment.

For this experiment, there were N conditions, in the following order:

1. GVE, TSAS Off
2. DVEL, TSAS Off
3. DVEH, TSAS Off
4. GVE, TSAS On
5. DVEL, TSAS On
6. DVEH, TSAS On
7. GVE, TSAS Off
8. DVEL, TSAS Off
9. DVEH, TSAS Off
10. GVE, TSAS On
11. DVEL, TSAS On
12. DVEH, TSAS On

Note that each trial condition occurs twice.

The final determined counterbalanced experimental trial order for all twelve subjects is shown in Table C-1.

| SUBJECT | A | B | C | D | E | F | G | H | I | J | K | L |
|----------------|----------|----------|----------|----------|----------|----------|----------|----------|----------|----------|----------|----------|
| Trial 1 | 0, 0 | 1, 0 | 2, 0 | 0, 1 | 1, 1 | 2, 1 | 0, 0 | 1, 0 | 2, 0 | 0, 1 | 1, 1 | 2, 1 |
| 2 | 1, 0 | 2, 0 | 0, 1 | 1, 1 | 2, 1 | 0, 0 | 1, 0 | 2, 0 | 0, 1 | 1, 1 | 2, 1 | 0, 0 |
| 3 | 2, 1 | 0, 0 | 1, 0 | 2, 0 | 0, 1 | 1, 1 | 2, 1 | 0, 0 | 1, 0 | 2, 0 | 0, 1 | 1, 1 |
| 4 | 2, 0 | 0, 1 | 1, 1 | 2, 1 | 0, 0 | 1, 0 | 2, 0 | 0, 1 | 1, 1 | 2, 1 | 0, 0 | 1, 0 |
| 5 | 1, 1 | 2, 1 | 0, 0 | 1, 0 | 2, 0 | 0, 1 | 1, 1 | 2, 1 | 0, 0 | 1, 0 | 2, 0 | 0, 1 |
| 6 | 0, 1 | 1, 1 | 2, 1 | 0, 0 | 1, 0 | 2, 0 | 0, 1 | 1, 1 | 2, 1 | 0, 0 | 1, 0 | 2, 0 |
| 7 | 0, 1 | 1, 1 | 2, 1 | 0, 0 | 1, 0 | 2, 0 | 0, 1 | 1, 1 | 2, 1 | 0, 0 | 1, 0 | 2, 0 |
| 8 | 1, 1 | 2, 1 | 0, 0 | 1, 0 | 2, 0 | 0, 1 | 1, 1 | 2, 1 | 0, 0 | 1, 0 | 2, 0 | 0, 1 |
| 9 | 2, 0 | 0, 1 | 1, 1 | 2, 1 | 0, 0 | 1, 0 | 2, 0 | 0, 1 | 1, 1 | 2, 1 | 0, 0 | 1, 0 |
| 10 | 2, 1 | 0, 0 | 1, 0 | 2, 0 | 0, 1 | 1, 1 | 2, 1 | 0, 0 | 1, 0 | 2, 0 | 0, 1 | 1, 1 |
| 11 | 1, 0 | 2, 0 | 0, 1 | 1, 1 | 2, 1 | 0, 0 | 1, 0 | 2, 0 | 0, 1 | 1, 1 | 2, 1 | 0, 0 |
| 12 | 0, 0 | 1, 0 | 2, 0 | 0, 1 | 1, 1 | 2, 1 | 0, 0 | 1, 0 | 2, 0 | 0, 1 | 1, 1 | 2, 1 |

Table C-1 Trial Condition Order for All Subjects

In Table C-1, the first number in each column represents the Visual Condition (GVE = 0, DVEL = 1, and DVEH = 2). The second number represents the availability of TSAS (TSAS Off = 0, and TSAS On = 1).

Appendix D Pilot Questionnaires

| | |
|---|-----|
| Preflight Questionnaire | 189 |
| Intra Trial Questionnaire..... | 190 |
| Post Trial Questionnaire –Part 1 | 192 |
| Post Trial Questionnaire – Part 2 | 193 |

**PILOT QUESTIONNAIRE – TSAS Study
Pre-Flight Questionnaire**

Date: _____ Subject Letter: _____

Pilot Name: _____ Age: _____

Pilot Height: _____

Pilot Qualifications:

| | Total Hours | QTP | IP | Fixed Wing | Helicopter Hours | NVG Hours |
|--------------|-------------|-----|----|------------|------------------|-----------|
| Career | | | | | | |
| Last 90 Days | | | | | | |

Aircraft in which Current: _____

Pilot Vision: _____ / _____

Are Glasses Required (Y/N): _____

Prescription Used Normally: _____ During Testing: _____

Is Pilot taking any medication that may increase effects of nausea: _____

| In the past have you experienced, (Please check) | YES | NO |
|---|--------|--------|
| ■ motion sickness in an a/c, no visual aids | () | () |
| ■ motion sickness in an a/c, using NVG of IHAADS | () | () |
| ■ vertigo (spatial disorientation) in and a/c, no visual aids | () | () |
| ■ vertigo using NVG of IHAADS | () | () |
| ■ simulator sickness | () | () |

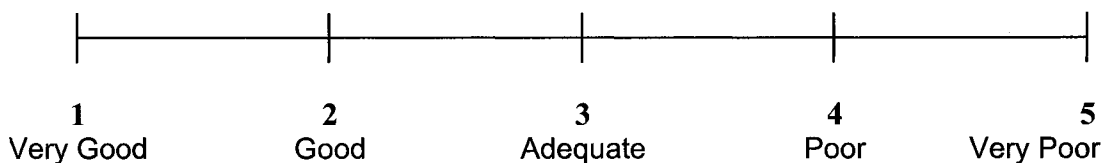
PILOT QUESTIONNAIRE – TSAS (Intra Trial)
Simulator Hover Task Subject Letter _____

Run #

TSAS ON / OFF (Circle One)
Good / DVE Light / DVE Heavy (Circle One)

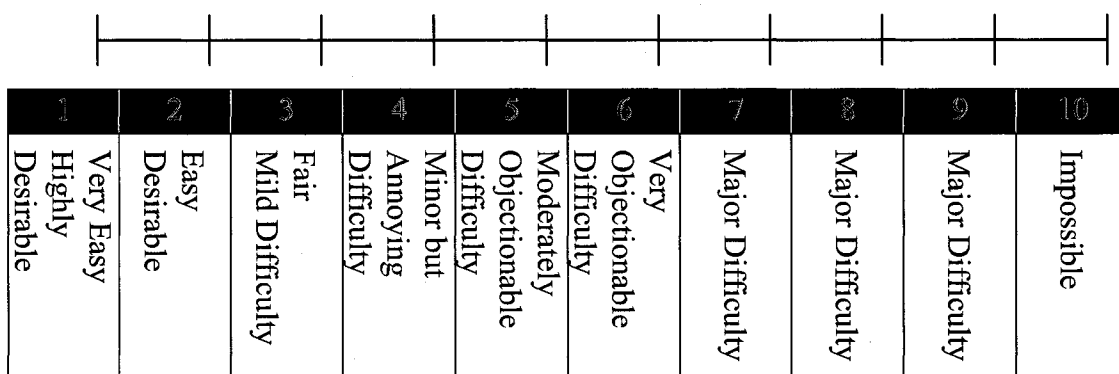
China Lake SA

- How would you rate your overall Situational Awareness during the previous run:



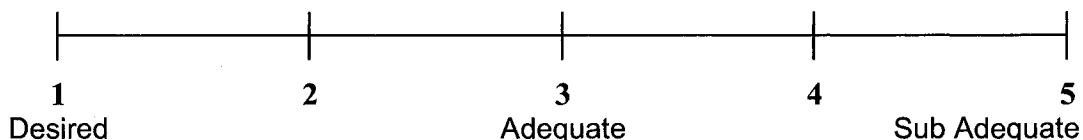
Modified Cooper-Harper Rating Scale

- How would you rate your mental effort during the previous run:



Subjective Performance Self Evaluation

- Rate your performance during the previous run:



Perceptual Cue Rating Scale

- o Rate the quality of the cues (Visual and/or Tactile) during the previous run:

| | | | | | | | |
|-----------------|---------|---|-------------|-------------------------------|---------|---|-------------|
| 1 | Good | 1 | Good | 1 | Good | 1 | Good |
| 2 | | 2 | | 2 | | 2 | |
| 3 | Fair | 3 | Fair | 3 | Fair | 3 | Fair |
| 4 | | 4 | | 4 | | 4 | |
| 5 | Poor | 5 | Poor | 5 | Poor | 5 | Poor |
| | Outside | | Instruments | | Outside | | Instruments |
| Attitude | | | | Horizontal Translation | | | |

Good : Can make aggressive and precise corrections with confidence and precision is good.

Fair : Can make limited corrections with confidence and precision is only fair.

Poor: Only small and gentle corrections are possible, and consistent precision is not attainable.

- o Indicate % of attention spent on each visual instrument during GVE and DVE.

| | | | |
|-----|----------------------|--------------------|--------------------------|
| | Visual Environment | | |
| GVE | <input type="text"/> | Flight Director | DVE <input type="text"/> |
| | | Artificial Horizon | |

- o Indicate % of information derived from TSAS or Vision during GVE and DVE

| | | | |
|-----|----------------------|-----|----------------------|
| GVE | <input type="text"/> | DVE | <input type="text"/> |
|-----|----------------------|-----|----------------------|

- o Did you feel disoriented or uncomfortable at any time during the maneuver

Physiological Response Questionnaire

Did you experience any of the following during or after the maneuver? (Please check)

| <u>ONSET</u> | <u>SLIGHT</u> | <u>MODERATE</u> | <u>STRONG</u> | <u>NOTHING</u> |
|-----------------------------------|---------------|-----------------|---------------|----------------|
| ■ DIZZINESS | () | () | () | () |
| ■ UNEASINESS | () | () | () | () |
| ■ SWEATING | () | () | () | () |
| ■ HEADACHE | () | () | () | () |
| ■ EYE STRAIN | () | () | () | () |
| ■ IMBALANCE | () | () | () | () |
| ■ STOMACH AWARENESS | () | () | () | () |
| ■ NAUSEA | () | () | () | () |
| ■ VERTIGO | () | () | () | () |
| ■ LOSS OF BRIGHTNESS OF THE IMAGE | () | () | () | () |
| ■ LOSS OF IMAGE | () | () | () | () |
| ■ FATIGUE | () | () | () | () |

**PILOT QUESTIONNAIRE – TSAS Study
Post-Flight Questionnaire - Part 1**

Date: _____

Pilot Name: _____

Subjective WORKload Dominance (SWORD)

Please compare each of the trials you flew based on the degree to which it reduced your mental workload in comparison to the other trials. Make a check mark in the column in each row corresponding to your preference for one trial configuration over another. Cross off the Task that was not completed.

For example, if you felt that the condition “Driving with Cruise Control” was absolutely more effective than “Driving while blindfolded” in reducing your mental workload, you should mark the box :

| | absOL UTE | | VERY STRONG | | STRON G | | weak | | equal | | weak | | STRONG | | VERY STRONG | | absOL UTE | |
|--------------------------------|--------------|--|----------------|--|------------|--|------|--|-------|--|------|--|--------|--|----------------|--|--------------|------------------------------|
| Driving with Cruise Control | 6.1. | | | | | | | | | | | | | | | | | Driving while Blindfolded |

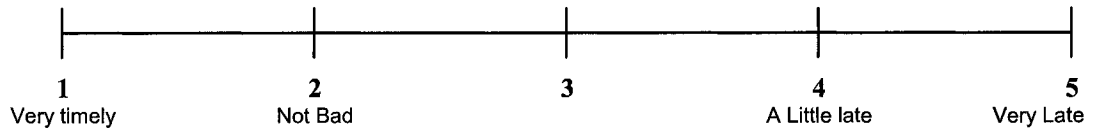
Task: High Hover

| | absOL UTE | | VERY STRONG | | STRON G | | weak | | equal | | weak | | STRONG | | VERY STRONG | | absOL UTE | |
|----------------------------|--------------|--|----------------|--|------------|--|------|--|-------|--|------|--|--------|--|----------------|--|--------------|------------------------------|
| Good Vision No TSAS | | | | | | | | | | | | | | | | | | Good Vision with TSAS |
| Good Vision No TSAS | | | | | | | | | | | | | | | | | | Occluded Vision No TSAS |
| Good Vision No TSAS | | | | | | | | | | | | | | | | | | Occluded Vision with TSAS |
| Good Vision with TSAS | | | | | | | | | | | | | | | | | | Occluded Vision No TSAS |
| Good Vision with TSAS | | | | | | | | | | | | | | | | | | Occluded Vision with TSAS |
| Occluded Vision No TSAS | | | | | | | | | | | | | | | | | | Occluded Vision with TSAS |

Task: Superslide

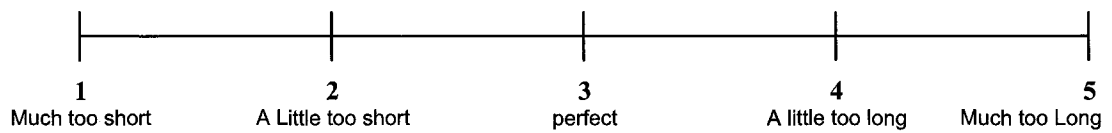
| | absOL UTE | | VERY STRONG | | STRON G | | weak | | equal | | weak | | STRONG | | VERY STRONG | | absOL UTE | |
|-------------------------|--------------|--|----------------|--|------------|--|------|--|-------|--|------|--|--------|--|----------------|--|--------------|----------------------------|
| Superslide with TSAS | | | | | | | | | | | | | | | | | | Superslide without TSAS |

5. Was the TSAS cue too late or unsynchronized with other cues for a/c control?



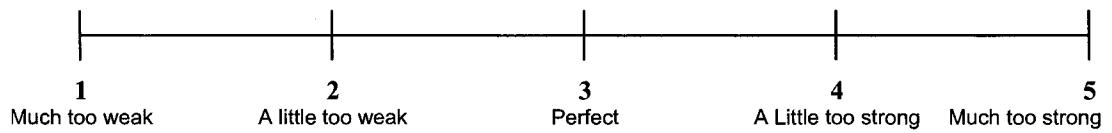
Comment: _____

6. Was the duration of the TSAS cue too short, too long or OK?



Comment: _____

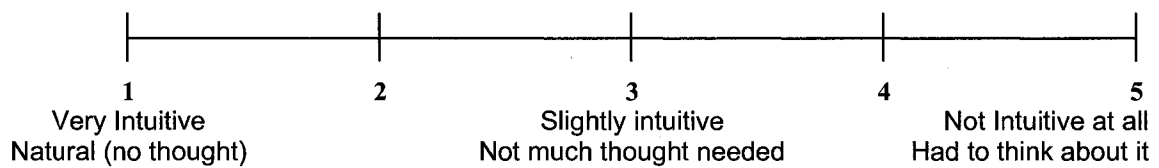
7. Was the TSAS cue too strong or too weak? _____



Comment: _____

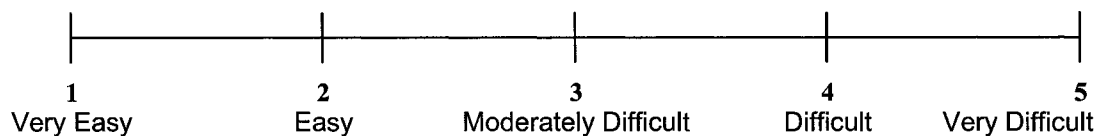
8. Could you comment on factor intensity during tactical conditions? _____

9. How intuitive was the TSAS?



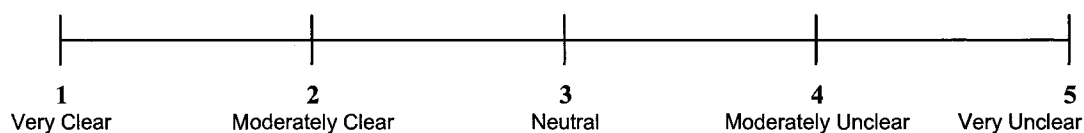
Comment: _____

10. How difficult was localizing the TSAS cue (i.e., difficult to determine if the cue was back, front, left, or right)?



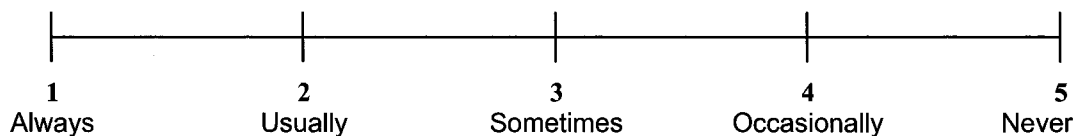
Comment: _____

11. In the case of multiple cues (e.g., back & side), how clear was it what action was required?



Comment: _____

12. Did you always interpret the TSAS cue correctly (i.e., always make the correct control input based on the TSAS cue)? (e.g., reversals)



Comment: _____

13. Should the TSAS provide cues for the direction of a/c motion or for the direction of the stick input required to correct the drift? _____

14. In which task was the TSAS most useful (HH/MH/Both/Neither)? _____
-

15. Were there any test conditions that led to disorientation (including mild or temporary disorientation)? _____
-

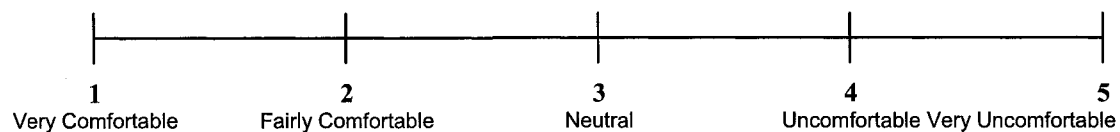
16. Where there any other aspects of the TSAS cueing that presented any difficulties? _____

17. Please comment on workload during high hover (shipboard landing) operations? _____

18. Any suggestions for improvements of the tactors and/or tactile information? _____

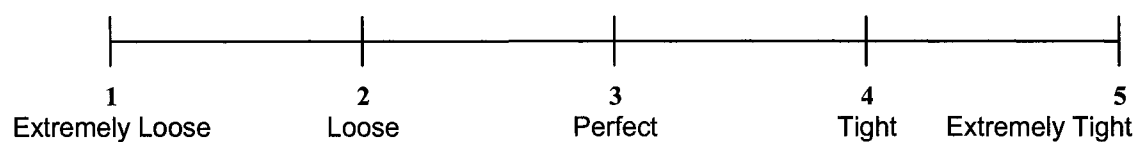
Fit & Comfort

1. Was the cooling suit comfortable?



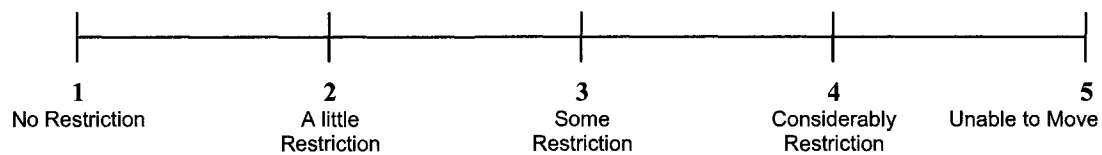
Comment: _____

2. Was TSAS too tight/loose?



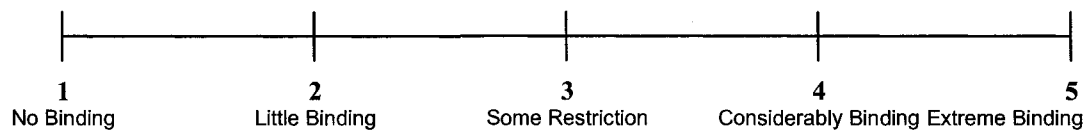
Comment: _____

3. Did the TSAS restrict movement in any way?



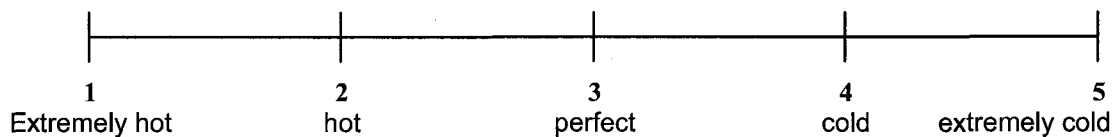
Comment: _____

4. Did you notice any binding in TSAS when you moved?



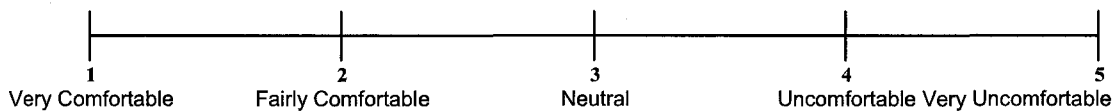
Comment: _____

5. Did you feel too hot/cold when wearing TSAS?



Comment: _____

6. Did you experience any discomfort from TSAS cues?



Comment: _____

7. Any suggestions for improvement of the cooling suit fit? _____

8. Any further comments? _____

Appendix E Analysis Scripts

| | |
|--------------------------------|-----|
| FINAL_DATA_ANALYZE..... | 200 |
| PATH_ERROR_PLOT..... | 202 |
| XAXIS_NM_MODELCALC..... | 206 |
| PILOT_PARAM..... | 210 |
| XAXIS_NONLINEAR_ANALYZE..... | 211 |
| YAXIS_MODEL_SIM_LINEAR..... | 223 |
| YAXIS_MODEL_SIM_NONLINEAR..... | 227 |
| YAXIS_SIM_PLOT_NONLINEAR..... | 235 |
| YAXIS_SIM_PLOT_LINEAR..... | 238 |
| XAXIS_ESTIMATORCOMPARE..... | 239 |
| XAXIS_MODEL_REVIEW..... | 243 |

```

%%%%%%%% Data Analysis
%%%%%%%% Karl Schultz
%%%%%%%% January 2005
%%%%%%%% This program will load and parse data saved by LabView
clear
%%% Set Datapath
loadpath='C:\KarlPhd\ExperimentsFall2004\Data';
eval(['addpath ',loadpath]);
%filename=input('Please Enter the name of the file you would like to analyze.','s');
CONDTSAS=[0 0 0 1 1 1 1 1 0 1 0 0;0 0 0 1 1 1 1 1 1 0 0 0;0 1 0 1 0 1 1 0 1 0 1 0;1 1 0 1 0 0 0 0 1 0 1 1;...
          1 1 1 0 0 0 0 0 0 1 1 1;1 0 1 0 1 0 0 1 0 1 0 1;0 0 1 0 1 1 1 1 0 1 0 0;0 0 0 1 1 1 1 1 1 0 0 0;...
          0 1 0 1 0 1 1 0 1 0 1 0;1 1 0 1 0 0 0 0 1 0 1 1;1 1 1 0 0 0 0 0 0 1 1 1;1 0 1 0 1 0 0 1 0 1 0 1];
CONDVE= [0 1 2 2 1 0 0 1 2 2 1 0;1 2 0 0 2 1 1 2 0 0 2 1;2 0 1 1 0 2 2 0 1 1 0 2;0 1 2 2 1 0 0 1 2 2 1 0;...
         1 2 0 0 2 1 1 2 0 0 2 1;2 0 1 1 0 2 2 0 1 1 0 2;0 1 2 2 1 0 0 1 2 2 1 0;1 2 0 0 2 1 1 2 0 0 2 1;...
         2 0 1 1 0 2 2 0 1 1 0 2;0 1 2 2 1 0 0 1 2 2 1 0;1 2 0 0 2 1 1 2 0 0 2 1;2 0 1 1 0 2 2 0 1 1 0 2];
SUBJ='ABCDEFGHIJKL';
for j=1:12
Subj=SUBJ(j);CondTSAS=CONDTSAS(j,:);CondVE=CONDVE(j,:);
baselinecount=1;DVELightcount=1;DVEheavycount=1;TSAScount=1;TSASDVELightcount=1;TSASDVE
heavycount=1;
for i=1:12
string = ['load ',Subj,num2str(CondTSAS(i)),num2str(CondVE(i)),'T',num2str(i)]; eval([string])
%%% Parse Data
eval(['data=',Subj,num2str(CondTSAS(i)),num2str(CondVE(i)),'T',num2str(i),']; data=data';
eval(['clear ',Subj,num2str(CondTSAS(i)),num2str(CondVE(i)),'T',num2str(i)];
height=data(:,1); pitch=data(:,2); roll=data(:,3); x=data(:,4); y=data(:,5); z=data(:,6);
xd=data(:,7); yd=data(:,8); ud=data(:,9); vd=data(:,10); wd=data(:,11); hd=data(:,12);
pd=data(:,13); rd=data(:,14); deltat=data(:,15); lightness=data(:,16); xdist=data(:,17);
ydist=data(:,18);
time=data(:,19); rudder=data(:,20); elevator=data(:,21); aileron=data(:,22); collective=data(:,23);
Var='x';%aileron to X error';
string=['error=',Var,']; eval([string])
if CondTSAS(i)==0
if CondVE(i)==0
Baseline(:,baselinecount)=error; baselinecount=baselinecount+1;
elseif CondVE(i)==1
DVELight(:,DVELightcount)=error; DVELightcount=DVELightcount+1;
else
DVEheavy(:,DVEheavycount)=error; DVEheavycount=DVEheavycount+1;
end
end
else
if CondVE(i)==0
TSAS(:,TSAScount)=error; TSAScount=TSAScount+1;
elseif CondVE(i)==1
TSASDVELight(:,TSASDVELightcount)=error; TSASDVELightcount=TSASDVELightcount+1;
else
TSASDVEheavy(:,TSASDVEheavycount)=error;
TSASDVEheavycount=TSASDVEheavycount+1;
end
end
end
BL=mean(Baseline');DVEL=mean(DVELight');DVEH=mean(DVEheavy');T=mean(TSAS');TDVEL=mean
(TSASDVELight');TDVEH=mean(TSASDVEheavy');
NDVEL=DVEL./BL;NDVEH=DVEH./BL;NT=T./BL;NTDVEL=TDVEL./BL;NTDVEH=TDVEH./BL;S
ubjBL(:,j)=BL;SubjDVEL(:,j)=DVEL;SubjDVEH(:,j)=DVEH';

```

```
SubjT(:,j)=T';SubjTDVEL(:,j)=TDVEL';SubjTDVEH(:,j)=TDVEH';SubjNDVEL(:,j)=NDVEL';SubjNDV  
EH(:,j)=NDVEH';SubjNT(:,j)=NT';SubjNTDVEL(:,j)=NTDVEL';SubjNTDVEH(:,j)=NTDVEH';  
end  
string=['save ',Var,'10data.mat SubjBL SubjDVEL SubjDVEH SubjT SubjTDVEL SubjTDVEH  
SubjNDVEL SubjNDVEH SubjNT SubjNTDVEL SubjNTDVEH time'];  
eval([string])
```



```

%% Path Error Plot
clear
%% Set Datapath
loadpath='C:\KarlPhd\ExperimentsFall2004\Data';
eval(['addpath ',loadpath]);
string = ['load ailerontoXerrordata']
eval([string])
[crd,index1]=min(abs(time-10));[crd,index2]=min(abs(time-70));[crd,index3]=min(abs(time-100));[crd,index4]=min(abs(time-190));
ind1=index1;ind2=index2;
PVOMean(1)=mean(mean(SubjBL(ind1:ind2,:)));PVOMean(2)=mean(mean(SubjDVEL(ind1:ind2,:)));PVOMean(3)=mean(mean(SubjDVEH(ind1:ind2,:)));
PVOMean(4)=mean(mean(SubjT(ind1:ind2,:)));PVOMean(5)=mean(mean(SubjTDVEL(ind1:ind2,:)));PVOMean(6)=mean(mean(SubjTDVEH(ind1:ind2,:)));
PVOstd(1)=std(mean(SubjBL(ind1:ind2,:)));PVOstd(2)=std(mean(SubjDVEL(ind1:ind2,:)));PVOstd(3)=std(mean(SubjDVEH(ind1:ind2,:)));
PVOstd(4)=std(mean(SubjT(ind1:ind2,:)));PVOstd(5)=std(mean(SubjTDVEL(ind1:ind2,:)));PVOstd(6)=std(mean(SubjTDVEH(ind1:ind2,:)));
PVOrms(1)=mean(mean(abs(SubjBL(ind1:ind2,:))));PVOrms(2)=mean(mean(abs(SubjDVEL(ind1:ind2,:))));PVOrms(3)=mean(mean(abs(SubjDVEH(ind1:ind2,:))));
PVOrms(4)=mean(mean(abs(SubjT(ind1:ind2,:))));PVOrms(5)=mean(mean(abs(SubjTDVEL(ind1:ind2,:))));PVOrms(6)=mean(mean(abs(SubjTDVEH(ind1:ind2,:))));
PVOrmsstd(1)=std(mean(abs(SubjBL(ind1:ind2,:))));PVOrmsstd(2)=std(mean(abs(SubjDVEL(ind1:ind2,:))));PVOrmsstd(3)=std(mean(abs(SubjDVEH(ind1:ind2,:))));
PVOrmsstd(4)=std(mean(abs(SubjT(ind1:ind2,:))));PVOrmsstd(5)=std(mean(abs(SubjTDVEL(ind1:ind2,:))));PVOrmsstd(6)=std(mean(abs(SubjTDVEH(ind1:ind2,:))));
PVOrange(1)=mean(max(SubjBL(ind1:ind2,:))-min(SubjBL(ind1:ind2,:)));PVOrange(2)=mean(max(SubjDVEL(ind1:ind2,:))-min(SubjDVEL(ind1:ind2,:)));
PVOrange(3)=mean(max(SubjDVEH(ind1:ind2,:))-min(SubjDVEH(ind1:ind2,:)));PVOrange(4)=mean(max(SubjT(ind1:ind2,:))-min(SubjT(ind1:ind2,:)));
PVOrange(5)=mean(max(SubjTDVEL(ind1:ind2,:))-min(SubjTDVEL(ind1:ind2,:)));PVOrange(6)=mean(max(SubjTDVEH(ind1:ind2,:))-min(SubjTDVEH(ind1:ind2,:)));
PVOrangestd(1)=std(max(SubjBL(ind1:ind2,:))-min(SubjBL(ind1:ind2,:)));PVOrangestd(2)=std(max(SubjDVEL(ind1:ind2,:))-min(SubjDVEL(ind1:ind2,:)));
PVOrangestd(3)=std(max(SubjDVEH(ind1:ind2,:))-min(SubjDVEH(ind1:ind2,:)));PVOrangestd(4)=std(max(SubjT(ind1:ind2,:))-min(SubjT(ind1:ind2,:)));
PVOrangestd(5)=std(max(SubjTDVEL(ind1:ind2,:))-min(SubjTDVEL(ind1:ind2,:)));PVOrangestd(6)=std(max(SubjTDVEH(ind1:ind2,:))-min(SubjTDVEH(ind1:ind2,:)));
ind1=index2+1;ind2=index3;
XSTIONmean(1)=mean(mean(SubjBL(ind1:ind2,:)));XSTIONmean(2)=mean(mean(SubjDVEL(ind1:ind2,:)));XSTIONmean(3)=mean(mean(SubjDVEH(ind1:ind2,:)));
XSTIONmean(4)=mean(mean(SubjT(ind1:ind2,:)));XSTIONmean(5)=mean(mean(SubjTDVEL(ind1:ind2,:)));XSTIONmean(6)=mean(mean(SubjTDVEH(ind1:ind2,:)));
XSTIONstd(1)=std(mean(SubjBL(ind1:ind2,:)));XSTIONstd(2)=std(mean(SubjDVEL(ind1:ind2,:)));XSTIONstd(3)=std(mean(SubjDVEH(ind1:ind2,:)));
XSTIONstd(4)=std(mean(SubjT(ind1:ind2,:)));XSTIONstd(5)=std(mean(SubjTDVEL(ind1:ind2,:)));XSTIONstd(6)=std(mean(SubjTDVEH(ind1:ind2,:)));
XSTIONrms(1)=mean(mean(abs(SubjBL(ind1:ind2,:))));XSTIONrms(2)=mean(mean(abs(SubjDVEL(ind1:ind2,:))));
XSTIONrms(3)=mean(mean(abs(SubjDVEH(ind1:ind2,:))));XSTIONrms(4)=mean(mean(abs(SubjT(ind1:ind2,:))));

```

```

XSTIONrms(5)=mean(mean(abs(SubjTDVEL(ind1:ind2,:))));XSTIONrms(6)=mean(mean(abs(SubjTDVE
H(ind1:ind2,:))));
XSTIONrmsstd(1)=std(mean(abs(SubjBL(ind1:ind2,:))));XSTIONrmsstd(2)=std(mean(abs(SubjDVEL(ind
1:ind2,:))));
XSTIONrmsstd(3)=std(mean(abs(SubjDVEH(ind1:ind2,:))));XSTIONrmsstd(4)=std(mean(abs(SubjT(ind1
:ind2,:))));
XSTIONrmsstd(5)=std(mean(abs(SubjTDVEL(ind1:ind2,:))));XSTIONrmsstd(6)=std(mean(abs(SubjTDV
EH(ind1:ind2,:))));
XSTIONrange(1)=mean(max(SubjBL(ind1:ind2,:))-
(min(SubjBL(ind1:ind2,:))));XSTIONrange(2)=mean(max(SubjDVEL(ind1:ind2,:))-
(min(SubjDVEL(ind1:ind2,:))));
XSTIONrange(3)=mean(max(SubjDVEH(ind1:ind2,:))-
(min(SubjDVEH(ind1:ind2,:))));XSTIONrange(4)=mean(max(SubjT(ind1:ind2,:))-
(min(SubjT(ind1:ind2,:))));
XSTIONrange(5)=mean(max(SubjTDVEL(ind1:ind2,:))-
(min(SubjTDVEL(ind1:ind2,:))));XSTIONrange(6)=mean(max(SubjTDVEH(ind1:ind2,:))-
(min(SubjTDVEH(ind1:ind2,:))));
XSTIONrangestd(1)=std(max(SubjBL(ind1:ind2,:))-
(min(SubjBL(ind1:ind2,:))));XSTIONrangestd(2)=std(max(SubjDVEL(ind1:ind2,:))-
(min(SubjDVEL(ind1:ind2,:))));
XSTIONrangestd(3)=std(max(SubjDVEH(ind1:ind2,:))-
(min(SubjDVEH(ind1:ind2,:))));XSTIONrangestd(4)=std(max(SubjT(ind1:ind2,:))-
(min(SubjT(ind1:ind2,:))));
XSTIONrangestd(5)=std(max(SubjTDVEL(ind1:ind2,:))-
(min(SubjTDVEL(ind1:ind2,:))));XSTIONrangestd(6)=std(max(SubjTDVEH(ind1:ind2,:))-
(min(SubjTDVEH(ind1:ind2,:))));
ind1=index3+1;ind2=index4;VOSSmean(1)=mean(mean(SubjBL(ind1:ind2,:)));VOSSmean(2)=mean(mea
n(SubjDVEL(ind1:ind2,:)));VOSSmean(3)=mean(mean(SubjDVEH(ind1:ind2,:)));
VOSSmean(4)=mean(mean(SubjT(ind1:ind2,:)));VOSSmean(5)=mean(mean(SubjTDVEL(ind1:ind2,:)));V
OSSmean(6)=mean(mean(SubjTDVEH(ind1:ind2,:)));
VOSSstd(1)=std(mean(SubjBL(ind1:ind2,:)));VOSSstd(2)=std(mean(SubjDVEL(ind1:ind2,:)));VOSSstd(3
)=std(mean(SubjDVEH(ind1:ind2,:)));
VOSSstd(4)=std(mean(SubjT(ind1:ind2,:)));VOSSstd(5)=std(mean(SubjTDVEL(ind1:ind2,:)));VOSSstd(6
)=std(mean(SubjTDVEH(ind1:ind2,:)));
VOSSrms(1)=mean(mean(abs(SubjBL(ind1:ind2,:))));VOSSrms(2)=mean(mean(abs(SubjDVEL(ind1:ind2
,:))));VOSSrms(3)=mean(mean(abs(SubjDVEH(ind1:ind2,:))));
VOSSrms(4)=mean(mean(abs(SubjT(ind1:ind2,:))));VOSSrms(5)=mean(mean(abs(SubjTDVEL(ind1:ind2
,:))));VOSSrms(6)=mean(mean(abs(SubjTDVEH(ind1:ind2,:))));
VOSSrmsstd(1)=std(mean(abs(SubjBL(ind1:ind2,:))));VOSSrmsstd(2)=std(mean(abs(SubjDVEL(ind1:ind
2,:))));VOSSrmsstd(3)=std(mean(abs(SubjDVEH(ind1:ind2,:))));
VOSSrmsstd(4)=std(mean(abs(SubjT(ind1:ind2,:))));VOSSrmsstd(5)=std(mean(abs(SubjTDVEL(ind1:ind
2,:))));VOSSrmsstd(6)=std(mean(abs(SubjTDVEH(ind1:ind2,:))));
VOSSrange(1)=mean(max(SubjBL(ind1:ind2,:))-
(min(SubjBL(ind1:ind2,:))));VOSSrange(2)=mean(max(SubjDVEL(ind1:ind2,:))-
(min(SubjDVEL(ind1:ind2,:))));
VOSSrange(3)=mean(max(SubjDVEH(ind1:ind2,:))-
(min(SubjDVEH(ind1:ind2,:))));VOSSrange(4)=mean(max(SubjT(ind1:ind2,:))-
(min(SubjT(ind1:ind2,:))));
VOSSrange(5)=mean(max(SubjTDVEL(ind1:ind2,:))-
(min(SubjTDVEL(ind1:ind2,:))));VOSSrange(6)=mean(max(SubjTDVEH(ind1:ind2,:))-
(min(SubjTDVEH(ind1:ind2,:))));
VOSSrangestd(1)=std(max(SubjBL(ind1:ind2,:))-
(min(SubjBL(ind1:ind2,:))));VOSSrangestd(2)=std(max(SubjDVEL(ind1:ind2,:))-
(min(SubjDVEL(ind1:ind2,:))));

```

```

VOSSrangestd(3)=std(max(SubjDVEH(ind1:ind2,:))-
(min(SubjDVEH(ind1:ind2,:))));VOSSrangestd(4)=std(max(SubjT(ind1:ind2,:))-
(min(SubjT(ind1:ind2,:))));
VOSSrangestd(5)=std(max(SubjTDVEL(ind1:ind2,:))-
(min(SubjTDVEL(ind1:ind2,:))));VOSSrangestd(6)=std(max(SubjTDVEH(ind1:ind2,:))-
(min(SubjTDVEH(ind1:ind2,:))));
AvgBL=mean(abs(SubjBL'));AvgDVEL=mean(abs(SubjDVEL'));AvgDVEH=mean(abs(SubjDVEH'));Av
gT=mean(abs(SubjT'));AvgTDVEL=mean(abs(SubjTDVEL'));AvgTDVEH=mean(abs(SubjTDVEH'));
stdBL=std(abs(SubjBL'));stdDVEL=std(abs(SubjDVEL'));stdDVEH=std(abs(SubjDVEH'));stdT=std(abs(S
ubjT'));stdTDVEL=std(abs(SubjTDVEL'));stdTDVEH=std(abs(SubjTDVEH'));
NDVEL=AvgDVEL./AvgBL;NDVEH=AvgDVEH./AvgBL;NT=AvgT./AvgBL;NTDVEL=AvgTDVEL./
AvgBL;NTDVEH=AvgTDVEH./AvgBL;
for i=1:length(time);
    AvgSubjBL(i)=mean(SubjBL(i,:)); devSubjBL(i)=std(SubjBL(i,:)); AvgSubjT(i)=mean(SubjT(i,:));
devSubjT(i)=std(SubjT(i,:)); AvgSubjDVEL(i)=mean(SubjDVEL(i,:));
AvgSubjTDVEL(i)=mean(SubjTDVEL(i,:));
    AvgSubjDVEH(i)=mean(SubjDVEH(i,:)); AvgSubjTDVEH(i)=mean(SubjTDVEH(i,:));
AvgSubjNT(i)=mean(SubjNT(i,:)); AvgSubjNDVEL(i)=mean(SubjNDVEL(i,:));
AvgSubjNTDVEL(i)=mean(SubjNTDVEL(i,:)); AvgSubjNDVEH(i)=mean(SubjNDVEH(i,:));
    AvgSubjNTDVEH(i)=mean(SubjNTDVEH(i,:)); devSubjDVEL(i)=std(SubjDVEL(i,:));
devSubjTDVEL(i)=std(SubjTDVEL(i,:)); devSubjDVEH(i)=std(SubjDVEH(i,:));
devSubjTDVEH(i)=std(SubjTDVEH(i,:)); devSubjNT(i)=std(SubjNT(i,:));
devSubjNDVEL(i)=std(SubjNDVEL(i,:));
    devSubjNTDVEL(i)=std(SubjNTDVEL(i,:)); devSubjNDVEH(i)=std(SubjNDVEH(i,:));
devSubjNTDVEH(i)=std(SubjNTDVEH(i,:));
    x1=(abs(SubjBL(i,:))); n1=length(x1); x2=(abs(SubjT(i,:))); n2=length(x2);
    tBLtoT(i)=(mean(x1)-mean(x2))/sqrt( (sum(x1.^2)- (sum(x1)^2)/n1 + sum(x2.^2) -
(sum(x2)^2)/n2)/(n1+n2-2)*(1/n1+1/n2));
    x2=(abs(SubjDVEL(i,:))); n2=length(x2);
    tBLtoDVEL(i)=(mean(x1)-mean(x2))/sqrt( (sum(x1.^2)- (sum(x1)^2)/n1 + sum(x2.^2) -
(sum(x2)^2)/n2)/(n1+n2-2)*(1/n1+1/n2));
    x2=(abs(SubjDVEH(i,:))); n2=length(x2);
    tBLtoDVEH(i)=(mean(x1)-mean(x2))/sqrt( (sum(x1.^2)- (sum(x1)^2)/n1 + sum(x2.^2) -
(sum(x2)^2)/n2)/(n1+n2-2)*(1/n1+1/n2));
    x2=(abs(SubjTDVEH(i,:))); n2=length(x2);
    tBLtoTDVEH(i)=(mean(x1)-mean(x2))/sqrt( (sum(x1.^2)- (sum(x1)^2)/n1 + sum(x2.^2) -
(sum(x2)^2)/n2)/(n1+n2-2)*(1/n1+1/n2));
    x2=(abs(SubjTDVEL(i,:))); n2=length(x2);
    tBLtoTDVEL(i)=(mean(x1)-mean(x2))/sqrt( (sum(x1.^2)- (sum(x1)^2)/n1 + sum(x2.^2) -
(sum(x2)^2)/n2)/(n1+n2-2)*(1/n1+1/n2));
    x1=(abs(SubjT(i,:))); n1=length(x1); x2=(abs(SubjTDVEL(i,:))); n2=length(x2);
    tTtoTDVEL(i)=(mean(x1)-mean(x2))/sqrt( (sum(x1.^2)- (sum(x1)^2)/n1 + sum(x2.^2) -
(sum(x2)^2)/n2)/(n1+n2-2)*(1/n1+1/n2));
    x2=(abs(SubjTDVEH(i,:))); n2=length(x2);
    tTtoTDVEH(i)=(mean(x1)-mean(x2))/sqrt( (sum(x1.^2)- (sum(x1)^2)/n1 + sum(x2.^2) -
(sum(x2)^2)/n2)/(n1+n2-2)*(1/n1+1/n2));
    x1=(abs(SubjDVEL(i,:))); n1=length(x1); x2=(abs(SubjDVEH(i,:))); n2=length(x2);
    tDVELtoDVEH(i)=(mean(x1)-mean(x2))/sqrt( (sum(x1.^2)- (sum(x1)^2)/n1 + sum(x2.^2) -
(sum(x2)^2)/n2)/(n1+n2-2)*(1/n1+1/n2));
    x1=(abs(SubjTDVEL(i,:))); n1=length(x1); x2=(abs(SubjTDVEH(i,:))); n2=length(x2);
    tTDVELtoTDVEH(i)=(mean(x1)-mean(x2))/sqrt( (sum(x1.^2)- (sum(x1)^2)/n1 + sum(x2.^2) -
(sum(x2)^2)/n2)/(n1+n2-2)*(1/n1+1/n2));
    x1=ones(size(SubjNT(i,:))); x2=(abs(SubjNT(i,:))); n2=length(x2);
    tNtoNT(i)=(mean(x1)-mean(x2))/sqrt( (sum(x1.^2)- (sum(x1)^2)/n1 + sum(x2.^2) -
(sum(x2)^2)/n2)/(n1+n2-2)*(1/n1+1/n2));
    x2=(abs(SubjNDVEL(i,:))); n2=length(x2);

```

```

tNtoNDVEL(i)=(mean(x1)-mean(x2))/sqrt((sum(x1.^2)-(sum(x1)^2)/n1 + sum(x2.^2) -
(sum(x2)^2)/n2)/(n1+n2-2)*(1/n1+1/n2));
x2=(abs(SubjDVEH(i,:))); n2=length(x2);
tNtoNDVEH(i)=(mean(x1)-mean(x2))/sqrt((sum(x1.^2)-(sum(x1)^2)/n1 + sum(x2.^2) -
(sum(x2)^2)/n2)/(n1+n2-2)*(1/n1+1/n2));
x2=(abs(SubjNTDVEL(i,:))); n2=length(x2);
tNtoNTDVEL(i)=(mean(x1)-mean(x2))/sqrt((sum(x1.^2)-(sum(x1)^2)/n1 + sum(x2.^2) -
(sum(x2)^2)/n2)/(n1+n2-2)*(1/n1+1/n2));
x2=(abs(SubjNTDVEH(i,:))); n2=length(x2);
tNtoNTDVEH(i)=(mean(x1)-mean(x2))/sqrt((sum(x1.^2)-(sum(x1)^2)/n1 + sum(x2.^2) -
(sum(x2)^2)/n2)/(n1+n2-2)*(1/n1+1/n2));
end
%%%%%% Test Plot
figure(1)clfplot(time,AvgBL,'b','linewidth',2);hold
onplot(time,AvgDVEL,'r','linewidth',2);plot(time,AvgDVEH,'G','linewidth',2);
plot(time,AvgT,'C','linewidth',2);plot(time,AvgTDVEL,'M','linewidth',2);plot(time,AvgTDVEH,'Y','linewi
dth',2);
gridlegend('GVE','DVEL','DVEH','TSAS GVE','TSAS DVEL','TSAS DVEH')
figure(2)
clf plot(time,NDVEL,'r');hold
onplot(time,NDVEH,'G');plot(time,NT,'C');plot(time,NTDVEL,'M');plot(time,NTDVEH,'Y');
title('Normalized')
figure(3)
clf plot(PVOrms,'-x')hold on plot(PVOrms+PVOrmsstd,'+b')plot(PVOrms-PVOrmsstd,'+b')
grid plot(PVOrms,'-*r')plot(PVOrms+PVOrmsstd,'+r')plot(PVOrms-PVOrmsstd,'+r')
plot(PVOrange,'-ok')plot(PVOrange+PVOrangestd,'+k')plot(PVOrange-PVOrangestd,'+k')
title('PVO MEAN, RMS, and RANGE')
figure(4)
clf plot(XSTIONmean,'-x')hold onplot(XSTIONmean+XSTIONstd,'+b')plot(XSTIONmean-
XSTIONstd,'+b')
grid
plot(XSTIONrms,'-*r')plot(XSTIONrms+XSTIONrmsstd,'+r')plot(XSTIONrms-
XSTIONrmsstd,'+r')plot(XSTIONrange,'-ok')
plot(XSTIONrange+XSTIONrangestd,'+k')plot(XSTIONrange-XSTIONrangestd,'+k')
title('VOX MEAN, RMS, and RANGE')
figure(5)
clf plot(VOSSmean,'-x')hold onplot(VOSSmean+VOSSstd,'+b')plot(VOSSmean-VOSSstd,'+b')
grid
plot(VOSSrms,'-*r')plot(VOSSrms+VOSSrmsstd,'+r')plot(VOSSrms-VOSSrmsstd,'+r')plot(VOSSrange,'-
ok')
plot(VOSSrange+VOSSrangestd,'+k')plot(VOSSrange-VOSSrangestd,'+k')
title('VOSS MEAN, RMS, and RANGE')
figure(6)
clf
plot(time,abs(tBLtoDVEL),'r')
hold on
plot(time,abs(tBLtoDVEH),'g')plot(time,abs(tBLtoT),'C')plot(time,abs(tBLtoTDVEL),'M')plot(time,abs(tB
LtoTDVEH),'Y')
grid
title('t Value')

```

```

%%%% XAXIS_NM_MODEL.CALC.m
%%%% 11 June 2006
%%%% LCDR Karl U Schultz
%%%% This program will solve the compenstor block and
%%%% test the validity of several model structures
clear
%%%%% Define plant variables
g=9.81; Pfreq=3.0; Pdamp=.65; Pgain=500; Vydamp=4;
Rfreq=5; Rdamp=.4;Rgain=625;Vxdamp=4;
dt=.012; %% delta t for all trials
%%%%%mass=1000; Not used
%%%%% Basic plant
A=[-Vxdamp 0 0 g;1 0 0 0;0 0 -2*Rdamp*Rfreq -Rfreq^2;0 0 1 0];
B=[0;0;Rgain;0];C=[eye(4)];D=zeros(4,1);E=[0;1;0;0];sys=ss(A,B,C,D);
%%%%% Basic plant with TSAS
AT=A;BT=B;CT=[C;0 1 0 0]; %this includes the TSAS variable
DT=[D;0];sysT=ss(AT,BT,CT,DT);
%%%%% DVE Plant (no roll signal available)
AD=A;BD=B;CD=[1 0 0 0;0 1 0 0];DD=[0;0];sysD=ss(AD,BD,CD,DD);
%%%%% DVE Plant with TSAS
ADT=A;BDT=B;CDT=[CD;0 1 0 0];DDT=[DD;0];sysDT=ss(ADT,BDT,CDT,DDT);
%% Generate the important frequencies
w=.01;
for i=2:70
    w(i)=w(i-1)*1.2;
end
%%%% Set Datapath
loadpath='C:\KarlPhd\ExperimentsFall2004\Data';
eval(['addpath ',loadpath]);

CONDTSAS=[0 0 0 1 1 1 1 1 0 1 0 0;0 0 0 1 1 1 1 1 1 0 0 0;0 1 0 1 0 1 1 0 1 0 1 0;...
    1 1 0 1 0 0 0 0 1 0 1 1;1 1 1 0 0 0 0 0 0 1 1 1;1 0 1 0 1 0 0 1 0 1 0 1;...
    0 0 1 0 1 1 1 1 0 1 0 0;0 0 0 1 1 1 1 1 1 0 0 0;0 1 0 1 0 1 1 0 1 0 1 0;...
    1 1 0 1 0 0 0 0 1 0 1 1;1 1 1 0 0 0 0 0 0 1 1 1;1 0 1 0 1 0 0 1 0 1 0 1];
CONDVE=[0 1 2 2 1 0 0 1 2 2 1 0;1 2 0 0 2 1 1 2 0 0 2 1;2 0 1 1 0 2 2 0 1 1 0 2;...
    0 1 2 2 1 0 0 1 2 2 1 0;1 2 0 0 2 1 1 2 0 0 2 1;2 0 1 1 0 2 2 0 1 1 0 2;...
    0 1 2 2 1 0 0 1 2 2 1 0;1 2 0 0 2 1 1 2 0 0 2 1;2 0 1 1 0 2 2 0 1 1 0 2;...
    0 1 2 2 1 0 0 1 2 2 1 0;1 2 0 0 2 1 1 2 0 0 2 1;2 0 1 1 0 2 2 0 1 1 0 2];
SUBJ='ABCDEFGHIJKLM';
for j=1:12 % Subject
    BL=[]; DVEL=[]; DVEH=[]; TSAS=[]; TDVEL=[]; TDVEH=[];
    Gain=[]; Den=[]; Num=[]; Delay=[]; Data=[]; FIT=[];
    FIT1=[]; FIT2=[]; FIT3=[]; ERR1=[]; ERR2=[]; ERR3=[];
    CondTSAS=CONDTSAS(j,:); CondVE=CONDVE(j,:); Subj=SUBJ(j)
    NUM1=[]; DEL1=[]; DEN1=[]; GAIN1=[];
    NUM2=[]; DEL2=[]; DEN2=[]; GAIN2=[];
    NUM3=[]; DEL3=[]; DEN3=[]; GAIN3=[];
    for i=1:12
        i
        eval(['load
c:\karlphd\experimentsfall2004\data\',Subj,num2str(CondTSAS(i)),num2str(CondVE(i)), 'T',num2str(i)];
        %%% Parse Data
        eval(['data=',Subj,num2str(CondTSAS(i)),num2str(CondVE(i)), 'T',num2str(i),'']);
        eval(['clear ',Subj,num2str(CondTSAS(i)),num2str(CondVE(i)), 'T',num2str(i)];
        height=data(:,1); pitch=data(:,2); roll=data(:,3);
        x=data(:,4); y=data(:,5); z=data(:,6);

```

```

xd=data(:,7);   yd=data(:,8);   hd=data(:,12);
ud=data(:,9);   vd=data(:,10);  wd=data(:,11);
rd=data(:,14);  pd=data(:,13);
deltat=data(:,15); lightness=data(:,16);
xdist=data(:,17); ydist=data(:,18);
time=data(:,19); rudder=data(:,20);
aileron=data(:,22); elevator=data(:,21);collective=data(:,23);
%%%%% Define GVE, Xsition, and DVE
[crap,startlength]=min(abs(10-time));
[crap,gvelength]=min(abs(70-time));
[crap,xsitionlength]=min(abs(100-time));
[crap,totallength]=min(abs(190-time))
timeline=1; %PVO
%timeline=3; %VOSS
if timeline==1
    index1=startlength;
    index2=gvelength;
elseif timeline==2
    index1=gvelength;
    index2=xsitionlength;
else
    index1=xsitionlength;
    index2=totallength;
end
dt=abs(mean(time(1:length(time)-1)-time(2:length(time))));
T=time(index1:index2);
Xdist=xdist(index1:index2);
X=x(index1:index2);
dX=(xd(index1:index2)+xdist(index1:index2));
R=roll(index1:index2);
dR=rd(index1:index2);
Ail=aileron(index1:index2);
Ydist=ydist(index1:index2);
Y=y(index1:index2);
dY=(-yd(index1:index2)+ydist(index1:index2));
P=pitch(index1:index2);
dP=pd(index1:index2);
Elev=elevator(index1:index2);
T=T(1):dt:T(length(T));
minleng=min([length(T) length(Ail) length(X)]);
X=X(1:minleng);
dX=dX(1:minleng);
R=R(1:minleng);
dR=dR(1:minleng);
Xdist=Xdist(1:minleng);
T=T(1:minleng);
Ail=Ail(1:minleng);
%%%% Calculate Models using actual and estimated data
Q=[0 0 0 0;0 1 0 0;0 0 0 0;0 0 0 0];
Rr=1/100000;
Rr=Rr/100000;
[K,Scrap,Ecrap]=lqr(A,B,Q,Rr);
U=-K*[xd(index1-100:index1+length(T)) x(index1-100:index1+length(T)) rd(index1-
100:index1+length(T)) roll(index1-100:index1+length(T))];
U=-K*[dX X dR R]';
wn=20; % From Hess

```

```

damp=0.7; % From Hess
num2=[wn^2];
den2=[1 2*damp*wn wn^2];
lag=.1;
sys2=tf(num2,den2);
[Y2,Ttemp,state2]=lsim(sys2,U,T-T(1));
den3=conv(den2,[lag 1]);
sys3=tf(num2,den3);
[Y3,Ttemp,state3]=lsim(sys3,U,T-T(1));
DATA=iddata(Ail,U',dt);
DATA2=iddata(Ail,Y2,dt);
DATA3=iddata(Ail,Y3,dt);
guess=[.1 4 1 .01/max(K)]; %%delay num den gain
aux=0; %crap that I don't understand
global num den delay gain
InitialGuess=idgrey('PilotParam',guess,'cd',aux,0);
MODEL=pem(DATA,InitialGuess);
MODEL.A;
Num=conv([1 -6/delay 12/delay^2],[1 num])*gain;
Den=conv([1 6/delay 12/delay^2],[1 den]);
NUM1(i)=num;
DEN1(i)=den;
DEL1(i)=delay;
GAIN1(i)=gain;
[A1,B1,C1,D1]=tf2ss(Num,Den);
Sys=idss(A1,B1,C1,D1,'Ts',0);
[Txy,F]=TFE(U,Ail,length(Ail),1/dt);
MODEL2=pem(DATA2,InitialGuess);
MODEL2.A;
NUM2(i)=num;
DEN2(i)=den;
DEL2(i)=delay;
GAIN2(i)=gain;
Num=conv([1 -6/delay 12/delay^2],[1 num])*gain;
Den=conv([1 6/delay 12/delay^2],[1 den]);
Num=Num*wn^2;
Den=conv(Den,den2);
[A2,B2,C2,D2]=tf2ss(Num,Den);
Sys2=idss(A2,B2,C2,D2,'Ts',0);
MODEL3=pem(DATA3,InitialGuess);
MODEL3.A;
NUM3(i)=num;
DEN3(i)=den;
DEL3(i)=delay;
GAIN3(i)=gain;
Num=conv([1 -6/delay 12/delay^2],[1 num])*gain;
Den=conv([1 6/delay 12/delay^2],[1 den]);
Num=Num*wn^2;
Den=conv(Den,den3);
[A3,B3,C3,D3]=tf2ss(Num,Den);
Sys3=idss(A3,B3,C3,D3,'Ts',0);
cycles=[3 7 15 23 29 43 85 115 143 217 272 431];%% This is VOSS, not PVO
%cycles=[2 5 11 17 19 29 59 79 97 143 183 287];
freqs=cycles/90*2*pi;
freq=cycles/60*2*pi;
[MAG1,PH1]=bode(Sys,freqs);

```

```

[MAG2,PH2]=bode(Sys2,freqs);
[MAG3,PH3]=bode(Sys3,freqs);
for mag=1:length(MAG1)
    Mag1(mag)=MAG1(1,1,mag);
    Mag2(mag)=MAG2(1,1,mag);
    Mag3(mag)=MAG3(1,1,mag);
end
Err1=sum(abs(20*log10(Mag1')-20*log10(Txy(cycles+1))))
Err2=sum(abs(20*log10(Mag2')-20*log10(Txy(cycles+1))))
Err3=sum(abs(20*log10(Mag3')-20*log10(Txy(cycles+1))))
[crap,fit]=compare(DATA,Sys,Sys2,Sys3);
fit
FIT1(i)=fit(1); FIT2(i)=fit(2); FIT3(i)=fit(3);
ERR1(i)=Err1; ERR2(i)=Err2; ERR3(i)=Err3;

plotit=0;
if plotit==1;
    figure(1)
    clf
    bode(Sys,Sys2,Sys3,w)
    hold on
    grid
    semilogx(F(cycles+1)*2*pi,unwrap(angle(Txy(cycles+1)))*180/pi,'+b')
    semilogx(F*2*pi,unwrap(angle(Txy))*180/pi,'b')
    subplot(211)
    hold on
    grid
    loglog(F(cycles+1)*2*pi,(abs(Txy(cycles+1))),'ob')

    loglog(F*2*pi,(abs(Txy)), 'b:')
    loglog(freqs,Mag3,'*r')
    loglog(freqs,Mag2,'*g')
    loglog(freqs,Mag1,'*b')
    legend('Structured','2nd order NM','3rd order NM')
    figure(2)
    clf
    compare(DATA,Sys,Sys2,Sys3)
    beep
    pause
end
end
beep
clk=clock;
eval(['string=["Done Subject ",Subj," Time ",num2str(clk(4:6))]]')
eval(['save NMStructureSubject',Subj,' FIT1 FIT2 FIT3 ERR1 ERR2 ERR3 DEL1 DEL2 DEL3 DEN1
DEN2 DEN3 NUM1 NUM2 NUM3 GAIN1 GAIN2 GAIN3'])
end

```



```

function [A,B,C,D,K,X0]=PilotParam(input,ts,aux)
global delay num den gain
delay=input(1);
num=input(2);
den=input(3);
gain=input(4);
A=[-(6/delay+den) -(6/delay*den+12/delay^2) -(12/delay^2*den);1 0 0;0 1 0];
B=[1;0;0];
C=[((-6/delay+num)-(6/delay+den))*gain ((-6/delay*num+12/delay^2)-(6/delay*den+12/delay^2))*gain
((12/delay^2*num)-(12/delay^2*den))*gain];
D=gain;
K=[0;0;0];
X0=[0;0;0];
if ts>0 % sample interval
    s=expm([[A B]*ts;zeros(1,4)]);
    A=s(1:3,1:3);
    B=s(1:3,4);
end

```

```

%% XAXIS_NonLinear_Analyze
%% 11 June 2006
%% LCDR Karl U Schultz
%% This program investigates the nonlinear nature of
%% Pilot control response

clear
%% Define plant variables
g=9.81; Pfreq=3.0; Pdamp=.65; Pgain=500; Vydamp=4; Rfreq=5; Rdamp=.4; Rgain=625; Vxdamp=4;
dt=.012; %% delta t for all trials %% mass=1000; Not used
%% Basic plant
A=[-Vydamp 0 0 g; 1 0 0 0; 0 0 -2*Pdamp*Pfreq -Pfreq^2; 0 0 1 0]; B=[0;0;Pgain;0]; C=[eye(4)];
D=zeros(4,1); E=[0;1;0;0];
sys=ss(A,B,C,D);
%% Basic plant with TSAS
AT=A; BT=B; CT=[C;0 1 0 0]; %%this includes the TSAS variable
DT=[D;0]; sysT=ss(AT,BT,CT,DT);
%% DVE Plant (no roll signal available)
AD=A; BD=B; CD=[1 0 0 0; 0 1 0 0]; DD=[0;0]; sysD=ss(AD,BD,CD,DD);
%% DVE Plant with TSAS
ADT=A; BDT=B; CDT=[CD;0 1 0 0]; DDT=[DD;0]; sysDT=ss(ADT,BDT,CDT,DDT);
%% Generate the important frequencies
w=.01; for i=2:70
    w(i)=w(i-1)*1.2;
end
%% Set Datapath
loadpath='C:\KarlPhd\ExperimentsFall2004\Data'; eval(['addpath ',loadpath]);
CONDTSAS=[0 0 0 1 1 1 1 1 0 1 0 0; 0 0 0 1 1 1 1 1 1 0 0 0; 0 1 0 1 0 1 1 0 1 0 1 0; 1 1 0 1 0 0 0 0 1 0 1 1...
1 1 1 0 0 0 0 0 0 1 1 1; 1 0 1 0 1 0 0 1 0 1 0 1; 0 0 1 0 1 1 1 1 0 1 0 0; 0 0 0 1 1 1 1 1 1 0 0 0;...
0 1 0 1 0 1 1 0 1 0 1 0; 1 1 0 1 0 0 0 0 1 0 1 1; 1 1 1 0 0 0 0 0 0 1 1 1; 1 0 1 0 1 0 0 1 0 1 0 1];
CONDVE=[0 1 2 2 1 0 0 1 2 2 1 0; 1 2 0 0 2 1 1 2 0 0 2 1; 2 0 1 1 0 2 2 0 1 1 0 2; 0 1 2 2 1 0 0 1 2 2 1 0;...
1 2 0 0 2 1 1 2 0 0 2 1; 2 0 1 1 0 2 2 0 1 1 0 2; 0 1 2 2 1 0 0 1 2 2 1 0; 1 2 0 0 2 1 1 2 0 0 2 1;...
2 0 1 1 0 2 2 0 1 1 0 2; 0 1 2 2 1 0 0 1 2 2 1 0; 1 2 0 0 2 1 1 2 0 0 2 1; 2 0 1 1 0 2 2 0 1 1 0 2];
SUBJ='ABCDEFGHIJKL';
eval(['load YaxisNMMModel_PVO_Avg'])
bins=[-.5:.05:-.15 -.13:.02:.13 .15:.05:.5];
for j=1:12 % Subject
    BigSTATUS=[]; BigPHASE=[]; BigSTATNUM=[]; BigCOUNT=[]; BigCOUNTMD=[];
    BigCOUNTMU=[];
    BigCOUNTH=[]; BigCOUNTKHM=[]; BigCOUNTKHE=[]; BigCOUNTPHASE=[];
    BigCOUNTPHASEH=[];
    BigCOUNTPHASEMD=[]; BigCOUNTPHASEMU=[]; BigCOUNTPHASEHZ=[];
    BigCOUNTPHASEMDZ=[];
    BigCOUNTPHASEMUZ=[]; BigHCORRECT=[]; BigMDCORRECT=[]; BigMUCORRECT=[];
    BigHZCORRECT=[];
    BigMDZCORRECT=[]; BigMUZCORRECT=[]; BL=[]; DVEL=[]; DVEH=[]; TSAS=[];
    TDVEL=[]; TDVEH=[];
    Gain=[]; Den=[]; Num=[]; Delay=[]; Data=[]; FIT=[]; FIT1=[]; FIT2=[]; FIT3=[]; ERR1=[];
    ERR2=[]; ERR3=[];
    CondTSAS=CONDTSAS(j,:); CondVE=CONDVE(j,:); Subj=SUBJ(j)
    NUM1=[]; DEL1=[]; DEN1=[]; GAIN1=[]; NUM2=[]; DEL2=[]; DEN2=[]; GAIN2=[];
    NUM3=[]; DEL3=[]; DEN3=[]; GAIN3=[];
    for i=1:12
        eval(['load
c:\karlphd\experimentsfall2004\data\',Subj,num2str(CondTSAS(i)),num2str(CondVE(i)), 'T',num2str(i)]);
        %% Parse Data

```

```

eval(['data=',Subj,num2str(CondTSAS(i)),num2str(CondVE(i)),'T',num2str(i),'']);
eval(['clear ',Subj,num2str(CondTSAS(i)),num2str(CondVE(i)),'T',num2str(i)]);
height=data(:,1); pitch=data(:,2); roll=data(:,3); x=data(:,4); y=data(:,5); z=data(:,6);
xd=data(:,7); yd=data(:,8); hd=data(:,12); ud=data(:,9); vd=data(:,10);
wd=data(:,11);
rd=data(:,14); pd=data(:,13); deltat=data(:,15); lightness=data(:,16); xdist=data(:,17);
ydist=data(:,18);
time=data(:,19); rudder=data(:,20); aileron=data(:,22); elevator=data(:,21);collective=data(:,23);
%% Define GVE, Xsition, and DVE
[crd,startlength]=min(abs(10-time)); [crd,gvelength]=min(abs(70-time));
[crd,xsitionlength]=min(abs(100-time)); [crd,totallength]=min(abs(190-time));
timeline=3; %VOSS timeline=2; %VOX timeline=1; %PVO
if timeline==1
    index1=startlength; index2=gvelength;
elseif timeline==2
    index1=gvelength; index2=xsitionlength;
else
    index1=xsitionlength; index2=totallength;
end
dt=abs(mean(time(1:length(time)-1)-time(2:length(time))));
T=time(index1:index2); Xdist=xdist(index1:index2); X=x(index1:index2);
dX=(xd(index1:index2)+xdist(index1:index2));
R=roll(index1:index2); dR=rd(index1:index2); Ail=aileron(index1:index2);
Ydist=ydist(index1:index2); Y=y(index1:index2); dY=(-yd(index1:index2)+ydist(index1:index2));
P=pitch(index1:index2); dP=pd(index1:index2); Elev=elevator(index1:index2);
T=T(1):dt:T(length(T)); minleng=min([length(T) length(Ail) length(X)]);
X=Y(1:minleng); dX=dY(1:minleng); R=P(1:minleng); dR=dP(1:minleng); Xdist=Ydist(1:minleng);
T=T(1:minleng); Ail=Elev(1:minleng);
TSAS=zeros(size(X));
%% Calculate TSAS; TSASindxzero=abs(X)<=5;
TSASindx1=and(X>5,X<=10); TSASindx2=and(X>10,X<=20); TSASindx3=X>20;
TSASindxm1=and(X<-5,X>=-10); TSASindxm2=and(X<-10,X>=-20); TSASindxm3=X<-20;
TSAS(TSASindx1)=7.5*ones(size(TSAS(TSASindx1))); TSAS(TSASindxm1)=-
7.5*ones(size(TSAS(TSASindxm1)));
TSAS(TSASindx2)=15*ones(size(TSAS(TSASindx2))); TSAS(TSASindxm2)=-
15*ones(size(TSAS(TSASindxm2)));
TSAS(TSASindx3)=25*ones(size(TSAS(TSASindx3))); TSAS(TSASindxm3)=-
25*ones(size(TSAS(TSASindxm3)));
errorT=X-TSAS;
%% Determine the noise for each state
if or((CondVE(i)==0),(timeline==1));
    errorY=-.1881*abs(X)+15; errordX=.2723*abs(dX); errorR=.1013*abs(R)+1.4;
errordR=.45*abs(dR)/2;
elseif CondVE(i)==1;
    errorX=-.1881*abs(X)+15; errordX=.2723*abs(dX); errorR=.1013*abs(R)+1.4;
errordR=.45*abs(dR)/2;
else
    errorX=(.1164*abs(X)+1.1810)*1; errordX=(.45*abs(dX)+.36)*1;
end
randx=randn(size(errorX)); randdx=randn(size(errordX));randr=randn(size(errorRoll));
randdr=randn(size(errordRoll));
noisescale=1; noiseX=errorX.*randx*noisescale; noisedX=errordX.*randdx*noisescale;
noiseR=errorRoll.*randr*noisescale; noisedR=errordRoll.*randdr*noisescale;
noiseT=errorT; %this is the real error. Do NOT Scale
w=Xdist; vu=randn(size(Ail)).*abs(Ail)*.03; %%This helps match PSD (deltaNL) against
PSD(Ail)

```

```

%%%%%%%% Check the visual and tactile conditions
if CondTSAS(i)==0
    if and(timeline>1,CondVE(i)==2)
        C=CD; D=DD; outs=2; vy=[noisedX noiseX];% noisedR noiseR];
    else
        C=Cb; D=Db; outs=4; vy=[noisedX noiseX noisedR noiseR];
    end
else %TSAS on
    if and(timeline>1,CondVE(i)==2)
        C=CDT; D=DDT; outs=3; vy=[noisedX noiseX noiseT];%noiseR noiseR noiseT];
    else
        C=CT; D=DT; outs=5; vy=[noisedX noiseX noisedR noiseR noiseT];
    end
end
Vy=diag(mean(abs(vy))); W1=diag([mean(abs(Xdist)) mean(abs(vu))]);
%%%%%%%%% Neuromuscular Term
eval(['Sysc=Sys1',Subj,',']); eval(['Ac,Bc,Cc,Dc]=ssdata(Sysc,')
Sysc=ss(Ac,Bc,Cc,Dc); Sysnm=ss(Anm,Bnm,Cnm,Dnm); Cnl=eye(1);
%%%%%%%% Complete Term
A1=[A B*Cnm zeros(4,3);zeros(3,4) Anm Bnm*Cnl*Cc;zeros(3,4) zeros(3,3) Ac];
B1=[zeros(4,1);Bnm*Cnl*Dc;Bc]; C1=[C zeros(outs,3) zeros(outs,3)]; D1=[zeros(outs,1)];
Sys1=ss(A1,B1,C1,D1);
E1=[E B zeros(4,out);zeros(3,1) zeros(3,1) zeros(3,out);zeros(3,1) zeros(3,1) zeros(3,out)];
Q=[0 0 0 0;0 1 0 0;0 0 0 0;0 0 0 0];
Q1=[Q zeros(4,3) zeros(4,3);zeros(3,4) zeros(3,3) zeros(3,3);zeros(3,4) zeros(3,3) zeros(3,3)];
R1=10^-10; [K1,Scrd,Ecrd]=lqr(A1,B1,Q1,R1);
Sys1e=ss(A1,[B1 [E B;zeros(3,1) zeros(3,1);zeros(3,1) zeros(3,1)]],C1,[D1 zeros(outs,1)
zeros(outs,1)]); %Open Loop
[Kest,L1,P]=kalman(Sys1e,W1,Vy); %%%%%%%%%
ANLol=[A1-L1*C1-B1*K1 L1*C zeros(10,3);...
zeros(4,10) A zeros(4,3);...
-Bc*K1 zeros(3,4) Ac];
BNL=[zeros(10,1);B;zeros(3,1)];
ENL=[zeros(10,1) zeros(10,1) L1;...
E B zeros(4,out);...
zeros(3,1) zeros(3,1) zeros(3,out)];
BNLol=[BNL ENL]; CNLol=[-Dc*K1 zeros(1,4) Cc]; DNLol=[zeros(1,1) zeros(1,1) zeros(1,1)
zeros(1,out)];
SYSNLol=ss(ANLol,BNLol,CNLol,DNLol);
SYSol=ss(A,[B E],C,[D D]);
siminput=[Ail w vu vy]; [YNLol,TNLol,XNLol]=lsim(SYSNLol,siminput,T-T(1));
siminput=[Ail w]; [Yol,Tol,Xol]=lsim(SYSol,siminput,T-T(1));
Uc=YNLol; U=Uc;
%%%%%%%% Calculate Models using actual and estimated data
Qold=[0 0 0 0;0 1 0 0;0 0 0 0;0 0 0 0]; Rold=10^-10;
[Kold,Scrd,Ecrd]=lqr(A,B,Qold,Rold); Uold=-Kold*[dX X dR R]';
countit=8; %how far back to look to define the decision
timeit=300; % how far back to look to use the info in making the decision
AIL=Ail;
%%% determine holds and moves
keepholdcount=1; KHOLD=[]; KHT=[]; moveupcount=1; MOVEUP=[]; MUT=[];
movedowncount=1;MOVEDOWN=[];MDT=[]; holdcount=1; HOLD=[]; HT=[];
keepmovecount=1; KMOVE=[]; KMT=[];
for iii=timeit+1:length(AIL)-timeit
    if and((abs(AIL(iii))-mean(AIL(iii-countit:iii)))<mean(abs(AIL))*0.01),(AIL(iii)<AIL(iii+1)))

```

```

        MOVEUP(moveupcount)=AIL(iii); MUT(moveupcount)=iii;
moveupcount=moveupcount+1;
        elseif and((abs(AIL(iii)-mean(AIL(iii-countit:iii)))<mean(abs(AIL))*0.01),(AIL(iii)>AIL(iii+1)))
            MOVEDOWN(movedowncount)=AIL(iii); MDT(movedowncount)=iii;
movedowncount=movedowncount+1;
        elseif and((abs(AIL(iii)-mean(AIL(iii:iii+countit)))<mean(abs(AIL))*0.01),(AIL(iii)~=AIL(iii-1)))
            HOLD(holdcount)=AIL(iii); HT(holdcount)=iii; holdcount=holdcount+1;
        elseif or((abs(AIL(iii)-mean(AIL(iii-countit:iii)))<mean(abs(AIL))*0.01),(abs(AIL(iii)-
mean(AIL(iii:iii+countit)))<mean(abs(AIL))*0.01))
            KHOLD(keepholdcount)=AIL(iii); KHT(keepholdcount)=iii; keepholdcount=keepholdcount+1;
        else
            KMOVE(keepmovecount)=AIL(iii); KMT(keepmovecount)=iii;
keepmovecount=keepmovecount+1;
        end
    end
    end
    MT=[MUT MDT]; [Output,T,States]=lsim(Sys3A,U,T-T(1)); delay=20; Diff=U-Ail;
    %%%Find relationship between Diff and Ail
    DATA=iddata(Ail,Diff,dt); MODEL=n4sid(DATA,2,'Ts',0);
    timecount=1; phasecount=1; cont=1; status='Hold';
    if Diff(2)==Diff(1)
        status='Hold';
    elseif Diff(2)>Diff(1)
        status='MvUp';
    else
        status='MvDn';
    end
    STATUS(phasecount,:)= 'Hold'; STATNUM(phasecount)=1; thresh=(max(Ail)-min(Ail))*0.0001;
%
    %%%[start end deltat startDiff endDiff deltaDiff startAil EndAil
DiffAil
    PHASE(phasecount,:)= [timecount 0 0 Diff(timecount) 0 0 Ail(timecount) 0 0];
    timecount=2; stepup=1;
    while cont==1
        if status == 'Hold'
            if abs(mean(Ail(timecount+1:timecount+stepup))-Ail(timecount))<=thresh
                % timecount=timecount+1;
            elseif mean(Ail(timecount+1:timecount+stepup))>Ail(timecount)+thresh
                status='MvUp'; PHASE(phasecount,2)=timecount;
                PHASE(phasecount,3)=PHASE(phasecount,2)-PHASE(phasecount,1);
                PHASE(phasecount,5)=Diff(timecount);
                PHASE(phasecount,6)=abs(Diff(PHASE(phasecount,1)))-abs(Diff(timecount));
                PHASE(phasecount,8)=Ail(timecount);
                PHASE(phasecount,9)=PHASE(phasecount,8)-PHASE(phasecount,7);
                phasecount=phasecount+1;
                PHASE(phasecount,:)= [timecount 0 0 Diff(timecount) 0 0 Ail(timecount) 0 0];
                STATUS(phasecount,:)= 'MvUp';
            elseif mean(Ail(timecount+1:timecount+stepup))<Ail(timecount)-thresh
                status='MvDn'; PHASE(phasecount,2)=timecount;
                PHASE(phasecount,3)=PHASE(phasecount,2)-PHASE(phasecount,1);
                PHASE(phasecount,5)=Diff(timecount);
                PHASE(phasecount,6)=abs(Diff(PHASE(phasecount,1)))-abs(Diff(timecount));
                PHASE(phasecount,8)=Ail(timecount);
                PHASE(phasecount,9)=PHASE(phasecount,8)-PHASE(phasecount,7);
                phasecount=phasecount+1;
                PHASE(phasecount,:)= [timecount 0 0 Diff(timecount) 0 0 Ail(timecount) 0 0];
                STATUS(phasecount,:)= 'MvDn';
            end
        end
    end
end

```

```

end
elseif status=='MvUp'
if mean(Ail(timecount+1:timecount+stepup))>Ail(timecount)+thresh
% timecount=timecount+1;
elseif abs(mean(Ail(timecount+1:timecount+stepup))-Ail(timecount))<=thresh
status='Hold'; PHASE(phasecount,2)=timecount;
PHASE(phasecount,3)=PHASE(phasecount,2)-PHASE(phasecount,1);
PHASE(phasecount,5)=Diff(timecount);
PHASE(phasecount,6)=abs(Diff(PHASE(phasecount,1)))-abs(Diff(timecount));
PHASE(phasecount,8)=Ail(timecount);
PHASE(phasecount,9)=PHASE(phasecount,8)-PHASE(phasecount,7);
phasecount=phasecount+1;
PHASE(phasecount,:)=timecount 0 0 Diff(timecount) 0 0 Ail(timecount) 0 0];
STATUS(phasecount,:)= 'Hold';
elseif mean(Ail(timecount+1:timecount+stepup))<Ail(timecount)-thresh
status='MvDn'; PHASE(phasecount,2)=timecount;
PHASE(phasecount,3)=PHASE(phasecount,2)-PHASE(phasecount,1);
PHASE(phasecount,5)=Diff(timecount);
PHASE(phasecount,6)=abs(Diff(PHASE(phasecount,1)))-abs(Diff(timecount));
PHASE(phasecount,8)=Ail(timecount);
PHASE(phasecount,9)=PHASE(phasecount,8)-PHASE(phasecount,7);
phasecount=phasecount+1;
PHASE(phasecount,:)=timecount 0 0 Diff(timecount) 0 0 Ail(timecount) 0 0];
STATUS(phasecount,:)= 'MvDn';
end
else
if mean(Ail(timecount+1:timecount+stepup))<Ail(timecount)-thresh
%timecount=timecount+1;
elseif mean(Ail(timecount+1:timecount+stepup))>Ail(timecount)+thresh
status='MvUp'; PHASE(phasecount,2)=timecount;
PHASE(phasecount,3)=PHASE(phasecount,2)-PHASE(phasecount,1);
PHASE(phasecount,5)=Diff(timecount);
PHASE(phasecount,6)=abs(Diff(PHASE(phasecount,1)))-abs(Diff(timecount));
PHASE(phasecount,8)=Ail(timecount);
PHASE(phasecount,9)=PHASE(phasecount,8)-PHASE(phasecount,7);
phasecount=phasecount+1;
PHASE(phasecount,:)=timecount 0 0 Diff(timecount) 0 0 Ail(timecount) 0 0];
STATUS(phasecount,:)= 'MvUp';
elseif abs(mean(Ail(timecount+1:timecount+stepup))-Ail(timecount))<=thresh
status='Hold'; PHASE(phasecount,2)=timecount;
PHASE(phasecount,3)=PHASE(phasecount,2)-PHASE(phasecount,1);
PHASE(phasecount,5)=Diff(timecount);
PHASE(phasecount,6)=abs(Diff(PHASE(phasecount,1)))-abs(Diff(timecount));
PHASE(phasecount,8)=Ail(timecount);
PHASE(phasecount,9)=PHASE(phasecount,8)-PHASE(phasecount,7);
phasecount=phasecount+1;
PHASE(phasecount,:)=timecount 0 0 Diff(timecount) 0 0 Ail(timecount) 0 0];
STATUS(phasecount,:)= 'Hold';
end
end
timecount=timecount+1;
if timecount>(length(Ail)-stepup-1)
PHASE(phasecount,2)=timecount;
PHASE(phasecount,3)=PHASE(phasecount,2)-PHASE(phasecount,1);
PHASE(phasecount,5)=Diff(timecount);
PHASE(phasecount,6)=Diff(PHASE(phasecount,1))-Diff(timecount);

```

```

    PHASE(phasecount,8)=Ail(timecount);
    PHASE(phasecount,9)=PHASE(phasecount,8)-PHASE(phasecount,7);
    phasecount=phasecount+1;
    break
end
end
for count=1:length(PHASE)
    if STATUS(count,:)=='Hold'
        STATNUM(count)=1;
    elseif STATUS(count,:)=='MvDn'
        STATNUM(count)=2;
    elseif STATUS(count,:)=='MvUp';
        STATNUM(count)=3;
    end
end
clear NEWPHASE NEWSTATNUM
NEWPHASE(1,:)=[1 PHASE(2,2) PHASE(2,3)+PHASE(1,3) PHASE(1,4) PHASE(2,5)
abs(PHASE(2,6))-abs(PHASE(1,6)) PHASE(1,7) PHASE(2,8) PHASE(2,8)-PHASE(1,7)];
NEWSTATNUM=1;
NPcount=2;
%%% Apply logic to PHASE
for iii=2:length(PHASE)
    if and(STATNUM(iii)==STATNUM(iii+2),and(STATNUM(iii+1)==1,PHASE(iii+1,3)<=20))
        PHASE=[PHASE(1:iii,:);PHASE(iii+2:length(PHASE),:)];
        STATNUM=[STATNUM(1:iii) STATNUM(iii+2:length(STATNUM))];
    end
    if iii>=length(PHASE)-2
        break
    end
end
for iii=3:length(PHASE)
    if NEWSTATNUM(NPcount-1)==STATNUM(iii);
        NEWPHASE(NPcount-1,:)=[NEWPHASE(NPcount-1,1) PHASE(iii,2)
PHASE(iii,3)+NEWPHASE(NPcount-1,3) NEWPHASE(NPcount-1,4) PHASE(iii,5) abs(PHASE(iii,6))-
abs(NEWPHASE(NPcount-1,6)) NEWPHASE(NPcount-1,7) PHASE(iii,8) PHASE(iii,8)-
NEWPHASE(NPcount-1,7)];
    else
string='different';NEWPHASE(NPcount,:)=PHASE(iii,:);NEWSTATNUM(NPcount)=STATNUM(iii);
NPcount=NPcount+1;
    end
end
PHASE=NEWPHASE; STATNUM=NEWSTATNUM;
for count=1:length(PHASE)
    if and((STATNUM(count)==1),abs(PHASE(count,7))<=thresh)
        STATNUM(count)=4;
    elseif and((STATNUM(count)==2),abs(PHASE(count,8))<=thresh)
        STATNUM(count)=5;
    elseif and((STATNUM(count)==3),abs(PHASE(count,8))<=thresh)
        STATNUM(count)=6;
    end
end
dDiff=Diff(2:length(Diff))-Diff(1:length(Diff)-1); dDiff=[dDiff(1);dDiff];
COUNT=sum(Diff<bins(1)); COUNTMD=sum(Diff(MDT)<bins(1));
COUNTMU=sum(Diff(MUT)<bins(1));

```

```

COUNTH=sum(Diff(HT)<bins(1)); COUNTKM=sum(Diff(KMT)<bins(1));
COUNTKH=sum(Diff(KHT)<bins(1));
for BINS=2:length(bins)
    COUNT(BINS)=sum(and(Diff>bins(BINS-1),Diff<bins(BINS)));
    COUNTMD(BINS)=sum(and(Diff(MDT)>bins(BINS-1),Diff(MDT)<bins(BINS)));
    COUNTMU(BINS)=sum(and(Diff(MUT)>bins(BINS-1),Diff(MUT)<bins(BINS)));
    COUNTH(BINS)=sum(and(Diff(HT)>bins(BINS-1),Diff(HT)<bins(BINS)));
    COUNTKM(BINS)=sum(and(Diff(KMT)>bins(BINS-1),Diff(KMT)<bins(BINS)));
    COUNTKH(BINS)=sum(and(Diff(KHT)>bins(BINS-1),Diff(KHT)<bins(BINS)));
end
%%% Count PHASE Data
IndHold=STATNUM==1; IndMovDn=STATNUM==2; IndMovUp=STATNUM==3;
IndHoldZero=STATNUM==4; IndMovDnZero=STATNUM==5; IndMovUpZero=STATNUM==6;
COUNTPHASE=sum(PHASE(:,4)<bins(1)); %Start Diff
COUNTPHASEH=sum(PHASE(IndHold,4)<bins(1)); %Start Diff
COUNTPHASEMD=sum(PHASE(IndMovDn,4)<bins(1)); %Start Diff
COUNTPHASEMU=sum(PHASE(IndMovUp,4)<bins(1)); %Start Diff
COUNTPHASEMDZ=sum(PHASE(IndMovDnZero,4)<bins(1)); %Start Diff
COUNTPHASEMUZ=sum(PHASE(IndMovUpZero,4)<bins(1)); %Start Diff
COUNTPHASEHZ=sum(PHASE(IndHoldZero,4)<bins(1)); %Start Diff

HCCORRECT=sum(and(PHASE(IndHold,4)<bins(1),abs(PHASE(IndHold,5))<abs(PHASE(IndHold,4))));

MDCORRECT=sum(and(PHASE(IndMovDn,4)<bins(1),abs(PHASE(IndMovDn,5))<abs(PHASE(IndMo
vDn,4))));

MUCORRECT=sum(and(PHASE(IndMovUp,4)<bins(1),abs(PHASE(IndMovUp,5))<abs(PHASE(IndMo
vUp,4))));

HZCORRECT=sum(and(PHASE(IndHoldZero,4)<bins(1),abs(PHASE(IndHoldZero,5))<abs(PHASE(Ind
HoldZero,4))));

MDZCORRECT=sum(and(PHASE(IndMovDnZero,4)<bins(1),abs(PHASE(IndMovDnZero,5))<abs(PHA
SE(IndMovDnZero,4))));

MUZCORRECT=sum(and(PHASE(IndMovUpZero,4)<bins(1),abs(PHASE(IndMovUpZero,5))<abs(PHA
SE(IndMovUpZero,4))));
for BINS=2:length(bins)
    COUNTPHASE(BINS)=sum(and(PHASE(:,4)>bins(BINS-1),PHASE(:,4)<bins(BINS))); %Start
Diff
    COUNTPHASEH(BINS)=sum(and(PHASE(IndHold,4)>bins(BINS-
1),PHASE(IndHold,4)<bins(BINS))); %Start Diff
    COUNTPHASEMD(BINS)=sum(and(PHASE(IndMovDn,4)>bins(BINS-
1),PHASE(IndMovDn,4)<bins(BINS))); %Start Diff
    COUNTPHASEMU(BINS)=sum(and(PHASE(IndMovUp,4)>bins(BINS-
1),PHASE(IndMovUp,4)<bins(BINS))); %Start Diff
    COUNTPHASEHZ(BINS)=sum(and(PHASE(IndHoldZero,4)>bins(BINS-
1),PHASE(IndHoldZero,4)<bins(BINS))); %Start Diff
    COUNTPHASEMDZ(BINS)=sum(and(PHASE(IndMovDnZero,4)>bins(BINS-
1),PHASE(IndMovDnZero,4)<bins(BINS)));
    COUNTPHASEMUZ(BINS)=sum(and(PHASE(IndMovUpZero,4)>bins(BINS-
1),PHASE(IndMovUpZero,4)<bins(BINS)));
    HCCORRECT(BINS)=sum(and(and(PHASE(IndHold,4)>bins(BINS-
1),PHASE(IndHold,4)<bins(BINS)),abs(PHASE(IndHold,5))<abs(PHASE(IndHold,4))));
    MDCORRECT(BINS)=sum(and(and(PHASE(IndMovDn,4)>bins(BINS-
1),PHASE(IndMovDn,4)<bins(BINS)),abs(PHASE(IndMovDn,5))<abs(PHASE(IndMovDn,4)) ));

```



```

MUCORRECT(BINS)=sum(and(and(PHASE(IndMovUp,4)>bins(BINS-
1),PHASE(IndMovUp,4)<bins(BINS)),abs(PHASE(IndMovUp,5))<abs(PHASE(IndMovUp,4)) ));
HZCORRECT(BINS)=sum(and(and(PHASE(IndHoldZero,4)>bins(BINS-
1),PHASE(IndHoldZero,4)<bins(BINS)), abs(PHASE(IndHoldZero,5))<abs(PHASE(IndHoldZero,4))));
MDZCORRECT(BINS)=sum(and(and(PHASE(IndMovDnZero,4)>bins(BINS-
1),PHASE(IndMovDnZero,4)<bins(BINS)),abs(PHASE(IndMovDnZero,5))<abs(PHASE(IndMovDnZero,
4)) ));
MUZCORRECT(BINS)=sum(and(and(PHASE(IndMovUpZero,4)>bins(BINS-
1),PHASE(IndMovUpZero,4)<bins(BINS)),abs(PHASE(IndMovUpZero,5))<abs(PHASE(IndMovUpZero,
4)) ));
end
Delbins=1:200; [HIST]=hist(PHASE(:,3),Delbins);
Fhist=2*pi./(Delbins*dt);
[AA Fa]=psd(Ail,length(Ail),1/dt); AA=sqrt(AA);
[UU Fu]=psd(Output,length(Output),1/dt); UU=sqrt(UU);
Ptot=[]; Fu=Fu*2*pi;
%%%% Calculate additional noise
Fnew=zeros(length(Fhist),length(Fu));
for frq=1:length(Fhist)
    Ptemp=zeros(size(UU));
    if HIST(frq)>0
        Fs=Fhist(frq); Rat=HIST(frq)*Delbins(frq)/sum(PHASE(:,3));
        [crd,Find]=min(abs(Fs-Fu)); SCtemp=sinc(Fu./Fs);
        if Find<(length(Fu))
            for pwr=1:Find-1
                Ptemp(pwr)=UU(Find-pwr)*abs(SCtemp(pwr))+UU(pwr)*abs(SCtemp(pwr))-
UU(pwr);%*Rat;
            end
        end
        for fin=Find+1:length(Fu)
            n=floor((fin-1)/Find);
            Ptemp(fin)=UU(fin-n*Find)*abs(SCtemp(fin));%+UU(pwr)*abs(SCtemp(pwr))-
UU(pwr);%*Rat;
        end
        Ptemp=Ptemp*Rat;    Ptot(frq,:)=Ptemp;
    end
end
%    if and(CondVE(i)==2,CondTSAS(i)==1)
BigSTATUS=[BigSTATUS;STATUS]; BigPHASE=[BigPHASE;PHASE];
BigSTATNUM=[BigSTATNUM;STATNUM];
BigCOUNT=[BigCOUNT;COUNT]; BigCOUNTMD=[BigCOUNTMD;COUNTMD];
BigCOUNTMU=[BigCOUNTMU;COUNTMU];BigCOUNTH=[BigCOUNTH;
COUNTH];BigCOUNTKH=[BigCOUNTKH;COUNTKH]; BigCOUNTKM=[BigCOUNTKM;
COUNTKM];
BigCOUNTPHASE=[BigCOUNTPHASE;COUNTPHASE];
BigCOUNTPHASEH=[BigCOUNTPHASEH;COUNTPHASEH];
BigCOUNTPHASEMD=[BigCOUNTPHASEMD;COUNTPHASEMD];
BigCOUNTPHASEMU=[BigCOUNTPHASEMU;COUNTPHASEMU];
BigCOUNTPHASEHZ=[BigCOUNTPHASEHZ;COUNTPHASEHZ];
BigCOUNTPHASEMDZ=[BigCOUNTPHASEMDZ;COUNTPHASEMDZ];
BigCOUNTPHASEMUZ=[BigCOUNTPHASEMUZ;COUNTPHASEMUZ];
BigHCORRECT=[BigHCORRECT;HCORRECT];    BigMDCORRECT=[BigMDCORRECT;
MDCORRECT]; BigMUCORRECT=[BigMUCORRECT;MUCORRECT];
BigHZCORRECT=[BigHZCORRECT;HZCORRECT];    BigMDZCORRECT=[BigMDZCORRECT;
MDZCORRECT]; BigMUZCORRECT=[BigMUZCORRECT;MUZCORRECT];
%    end

```

```

end %for i
%%%%%% calculate equation
takeout=5; takeout2=5; shortbins=bins(1+takeout:30-takeout); sshortbins=bins(1+takeout2:30-
takeout2);
BC=mean(BigCOUNT); Indx=BC>0; IndX=Indx==1; Xbins=bins(Indx);
MUx=mean(BigCOUNTPHASEMU)./mean(BigCOUNTPHASE); MUx=MUx(Indx);
MUx=[ones(1,takeout)*MUx(takeout+1) MUx(1+takeout:length(MUx)-takeout)
ones(1,takeout)*MUx(length(MUx)-takeout)];
MDx=mean(BigCOUNTPHASEMD)./mean(BigCOUNTPHASE); MDx=MDx(Indx);
MDx=[ones(1,takeout)*MDx(takeout+1) MDx(1+takeout:length(MDx)-takeout)
ones(1,takeout)*MDx(length(MDx)-takeout)];
Hx=mean(BigCOUNTPHASEH)./mean(BigCOUNTPHASE); Hx=Hx(Indx);
Hx=[ones(1,takeout)*Hx(takeout+1) Hx(1+takeout:length(Hx)-takeout) ones(1,takeout)*Hx(length(Hx)-
takeout)];
MUZx=mean(BigCOUNTPHASEMUZ)./mean(BigCOUNTPHASE); MUZx=MUZx(Indx); MUZx=[
zeros(1,takeout2) MUZx(1+takeout2:length(MUZx)-takeout2) ones(1,takeout2)*MUZx(length(MUZx)-
takeout2)];
MDZx=mean(BigCOUNTPHASEMDZ)./mean(BigCOUNTPHASE); MDZx=MDZx(Indx);
MDZx=[ones(1,takeout2)*MDZx(1+takeout2) MDZx(1+takeout2:length(MDZx)-takeout2)
zeros(1,takeout2)];
HZx=mean(BigCOUNTPHASEHZ)./mean(BigCOUNTPHASE); HZx=HZx(Indx);
HZx=[ones(1,takeout2)*HZx(1+takeout2) HZx(1+takeout2:length(HZx)-takeout2)
ones(1,takeout2)*HZx(length(HZx)-takeout2)];
Xbins=Xbins(2:length(Xbins)-2); MUx=MUx(2:length(MUx)-2); MUx(1:3)=[0 0 0];
MDx=MDx(2:length(MDx)-2); MDx(length(MDx)-2:length(MDx))=[0 0 0];
Hx=Hx(2:length(Hx)-2);
MUZx=MUZx(2:length(MUZx)-2); MUZx(1:5)=[0 0 0 0 0];
MDZx=MDZx(2:length(MDZx)-2); MDZx(length(MDZx)-4:length(MDZx))=[0 0 0 0 0];
HZx=HZx(2:length(HZx)-2);
XXX=[bins' bins.^2' bins.^3' bins.^4' bins.^5' ones(size(bins))];
XXXX=[Xbins' Xbins.^2' Xbins.^3' Xbins.^4' Xbins.^5' ones(size(Xbins))];
XXXX=XXXX*inv(XXXX*XXXX);
MUGain=MUx*XXXX; MUprob=MUGain*XXX*100; % MUprob=[ones(1,takeout)*MUprob(1)
MUprob ones(1,takeout)*MUprob(length(MUprob))];
MDGain=MDx*XXXX; MDprob=MDGain*XXX*100; % MDprob=[ones(1,takeout)*MDprob(1)
MDprob ones(1,takeout)*MDprob(length(MDprob))];
Hgain=Hx*XXXX; Hprob=Hgain*XXX*100; % Hprob=[ones(1,takeout)*Hprob(1) Hprob
ones(1,takeout)*Hprob(length(Hprob))];
HZgain=HZx*XXXX; HZprob=HZgain*XXX*100; % HZprob=[ones(1,takeout2)*HZprob(1) HZprob
ones(1,takeout2)*HZprob(length(HZprob))];
MUZgain=MUZx*XXXX; MUZprob=MUZgain*XXX*100;
% MUZprob=[zeros(1,takeout2)*MUZprob(1) MUZprob ones(1,takeout2)*MUZprob(length(MUZprob))];
MDZgain=MDZx*XXXX; MDZprob=MDZgain*XXX*100;
% MDZprob=[zeros(1,takeout2)*MDZprob(1) MDZprob ones(1,takeout2)*MDZprob(length(MDZprob))];
MUZprob(1:5)=[0 0 0 0 0];
MDZprob(length(MDZprob)-4:length(MDZprob))=[0 0 0 0 0]; MUprob(1:5)=[0 0 0 0 0];
MDprob(length(MDprob)-4:length(MDprob))=[0 0 0 0 0];
for zeroout=1:length(MDprob)
if MDprob(zeroout)<0
MDprob(zeroout)=0;
end
if MUprob(zeroout)<0
MUprob(zeroout)=0;
end
if Hprob(zeroout)<0
Hprob(zeroout)=0;
end

```

```

end
  if MDZprob(zeroout)<0
    MDZprob(zeroout)=0;
  end
  if MUZprob(zeroout)<0
    MUZprob(zeroout)=0;
  end
  if HZprob(zeroout)<0
    HZprob(zeroout)=0;
  end
end
Tprob=(Hprob+MUprob+MDprob+HZprob+MUZprob+MDZprob)/100;
Hprob=Hprob./Tprob;MUprob=MUprob./Tprob;MDprob=MDprob./Tprob;HZprob=HZprob./Tprob;
MUZprob=MUZprob./Tprob;MDZprob=MDZprob./Tprob;
IndHold=BigSTATNUM==1;IndMovDn=BigSTATNUM==2;IndMovUp=BigSTATNUM==3;
IndHoldZero=BigSTATNUM==4;IndMovDnZero=BigSTATNUM==5;IndMovUpZero=BigSTATNUM==6;
%%%%% quantify likelihoods
%%%%% Hold
clear Ybtot Temp Distance
Diffbins=-.4:.01:.4; Samplebins=1:150; XX=BigPHASE(IndHold,4); YY=BigPHASE(IndHold,3);
for Probcount=1:length(Diffbins)-1
  XXind=and(XX>Diffbins(Probcount),XX<=Diffbins(Probcount+1));
  Yb=hist(YY(XXind),Samplebins);
  if sum(Yb)>0
    Yb=Yb./sum(Yb);
  end
  Ybtot(:,Probcount)=Yb';
end
Diffnums=(diag(1:80)*ones(80,150)); Samplenums=diag(1:150)*ones(150,80);
for Diffnum=1:length(Diffbins)-1
  for Samplenum=1:length(Samplebins)
    Distance=sqrt((Diffnums-Diffnum).^2+(Samplenums-Samplenum).^2);
    Temp(Diffnum,Samplenum)=sum(sum(radbas(Distance/5).*Ybtot));
  end
end
for tt=1:length(Diffbins)-1
  if sum(Temp(tt,:))>0
    Temp(tt,:)=Temp(tt,:)/sum(Temp(tt,:));
  end
end
for tt=length(Samplebins)-1:-1:1 %%% cumulative probability
  Temp(:,tt)=Temp(:,tt)+Temp(:,tt+1);
end
HoldSteps=Temp;
%%%%% Moveup
clear Ybtot Temp Distance
Diffbins=-.4:.01:.4; Samplebins2=1:50; XX=BigPHASE(IndMovUp,4);
YY=BigPHASE(IndMovUp,3);
for Probcount=1:length(Diffbins)-1
  XXind=and(XX>Diffbins(Probcount),XX<=Diffbins(Probcount+1));
  Yb=hist(YY(XXind),Samplebins2);
  if sum(Yb)>0
    Yb=Yb./sum(Yb);
  end
  Ybtot(:,Probcount)=Yb';

```

```

end
Diffnums2=(diag(1:80)*ones(80,length(Samplebins2)))';
Samplenums2=diag(1:length(Samplebins2))*ones(length(Samplebins2),80);
for Diffnum2=1:length(Diffbins)-1
    for Samplenum2=1:length(Samplebins2)
        Distance=sqrt((Diffnums2-Diffnum2).^2+(Samplenums2-Samplenum2).^2);
        Temp(Diffnum2,Samplenum2)=sum(sum(radbas(Distance/5).*Ybtot));
    end
end
for tt=1:length(Diffbins)-1
    if sum(Temp(tt,:))>0
        Temp(tt,:)=Temp(tt,:)/sum(Temp(tt,:));
    end
end
for tt=length(Samplebins2)-1:-1:1 %%% cumulative probability
    Temp(:,tt)=Temp(:,tt)+Temp(:,tt+1);
end
MoveUpSteps=Temp;
%%%% Movedown
clear Ybtot Temp Distance
XX=BigPHASE(IndMovDn,4); YY=BigPHASE(IndMovDn,3);
for Probcount=1:length(Diffbins)-1
    XXind=and(XX>Diffbins(Probcount),XX<=Diffbins(Probcount+1));
Yb=hist(YY(XXind),Samplebins2);
    if sum(Yb)>0
        Yb=Yb./sum(Yb);
    end
    Ybtot(:,Probcount)=Yb';
end
Diffnums2=(diag(1:80)*ones(80,length(Samplebins2)))';
Samplenums2=diag(1:length(Samplebins2))*ones(length(Samplebins2),80);
for Diffnum2=1:length(Diffbins)-1
    for Samplenum2=1:length(Samplebins2)
        Distance=sqrt((Diffnums2-Diffnum2).^2+(Samplenums2-Samplenum2).^2);
        Temp(Diffnum2,Samplenum2)=sum(sum(radbas(Distance/5).*Ybtot));
    end
end
for tt=1:length(Diffbins)-1
    if sum(Temp(tt,:))>0
        Temp(tt,:)=Temp(tt,:)/sum(Temp(tt,:));
    end
end
for tt=length(Samplebins2)-1:-1:1 %%% cumulative probability
    Temp(:,tt)=Temp(:,tt)+Temp(:,tt+1);
end
MoveDownSteps=Temp;
%%%% Aileron movement
%%%% Moveup
clear Ybtot Temp Distance
Ailbins=-1:.025:1; XX=BigPHASE(IndMovUp,3); YY=(BigPHASE(IndMovUp,9));
for Probcount=1:length(Samplebins2)-1
    XXind=and(XX>Samplebins2(Probcount),XX<=Samplebins2(Probcount+1));
Yb=hist(YY(XXind),Ailbins);
    if sum(Yb)>0
        Yb=Yb./sum(Yb);
    end
end

```

```

    Ybtot(:,Probcount)=Yb';
end
Ailnums=(diag(1:length(Ailbins))*ones(length(Ailbins),length(Samplebins2)-1));
Samplenums2=diag(1:length(Samplebins2)-1)*ones(length(Samplebins2)-1,length(Ailbins));
for Samplenum2=1:length(Samplebins2)-1
    for Ailnum=1:length(Ailbins)
        Distance=sqrt((Samplenums2-Samplenum2).^2+(Ailnums-Ailnum).^2);
        Temp(Samplenum2,Ailnum)=sum(sum(radbas(Distance/5).*Ybtot));
    end
end
for tt=1:length(Samplebins2)-1
    if sum(Temp(tt,:))>0
        Temp(tt,:)=Temp(tt,:)/sum(Temp(tt,:));
    end
end
for tt=length(Ailbins)-1:-1:1 %%% cumulative probability
    Temp(:,tt)=Temp(:,tt)+Temp(:,tt+1);
end
MoveUpAil=Temp
%%%%%% MoveDown
clear Ybtot Temp Distance
Ailbins=-1:.025:1; XX=BigPHASE(IndMovDn,3); YY=(BigPHASE(IndMovDn,9));
for Probcount=1:length(Samplebins2)-1
    XXind=and(XX>Samplebins2(Probcount),XX<=Samplebins2(Probcount+1));
Yb=hist(YY(XXind),Ailbins);
    if sum(Yb)>0
        Yb=Yb./sum(Yb);
    end
    Ybtot(:,Probcount)=Yb';
end
Ailnums=(diag(1:length(Ailbins))*ones(length(Ailbins),length(Samplebins2)-1));
Samplenums2=diag(1:length(Samplebins2)-1)*ones(length(Samplebins2)-1,length(Ailbins));
for Samplenum2=1:length(Samplebins2)-1
    for Ailnum=1:length(Ailbins)
        Distance=sqrt((Samplenums2-Samplenum2).^2+(Ailnums-Ailnum).^2);
        Temp(Samplenum2,Ailnum)=sum(sum(radbas(Distance/5).*Ybtot));
    end
end
for tt=1:length(Samplebins2)-1
    if sum(Temp(tt,:))>0
        Temp(tt,:)=Temp(tt,:)/sum(Temp(tt,:));
    end
end
for tt=length(Ailbins)-1:-1:1 %%% cumulative probability
    Temp(:,tt)=Temp(:,tt)+Temp(:,tt+1);
end
MoveDnAil=Temp;
eval(['save YaxisNLDataSubj',Subj,' BigMUCORRECT BigMDCORRECT BigHCORRECT
BigHZCORRECT BigMDZCORRECT BigMUZCORRECT BigCOUNTPHASE BigCOUNTPHASEMU
BigCOUNTPHASEMD BigCOUNTPHASEH BigCOUNTPHASEHZ BigCOUNTPHASEMDZ
BigCOUNTPHASEMUZ BigCOUNT BigCOUNTH BigCOUNTMD BigCOUNTMU BigPHASE
BigSTATUS BigSTATNUM bins Samplebins Samplebins2 Diffbins Ailbins MoveDnAil MoveUpAil
MoveDownSteps MoveUpSteps HoldSteps IndMovUp IndMovDn IndHold IndHoldZero IndMovUpZero
IndMovDnZero Hprob MUp prob MDprob HZprob MUZprob MDZprob'])
end %for j

```

```

%% 1 July 2006
%% yaxis model sim linear
%% LCDR Karl U Schultz
%% This program constructs the entire model and simulates an entire run
clear
%% Define plant variables
g=9.81; Pfreq=3.0; Pdamp=.65; Pgain=500; Vydamp=4; Rfreq=5; Rdamp=.4;Rgain=625;Vxdamp=4;
dt=.012; %% delta t for all trials %%mass=1000; Not used
%% Basic plant
A=[-Vydamp 0 0 g; 1 0 0 0; 0 0 -2*Pdamp*Pfreq -Pfreq^2; 0 0 1 0]; B=[0;0;Pgain;0]; C=[eye(4)];
D=zeros(4,1); E=[0;1;0;0];
sys=ss(A,B,C,D);
%% Basic plant with TSAS
AT=A; BT=B; CT=[C;0 1 0 0]; %this includes the TSAS variable
DT=[D;0]; sysT=ss(AT,BT,CT,DT);
%% DVE Plant (no roll signal available)
AD=A; BD=B; CD=[1 0 0 0; 0 1 0 0]; DD=[0;0]; sysD=ss(AD,BD,CD,DD);
%% DVE Plant with TSAS
ADT=A; BDT=B; CDT=[CD;0 1 0 0]; DDT=[DD;0]; sysDT=ss(ADT,BDT,CDT,DDT);
%% Generate the important frequencies
w=.01; for i=2:70
    w(i)=w(i-1)*1.2;
end
%% Set Datapath
loadpath='C:\KarlPhd\ExperimentsFall2004\Data'; eval(['addpath ',loadpath]);
CONDTSAS=[0 0 0 1 1 1 1 1 0 1 0 0;0 0 0 1 1 1 1 1 1 0 0 0;0 1 0 1 0 1 1 0 1 0 1 0;1 1 0 1 0 0 0 0 1 0 1 1...
1 1 1 0 0 0 0 0 0 1 1 1;1 0 1 0 1 0 0 1 0 1 0 1;0 0 1 0 1 1 1 1 0 1 0 0;0 0 0 1 1 1 1 1 1 0 0 0;...
0 1 0 1 0 1 1 0 1 0 1 0;1 1 0 1 0 0 0 0 1 0 1 1;1 1 1 0 0 0 0 0 0 1 1 1;1 0 1 0 1 0 0 1 0 1 0 1];
CONDVE=[0 1 2 2 1 0 0 1 2 2 1 0;1 2 0 0 2 1 1 2 0 0 2 1;2 0 1 1 0 2 2 0 1 1 0 2;0 1 2 2 1 0 0 1 2 2 1 0;...
1 2 0 0 2 1 1 2 0 0 2 1;2 0 1 1 0 2 2 0 1 1 0 2;0 1 2 2 1 0 0 1 2 2 1 0;1 2 0 0 2 1 1 2 0 0 2 1;...
2 0 1 1 0 2 2 0 1 1 0 2;0 1 2 2 1 0 0 1 2 2 1 0;1 2 0 0 2 1 1 2 0 0 2 1;2 0 1 1 0 2 2 0 1 1 0 2];
SUBJ='ABCDEFGHIJKL';
eval(['load YaxisNMMModel_PVO_Avg'])
%bins=[-.5:.05:-.15 -.13:.02:.13 .15:.05:.5];
%bins=-.15:.02:.15;
for j=1:12 % Subject
    CondTSAS=CONDTSAS(j,:); CondVE=CONDVE(j,:); Subj=SUBJ(j)
    for i=1:12
        eval(['load
c:\karlphd\experimentsfall2004\data\',Subj,num2str(CondTSAS(i)),num2str(CondVE(i)),T',num2str(i)]];
        %%% Parse Data
        eval(['data=',Subj,num2str(CondTSAS(i)),num2str(CondVE(i)),T',num2str(i),'']);
        eval(['clear ',Subj,num2str(CondTSAS(i)),num2str(CondVE(i)),T',num2str(i)]];
        height=data(:,1); pitch=data(:,2); roll=data(:,3); x=data(:,4); y=data(:,5); z=data(:,6);
        xd=data(:,7); yd=data(:,8); hd=data(:,12); ud=data(:,9); vd=data(:,10);
        wd=data(:,11);
        rd=data(:,14); pd=data(:,13); deltat=data(:,15); lightness=data(:,16);
        xdist=data(:,17); ydist=data(:,18); time=data(:,19); rudder=data(:,20);
        aileron=data(:,22); elevator=data(:,21);collective=data(:,23); %%% Define GVE, Xsition, and
DVE
        [crd,startlength]=min(abs(10-time)); [crd,gvelength]=min(abs(70-time));
[crd,xsitionlength]=min(abs(100-time));
        [crd,totallength]=min(abs(190-time)); timeline=1; % PVO
        timeline=3; %VOSS
        if timeline==1
            index1=startlength; index2=gvelength;

```

```

elseif timeline==2
    index1=gvelength;    index2=xsitionlength;
else
    index1=xsitionlength;    index2=totallength;
end
dt=abs(mean(time(1:length(time)-1)-time(2:length(time))));
T=time(index1:index2); Xdist=xdist(index1:index2); X=x(index1:index2);
dX=(xd(index1:index2)+xdist(index1:index2));
R=roll(index1:index2); dR=rd(index1:index2); Ail=aileron(index1:index2);
Ydist=ydist(index1:index2); Y=y(index1:index2); dY=(-yd(index1:index2)+ydist(index1:index2));
P=pitch(index1:index2); dP=pd(index1:index2); Elev=elevator(index1:index2);
T=T(1):dt:T(length(T)); minleng=min([length(T) length(Elev) length(Y)]);
Y=Y(1:minleng); dY=dY(1:minleng); P=P(1:minleng); dP=dP(1:minleng); Ydist=Ydist(1:minleng);
T=T(1:minleng); Elev=Elev(1:minleng);
TSAS=zeros(size(Y));
%% Calculate TSAS; TSASindxzero=abs(X)<=5;
TSASindx1=and(Y>5,Y<=10); TSASindx2=and(Y>10,Y<=20); TSASindx3=Y>20;
TSASindxm1=and(Y<-5,Y>=-10); TSASindxm2=and(Y<-10,Y>=-20); TSASindxm3=Y<-20;
TSAS(TSASindx1)=7.5*ones(size(TSAS(TSASindx1))); TSAS(TSASindxm1)=-
7.5*ones(size(TSAS(TSASindxm1)));
TSAS(TSASindx2)=15*ones(size(TSAS(TSASindx2))); TSAS(TSASindxm2)=-
15*ones(size(TSAS(TSASindxm2)));
TSAS(TSASindx3)=25*ones(size(TSAS(TSASindx3))); TSAS(TSASindxm3)=-
25*ones(size(TSAS(TSASindxm3)));
errorT=Y-TSAS;
%% Determine the noise for each state
if or((CondVE(i)==0),(timeline==1));
    errorY=.1881*abs(Y)+15;    errordY=.2723*abs(dY);    errorP=.1013*abs(P)+1.4;
errordP=.45*abs(dP)/2;
elseif CondVE(i)==1;
    errorY=(.1881*abs(Y)+15)*1.5; errordY=.2723*abs(dY)*1.5;    errorP=(.1013*abs(P)+1.4)*1.5;
errordP=.45*abs(dP)/2*1.5;
else
    errorY=(.1164*abs(Y)+1.1810)*1; errordY=(.45*abs(dY)+.36)*1;
end
for tenruns=1:10
    randY=randn(size(errorY)); randdY=randn(size(errordY)); randP=randn(size(errorP));
randdP=randn(size(errordP));
noisescale=1; noiseY=errorY.*randY*noisescale; noisedY=errordY.*randdY*noisescale;
noiseP=errorP.*randP*noisescale; noisedP=errordP.*randdP*noisescale;
noiseT=errorT; %this is the real error. Do NOT Scale
w=Ydist; vu=randn(size(Elev)).*abs(Elev)*.3; %%This helps match PSD (deltaNL) against
PSD(Elev)
%% Check the visual and tactile conditions
if CondTSAS(i)==0
    if and(timeline>1,CondVE(i)==2)
        C=CD; D=DD; outs=2;    vy=[noisedY noiseY;% noisedR noiseR];
    else
        C=Cb; D=Db; outs=4;    vy=[noisedY noiseY noisedP noiseP];
    end
else %TSAS on
    if and(timeline>1,CondVE(i)==2)
        C=CDT; D=DDT; outs=3;    vy=[noisedY noiseY noiseT;%noiseR noiseR noiseT];
    else
        C=CT; D=DT; outs=5;    vy=[noisedY noiseY noisedP noiseP noiseT];
    end
end

```

```

end
Vy=diag(mean(abs(vy))); W1=diag([mean(abs(Ydist)) mean(abs(vu))]);
%%%%%%%%% Neuromuscular Term
eval(['Sysc=Sys1',Subj,',';]); eval(['[Ac,Bc,Cc,Dc]=ssdata(Sysc);'])
Sysc=ss(Ac,Bc,Cc,Dc); Sysnm=ss(Anm,Bnm,Cnm,Dnm); Cnl=eye(1);
%%%%%%%%% Complete Term
A1=[A B*Cnm zeros(4,3);zeros(3,4) Anm Bnm*Cnl*Cc;zeros(3,4) zeros(3,3) Ac];
B1=[zeros(4,1);Bnm*Cnl*Dc;Bc]; C1=[C zeros(outs,3) zeros(outs,3)]; D1=[zeros(outs,1)];
Sys1=ss(A1,B1,C1,D1);
E1=[E B zeros(4,outs);zeros(3,1) zeros(3,1) zeros(3,outs);zeros(3,1) zeros(3,1) zeros(3,outs)];
Q=[0 0 0 0;0 1 0 0;0 0 0 0;0 0 0 0];
Q1=[Q zeros(4,3) zeros(4,3);zeros(3,4) zeros(3,3) zeros(3,3);zeros(3,4) zeros(3,3) zeros(3,3)];
R1=10^-10;
[K,Scrd,Ecrd]=lqr(A,B,Q,R1); Syscl=ss(A-B*K,E,C,D); %Plant Only
[K1,Scrd,Ecrd]=lqr(A1,B1,Q1,R1);
Sys1e=ss(A1,[B1 [E B;zeros(3,1) zeros(3,1)];zeros(3,1) zeros(3,1)]),C1,[D1 zeros(outs,1)
zeros(outs,1)]); %Open Loop
Sys1cl=ss(A1-B1*K1,E1,C1,[zeros(outs,1) zeros(outs,1) eye(outs)]); %Closed Loop no Est
[Kest,L1,Pcrd]=kalman(Sys1e,W1,Vy
ANLol=[A1-L1*C1-B1*K1 L1*C zeros(10,3);...
zeros(4,10) A zeros(4,3);...
-Bc*K1 zeros(3,4) Ac];
BNL=[zeros(10,1);B;zeros(3,1)];
ENL=[zeros(10,1) zeros(10,1) L1;...
E B zeros(4,outs);...
zeros(3,1) zeros(3,1) zeros(3,outs)];
BNLol=[BNL ENL]; CNLol=[-Dc*K1 zeros(1,4) Cc];
DNLol=[zeros(1,1) zeros(1,1) zeros(1,1) zeros(1,outs)];
SYSNLol=ss(ANLol,BNLol,CNLol,DNLol); SYSol=ss(A,[B E],C,[D D]);
siminput=[Elev w]; [Yol,Tol,Xol]=lsim(SYSol,siminput,T-T(1));
ANLcl=[A1-L1*C1-B1*K1 L1*C1;-B1*K1 A1];
BNLcl=[zeros(10,1) zeros(10,1) L1;E1];
CNLcl=[zeros(1,10) 0 1 0 0 zeros(1,3) zeros(1,3)];
DNLcl=[zeros(1,1) zeros(1,1) zeros(1,outs)];
SYSNLcl=ss(ANLcl,BNLcl,CNLcl,DNLcl);
siminput=[w vu vy]; [YNLcl,TNLcl,XNLcl]=lsim(SYSNLcl,siminput,T-T(1));
Elevcl=Cnm*XNLcl(:,15:17)+vu';
Uc=-K1*XNLcl(:,1:10)'; Uact=-K*XNLcl(:,11:14)';
[m,p]=bode(SYSNLcl(1),wf);
for mm=1:length(m)
MAG(mm)=m(1,1,mm); PHS(mm)=p(1,1,mm);
end
Elevsmooth=1; Elevol=Elevcl; XNLol=zeros(1,17); %%%%%%%%%% This puts in a random discretization of
the Elevator signal
while Elevsmooth<length(Elev)-2
steps=round(abs(randn(1))*1/dt)+1;
if (Elevsmooth+steps)>length(Elev)
steps=length(Elev)-Elevsmooth;
end
Elevol(Elevsmooth:Elevsmooth+steps)=ones(size(Elevcl(Elevsmooth:Elevsmooth+steps)))*(Elevcl(Elevsmooth:Elevsmooth+steps))*1.3; Elevsmooth=Elevsmooth+steps+1;
end
Elevol=Elevol'; siminput=[Elevol w vu vy]; [YNLol,TNLol,XNLol]=lsim(SYSNLol,siminput,T-T(1));
Elev=Elev(1:minleng); Elevcl=Elevcl(1:minleng); Elevol=Elevol(1:minleng);
Ymean(tenruns)=mean(abs(XNLcl(:,12))); dYmean(tenruns)=mean(abs(XNLcl(:,11)));

```



```

Pmean(tenruns)=mean(abs(XNLcl(:,14)));    dPmean(tenruns)=mean(abs(XNLcl(:,13)));
Yomean(tenruns)=mean(abs(XNLol(:,12)));    dYomean(tenruns)=mean(abs(XNLol(:,11)));
Pomean(tenruns)=mean(abs(XNLol(:,14)));    dPomean(tenruns)=mean(abs(XNLol(:,13)));
Elevmean(tenruns)=mean(abs(Elevcl));    Elevolmean(tenruns)=mean(abs(Elevol));
Yolmean(tenruns)=mean(abs(XNLol(:,12)));    [Yp(:,tenruns) F]=psd(Y,length(Y),1/dt);
[Yclp(:,tenruns) F]=psd(XNLcl(:,12),length(Y),1/dt);    [Yolp(:,tenruns)
F]=psd(XNLol(:,12),length(Y),1/dt);
[Elevp(:,tenruns) F]=psd(Elev,length(Elev),1/dt);    [Elevclp(:,tenruns)
F]=psd(Elevcl,length(Elev),1/dt);
[Elevolp(:,tenruns) F]=psd(Elevol,length(Elev),1/dt);    [Wp(:,tenruns) F]=psd(w,length(Y),1/dt);
[WY(:,tenruns) F]=tfe(w,Y,length(Y),1/dt);    [WYc(:,tenruns)
F]=tfe(w,XNLcl(:,12),length(Y),1/dt);
[WYo(:,tenruns) F]=tfe(w,XNLol(:,12),length(Y),1/dt);    [EY(:,tenruns)
F]=tfe(Y,Elev,length(Y),1/dt);
[EYc(:,tenruns) F]=tfe(XNLcl(:,12),Elevcl,length(Y),1/dt);    [EYo(:,tenruns)
F]=tfe(XNLol(:,12),Elevol,length(Y),1/dt);
end %tenruns
    YmeanActual(j,i)=mean(abs(Y)); YmeanNLcl(j,i)=mean(Ymean); YmeanNLol(j,i)=mean(Yomean);
    dYmeanActual(j,i)=mean(abs(dY)); dYmeanNLcl(j,i)=mean(dYmean);
dYmeanNLol(j,i)=mean(dYomean);
    PmeanActual(j,i)=mean(abs(P)); PmeanNLcl(j,i)=mean(Pmean); PmeanNLol(j,i)=mean(Pomean);
    dPmeanActual(j,i)=mean(abs(dP)); dPmeanNLcl(j,i)=mean(dPmean);
dPmeanNLol(j,i)=mean(dPomean);
    ElevmeanActual(j,i)=mean(abs(Elev)); ElevmeanNLcl(j,i)=mean(abs(Elevcl));
ElevmeanNLol(j,i)=mean(abs(Elevol));
    PSDElev(i,:)=mean(abs(Elevp'));    PSDElevcl(i,:)=mean(abs(Elevclp'));
PSDElevol(i,:)=mean(abs(Elevolp'));
    PSDYol(i,:)=mean(abs(Yolp'));    PSDYcl(i,:)=mean(abs(Yclp'));    PSDY(i,:)=mean(abs(Yp'));
    PSDW(i,:)=mean(abs(Wp'));    TFEWY(i,:)=mean(abs(WY'));    TFEWYc(i,:)=mean(abs(WYc'));
    TFEWYo(i,:)=mean(abs(WYo'));    TFEEY(i,:)=mean(abs(EY'));    TFEEYc(i,:)=mean(abs(EYc'));
    TFEEYo(i,:)=mean(abs(EYo'));
end %%% i (trials)
    eval(['save YaxisMODELVOSSSubj',Subj,'PSDData PSDElev PSDElevcl PSDElevol PSDY PSDYol
PSDYcl PSDW TFEWY TFEWYc TFEWYo TFEEY TFEEYc F'])
end % j Subject)
eval(['save YaxisMODELVOSSSummaryData.mat YmeanActual dYmeanActual PmeanActual
dPmeanActual ElevmeanActual YmeanNLcl dYmeanNLcl PmeanNLcl dPmeanNLcl ElevmeanNLcl
YmeanNLol dYmeanNLol PmeanNLol dPmeanNLol ElevmeanNLol CONDVE CONDTSAS'])

```

```

%%%% Yaxis MODEL SIM NONLINEAR
%%%% 1 July 2006
%%%% LCDR Karl U Schultz
%%%% This program constructs the entire NonLinear
%%%% model and simulates an entire run
clear
%%%% Define plant variables
g=9.81; Pfreq=3.0; Pdamp=.65; Pgain=500; Vydamp=4; Rfreq=5; Rdamp=.4;Rgain=625;Vxdamp=4;
dt=.012; %% delta t for all trials %%mass=1000; Not used
%%%% Basic plant
A=[-Vydamp 0 0 g; 1 0 0 0; 0 0 -2*Pdamp*Pfreq -Pfreq^2; 0 0 1 0]; B=[0;0;Pgain;0]; C=[eye(4)];
D=zeros(4,1); E=[0;1;0;0];
sys=ss(A,B,C,D);
%%%% Basic plant with TSAS
AT=A; BT=B; CT=[C;0 1 0 0]; %this includes the TSAS variable
DT=[D;0]; sysT=ss(AT,BT,CT,DT);
%%%% DVE Plant (no roll signal available)
AD=A; BD=B; CD=[1 0 0 0; 0 1 0 0]; DD=[0;0]; sysD=ss(AD,BD,CD,DD);
%%%% DVE Plant with TSAS
ADT=A; BDT=B; CDT=[CD;0 1 0 0]; DDT=[DD;0]; sysDT=ss(ADT,BDT,CDT,DDT);
%% Generate the important frequencies
w=.01; for i=2:70
    w(i)=w(i-1)*1.2;
end
%%%% Set Datapath
loadpath='C:\KarlPhd\ExperimentsFall2004\Data'; eval(['addpath ',loadpath]);
CONDTSAS=[0 0 0 1 1 1 1 1 0 1 0 0; 0 0 0 1 1 1 1 1 1 0 0 0; 0 1 0 1 0 1 1 0 1 0 1 0; 1 1 0 1 0 0 0 0 1 0 1 1 ...
1 1 1 0 0 0 0 0 0 1 1 1; 1 0 1 0 1 0 0 1 0 1 0 1; 0 0 1 0 1 1 1 1 0 1 0 0; 0 0 0 1 1 1 1 1 1 0 0 0; ...
0 1 0 1 0 1 1 0 1 0 1 0; 1 1 0 1 0 0 0 0 1 0 1 1; 1 1 1 0 0 0 0 0 0 1 1 1; 1 0 1 0 1 0 0 1 0 1 0 1];
CONDVE=[0 1 2 2 1 0 0 1 2 2 1 0; 1 2 0 0 2 1 1 2 0 0 2 1; 2 0 1 1 0 2 2 0 1 1 0 2; 0 1 2 2 1 0 0 1 2 2 1 0; ...
1 2 0 0 2 1 1 2 0 0 2 1; 2 0 1 1 0 2 2 0 1 1 0 2; 0 1 2 2 1 0 0 1 2 2 1 0; 1 2 0 0 2 1 1 2 0 0 2 1; ...
2 0 1 1 0 2 2 0 1 1 0 2; 0 1 2 2 1 0 0 1 2 2 1 0; 1 2 0 0 2 1 1 2 0 0 2 1; 2 0 1 1 0 2 2 0 1 1 0 2];
SUBJ='ABCDEFGHIJKL';
eval(['load YaxisNMMModel_PVO_Avg'])
for j=1:12 % Subject
    CondTSAS=CONDTSAS(j,:); CondVE=CONDVE(j,:); Subj=SUBJ(j)
    for i=1:12
        eval(['load
c:\karlphd\experimentsfall2004\data\',Subj,num2str(CondTSAS(i)),num2str(CondVE(i)), 'T',num2str(i)];
        %%% Parse Data
        eval(['data=',Subj,num2str(CondTSAS(i)),num2str(CondVE(i)), 'T',num2str(i),',';]);
        eval(['clear ',Subj,num2str(CondTSAS(i)),num2str(CondVE(i)), 'T',num2str(i)];
        height=data(:,1); pitch=data(:,2); roll=data(:,3); x=data(:,4); y=data(:,5); z=data(:,6);
        xd=data(:,7); yd=data(:,8); hd=data(:,12); ud=data(:,9); vd=data(:,10);
        wd=data(:,11);
        rd=data(:,14); pd=data(:,13); deltat=data(:,15); lightness=data(:,16);
        xdist=data(:,17); ydist=data(:,18); time=data(:,19); rudder=data(:,20);
        aileron=data(:,22); elevator=data(:,21); collective=data(:,23);
        %%% Define GVE, Xsition, and DVE
        [crd,startlength]=min(abs(10-time)); [crd,gvelength]=min(abs(70-time));
        [crd,xsitionlength]=min(abs(100-time)); [crd,totallength]=min(abs(190-time));
        timeline=1; % PVO
        timeline=3; %VOSS
        if timeline==1
            index1=startlength; index2=gvelength;
        elseif timeline==2

```

```

    index1=gvelength;    index2=xsitionlength;
else
    index1=xsitionlength;    index2=totallength;
end
dt=abs(mean(time(1:length(time)-1)-time(2:length(time))));
T=time(index1:index2); Xdist=xdist(index1:index2); X=x(index1:index2);
dX=(xd(index1:index2)+xdist(index1:index2));
R=roll(index1:index2); dR=rd(index1:index2); Ail=aileron(index1:index2);
Ydist=ydist(index1:index2); Y=y(index1:index2); dY=(-yd(index1:index2)+ydist(index1:index2));
P=pitch(index1:index2); dP=pd(index1:index2); Elev=elevator(index1:index2);
T=T(1):dt:T(length(T)); minleng=min([length(T) length(Elev) length(Y)]);
Y=Y(1:minleng); dY=dY(1:minleng); P=P(1:minleng); dP=dP(1:minleng); Ydist=Ydist(1:minleng);
T=T(1:minleng); Elev=Elev(1:minleng);
TSAS=zeros(size(Y));
%% Calculate TSAS; TSASindxzero=abs(X)<=5;
TSASindx1=and(Y>5,Y<=10); TSASindx2=and(Y>10,Y<=20); TSASindx3=Y>20;
TSASindxm1=and(Y<-5,Y>=-10); TSASindxm2=and(Y<-10,Y>=-20); TSASindxm3=Y<-20;
TSAS(TSASindx1)=7.5*ones(size(TSAS(TSASindx1))); TSAS(TSASindxm1)=
7.5*ones(size(TSAS(TSASindxm1)));
TSAS(TSASindx2)=15*ones(size(TSAS(TSASindx2))); TSAS(TSASindxm2)=
15*ones(size(TSAS(TSASindxm2)));
TSAS(TSASindx3)=25*ones(size(TSAS(TSASindx3))); TSAS(TSASindxm3)=
25*ones(size(TSAS(TSASindxm3)));
errorT=(Y-TSAS)/2;
%% Determine the noise for each state
if or((CondVE(i)==0),(timeline==1));
    errorY=-.1881*abs(Y)+15;    errordY=.2723*abs(dY);    errorP=.1013*abs(P)+1.4;
errordP=.45*abs(dP)/2;
elseif CondVE(i)==1;
    errorY=(-.1881*abs(Y)+15)*1.5; errordY=.2723*abs(dY)*1.5; errorP=(.1013*abs(P)+1.4)*1.5;
errordP=.45*abs(dP)*1.5/2;
else
    errorY=(.1164*abs(Y)+1.1810)*1;
errordY=(.45*abs(dY)+.36)*1;errorP=.2229*abs(P)*2000*1;errordP=.45*abs(dP)*2000*1;
end
for tenruns=1:5
    randY=randn(size(errorY)); randdY=randn(size(errordY));randP=randn(size(errorP));
randdP=randn(size(errordP));
    noisescale=1; noiseY=errorY.*randY*noisescale; noisedY=errordY.*randdY*noisescale;
    noiseP=errorP.*randP*noisescale; noisedP=errordP.*randdP*noisescale;noiseT=errorT; %this is the
real error. Do NOT Scale
    w=Ydist; vu=randn(size(Elev)).*abs(Elev)*.03; %%This helps match PSD (deltaNL) against
PSD(Elev)
    %%% Check the visual and tactile conditions
    if CondTSAS(i)==0
        if and(timeline>1,CondVE(i)==2)
            C=CD; D=DD; outs=2;    vy=[noisedY noiseY];% noisedR noiseR];
        else
            C=Cb; D=Db; outs=4;    vy=[noisedY noiseY noisedP noiseP];
        end
    else %TSAS on
        if and(timeline>1,CondVE(i)==2)
            C=CDT; D=DDT; outs=3;    vy=[noisedY noiseY noiseT];%noiseR noiseR noiseT];
        else
            C=CT; D=DT; outs=5;    vy=[noisedY noiseY noisedP noiseP noiseT];
        end
    end
end

```

```

end
Vy=diag(mean(abs(vy)));      W1=diag([mean(abs(Ydist)) mean(abs(vu))]);
%%%%%%%%% Neuromuscular Term
eval(['Sysc=Sys1',Subj,'];)
eval(['[Ac,Bc,Cc,Dc]=ssdata(Sysc);'])
Sysc=ss(Ac,Bc,Cc,Dc); Sysnm=ss(Anm,Bnm,Cnm,Dnm); Cnl=eye(1);
%%%%%%%% Complete Term
A1=[A B*Cnm zeros(4,3);zeros(3,4) Anm Bnm*Cnl*Cc;zeros(3,4) zeros(3,3) Ac];
B1=[zeros(4,1);Bnm*Cnl*Dc;Bc];      C1=[C zeros(outs,3) zeros(outs,3)];
D1=[zeros(outs,1)];
Sys1=ss(A1,B1,C1,D1);
E1=[E B zeros(4,outs);zeros(3,1) zeros(3,1) zeros(3,outs);zeros(3,1) zeros(3,1) zeros(3,outs)];
Q=[0 0 0 0;0 1 0 0;0 0 0 0;0 0 0 0];
Q1=[Q zeros(4,3) zeros(4,3);zeros(3,4) zeros(3,3) zeros(3,3);zeros(3,4) zeros(3,3) zeros(3,3)];
R1=10^-10;
[K1,Scrd,Ecrd]=lqr(A1,B1,Q1,R1);
Sys1e=ss(A1,[E B;zeros(3,1) zeros(3,1);zeros(3,1) zeros(3,1)],C1,[D1 zeros(outs,1)
zeros(outs,1)]); %Open Loop
[Kest,L1,eCRD]=kalman(Sys1e,W1,Vy); %%%
ANLol=[A1-L1*C1-B1*K1  L1*C  zeros(10,3);...
zeros(4,10)  A  zeros(4,3);...
-Bc*K1  zeros(3,4)  Ac];
BNL=[zeros(10,1);B;zeros(3,1)];
ENL=[zeros(10,1) zeros(10,1)  L1;...
E  B  zeros(4,outs);...
zeros(3,1) zeros(3,1) zeros(3,outs)];
BNLol=[BNL ENL];      CNLol=[-Dc*K1 zeros(1,4) Cc];      DNLol=[zeros(1,1) zeros(1,1)
zeros(1,1) zeros(1,outs)];
SYSNLol=ss(ANLol,BNLol,CNLol,DNLol);      SYSol=ss(A,[B E],C,[D D]);
siminput=[Elev w vu vy];      [YNLol,TNLol,XNLol]=lsim(SYSNLol,siminput,T-T(1));
siminput=[Elev w];      [Yol,Tol,Xol]=lsim(SYSol,siminput,T-T(1));
ANLcl=[A1-L1*C1-B1*K1  L1*C1;-B1*K1  A1];
BNLcl=[zeros(10,1) zeros(10,1) L1;E1];      CNLcl=[zeros(1,10) 0 1 0 0 zeros(1,3) zeros(1,3)];
DNLcl=[zeros(1,1) zeros(1,1) zeros(1,outs)];      SYSNLcl=ss(ANLcl,BNLcl,CNLcl,DNLcl);
siminput=[w vu vy];      [YNLcl,TNLcl,XNLcl]=lsim(SYSNLcl,siminput,T-T(1));
%%%%%%%% Step by step simulation - Nonlinear
%%%%%%%% Try to step through the simulation for NonLinear Stuff
ControlGain=1;  eval(['load NLDATASubj',Subj])
Hprob=(Hprob); MUprob=(MUprob); MDprob=(MDprob); MUZprob=(MUZprob);
MDZprob=(MDZprob);
SIM=1;      SIMold=1; NLcompute='y';
deltaNL=zeros(size(Elev)); Uc=zeros(size(Elev)); deltaNL(1)=Elev(1); DIFF=((Uc(1)-
deltaNL(1)));
X2comp=[dY(1) Y(1) dR(1) R(1) 0 0 0 0 0 dY(1) Y(1) dR(1) R(1) 0 0 0];
%% Choose the appropriate bin
[bin,bIndx]=min(abs(DIFF-bins));
%%%%%%%% look up probabilities
H=Hprob(bIndx); MU=MUprob(bIndx); MD=MDprob(bIndx);
tot=sum([H MU MD]); %this is to normalize the probabilities (due to math limits, they may not
add to 100%)
%%%%%%%% choose the action
pick=rand(1)*tot;
if pick<=(H)
decision='Hold';
elseif pick<=(H+MU)
decision='MvUp';

```

```

else
    decision='MvDn';
end
while NLcompute=='y';
    SIMoldold=SIMold; SIMold=SIM;
    if decision=='Hold'
        %%% Hold
        %% How long to hold
        [hdiff,hIndx]=min(abs(DIFF-Diffbins));
        if hIndx==81
            hIndx=80;
        end
        hline=HoldSteps(hIndx,:); steps=rand(1); hcount=sum((hline>steps));
        deltaNL(SIM+1:SIM+hcourt)=ones(1,hcount)*deltaNL(SIM);           SIM=SIM+hcourt;
    elseif decision=='MvUp'
        %%% Move up
        % how long to move up
        [mudiff,muIndx]=min(abs(DIFF-Diffbins));
        if muIndx==81
            muIndx=80;
        end
        muline=MoveUpSteps(muIndx,:); steps=(rand(1)); mucount=sum((muline>steps));
        %% How far to move Aileron(Elevator, but keep ail as convention
        [mudiff,muIndx]=min(abs(mucount-Samplebins2));
        if muIndx==50
            muIndx=49;
        end
        muAilline=MoveUpAil(muIndx,:); steps=(rand(1)); ailcount=sum((muAilline>steps));
        ailmove=Ailbins(ailcount); %total Aileron to move
        %%% compute change in Aileron
        stepgain=(1:mucount)/mucount; ailgain=stepgain*ailmove;
        deltaNL(SIM+1:SIM+mucourt)=ones(1,mucourt)*deltaNL(SIM)+ailgain;
    SIM=SIM+mucourt;
    elseif decision=='MvDn'
        %%% move down
        [mddiff,mdIndx]=min(abs(DIFF-Diffbins)); mdline=MoveDownSteps(mdIndx,:);
        steps=(rand(1)); mdcount=sum((mdline>steps));
        %% How far to move Aileron
        [mddiff,mdIndx]=min(abs(mdcount-Samplebins2));
        if mdIndx==50;
            mdIndx=49;
        end
        mdAilline=MoveDnAil(mdIndx,:); steps=rand(1); ailcount=sum((mdAilline>steps));
        ailmove=Ailbins(ailcount); %total Aileron to move
        %%% compute change in Aileron
        stepgain=(1:mdcount)/mdcount; ailgain=stepgain*ailmove;
        deltaNL(SIM+1:SIM+mdcount)=ones(1,mdcount)*deltaNL(SIM)+ailgain;
    SIM=SIM+mdcount;
    elseif decision=='MvUZ'
        %%% move Up to zero
        [mddiff,muIndx]=min(abs(DIFF-Diffbins));
        if muIndx==81;
            muIndx=80;
        end
        muline=MoveUpSteps(muIndx,:); steps=(rand(1)); mucount=sum((muline>steps));
        %% Aileron ends at zero

```

```

    ailmove=-deltaNL(SIM);
    %%% compute change in Aileron
    stepgain=(1:muccount)/muccount; ailgain=stepgain*ailmove;
    deltaNL(SIM+1:SIM+muccount)=ones(1,muccount)*deltaNL(SIM)+ailgain;
SIM=SIM+muccount;
    else
    %%% move down to zero
    [mddiff,mdIndx]=min(abs(DIFF-Diffbins));
    if mdIndx==81
        mdIndx=80;
    end
    mdlines=MoveDownSteps(mdIndx,:);          steps=(rand(1));
mcount=sum((mdlines>steps));
    %% Aileron ends at zero
    ailmove=-deltaNL(SIM);
    %%% compute change in Aileron
    stepgain=(1:mcount)/mcount; ailgain=stepgain*ailmove;
    deltaNL(SIM+1:SIM+mcount)=ones(1,mcount)*deltaNL(SIM)+ailgain;
SIM=SIM+mcount;
    end
    if SIM>=length(Y)
        deltaNL=deltaNL(1:length(Y));          NLcompute='n';          SIM=length(Y);
    end
    %%%% Recompute Vy
    %%%% Check the visual and tactile conditions
    if CondTSAS(i)==0
        if and(timeline>1,CondVE(i)==2)
            C=CD; D=DD; outs=2;
vy(SIMoldold:SIMold,:)=X2comp(SIMoldold:SIMold,11).*randdY(SIMoldold:SIMold)*noisescale ...
            X2comp(SIMoldold:SIMold,12).*randY(SIMoldold:SIMold)*noisescale];
        else
            C=C; D=D; outs=4;
vy(SIMoldold:SIMold,:)=X2comp(SIMoldold:SIMold,11).*randdY(SIMoldold:SIMold)*noisescale ...
            X2comp(SIMoldold:SIMold,12).*randY(SIMoldold:SIMold)*noisescale ...
            X2comp(SIMoldold:SIMold,13).*randdP(SIMoldold:SIMold)*noisescale ...
            X2comp(SIMoldold:SIMold,14).*randP(SIMoldold:SIMold)*noisescale];
        end
    else %TSAS on
        if and(timeline>1,CondVE(i)==2)
            C=CDT; D=DDT; outs=3;
vy(SIMoldold:SIMold,:)=X2comp(SIMoldold:SIMold,11).*randdY(SIMoldold:SIMold)*noisescale .
            X2comp(SIMoldold:SIMold,12).*randY(SIMoldold:SIMold)*noisescale ...
            noiseT(SIMoldold:SIMold)];
        else
            C=CT; D=DT; outs=5;
vy(SIMoldold:SIMold,:)=X2comp(SIMoldold:SIMold,11).*randdY(SIMoldold:SIMold)*noisescale ...
            X2comp(SIMoldold:SIMold,12).*randY(SIMoldold:SIMold)*noisescale ...
            X2comp(SIMoldold:SIMold,13).*randdP(SIMoldold:SIMold)*noisescale ...
            X2comp(SIMoldold:SIMold,14).*randP(SIMoldold:SIMold)*noisescale ...
            noiseT(SIMoldold:SIMold)];
        end
    end
    end
    Vy=diag(mean(abs(vy(SIMoldold:SIMold,:))));
    if SIMoldold==SIMold;
        Vy=diag((abs(vy(SIMold,:))));
    end
end

```

```

WW=diag([mean(abs(Ydist(SIMoldold:SIMold))) mean(abs(vu(SIMoldold:SIMold)))]);
for WWW=1:length(WW)
    if WW(WWW,WWW)==0
        WW(WWW,WWW)=.001;
    end
end
for VVy=1:length(Vy)
    if Vy(VVy,VVy)==0
        Vy(VVy,VVy)=.001;
    end
end
[S,L,Ecrd] = kalman(Sys1e,WW,Vy);
ANLol=[A1-L*C1-B1*K1 L*C zeros(10,3);...
        zeros(4,10) A zeros(4,3);...
        -Bc*K1 zeros(3,4) Ac];
BNL=[zeros(10,1);B;zeros(3,1)];
ENL=[zeros(10,1) zeros(10,1) L;...
      E B zeros(4,outs);...
      zeros(3,1) zeros(3,1) zeros(3,outs)];
BNLol=[BNL ENL]; CNLol=[-Dc*K1 zeros(1,4) Cc]; DNLol=[zeros(1,1) zeros(1,1)
zeros(1,1) zeros(1,outs)];
SYSNLol=ss(ANLol,BNLol,CNLol,DNLol); simadd=2;
if (SIM+simadd)>length(Y)
    simadd=length(Y)-SIM;
end
% deltaNL(SIMold:SIM+simadd)=Ail(SIMold:SIM+simadd); %%This tests the system
siminput=[deltaNL(SIMold:SIM+simadd) w(SIMold:SIM+simadd) vu(SIMold:SIM+simadd)
vy(SIMold:SIM+simadd,:)];
[Output,Tt,Statescomp]=lism(SYSNLol,siminput,[0:dt:dt*(SIM+simadd-
SIMold)],X2comp(SIMold,:));
X2comp(SIMold+1:SIM,:)=Statescomp(2:(SIM-SIMold+1),:);
Uc(SIMold+1:SIM)=Output(2:SIM-SIMold+1)*ControlGain;
Uc(SIM+1)=Uc(SIM);
if decision=='Hold'
    %%% Hold
    %%% Choose next action
    DIFF=(Uc(SIM)-deltaNL(SIM));
    %%% Choose the appropriate bin
    [bin,bIndx]=min(abs(DIFF-bins));
    %%% look up probabilities
    H=Hprob(bIndx); MU=MUprob(bIndx); MD=MDprob(bIndx); MUZ=MUZprob(bIndx);
    MDZ=MDZprob(bIndx);
    tot=sum([H MU MD MUZ MDZ]); %this is to normalize the probs (due to math limits, they
may not add to 100%)
    %%% choose the action
    pick=rand(1)*tot;
    if pick<=(H)
        decision='Hold';
    elseif pick<=(H+MU)
        decision='MvUp';
    elseif pick<=(H+MU+MUZ)
        decision='MvUZ';
    elseif pick<=(H+MU+MUZ+MD)
        decision='MvDn';
    else
        decision='MvDZ';
    end
end

```

```

end
elseif decision=='MvUp'
    %%% Move up
    %% Choose next action
    DIFF=(Uc(SIM)-deltaNL(SIM));
    %% Choose the appropriate bin
    [bin,bIndx]=min(abs(DIFF-bins));
    %%% look up probabilities
    H=Hprob(bIndx); MD=MDprob(bIndx); MDZ=MDZprob(bIndx);
    tot=sum([H MD MDZ]); %this is to normalize the probabilities (due to math limits, they may
not add to 100%)
    %%% choose the action
    pick=rand(1)*tot;
    if pick<=(H)
        decision='Hold';
    elseif pick<=(H+MD)
        decision='MvDn';
    else
        decision='MvDZ';
    end
elseif decision=='MvDn'
    %%% move down
    %% Choose next action
    DIFF=(Uc(SIM)-deltaNL(SIM));
    %% Choose the appropriate bin
    [bin,bIndx]=min(abs(DIFF-bins));
    %%% look up probabilities
    H=Hprob(bIndx); MD=MDprob(bIndx); MDZ=MDZprob(bIndx);
    tot=sum([H MD MDZ]); %this is to normalize the probabilities (due to math limits, they may
not add to 100%)
    %%% choose the action
    pick=rand(1)*tot;
    if pick<=(H)
        decision='Hold';
    elseif pick<=(H+MD)
        decision='MvDn';
    else
        decision='MvDZ';
    end
elseif decision=='MvUZ'
    %% Choose next action
    DIFF=(Uc(SIM)-deltaNL(SIM));
    %% Choose the appropriate bin
    [bin,bIndx]=min(abs(DIFF-bins));
    %%% look up probabilities
    H=Hprob(bIndx); MD=MDprob(bIndx); MDZ=MDZprob(bIndx);
    tot=sum([H MD MDZ]); %this is to normalize the probabilities (due to math limits, they may
not add to 100%)
    %%% choose the action
    pick=rand(1)*tot;
    if pick<=(H)
        decision='Hold';
    elseif pick<=(H+MD)

        decision='MvDn';
    else

```



```

        decision='MvDZ';
    end
else
    %%% move down to zero
    %% Choose next action
    DIFF=(Uc(SIM)-deltaNL(SIM));
    % Choose the appropriate bin
    [bin,bIndx]=min(abs(DIFF-bins));
    %% look up probabilities
    H=Hprob(bIndx); MU=MUprob(bIndx); MUZ=MUZprob(bIndx);
    tot=sum([H MU MUZ]); %this is to normalize the probabilities (due to math limits, they may
not add to 100%)
    %% choose the action
    pick=rand(1)*tot;
    if pick<=(H)
        decision='Hold';
    elseif pick<=(H+MU)
        decision='MvUp';
    else
        decision='MvUZ';
    end
end
end
if SIM>=length(Y)
    deltaNL=deltaNL(1:length(Y)); NLcompute='n'; SIM=length(Y);
end
end %WHILE
Uc=Uc(1:length(Uc)-1);
Ymean(tenruns)=mean(abs(X2comp(:,12))); dYmean(tenruns)=mean(abs(X2comp(:,11)));
Pmean(tenruns)=mean(abs(X2comp(:,14))); dPmean(tenruns)=mean(abs(X2comp(:,13)));
Elevmean(tenruns)=mean(abs(deltaNL));
[Ycp(:,tenruns) F]=psd(Y,length(Y),1/dt); [Yclp(:,tenruns)
F]=psd(X2comp(:,12),length(Y),1/dt);
[Elevp(:,tenruns) F]=psd(Elev,length(Elev),1/dt); [Elevclp(:,tenruns)
F]=psd(deltaNL,length(Ail),1/dt);
[CLp(:,tenruns) F]=tfe(w,Y,length(Y),1/dt); [CLclp(:,tenruns)
F]=tfe(w,X2comp(:,12),length(Y),1/dt);
end %% tenruns
YmeanActual(j,i)=mean(abs(Y)); YmeanNLcl(j,i)=mean(Ymean);
dYmeanActual(j,i)=mean(abs(dY)); dYmeanNLcl(j,i)=mean(dYmean);
PmeanActual(j,i)=mean(abs(P)); PmeanNLcl(j,i)=mean(Pmean);
dPmeanActual(j,i)=mean(abs(dP)); dPmeanNLcl(j,i)=mean(dPmean);
ElevmeanActual(j,i)=mean(abs(Elev)); ElevmeanNLcl(j,i)=mean(abs(Elevmean));
PSDElev(i,:)=mean(abs(Elevp)); PSDElevcl(i,:)=mean(abs(Elevclp));
PSDYcl(i,:)=mean(abs(Ycp));
PSDY(i,:)=mean(abs(Yp)); PSDCL(i,:)=mean(abs(CLp)); PSDCLcl(i,:)=mean(abs(CLclp));
end %% i
eval(['save YaxisNonLinearMODELVOSSSubj',Subj,'PSDData.mat PSDY PSDYcl PSDElev
PSDElevcl PSDCL PSDCLcl F CONDVE CONDTAS'])
end % j Subject)
eval(['save YaxisNonLinearMODELVOSSSummaryData.mat YmeanActual dYmeanActual PmeanActual
dPmeanActual ElevmeanActual YmeanNLcl dYmeanNLcl PmeanNLcl dPmeanNLcl ElevmeanNLcl
CONDVE CONDTAS'])

```

```

%%%%% 7 July
%%%% YAXIS_SIM_PLOT_NONLINEAR
%%%%% This program loads the simulator data, parses it, and plots it
clear
eval(['load YaxisNonLinearMODELVOSSSummaryData'])
YV=[]; dYV=[]; dPV=[]; PV=[]; ElevV=[]; YclV=[]; dYclV=[]; dPclV=[]; PclV=[]; ElevclV=[];
for i=1:12
    YV=[YV YmeanActual(i,:); dYV=[dYV dYmeanActual(i,:); PV=[PV PmeanActual(i,:); dPV=[dPV
dPmeanActual(i,:); ElevV=[ElevV ElevmeanActual(i,:);
    YclV=[YclV YmeanNLcl(i,:); dYclV=[dYclV dYmeanNLcl(i,:); PclV=[PclV PmeanNLcl(i,:);
dPclV=[dPclV dPmeanNLcl(i,:); ElevclV=[ElevclV ElevmeanNLcl(i,:);
    CondTSAS=[CondTSAS CONDTASAS(i,:); CondVE=[CondVE CONDVVE(i,:);
end
%%%% SET INDICES FOR MEANS
TSASindx=CondTSAS==1; NoTSASindx=CondTSAS==0; GTindx=and(CondTSAS==1, CondVE==0);
DLTindx=and(CondTSAS==1, CondVE==1); DHTindx=and(CondTSAS==1, CondVE==2);
Gindx=and(CondTSAS==0, CondVE==0); DLindx=and(CondTSAS==0, CondVE==1);
DHindx=and(CondTSAS==0, CondVE==2);
figure(1) XX=YV(DHindx); XX=[XX(1:4) XX(7:24)]; clf subplot(121)
plot([1 2 3],[mean(YV(Gindx)) mean(YV(DLindx)) mean(XX)] ,'-ob') hold on
plot([1 2 3],[mean(YV(GTindx)) mean(YV(DLTindx)) mean(YV(DHTindx))],'-sr')
plot([1 1],[mean(YV(GTindx))+std(YV(GTindx)) mean(YV(GTindx))-std(YV(GTindx))],'-+r')
plot([1 1],[mean(YV(Gindx))+std(YV(Gindx)) mean(YV(Gindx))-std(YV(Gindx))],'-+b')
plot([2 2],[mean(YV(DLTindx))+std(YV(DLTindx)) mean(YV(DLTindx))-std(YV(DLTindx))],'-+r')
plot([2 2],[mean(YV(DLindx))+std(YV(DLindx)) mean(YV(DLindx))-std(YV(DLindx))],'-+b')
plot([3 3],[mean(YV(DHTindx))+std(YV(DHTindx)) mean(YV(DHTindx))-std(YV(DHTindx))],'-+r')
plot([3 3],[mean(XX)+std(XX) mean(XX)-std(XX)],'-+b')
a=axis; gridaxis([.5 3.5 0 a(4)]);
ylabel('RMS Error') title('Y Error - Actual Trials') xlabel('GVE DVEL DVEH')
subplot(122)
plot([1 2 3],[mean(YclV(Gindx)) mean(YclV(DLindx)) mean(YclV(DHindx))],'-ob')
hold on
plot([1 2 3],[mean(YclV(GTindx)) mean(YclV(DLTindx)) mean(YclV(DHTindx))],'-sr')
plot([1 1],[mean(YclV(GTindx))+std(YclV(GTindx)) mean(YclV(GTindx))-std(YclV(GTindx))],'-+r')
plot([1 1],[mean(YclV(Gindx))+std(YclV(Gindx)) mean(YclV(Gindx))-std(YclV(Gindx))],'-+b')
plot([2 2],[mean(YclV(DLTindx))+std(YclV(DLTindx)) mean(YclV(DLTindx))-std(YclV(DLTindx))],'-+r')
plot([2 2],[mean(YclV(DLindx))+std(YclV(DLindx)) mean(YclV(DLindx))-std(YclV(DLindx))],'-+b')
plot([3 3],[mean(YclV(DHTindx))+std(YclV(DHTindx)) mean(YclV(DHTindx))-std(YclV(DHTindx))],'-+r')
plot([3 3],[mean(YclV(DHindx))+std(YclV(DHindx)) mean(YclV(DHindx))-std(YclV(DHindx))],'-+b')
axis([.5 3.5 0 a(4)]) gridylabel('RMS Error') title('Y Error - Simulated Trials') xlabel('GVE DVEL DVEH')
figure(2) clf subplot(121)
plot([1 2 3],[mean(dYV(Gindx)) mean(dYV(DLindx)) mean(dYV(DHindx))],'-ob')
hold on plot([1 2 3],[mean(dYV(GTindx)) mean(dYV(DLTindx)) mean(dYV(DHTindx))],'-sr')
plot([1 1],[mean(dYV(GTindx))+std(dYV(GTindx)) mean(dYV(GTindx))-std(dYV(GTindx))],'-+r')
plot([1 1],[mean(dYV(Gindx))+std(dYV(Gindx)) mean(dYV(Gindx))-std(dYV(Gindx))],'-+b')
plot([2 2],[mean(dYV(DLTindx))+std(dYV(DLTindx)) mean(dYV(DLTindx))-std(dYV(DLTindx))],'-+r')
plot([2 2],[mean(dYV(DLindx))+std(dYV(DLindx)) mean(dYV(DLindx))-std(dYV(DLindx))],'-+b')
plot([3 3],[mean(dYV(DHTindx))+std(dYV(DHTindx)) mean(dYV(DHTindx))-std(dYV(DHTindx))],'-+r')
plot([3 3],[mean(dYV(DHindx))+std(dYV(DHindx)) mean(dYV(DHindx))-std(dYV(DHindx))],'-+b')
a=axis; gridaxis([.5 3.5 0 a(4)]); ylabel('RMS Error') title('Y Error Rate - Actual Trials') xlabel('GVE DVEL DVEH')
subplot(122) plot([1 2 3],[mean(dYclV(Gindx)) mean(dYclV(DLindx)) mean(dYclV(DHindx))],'-ob')
hold on plot([1 2 3],[mean(dYclV(GTindx)) mean(dYclV(DLTindx)) mean(dYclV(DHTindx))],'-sr')
plot([1 1],[mean(dYclV(GTindx))+std(dYclV(GTindx)) mean(dYclV(GTindx))-std(dYclV(GTindx))],'-+r')

```

```

plot([1 1],[mean(dYclV(Gindx))+std(dYclV(Gindx)) mean(dYclV(Gindx))-std(dYclV(Gindx))],'-+b')
plot([2 2],[mean(dYclV(DLTindx))+std(dYclV(DLTindx)) mean(dYclV(DLTindx))-std(dYclV(DLTindx))],'-+r')
plot([2 2],[mean(dYclV(DLindx))+std(dYclV(DLindx)) mean(dYclV(DLindx))-std(dYclV(DLindx))],'-+b')
plot([3 3],[mean(dYclV(DHTindx))+std(dYclV(DHTindx)) mean(dYclV(DHTindx))-std(dYclV(DHTindx))],'-+r')
plot([3 3],[mean(dYclV(DHindx))+std(dYclV(DHindx)) mean(dYclV(DHindx))-std(dYclV(DHindx))],'-+b')
axis([.5 3.5 0 a(4)]);gridylabel('RMS Error')title('Y Error Rate - Simulated Trials')xlabel('GVE DVEL DVEH')
figure(3) clf subplot(121) plot([1 2 3],[mean(PV(Gindx)) mean(PV(DLindx)) mean(PV(DHindx))], '-ob')
hold on plot([1 2 3],[mean(PV(GTindx)) mean(PV(DLTindx)) mean(PV(DHTindx))], '-sr')
plot([1 1],[mean(PV(GTindx))+std(PV(GTindx)) mean(PV(GTindx))-std(PV(GTindx))],'-+r')
plot([1 1],[mean(PV(Gindx))+std(PV(Gindx)) mean(PV(Gindx))-std(PV(Gindx))],'-+b')
plot([2 2],[mean(PV(DLTindx))+std(PV(DLTindx)) mean(PV(DLTindx))-std(PV(DLTindx))],'-+r')
plot([2 2],[mean(PV(DLindx))+std(PV(DLindx)) mean(PV(DLindx))-std(PV(DLindx))],'-+b')
plot([3 3],[mean(PV(DHTindx))+std(PV(DHTindx)) mean(PV(DHTindx))-std(PV(DHTindx))],'-+r')
plot([3 3],[mean(PV(DHindx))+std(PV(DHindx)) mean(PV(DHindx))-std(PV(DHindx))],'-+b')
a=axis;grid axis([.5 3.5 0 a(4)]);ylabel('RMS Error')title('Pitch Error - Actual Trials')xlabel('GVE DVEL DVEH')
subplot(122) plot([1 2 3],[mean(PclV(Gindx)) mean(PclV(DLindx)) mean(PclV(DHindx))], '-ob')
hold on plot([1 2 3],[mean(PclV(GTindx)) mean(PclV(DLTindx)) mean(PclV(DHTindx))], 'sr')
plot([1 1],[mean(PclV(GTindx))+std(PclV(GTindx)) mean(PclV(GTindx))-std(PclV(GTindx))],'-+r')
plot([1 1],[mean(PclV(Gindx))+std(PclV(Gindx)) mean(PclV(Gindx))-std(PclV(Gindx))],'-+b')
plot([2 2],[mean(PclV(DLTindx))+std(PclV(DLTindx)) mean(PclV(DLTindx))-std(PclV(DLTindx))],'-+r')
plot([2 2],[mean(PclV(DLindx))+std(PclV(DLindx)) mean(PclV(DLindx))-std(PclV(DLindx))],'-+b')
plot([3 3],[mean(PclV(DHTindx))+std(PclV(DHTindx)) mean(PclV(DHTindx))-std(PclV(DHTindx))],'-+r')
plot([3 3],[mean(PclV(DHindx))+std(PclV(DHindx)) mean(PclV(DHindx))-std(PclV(DHindx))],'-+b')
axis([.5 3.5 0 a(4)])ylabel('RMS Error')title('Pitch Error - Simulated Trials')xlabel('GVE DVEL DVEH')grid
figure(4) clf subplot(121)
plot([1 2 3],[mean(dPV(Gindx)) mean(dPV(DLindx)) mean(dPV(DHindx))], '-ob') hold on
plot([1 2 3],[mean(dPV(GTindx)) mean(dPV(DLTindx)) mean(dPV(DHTindx))], '-sr')
plot([1 1],[mean(dPV(GTindx))+std(dPV(GTindx)) mean(dPV(GTindx))-std(dPV(GTindx))],'-+r')
plot([1 1],[mean(dPV(Gindx))+std(dPV(Gindx)) mean(dPV(Gindx))-std(dPV(Gindx))],'-+b')
plot([2 2],[mean(dPV(DLTindx))+std(dPV(DLTindx)) mean(dPV(DLTindx))-std(dPV(DLTindx))],'-+r')
plot([2 2],[mean(dPV(DLindx))+std(dPV(DLindx)) mean(dPV(DLindx))-std(dPV(DLindx))],'-+b')
plot([3 3],[mean(dPV(DHTindx))+std(dPV(DHTindx)) mean(dPV(DHTindx))-std(dPV(DHTindx))],'-+r')
plot([3 3],[mean(dPV(DHindx))+std(dPV(DHindx)) mean(dPV(DHindx))-std(dPV(DHindx))],'-+b')
a=axis;gridaxis([.5 3.5 0 a(4)]);ylabel('RMS Error')title('Pitch Rate Error - Actual Trials')xlabel('GVE DVEL DVEH')
subplot(122)
plot([1 2 3],[mean(dPclV(Gindx)) mean(dPclV(DLindx)) mean(dPclV(DHindx))], '-ob')
hold on
plot([1 2 3],[mean(dPclV(GTindx)) mean(dPclV(DLTindx)) mean(dPclV(DHTindx))], '-sr')
plot([1 1],[mean(dPclV(GTindx))+std(dPclV(GTindx)) mean(dPclV(GTindx))-std(dPclV(GTindx))],'-+r')
plot([1 1],[mean(dPclV(Gindx))+std(dPclV(Gindx)) mean(dPclV(Gindx))-std(dPclV(Gindx))],'-+b')
plot([2 2],[mean(dPclV(DLTindx))+std(dPclV(DLTindx)) mean(dPclV(DLTindx))-std(dPclV(DLTindx))],'-+r')
plot([2 2],[mean(dPclV(DLindx))+std(dPclV(DLindx)) mean(dPclV(DLindx))-std(dPclV(DLindx))],'-+b')
plot([3 3],[mean(dPclV(DHTindx))+std(dPclV(DHTindx)) mean(dPclV(DHTindx))-std(dPclV(DHTindx))],'-+r')
plot([3 3],[mean(dPclV(DHindx))+std(dPclV(DHindx)) mean(dPclV(DHindx))-std(dPclV(DHindx))],'-+b')

```

```

axis([.5 3.5 0 a(4)])ylabel('RMS Error')title('Pitch Rate Error - Simulated Trials')xlabel('GVE DVEL
DVEH')grid
figure(5) clf subplot(121)
plot([1 2 3],[mean(ElevV(Gindx)) mean(ElevV(DLindx)) mean(ElevV(DHindx))], '-ob')
hold on
plot([1 2 3],[mean(ElevV(GTindx)) mean(ElevV(DLTindx)) mean(ElevV(DHTindx))], 'sr')
plot([1 1],[mean(ElevV(GTindx))+std(ElevV(GTindx)) mean(ElevV(GTindx))-std(ElevV(GTindx))], '-+r')
plot([1 1],[mean(ElevV(Gindx))+std(ElevV(Gindx)) mean(ElevV(Gindx))-std(ElevV(Gindx))], '-+b')
plot([2 2],[mean(ElevV(DLTindx))+std(ElevV(DLTindx)) mean(ElevV(DLTindx))-
std(ElevV(DLTindx))], '-+r')
plot([2 2],[mean(ElevV(DLindx))+std(ElevV(DLindx)) mean(ElevV(DLindx))-std(ElevV(DLindx))], '-+b')
plot([3 3],[mean(ElevV(DHTindx))+std(ElevV(DHTindx)) mean(ElevV(DHTindx))-
std(ElevV(DHTindx))], '-+r')
plot([3 3],[mean(ElevV(DHindx))+std(ElevV(DHindx)) mean(ElevV(DHindx))-std(ElevV(DHindx))], '-
+b')
a=axis;gridaxis([.5 3.5 0 a(4)]);ylabel('RMS Elevator Signal')title('Elevator - Actual Trials')xlabel('GVE
DVEL DVEH')
subplot(122)
plot([1 2 3],[mean(ElevclV(Gindx)) mean(ElevclV(DLindx)) mean(ElevclV(DHindx))], '-ob')
hold on
plot([1 2 3],[mean(ElevclV(GTindx)) mean(ElevclV(DLTindx)) mean(ElevclV(DHTindx))], '-sr')
plot([1 1],[mean(ElevclV(GTindx))+std(ElevclV(GTindx)) mean(ElevclV(GTindx))-
std(ElevclV(GTindx))], '-+r')
plot([1 1],[mean(ElevclV(Gindx))+std(ElevclV(Gindx)) mean(ElevclV(Gindx))-std(ElevclV(Gindx))], '-
+b')
plot([2 2],[mean(ElevclV(DLTindx))+std(ElevclV(DLTindx)) mean(ElevclV(DLTindx))-
std(ElevclV(DLTindx))], '-+r')
plot([2 2],[mean(ElevclV(DLindx))+std(ElevclV(DLindx)) mean(ElevclV(DLindx))-
std(ElevclV(DLindx))], '-+b')
plot([3 3],[mean(ElevclV(DHTindx))+std(ElevclV(DHTindx)) mean(ElevclV(DHTindx))-
std(ElevclV(DHTindx))], '-+r')
plot([3 3],[mean(ElevclV(DHindx))+std(ElevclV(DHindx)) mean(ElevclV(DHindx))-
std(ElevclV(DHindx))], '-+b')
axis([.5 3.5 0 a(4)])ylabel('RMS Elevator Signal')title('Elevator - Simulated Trials')xlabel('GVE DVEL
DVEH')grid

```

```

%% YAXIS_SIM_PLOT_LINEAR
%% This program will plot the PSD Data saved by Xaxis_MODELSSIMNonLinear
clear
wf=.01;
for i=2:70
    wf(i)=wf(i-1)*1.2;
end
cycles=[3 7 15 23 29 43 85 115 143 217 272 431];%% This is VOSS, not PVO
%% Set Datapath
loadpath='C:\KarlPhd\ExperimentsFall2004\Data';
eval(['addpath ',loadpath]);
CONDTSAS=[0 0 0 1 1 1 1 1 1 0 1 0 0;0 0 0 1 1 1 1 1 1 0 0 0;0 1 0 1 0 1 1 0 1 0 1 0;1 1 0 1 0 0 0 0 1 0 1 1;
1 1 1 0 0 0 0 0 1 1 1 1;1 0 1 0 1 0 0 1 0 1 0 1;0 0 1 0 1 1 1 1 0 1 0 0;0 0 0 1 1 1 1 1 1 0 0 0;...
0 1 0 1 0 1 1 0 1 0 1 0;1 1 0 1 0 0 0 0 1 0 1 1;1 1 1 0 0 0 0 0 1 1 1 1;1 0 1 0 1 0 0 1 0 1 0 1];
CONDVE=[0 1 2 2 1 0 0 1 2 2 1 0;1 2 0 0 2 1 1 2 0 0 2 1;2 0 1 1 0 2 2 0 1 1 0 2;0 1 2 2 1 0 0 1 2 2 1 0;...
1 2 0 0 2 1 1 2 0 0 2 1;2 0 1 1 0 2 2 0 1 1 0 2;0 1 2 2 1 0 0 1 2 2 1 0;1 2 0 0 2 1 1 2 0 0 2 1;...
2 0 1 1 0 2 2 0 1 1 0 2;0 1 2 2 1 0 0 1 2 2 1 0;1 2 0 0 2 1 1 2 0 0 2 1;2 0 1 1 0 2 2 0 1 1 0 2];
SUBJ='ABCDEFGHIJKL';
for j=1:12 % Subject
    CondTSAS=CONDTSAS(j,:); CondVE=CONDVE(j,:); Subj=SUBJ(j)
    GTindx=and(CondTSAS==1,CondVE==0); DLTindx=and(CondTSAS==1,CondVE==1);
    DHTindx=and(CondTSAS==1,CondVE==2);
    Gindx=and(CondTSAS==0,CondVE==0); DLindx=and(CondTSAS==0,CondVE==1);
    DHindx=and(CondTSAS==0,CondVE==2);
    eval(['load YAXISNonLinearMODELVOSSSubj',Subj,'PSDData.mat'])
    figure(1) clf
    semilogx(F*2*pi,20*log10(mean(abs(PSDElevcl))), 'g');
    hold on
    semilogx(F*2*pi,20*log10(mean(abs(PSDElev))), 'k');
    semilogx(F(cycles+1)*2*pi,20*log10(mean(abs(PSDElevcl(:,cycles+1)))), 'og')
    semilogx(F(cycles+1)*2*pi,20*log10(mean(abs(PSDElev(:,cycles+1)))), 'dk')
    eval(['title(["PSD of Eleveron Signal - Subject ",Subj])'])
    legend('Closed Loop Simulation','Actual Eleveron')
    figure(2) clf
    semilogx(F*2*pi,20*log10(mean(abs(PSDYcl))), 'g');
    hold on
    semilogx(F*2*pi,20*log10(mean(abs(PSDY))), 'k');
    semilogx(F(cycles+1)*2*pi,20*log10(mean(abs(PSDYcl(:,cycles+1)))), 'og')
    semilogx(F(cycles+1)*2*pi,20*log10(mean(abs(PSDY(:,cycles+1)))), 'dk')
    eval(['title(["PSD of X axis Error - Subject ",Subj])'])
    legend('Closed Loop Simulation','Actual X axis Error')
    figure(3) clf
    semilogx(F*2*pi,20*log10(mean(abs(PSDCLcl))), 'g');
    hold on
    semilogx(F*2*pi,20*log10(mean(abs(PSDCL))), 'k');
    semilogx(F(cycles+1)*2*pi,20*log10(mean(abs(PSDCLcl(:,cycles+1)))), 'og')
    semilogx(F(cycles+1)*2*pi,20*log10(mean(abs(PSDCL(:,cycles+1)))), 'dk')
    eval(['title(["PSD of Closed Loop - Subject ",Subj])'])
    legend('Closed Loop Simulation','Actual X axis Error')
    pause end

```

```

%% XAXIS_ESTIMATORCOMPARE
%% 1 July 2006
%% LCDR Karl U Schultz
%% This program constructs the entire model
%% and compares high and low noise estimator dynamics
clear
%% Define plant variables
g=9.81; Pfreq=3.0; Pdamp=.65; Pgain=500; Vydamp=4;
Rfreq=5; Rdamp=.4; Rgain=625; Vxdamp=4;
dt=.012; %% delta t for all trials
%% mass=1000; Not used
%% Basic plant
A=[-Vxdamp 0 0 g; 1 0 0 0; 0 0 -2*Rdamp*Rfreq -Rfreq^2; 0 0 1 0];
B=[0;0;Rgain;0];C=[eye(4)];D=zeros(4,1);E=[0;1;0;0];sys=ss(A,B,C,D);
%% Basic (to prevent overwriting
Cb=C;Db=D;
%% Basic plant with TSAS
AT=A;BT=B;CT=[C;0 1 0 0]; %%this includes the TSAS variable
DT=[D;0];sysT=ss(AT,BT,CT,DT);
%% DVE Plant (no roll signal available)
AD=A;BD=B;CD=[1 0 0 0;0 1 0 0];DD=[0;0];sysD=ss(AD,BD,CD,DD);
%% DVE Plant with TSAS
ADT=A;BDT=B;CDT=[CD;0 1 0 0];DDT=[DD;0];sysDT=ss(ADT,BDT,CDT,DDT);
%% Neuromuscular Model
wn=20;damp=.7;num2=[wn^2];den2=[1 2*damp*wn wn^2];lag=.1;sys2=tf(num2,den2);
den3=conv(den2,[lag 1]);sys3=tf(num2,den3);[Anm,Bnm,Cnm,Dnm]=tf2ss(num2,den3);
%% Generate the important frequencies
wf=.01;
for i=2:70
    wf(i)=wf(i-1)*1.2;
end
%% Set cycles for PVO
cycles=[2 5 11 17 19 29 59 79 97 143 183 287];
%% Set Datapath
loadpath='C:\KarlPhd\ExperimentsFall2004\Data';
eval(['addpath ',loadpath]);
CONDTSAS=[0 0 0 1 1 1 1 1 0 1 0 0;0 0 0 1 1 1 1 1 0 0 0;0 1 0 1 0 1 1 0 1 0 1 0;...
    1 1 0 1 0 0 0 1 0 1 1;1 1 1 0 0 0 0 0 1 1 1;1 0 1 0 1 0 0 1 0 1 0 1;...
    0 0 1 0 1 1 1 1 0 1 0 0;0 0 0 1 1 1 1 1 0 0 0;0 1 0 1 0 1 1 0 1 0 1 0;...
    1 1 0 1 0 0 0 1 0 1 1;1 1 1 0 0 0 0 0 1 1 1;1 0 1 0 1 0 0 1 0 1 0 1];
CONDVE=[0 1 2 2 1 0 0 1 2 2 1 0;1 2 0 0 2 1 1 2 0 0 2 1;2 0 1 1 0 2 2 0 1 1 0 2;...
    0 1 2 2 1 0 0 1 2 2 1 0;1 2 0 0 2 1 1 2 0 0 2 1;2 0 1 1 0 2 2 0 1 1 0 2;...
    0 1 2 2 1 0 0 1 2 2 1 0;1 2 0 0 2 1 1 2 0 0 2 1;2 0 1 1 0 2 2 0 1 1 0 2;...
    0 1 2 2 1 0 0 1 2 2 1 0;1 2 0 0 2 1 1 2 0 0 2 1;2 0 1 1 0 2 2 0 1 1 0 2];
SUBJ='ABCDEFGHIJKL';
eval(['load NMMModel_PVO_Avg']);
for j=1:12 % Subject
    CondTSAS=CONDTSAS(j,:); CondVE=CONDVE(j,:); Subj=SUBJ(j)
    for i=1:12
        eval(['load
c:\karlphd\experimentsfall2004\data\',Subj,num2str(CondTSAS(i)),num2str(CondVE(i)), 'T',num2str(i)];
        %% Parse Data
        eval(['data=',Subj,num2str(CondTSAS(i)),num2str(CondVE(i)), 'T',num2str(i),'']);
        eval(['clear ',Subj,num2str(CondTSAS(i)),num2str(CondVE(i)), 'T',num2str(i)];
        height=data(:,1); pitch=data(:,2); roll=data(:,3);
        x=data(:,4); y=data(:,5); z=data(:,6);

```

```

xd=data(:,7); yd=data(:,8); hd=data(:,12);
ud=data(:,9); vd=data(:,10); wd=data(:,11);
rd=data(:,14); pd=data(:,13);
deltat=data(:,15); lightness=data(:,16);
xdist=data(:,17); ydist=data(:,18);
time=data(:,19); rudder=data(:,20);
aileron=data(:,22); elevator=data(:,21);collective=data(:,23);
%%%% Define GVE, Xsition, and DVE
[crd,startlength]=min(abs(10-time));
[crd,gvelength]=min(abs(70-time));
[crd,xsitionlength]=min(abs(100-time));
[crd,totallength]=min(abs(190-time));
timeline=1; % PVO
        timeline=3; %VOSS
if timeline==1
    index1=startlength; index2=gvelength;
elseif timeline==2
    index1=gvelength; index2=xsitionlength;
else
    index1=xsitionlength; index2=totallength;
end
dt=abs(mean(time(1:length(time)-1)-time(2:length(time))));
T=time(index1:index2); Xdist=xdist(index1:index2); X=x(index1:index2);
dX=(xd(index1:index2)+xdist(index1:index2));
R=roll(index1:index2); dR=rd(index1:index2); Ail=aileron(index1:index2);
Ydist=ydist(index1:index2); Y=y(index1:index2); dY=(-yd(index1:index2)+ydist(index1:index2));
P=pitch(index1:index2); dP=pd(index1:index2); Elev=elevator(index1:index2);
T=T(1):dt:T(length(T)); minleng=min([length(T) length(Ail) length(X)]);
X=X(1:minleng); dX=dX(1:minleng); R=R(1:minleng); dR=dR(1:minleng); Xdist=Xdist(1:minleng);
T=T(1:minleng); Ail=Ail(1:minleng);
TSAS=zeros(size(X));
%%%% Calculate TSAS; TSASindxzero=abs(X)<=5;
TSASindx1=and(X>5,X<=10); TSASindx2=and(X>10,X<=20); TSASindx3=X>20;
TSASindxm1=and(X<-5,X>=-10); TSASindxm2=and(X<-10,X>=-20); TSASindxm3=X<-20;
TSAS(TSASindx1)=7.5*ones(size(TSAS(TSASindx1))); TSAS(TSASindxm1)=-
7.5*ones(size(TSAS(TSASindxm1)));
TSAS(TSASindx2)=15*ones(size(TSAS(TSASindx2))); TSAS(TSASindxm2)=-
15*ones(size(TSAS(TSASindxm2)));
TSAS(TSASindx3)=25*ones(size(TSAS(TSASindx3))); TSAS(TSASindxm3)=-
25*ones(size(TSAS(TSASindxm3)));
errorT=X-TSAS;
%%%% Determine the noise for each state
if or((CondVE(i)==0),(timeline==1));
    errorX=.1371*abs(X); errordX=.2551*abs(dX);
    errorRoll=.2229*abs(R); errordRoll=.45*abs(dR)/2;
elseif CondVE(i)==1;
    errorX=.1371*abs(X)*1.5; errordX=.2551*abs(dX)*1.5;
    errorRoll=.2229*abs(R)*1.5; errordRoll=.45*abs(dR)*1.5/2;
else
    errorX=(.2287*abs(X)+.1810); errordX=(.45*abs(dX)+.36);
    errorRoll=.2229*abs(R); errordRoll=.45*abs(dR);
end
for tenruns=1:3
    randx=randn(size(errorX)); randdx=randn(size(errordX));
    randr=randn(size(errorRoll)); randdr=randn(size(errordRoll));
    noisescale=1;

```

```

noiseX=errorX.*randx*noisescale; noisedX=errorDX.*randdx*noisescale;
noiseR=errorRoll.*randr*noisescale; noisedR=errordRoll.*randdr*noisescale;
noiseT=errorT; %this is the real error. Do NOT Scale
w=Xdist; vu=randn(size(Ail)).*abs(Ail)*.3; %%%This helps match PSD (deltaNL) against PSD(Ail)
%%%%% Check the visual and tactile conditions
if CondTSAS(i)==0
    if and(timeline>1,CondVE(i)==2)
        C=CD; D=DD; outs=2;vy=[noisedX noiseX];% noisedR noiseR];
    else
        C=Cb; D=Db; outs=4;vy=[noisedX noiseX noisedR noiseR];
    end
else %TSAS on
    if and(timeline>1,CondVE(i)==2)
        C=CDT; D=DDT; outs=3;vy=[noisedX noiseX noiseT];%noiseR noiseR noiseT];
    else
        C=CT; D=DT; outs=5;vy=[noisedX noiseX noisedR noiseR noiseT];
    end
end
Vy=diag(mean(abs(vy)));W1=diag([mean(abs(Xdist)) mean(abs(vu))]);
%%%%%% Neuromuscular Term
eval(['Sysc=Sys3',Subj,',';]);
eval(['Sysc=Sys1',Subj,',';]); eval(['[Ac,Bc,Cc,Dc]=ssdata(Sysc);'])
Sysc=ss(Ac,Bc,Cc,Dc); Sysnm=ss(Anm,Bnm,Cnm,Dnm); Cnl=eye(1);
%%%% Complete Term
A1=[A B*Cnm zeros(4,3);zeros(3,4) Anm Bnm*Cnl*Cc;zeros(3,4) zeros(3,3) Ac];
B1=[zeros(4,1);Bnm*Cnl*Dc;Bc]; C1=[C zeros(outs,3) zeros(outs,3)];
D1=[zeros(outs,1)];Sys1=ss(A1,B1,C1,D1);
E1=[E B zeros(4,out);zeros(3,1) zeros(3,1) zeros(3,out);zeros(3,1) zeros(3,1) zeros(3,out)];
Q=[0 0 0 0;0 1 0 0;0 0 0 0;0 0 0 0];
Q1=[Q zeros(4,3) zeros(4,3);zeros(3,4) zeros(3,3) zeros(3,3);zeros(3,4) zeros(3,3) zeros(3,3)];
R1=10^-10;
[K,Scrd,Ecrd]=lqr(A,B,Q,R1); Syscl=ss(A-B*K,E,C,D); %Plant Only
[K1,Scrd,Ecrd]=lqr(A1,B1,Q1,R1);
Sys1e=ss(A1,[B1 [E B;zeros(3,1) zeros(3,1);zeros(3,1) zeros(3,1)]],C1,[D1 zeros(outs,1)
zeros(outs,1)]); %Open Loop
Sys1cl=ss(A1-B1*K1,E1,C1,[zeros(outs,1) zeros(outs,1) eye(outs)]); %Closed Loop no Est
[Kest,L1,P]=kalman(Sys1e,W1,Vy); %%%
ANLol=[A1-L1*C1-B1*K1 L1*C zeros(10,3);...
zeros(4,10) A zeros(4,3);...
-Bc*K1 zeros(3,4) Ac];
BNLol=[zeros(10,1);B;zeros(3,1)];
ENLol=[zeros(10,1) zeros(10,1) L1;...
E B zeros(4,out);...
zeros(3,1) zeros(3,1) zeros(3,out)];
BNLcl=[BNLol ENLol];CNLcl=[-Dc*K1 zeros(1,4) Cc];
DNLcl=[zeros(1,1) zeros(1,1) zeros(1,1) zeros(1,out)];
SYSNLol=ss(ANLol,BNLol,CNLcl,DNLcl);
SYSol=ss(A,[B E],C,[D D]);
siminput=[Ail w];
[Yol,Tol,Xol]=lsim(SYSol,siminput,T-T(1));
ANLcl=[A1-L1*C1-B1*K1 L1*C1;-B1*K1 A1];
BNLcl=[zeros(10,1) zeros(10,1) L1;E1];
CNLcl=[zeros(1,10) 0 1 0 0 zeros(1,3) zeros(1,3)];
DNLcl=[zeros(1,1) zeros(1,1) zeros(1,out)];
SYSNcl=ss(ANLcl,BNLcl,CNLcl,DNLcl);
siminput=[w vu vy];

```



```

[YNLcl,TNLcl,XNLcl]=lsim(SYSNLcl,siminput,T-T(1));
Ailcl=Cnm*XNLcl(:,15:17)'+vu';
Uc=-K1*XNLcl(:,1:10)'; Uact=-K*XNLcl(:,11:14)';
[m,p]=bode(SYSNLcl(1),wf);
for mm=1:length(m)
    MAG(mm)=m(1,1,mm); PHS(mm)=p(1,1,mm);
end
if and(CondTSAS(i)==0,CondVE(i)==2)
    SYSDVE=SYSNLcl;
elseif and(CondTSAS(i)==1,CondVE(i)==0)
    SYSGVE=SYSNLcl;
end
end % tenruns

end %%% i (trials)
[mg,pg]=bode(SYSGVE(1),wf);
[md,pd]=bode(SYSDVE(1),wf);
for crd=1:length(mg)
    Mg(crd)=mg(1,1,crd);Pg(crd)=pg(1,1,crd);Md(crd)=md(1,1,crd);Pd(crd)=pd(1,1,crd);
end
figure(1)
clf
subplot(211)
semilogx(wf,20*log10(Mg),'g','Linewidth',1)
hold on
semilogx(wf,20*log10(Md),'r','Linewidth',3)
grid
ylabel('Magnitude (dB)')
xlabel('Frequency (rad/sec)')
title('Effect of Noise on Estimator and Closed Loop Bode Plot')
legend('Good Visual Environment Closed Loop','Degraded Visual Environment Closed Loop')
subplot(212)
semilogx(wf,unwrap(Pg)*180/pi,'g','Linewidth',1)
hold on
semilogx(wf,unwrap(Pd)*180/pi,'r','Linewidth',3)
grid
ylabel('Frequency (rad/sec)')
xlabel('Phase (degrees)')
figure(2)
clf
plot(pole(SYSGVE(1)),'x','Markersize',10,'Linewidth',2)
hold on
plot(zero(SYSGVE(1)),'ob','Markersize',10,'Linewidth',2)
plot(pole(SYSDVE(1)),'+r','Markersize',10)
plot(zero(SYSDVE(1)),'sr','Markersize',10)
grid
ylabel('Imaginary Axis')
xlabel('Real Axis')
title('Poles and Zeros of Closed Loop System - GVE and DVE')
legend('GVE Closed Loop Poles','GVE Closed Loop Zeros','DVE Closed Loop Poles','DVE Closed Loop
Zeros')
string=['Done with Subj ',Subj]
beep
pause
end % j Subject)

```

```

%% XAXIS_MODEL_REVIEW
%% 11 June 2006
%% LCDR Karl U Schultz
%% This program will summarize the model parts, assumptions, and performance.
clear
%% Define plant variables
g=9.81; Pfreq=3.0; Pdamp=.65; Pgain=500; Vydamp=4;
dt=.012; %% delta t for all trials
%% Basic plant
A=[-Vydamp 0 0 g; 1 0 0 0; 0 0 -2*Pdamp*Pfreq -Pfreq^2; 0 0 1 0];
B=[0;0;Pgain;0];E=[0;1;0;0];C=[eye(4)];D=zeros(4,1);sys=ss(A,B,C,D);
%% Basic plant with TSAS
AT=A;BT=B;CT=[C;0 1 0 0]; %%this includes the TSAS variable
DT=[D;0];sysT=ss(AT,BT,CT,DT);
%% DVE Plant (no roll signal available)
AD=A;BD=B;CD=[1 0 0 0; 0 1 0 0];DD=[0;0];sysD=ss(AD,BD,CD,DD);
%% DVE Plant with TSAS
ADT=A;BDT=B;CDT=[CD;0 1 0 0];DDT=[DD;0];sysDT=ss(ADT,BDT,CDT,DDT);
%% Generate the important frequencies
w=.01;
for i=2:70
    w(i)=w(i-1)*1.2;
end
%% Set Datapath
loadpath='C:\KarlPhd\ExperimentsFall2004\Data';
eval(['addpath ',loadpath]);
CONDTSAS=[0 0 0 1 1 1 1 1 0 1 0 0;0 0 0 1 1 1 1 1 0 0 0;0 1 0 1 0 1 1 0 1 0 1 0;...
    1 1 0 1 0 0 0 0 1 0 1 1;1 1 1 0 0 0 0 0 0 1 1 1;1 0 1 0 1 0 0 1 0 1 0 1;...
    0 0 1 0 1 1 1 1 0 1 0 0;0 0 0 1 1 1 1 1 1 0 0 0;0 1 0 1 0 1 1 0 1 0 1 0;...
    1 1 0 1 0 0 0 0 1 0 1 1;1 1 1 0 0 0 0 0 0 1 1 1;1 0 1 0 1 0 0 1 0 1 0 1];
CONDVE=[0 1 2 2 1 0 0 1 2 2 1 0;1 2 0 0 2 1 1 2 0 0 2 1;2 0 1 1 0 2 2 0 1 1 0 2;...
    0 1 2 2 1 0 0 1 2 2 1 0;1 2 0 0 2 1 1 2 0 0 2 1;2 0 1 1 0 2 2 0 1 1 0 2;...
    0 1 2 2 1 0 0 1 2 2 1 0;1 2 0 0 2 1 1 2 0 0 2 1;2 0 1 1 0 2 2 0 1 1 0 2;...
    0 1 2 2 1 0 0 1 2 2 1 0;1 2 0 0 2 1 1 2 0 0 2 1;2 0 1 1 0 2 2 0 1 1 0 2];
SUBJ='ABCDEFGHIJKL';
j=1; %%subject A
BL=[]; DVEL=[]; DVEH=[]; TSAS=[]; TDVEL=[]; TDVEH=[];
Gain=[]; Den=[]; Num=[]; Delay=[]; Data=[]; FIT=[];
FIT1=[]; FIT2=[]; FIT3=[]; ERR1=[]; ERR2=[]; ERR3=[];
CondTSAS=CONDTSAS(j,:); CondVE=CONDVE(j,:); Subj=SUBJ(j)
NUM1=[]; DEL1=[]; DEN1=[]; GAIN1=[];
NUM2=[]; DEL2=[]; DEN2=[]; GAIN2=[];
NUM3=[]; DEL3=[]; DEN3=[]; GAIN3=[];
i=1; %%trial #1
eval(['load
c:\karlphd\experimentsfall2004\data\',Subj,num2str(CondTSAS(i)),num2str(CondVE(i)),T',num2str(i)]);
%% Parse Data
eval(['data=',Subj,num2str(CondTSAS(i)),num2str(CondVE(i)),T',num2str(i),''];]);
eval(['clear ',Subj,num2str(CondTSAS(i)),num2str(CondVE(i)),T',num2str(i)]);
height=data(:,1); pitch=data(:,2); roll=data(:,3);
x=data(:,4); y=data(:,5); z=data(:,6);
xd=data(:,7); yd=data(:,8); hd=data(:,12);
ud=data(:,9); vd=data(:,10); wd=data(:,11);
rd=data(:,14); pd=data(:,13);
deltat=data(:,15); lightness=data(:,16);
xdist=data(:,17); ydist=data(:,18);

```

```

time=data(:,19); rudder=data(:,20);
aileron=data(:,22); elevator=data(:,21);collective=data(:,23);
%%%% Define GVE, Xsition, and DVE
[crd,startlength]=min(abs(10-time));
[crd,gvelength]=min(abs(70-time));
[crd,xsitionlength]=min(abs(100-time));
[crd,totallength]=min(abs(190-time));
timeline=1; %PVO
if timeline==1
    index1=startlength; index2=gvelength;
elseif timeline==2
    index1=gvelength; index2=xsitionlength;
else
    index1=xsitionlength; index2=totallength;
end
dt=abs(mean(time(1:length(time)-1)-time(2:length(time))));
T=time(index1:index2);Xdist=xdist(index1:index2);
X=x(index1:index2);dX=(xd(index1:index2)+xdist(index1:index2));
R=roll(index1:index2);dR=rd(index1:index2);
Ail=aileron(index1:index2);
Ydist=ydist(index1:index2);
Y=y(index1:index2);dY=(-yd(index1:index2)+ydist(index1:index2));
P=pitch(index1:index2);dP=pd(index1:index2);
Elev=elevator(index1:index2);T=T(1):dt:T(length(T));
minleng=min([length(T) length(Ail) length(X)]);
X=X(1:minleng);dX=dX(1:minleng);R=R(1:minleng);dR=dR(1:minleng);
Xdist=Xdist(1:minleng);T=T(1:minleng);Ail=Ail(1:minleng);

cycles=[2 5 11 17 19 29 59 79 97 143 183 287];
freqs=(cycles*2*pi)/60;
%%%% Calculate Models using actual and estimated data
Q=[0 0 0 0;0 1 0 0;0 0 0 0;0 0 0 0];
Rr=1*10000;
[K,Scrd,Ecrd]=lqr(A,B,Q,Rr);KHigh=K;
%%%% Optimal Feedback, no Estimator
%% closed loop, High control cost
[Twy,F]=tfe(Xdist, X,length(X),1/dt);
Acl=[A-B*K];Bcl=E;Ccl=[0 1 0 0];Dcl=0;Syscl=ss(Acl,Bcl,Ccl,Dcl);
[Magcrd,Phasecrd]=bode(Syscl,w);
for BOD=1:length(Magcrd);
    Mag(BOD)=Magcrd(1,1,BOD); Phase(BOD)=Phasecrd(1,1,BOD);
end
figure(1)
clf
subplot(211)
semilogx(F*2*pi,20*log10(abs(Twy)), 'r', 'LineWidth', 2)
hold on
semilogx(w,20*log10(Mag), 'b');
semilogx(F*(cycles+1)*2*pi,20*log10(abs(Twy*(cycles+1))), '*r')
grid
title('Bode plot of Experimental Data and Solved Optimal Gain Closed Loop Model - High Control Cost')
legend('Experimental Transfer Function','Solved Closed Loop System','Experimental Transfer Function at Disturbance Freqs')
xlabel('Frequency (rad/sec)')
ylabel('Magnitude (dB)')
subplot(212)

```

```

semilogx(F*2*pi,unwrap(angle(Twy)), 'r', 'LineWidth', 2)
hold on
semilogx(w, (Phase), ':b');
grid
ylabel('Angle (degrees)')
xlabel('Frequency (rad/sec)')
[Y, T, XstateHigh] = lsim(Syscl, Xdist, T);
figure(2)
clf
plot(T, Xdist, 'k', 'LineWidth', 2)
hold on
plot(T, X, ':r')
plot(T, Y, '--b')
grid
legend('Disturbance', 'Measured Lateral Axis Position Error', 'Linear Model Calculated Position Error')
title('Time Domain Plot of Measured Data and Linear Optimal Gain Closed Loop Model - High Control Cost')
xlabel('Time (sec)')
ylabel('Position Error (m)')
SysclHigh = Syscl;
%% Calculate Models using actual and estimated data
Q = [0 0 0 0; 0 1 0 0; 0 0 0 0; 0 0 0 0];
Rr = 1/100000;
[K, Scrd, Ecrd] = lqr(A, B, Q, Rr); K = K*(Rr); KLow = K;
%% Optimal Feedback, no Estimator
%% closed loop, low control cost
[Twy, F] = tfe(Xdist, X, length(X), 1/dt);
Acl = [A - B*K]; Bcl = E; Ccl = [0 1 0 0]; Dcl = 0; Syscl = ss(Acl, Bcl, Ccl, Dcl);
[Magcrd, Phasecrd] = bode(Syscl, w);
for BOD = 1:length(Magcrd);
    Mag(BOD) = Magcrd(1, 1, BOD); Phase(BOD) = Phasecrd(1, 1, BOD);
end
figure(3)
clf
subplot(211)
semilogx(F*2*pi, 20*log10(abs(Twy)), 'r', 'LineWidth', 2)
hold on
semilogx(w, 20*log10(Mag), ':b', 'LineWidth', 2);
semilogx(F(cycles+1)*2*pi, 20*log10(abs(Twy(cycles+1))), '*r')
grid
title('Bode plot of Experimental Data and Solved Optimal Gain Closed Loop Model - Low Control Cost')
legend('Experimental Transfer Function', 'Solved Closed Loop System', 'Experimental Transfer Function at Disturbance Freqs')
xlabel('Frequency (rad/sec)')
ylabel('Magnitude (dB)')
subplot(212)
semilogx(F*2*pi, unwrap(angle(Twy)), 'r', 'LineWidth', 2)
hold on
semilogx(w, (Phase), ':b', 'LineWidth', 2);
grid
ylabel('Angle (degrees)')
xlabel('Frequency (rad/sec)')
%% simulate closed loop output (State X)
[Y, T, XstateLow] = lsim(Syscl, Xdist, T);
figure(4)
clf

```

```

plot(T,(-K*[dX X dR R])*3,'k','LineWidth',2)
hold on
plot(T,Ail,':r','LineWidth',2)
%plot(T,Y,'--b','LineWidth',2)
grid
legend('Optimal Feedback Signal','Actual Aileron Signal')
title('Time Domain Plot of Measured Data and Linear Optimal Gain Closed Loop Model - Low Control
Cost')
SysclLow=Syscl;
xlabel('Time (sec)')
ylabel('Aileron Signal')
XX=[dX X dR R]; %remove +Xdist since reconstruction is of true dynamics (Xdist already added)
ULow=-KLow*XX;UHigh=-KHigh*XX'
wn=20;damp=0.7; % From Hess
num2=[wn^2];den2=[1 2*damp*wn wn^2];lag=.1;sys2=tf(num2,den2);
[Y2Low,Ttemp,state2]=lsim(sys2,ULow,T);
[Y2High,Ttemp,state2]=lsim(sys2,UHigh,T);
den3=conv(den2,[lag 1]);sys3=tf(num2,den3);
[Y3Low,Ttemp,state3]=lsim(sys3,ULow,T);
[Y3High,Ttemp,state3]=lsim(sys3,UHigh,T);
DATA2Low=iddata(Ail,ULow',dt);DATA2High=iddata(Ail,Y2High,dt);DATA3Low=iddata(Ail,Y3Low,dt);
guess=[.1 1 4 .01/max(K)]; %%delay num den gain
aux=0; %crd that I don't understand
global num den delay gain
InitialGuess=idgrey('PilotParam',guess,'cd',aux,0);
MODELLow=pem(DATA2Low,InitialGuess);
MODELLow1=n4sid(DATA2Low,1,'Ts',0);
MODELLow2=n4sid(DATA2Low,2,'Ts',0);
MODELLow3=n4sid(DATA2Low,3,'Ts',0);
Num=conv([1 -6/delay 12/delay^2],[1 num])*gain;
Den=conv([1 6/delay 12/delay^2],[1 den]);
[A1,B1,C1,D1]=tf2ss(Num,Den);
SysLow=idss(A1,B1,C1,D1,'Ts',0);
[TLowuail,F]=TFE(ULow,Ail,length(Ail),1/dt);
Aileron=DATA2Low;Structured=MODELLow;FirstOrderUnstruc=MODELLow1;
SecondOrderUnstruc=MODELLow2;ThirdOrderUnstruc=MODELLow3;
figure(11)
clf
compare(Aileron,Structured,FirstOrderUnstruc,SecondOrderUnstruc,ThirdOrderUnstruc)
MODEL2Low=pem(DATA2High,InitialGuess);
Num=conv([1 -6/delay 12/delay^2],[1 num])*gain;
Den=conv([1 6/delay 12/delay^2],[1 den]);
Num=Num*wn^2;Den=conv(Den,den2);[A2,B2,C2,D2]=tf2ss(Num,Den);
Sys2Low=idss(A2,B2,C2,D2,'Ts',0);
MODEL3Low=pem(DATA3Low,InitialGuess);
Num=conv([1 -6/delay 12/delay^2],[1 num])*gain;
Den=conv([1 6/delay 12/delay^2],[1 den]);
Num=Num*wn^2;Den=conv(Den,den3);[A3,B3,C3,D3]=tf2ss(Num,Den);
Sys3Low=idss(A3,B3,C3,D3,'Ts',0);
DATA2High=iddata(Ail,UHigh',dt);DATA3High=iddata(Ail,Y3High,
dt);
guess=[.1 1 4 .01/max(K)]; %%delay num den gain
aux=0; %crd that I don't understand
global num den delay gain
InitialGuess=idgrey('PilotParam',guess,'cd',aux,0);
[THighuail,F]=TFE(UHigh,Ail,length(Ail),1/dt);

```

```

MODELHigh=pem(DATAHigh,InitialGuess);
Num=conv([1 -6/delay 12/delay^2],[1 num])*gain;
Den=conv([1 6/delay 12/delay^2],[1 den]);
[A1,B1,C1,D1]=tf2ss(Num,Den);
SysHigh=idss(A1,B1,C1,D1,'Ts',0);
MODEL2High=pem(DATA2High,InitialGuess);
Num=conv([1 -6/delay 12/delay^2],[1 num])*gain;
Den=conv([1 6/delay 12/delay^2],[1 den]);
Num=Num*wn^2;Den=conv(Den,den2);[A2,B2,C2,D2]=tf2ss(Num,Den);
Sys2High=idss(A2,B2,C2,D2,'Ts',0);
MODEL3High=pem(DATA3High,InitialGuess);
Num=conv([1 -6/delay 12/delay^2],[1 num])*gain;
Den=conv([1 6/delay 12/delay^2],[1 den]);
Num=Num*wn^2;Den=conv(Den,den3);[A3,B3,C3,D3]=tf2ss(Num,Den);
Sys3High=idss(A3,B3,C3,D3,'Ts',0);
cycles=[2 5 11 17 19 29 59 79 97 143 183 287];
%cycles=[3 7 15 23 29 43 85 115 143 217 272 431];
freqs=cycles/60*2*pi;
[MAG1,PH1]=bode(SysLow,freqs);[MAG2,PH2]=bode(Sys2Low,freqs);[MAG3,PH3]=bode(Sys3Low,freqs);
for mag=1:length(MAG1)
    Mag1Low(mag)=MAG1(1,1,mag); Mag2Low(mag)=MAG2(1,1,mag);
    Mag3Low(mag)=MAG3(1,1,mag);
end
Err1=sum(abs(20*log10(Mag1Low')-20*log10(TLowuail(cycles+1))))
Err2=sum(abs(20*log10(Mag2Low')-20*log10(TLowuail(cycles+1))))
Err3=sum(abs(20*log10(Mag3Low')-20*log10(TLowuail(cycles+1))))
[MAG1,PH1]=bode(SysHigh,freqs);[MAG2,PH2]=bode(Sys2High,freqs);[MAG3,PH3]=bode(Sys3High,freqs);
for mag=1:length(MAG1)
    Mag1High(mag)=MAG1(1,1,mag); Mag2High(mag)=MAG2(1,1,mag);
    Mag3High(mag)=MAG3(1,1,mag);
end
Err1=sum(abs(20*log10(Mag1High')-20*log10(THighuail(cycles+1))))
Err2=sum(abs(20*log10(Mag2High')-20*log10(THighuail(cycles+1))))
Err3=sum(abs(20*log10(Mag3High')-20*log10(THighuail(cycles+1))))
figure(5)
clf
[m1,p1]=bode(SysLow,w);[m2,p2]=bode(Sys2Low,w);[m3,p3]=bode(Sys3Low,w);
for crd=1:length(m1);
    M1(crd)=m1(1,1,crd); M2(crd)=m2(1,1,crd); M3(crd)=m3(1,1,crd);
    P1(crd)=p1(1,1,crd); P2(crd)=p2(1,1,crd); P3(crd)=p3(1,1,crd);
end
bode(SysLow,Sys2Low,Sys3Low,w);%,SysHigh,Sys2High,Sys3High,w)
hold on
grid
semilogx(F(cycles+1)*2*pi,unwrap(angle(TLowuail(cycles+1)))*180/pi,'ob')
semilogx(F*2*pi,unwrap(angle(TLowuail))*180/pi,'b')
subplot(211)
hold on
grid
a=axis;
axis([a(1:2) 10^-1 10^6])
loglog(F(cycles+1)*2*pi,(abs(TLowuail(cycles+1))),'ob')
loglog(F*2*pi,(abs(TLowuail)), 'b:')
loglog(freqs,Mag3Low,'sr')

```

```

loglog(freqs,Mag2Low,'*g')
loglog(freqs,Mag1Low,'*b')
loglog(w,(abs(M3)),':r','Linewidth',3)
loglog(w,abs(M2),'--g','Linewidth',2)
ylabel('Magnitude (dB)')
legend('Modeled TF - No NM Model','Modeled TF - 2nd Order NM Model','Modeled TF - 3rd Order NM
Model','Actual TF at Disturbance Freqs','Actual TF - All Freqs','No NM Model - Dist Freqs','2nd Order NM
Model - Dist Freqs','3rd Order NM Model - Dist Freqs')
figure(6)
clf
bode(SysHigh,Sys2High,Sys3High,w),%,SysHigh,Sys2High,Sys3High,w)
hold on
grid
semilogx(F*(cycles+1)*2*pi,unwrap(angle(THighuail(cycles+1)))*180/pi,'ob')
semilogx(F*2*pi,unwrap(angle(THighuail))*180/pi,'b')
subplot(211)
hold on
grid
loglog(F*(cycles+1)*2*pi,(abs(THighuail(cycles+1))),'ob')
loglog(F*2*pi,(abs(THighuail)),':b')
loglog(freqs,Mag3High,'*r')
loglog(freqs,Mag2High,'*g')
loglog(freqs,Mag1High,'*b')
legend('No NM Model','2nd Order NM Model','3rd Order NM Model','Actual TF at Disturbance
Freqs','Actual TF - All Freqs','No NM Model - Dist Freqs','2nd Order NM Model - Dist Freqs','3rd Order
NM Model - Dist Freqs')
figure(7)
clf
compare(DATAHigh,SysHigh,Sys2High,Sys3High)
figure(8)
clf
Aileron=DATAHigh;ZeroOrder=SysHigh;SecondOrder=Sys2High;ThirdOrder=Sys3High;
compare(Aileron,ZeroOrder,SecondOrder,ThirdOrder)
compare(DATAHigh,SysHigh,Sys2High,Sys3High)
%%%%%% Nonlinear part
Diff=ULow'-Ail;
bins=[-.5:.05:-.15 -.13:.02:.13 .15:.05:.5];
timecount=1; phasecount=1; cont=1;
status='Hold';
if Diff(2)==Diff(1)
    status='Hold';
elseif Diff(2)>Diff(1)
    status='MvUp';
else
    status='MvDn';
end
STATUS(phasecount,:)=Diff(1); STATNUM(phasecount)=1;
thresh=(max(Ail)-min(Ail))*0.0001; %
%%%%%%%%%%%%%%[start end deltat startDiff endDiff deltaDiff startAil
EndAil DiffAil
PHASE(phasecount,:)=timecount 0 0 Diff(timecount) 0 0 Ail(timecount) 0 0];
timecount=2;
looklen=1;
while cont==1
    if status == 'Hold'
        if abs(mean(Ail(timecount+1:timecount+looklen))-Ail(timecount))<=thresh

```

```

    % timecount=timecount+1;
elseif mean(Ail(timecount+1:timecount+looklen))>Ail(timecount)+thresh
    status='MvUp';
    PHASE(phasecount,2)=timecount;
    PHASE(phasecount,3)=PHASE(phasecount,2)-PHASE(phasecount,1);
    PHASE(phasecount,5)=Diff(timecount);
    PHASE(phasecount,6)=abs(Diff(PHASE(phasecount,1)))-abs(Diff(timecount));
    PHASE(phasecount,8)=Ail(timecount);
    PHASE(phasecount,9)=PHASE(phasecount,8)-PHASE(phasecount,7);
    phasecount=phasecount+1;
    PHASE(phasecount,:)= [timecount 0 0 Diff(timecount) 0 0 Ail(timecount) 0 0];
    STATUS(phasecount,:)= 'MvUp';
elseif mean(Ail(timecount+1:timecount+looklen))<Ail(timecount)-thresh
    status='MvDn';
    PHASE(phasecount,2)=timecount;
    PHASE(phasecount,3)=PHASE(phasecount,2)-PHASE(phasecount,1);
    PHASE(phasecount,5)=Diff(timecount);
    PHASE(phasecount,6)=abs(Diff(PHASE(phasecount,1)))-abs(Diff(timecount));
    PHASE(phasecount,8)=Ail(timecount);
    PHASE(phasecount,9)=PHASE(phasecount,8)-PHASE(phasecount,7);
    phasecount=phasecount+1;
    PHASE(phasecount,:)= [timecount 0 0 Diff(timecount) 0 0 Ail(timecount) 0 0];
    STATUS(phasecount,:)= 'MvDn';
end
elseif status=='MvUp'
    if mean(Ail(timecount+1:timecount+looklen))>Ail(timecount)+thresh
        % timecount=timecount+1;
    elseif abs(mean(Ail(timecount+1:timecount+looklen))-Ail(timecount))<=thresh
        status='Hold';
        PHASE(phasecount,2)=timecount;
        PHASE(phasecount,3)=PHASE(phasecount,2)-PHASE(phasecount,1);
        PHASE(phasecount,5)=Diff(timecount);
        PHASE(phasecount,6)=abs(Diff(PHASE(phasecount,1)))-abs(Diff(timecount));
        PHASE(phasecount,8)=Ail(timecount);
        PHASE(phasecount,9)=PHASE(phasecount,8)-PHASE(phasecount,7);
        phasecount=phasecount+1;
        PHASE(phasecount,:)= [timecount 0 0 Diff(timecount) 0 0 Ail(timecount) 0 0];
        STATUS(phasecount,:)= 'Hold';
    elseif mean(Ail(timecount+1:timecount+looklen))<Ail(timecount)-thresh
        status='MvDn';
        PHASE(phasecount,2)=timecount;
        PHASE(phasecount,3)=PHASE(phasecount,2)-PHASE(phasecount,1);
        PHASE(phasecount,5)=Diff(timecount);
        PHASE(phasecount,6)=abs(Diff(PHASE(phasecount,1)))-abs(Diff(timecount));
        PHASE(phasecount,8)=Ail(timecount);
        PHASE(phasecount,9)=PHASE(phasecount,8)-PHASE(phasecount,7);
        phasecount=phasecount+1;
        PHASE(phasecount,:)= [timecount 0 0 Diff(timecount) 0 0 Ail(timecount) 0 0];
        STATUS(phasecount,:)= 'MvDn';
    end
end
else
    if mean(Ail(timecount+1:timecount+looklen))<Ail(timecount)-thresh
        %timecount=timecount+1;
    elseif mean(Ail(timecount+1:timecount+looklen))>Ail(timecount)+thresh
        status='MvUp';
        PHASE(phasecount,2)=timecount;

```



```

    PHASE(phasecount,3)=PHASE(phasecount,2)-PHASE(phasecount,1);
    PHASE(phasecount,5)=Diff(timecount);
    PHASE(phasecount,6)=abs(Diff(PHASE(phasecount,1)))-abs(Diff(timecount));
    PHASE(phasecount,8)=Ail(timecount);
    PHASE(phasecount,9)=PHASE(phasecount,8)-PHASE(phasecount,7);
    phasecount=phasecount+1;
    PHASE(phasecount,:)=[timecount 0 0 Diff(timecount) 0 0 Ail(timecount) 0 0];
    STATUS(phasecount,:)= 'MvUp';
elseif abs(mean(Ail(timecount+1:timecount+looklen))-Ail(timecount))<=thresh
    status='Hold';
    PHASE(phasecount,2)=timecount;
    PHASE(phasecount,3)=PHASE(phasecount,2)-PHASE(phasecount,1);
    PHASE(phasecount,5)=Diff(timecount);
    PHASE(phasecount,6)=abs(Diff(PHASE(phasecount,1)))-abs(Diff(timecount));
    PHASE(phasecount,8)=Ail(timecount);
    PHASE(phasecount,9)=PHASE(phasecount,8)-PHASE(phasecount,7);
    phasecount=phasecount+1;
    PHASE(phasecount,:)=[timecount 0 0 Diff(timecount) 0 0 Ail(timecount) 0 0];
    STATUS(phasecount,:)= 'Hold';
end
end
timecount=timecount+1;
if timecount>(length(Ail)-looklen-1)
    PHASE(phasecount,2)=timecount;
    PHASE(phasecount,3)=PHASE(phasecount,2)-PHASE(phasecount,1);
    PHASE(phasecount,5)=Diff(timecount);
    PHASE(phasecount,6)=Diff(PHASE(phasecount,1))-Diff(timecount);
    PHASE(phasecount,8)=Ail(timecount);
    PHASE(phasecount,9)=PHASE(phasecount,8)-PHASE(phasecount,7);
    phasecount=phasecount+1;
    break
end
end
for count=1:length(PHASE)
    if STATUS(count,:)== 'Hold'
        STATNUM(count)=1;
    elseif STATUS(count,:)== 'MvDn'
        STATNUM(count)=2;
    elseif STATUS(count,:)== 'MvUp';
        STATNUM(count)=3;
    end
    if and((STATUS(count,:)== 'Hold'),abs(PHASE(count,7))<=thresh)
        STATUS(count,:)= 'HldZ';
        STATNUM(count)=4;
    elseif and((STATUS(count,:)== 'MvDn'),abs(PHASE(count,8))<=thresh)
        STATUS(count,:)= 'MvDZ';
        STATNUM(count)=5;
    elseif and((STATUS(count,:)== 'MvUp'),abs(PHASE(count,8))<=thresh)
        STATUS(count,:)= 'MvUZ';
        STATNUM(count)=6;
    end
end
end
%%% Count PHASE Data
IndHold=STATNUM==1;    IndMovDn=STATNUM==2;    IndMovUp=STATNUM==3;
IndHoldZero=STATNUM==4;    IndMovDnZero=STATNUM==5;
IndMovUpZero=STATNUM==6;

```

```

COUNTPHASE=sum(PHASE(:,4)<bins(1)); %Start Diff
COUNTPHASEH=sum(PHASE(IndHold,4)<bins(1)); %Start Diff
COUNTPHASEMD=sum(PHASE(IndMovDn,4)<bins(1)); %Start Diff
COUNTPHASEMU=sum(PHASE(IndMovUp,4)<bins(1)); %Start Diff
COUNTPHASEMDZ=sum(PHASE(IndMovDnZero,4)<bins(1)); %Start Diff
COUNTPHASEMUZ=sum(PHASE(IndMovUpZero,4)<bins(1)); %Start Diff
COUNTPHASEHZ=sum(PHASE(IndHoldZero,4)<bins(1)); %Start Diff
HCORRECT=sum(and(PHASE(IndHold,4)<bins(1),abs(PHASE(IndHold,5))<abs(PHASE(IndHold,4))));
MDCORRECT=sum(and(PHASE(IndMovDn,4)<bins(1),abs(PHASE(IndMovDn,5))<abs(PHASE(IndMovDn,4))));
MUCORRECT=sum(and(PHASE(IndMovUp,4)<bins(1),abs(PHASE(IndMovUp,5))<abs(PHASE(IndMovUp,4))));
HZCORRECT=sum(and(PHASE(IndHoldZero,4)<bins(1),abs(PHASE(IndHoldZero,5))<abs(PHASE(IndHoldZero,4))));
MDZCORRECT=sum(and(PHASE(IndMovDnZero,4)<bins(1),abs(PHASE(IndMovDnZero,5))<abs(PHASE(IndMovDnZero,4))));
MUZCORRECT=sum(and(PHASE(IndMovUpZero,4)<bins(1),abs(PHASE(IndMovUpZero,5))<abs(PHASE(IndMovUpZero,4))));
for BINS=2:length(bins)
    COUNTPHASE(BINS)=sum(and(PHASE(:,4)>bins(BINS-1),PHASE(:,4)<bins(BINS))); %Start Diff
    COUNTPHASEH(BINS)=sum(and(PHASE(IndHold,4)>bins(BINS-1),PHASE(IndHold,4)<bins(BINS))); %Start Diff
    COUNTPHASEMD(BINS)=sum(and(PHASE(IndMovDn,4)>bins(BINS-1),PHASE(IndMovDn,4)<bins(BINS))); %Start Diff
    COUNTPHASEMU(BINS)=sum(and(PHASE(IndMovUp,4)>bins(BINS-1),PHASE(IndMovUp,4)<bins(BINS))); %Start Diff
    COUNTPHASEHZ(BINS)=sum(and(PHASE(IndHoldZero,4)>bins(BINS-1),PHASE(IndHoldZero,4)<bins(BINS))); %Start Diff
    COUNTPHASEMDZ(BINS)=sum(and(PHASE(IndMovDnZero,4)>bins(BINS-1),PHASE(IndMovDnZero,4)<bins(BINS))); %Start Diff
    COUNTPHASEMUZ(BINS)=sum(and(PHASE(IndMovUpZero,4)>bins(BINS-1),PHASE(IndMovUpZero,4)<bins(BINS))); %Start Diff
    HCORRECT(BINS)=sum(and(and(PHASE(IndHold,4)>bins(BINS-1),PHASE(IndHold,4)<bins(BINS)),abs(PHASE(IndHold,5))<abs(PHASE(IndHold,4)))); %Start Diff
    MDCORRECT(BINS)=sum(and(and(PHASE(IndMovDn,4)>bins(BINS-1),PHASE(IndMovDn,4)<bins(BINS)),abs(PHASE(IndMovDn,5))<abs(PHASE(IndMovDn,4)) )); %Start Diff
    MUCORRECT(BINS)=sum(and(and(PHASE(IndMovUp,4)>bins(BINS-1),PHASE(IndMovUp,4)<bins(BINS)),abs(PHASE(IndMovUp,5))<abs(PHASE(IndMovUp,4)) )); %Start Diff
    HZCORRECT(BINS)=sum(and(and(PHASE(IndHoldZero,4)>bins(BINS-1),PHASE(IndHoldZero,4)<bins(BINS)), abs(PHASE(IndHoldZero,5))<abs(PHASE(IndHoldZero,4)))); %Start Diff
    MDZCORRECT(BINS)=sum(and(and(PHASE(IndMovDnZero,4)>bins(BINS-1),PHASE(IndMovDnZero,4)<bins(BINS)),abs(PHASE(IndMovDnZero,5))<abs(PHASE(IndMovDnZero,4)) )); %Start Diff
    MUZCORRECT(BINS)=sum(and(and(PHASE(IndMovUpZero,4)>bins(BINS-1),PHASE(IndMovUpZero,4)<bins(BINS)),abs(PHASE(IndMovUpZero,5))<abs(PHASE(IndMovUpZero,4)) )); %Start Diff
end
Delbins=1:200; [HIST]=hist(PHASE(:,3),Delbins);
Fhist=2*pi./(Delbins*dt); semilogx(Fhist,20*log10(HIST),'-');
[AA Fa]=psd(Ail,length(Ail),1/dt); AA=sqrt(AA);
[UU Fu]=psd(ULow,length(ULow),1/dt); UU=sqrt(UU);
Ptot=[]; Fu=Fu*2*pi;
%% Calculate additional noise

```

```

Fnew=zeros(length(Fhist),length(Fu));
for frq=1:length(Fhist)
    Ptemp=zeros(size(UU));
    if HIST(frq)>0
        Fs=Fhist(frq);
        Rat=HIST(frq)*Delbins(frq)/sum(PHASE(:,3));
        [crd,Find]=min(abs(Fs-Fu));
        SCtemp=sinc(Fu./Fs);
        if Find<(length(Fu))
            for pwr=1:Find-1
                Ptemp(pwr)=UU(Find-pwr)*abs(SCtemp(pwr))+UU(pwr)*abs(SCtemp(pwr))-UU(pwr);%*Rat;
            end
        end
        for fin=Find+1:length(Fu)
            n=floor((fin-1)/Find);
            Ptemp(fin)=UU(fin-n*Find)*abs(SCtemp(fin));%+UU(pwr)*abs(SCtemp(pwr))-UU(pwr);%*Rat;
        end
        Ptemp=Ptemp*Rat;          Ptot(frq,:)=Ptemp;
    end
end
figure(9)
clf
plot(PHASE(IndHold,4),PHASE(IndHold,3),'ob')
hold on
plot(PHASE(IndMovDn,4),PHASE(IndMovDn,3),'vr')
plot(PHASE(IndMovUp,4),PHASE(IndMovUp,3),'^g')
plot(PHASE(IndHoldZero,4),PHASE(IndHoldZero,3),'sb')
plot(PHASE(IndMovDnZero,4),PHASE(IndMovDnZero,3),'<r')
plot(PHASE(IndMovUpZero,4),PHASE(IndMovUpZero,3),'>g')
legend('Hold','Move Down','Move Up','Hold at Zero','Move Down to Zero','Move Up to Zero')
grid
xlabel('Command Signal Error at Beginning of Step')
ylabel('Duration of Input')
title('Duration of Input vs. Command Signal Error at Time of Action')
figure(11) %% percentage of correct responses
clf
%    plot(bins,COUNTPHASE./COUNTPHASE,'k')
hold on
plot(bins,HCORRECT./COUNTPHASEH,'ob')
hold on
plot(bins,MDCORRECT./COUNTPHASEMD,'vg')
plot(bins,MUCORRECT./COUNTPHASEMU,'^r')
plot(bins,HZCORRECT./COUNTPHASEHZ,'sb')
plot(bins,MDZCORRECT./COUNTPHASEMDZ,'<g')
plot(bins,MUZCORRECT./COUNTPHASEMUZ,'>r')
%%%%% HISTOGRAM
figure(12)
clf
bar(Delbins*dt,HIST)
%% BODE PLOT OF EXTRA NOISE
figure(13)
PPP=sum(Ptot);
clf
semilogx(Fu,20*log10(UU))
hold on
semilogx(Fu,20*log10(AA),'r')

```

```
semilogx(Fu,20*log10(UU+PPP),'g')
legend('Linear Signal','NonLinear Signal')%,'Linear Signal with Sampling Noise')
grid
semilogx(Fu(cycles+1),20*log10(UU(cycles+1)),'oc')
semilogx(Fu(cycles+1),20*log10(AA(cycles+1)),'om')
semilogx(Fu(cycles+1),20*log10(UU(cycles+1)+PPP(cycles+1)),'oy')
```